UNIVERSITY OF SOUTHAMPTON

Solid phase synthesis of polyamine conjugates in the search for new inhibitors of trypanothione reductase and transfection agents for gene therapy.

by

Bordin Chitkul

Doctor of Philosophy

Department of Chemistry
Faculty of Science

September 2001

University of Southampton

FACULTY OF SCIENCE

DEPARTMENT OF CHEMISTRY

Doctor of Philosophy

Solid phase synthesis of polyamine conjugates in the search for new inhibitors of trypanothione reductase and transfection agents.

By Bordin Chitkul

Abstract

The enzyme trypanothione reductase (TR) is unique to the parasitic protozoa known as *Trypanosomes* and *Leishmania*. This enzyme and its substrate trypanothione (N^1,N^8-*bis*(glutathionyl)spermidine) play an essential role in the maintenance of a reducing cellular environment within these parasites. The trypanothione reductase system is made more attractive as a target for rational drug design because of the highly specific substrate specificity of TR.

This thesis describes the synthesis of a range of immobilised polyamines (spermine, spermidine and norspermidine) which allowed the synthesis of a number of polyamine derivatives. A series of TR inhibitors were identified using directed solid phase chemistry, with compounds based on the natural product kukoamine A as a lead structure. Several potent inhibitors of TR were discovered with K_i values as low as 76 nM.

A biocompatible safety-catch linker was developed for the solid phase synthesis and release of transfection agents. The linkers were evaluated using both peptides and small organic molecules on polystyrene and TentaGel resin. A library of transfection agents based on bile and long chain fatty acids was prepared by solid phase synthesis. The biological activity of these compounds was screened using green fluorescent protein (GFP) as a marker. The results showed that N^1-(3α, 7α–dihydroxy-5β-cholane-24-carbonyl)-1,5,10,14-tetraazatetradecane was the most potent compound. The transfection efficiency, in association with its relatively low toxicity and ease of preparation make it a promising candidate for general gene therapy.

Table of Contents

Acknowledgements

I wish to express my sincere gratitude to my supervisor Professor Mark Bradley for his kind and helpful supervision, patience and encouragement throughout this project.

Special thanks to Dr. Ashley Pringel and Dr. Lars Sundstrom for teaching me how to use the fluorescent microscope and for the use of their facilities during the transfection project at Southampton General Hospital. Thanks to Professor Tom Brown for use of his fluorescence spectrometer.
Thanks to Joan Street, John Langley and Julie Herimann for NMR and mass specs.

Many thanks to all my friends and colleagues in the Bradley group, past and present, it's been a pleasure working with you. Special thanks goes to Dr. Patric Page, for teaching me the techniques of solid phase chemistry and for his friendship. Thanks to who showed me how to purify trypanothione reductase. Thanks to Sachin, my flat mate who helped me to improve my English language and also thanks to Sunil for his help especially when I got ill. A big thanks goes to all those who proof read this thesis. Thanks to Neil, Iain for HPLC and Boon-ek for such unlimited access to the 400 NMR during weekends.

Thanks also to my grandmother, mother and father for their the love and support.
I would like to thank Professor Apichart Suksamrarn and Professor Yodhathai Thebtaranonth for all their exemplary help, (I can stand today in this way because of both of you).
Special thanks to my wife Nutcha for her love, patience and her supporting role toward my success.
Thanks to all staff at Department of Chemistry, Ramkhamhaeng University for all their support. Also thanks to departmental staff (Julia, Jill and Sue).
I acknowledge and appreciate the financial support of the Royal Thai government.

Abbreviations

aa	amino acid
Acbz	4-azidobenzyloxycarbonyl
Aloc	allyloxycarbonyl
AP	alkaline phosphatase
BGCT	bis(guanidium) TREN-cholesterol
Boc	*t*-butyloxycarbonyl
BSA	bovine serum albumin
CAT	chloramphenicol acetyl transferase
C. fasciculata	*Crithidia fasciculata*
δ	chemical shift (ppm)
δ_C	chemical shift ^{13}C
δ_H	chemical shift ^{1}H
DCC	dicyclohexylcarbodiimide
DC-Chol	3β-[*N-(N', N'*-dimethylaminoethyll) carbamoyl]cholesterol
DCM	dichloromethane
DIC	diisopropylcarbodiimide
DIPEA	diisopropylethylamine
DMF	dimethylformamide
DMSO	dimethylsulfoxide
DOGS	dioctadecylamidoglycylspermine
DOTAP	1,2-dioleyloxy-3-(trimethylammonio)-propane
E. coli	*Eschericia coli*
EDT	ethanedithiol
EDTA	ethylenediaminetetraacetic acid
ES+	electrospray (positive ion)
EtOH	ethanol
FAB	fast atom bombardment
FAD	flavin adenine dinucleotide (oxidised)
Fmoc	9-fluorenylmethoxycarbonyl
FTIR	Fourier transform infrared
GFP	green fluorescent protein

GR	glutathione reductase
GSSG	oxidised glutathione
HOBt	N-hydroxybenzotriazole
IR	Infrared
IPTG	isopropyl-β-D-1-thiogalactopyranoside
J	coupling constant (Hz)
MALDI-TOF MS	matrix assisted laser desorption ionisation time of flight mass spectrometry
MeOH	methanol
M_r	relative molecular weight
MS	mass spectrometry
NADPH	nicotinamide adenine dinucleotide phosphate (reduced form)
NMR	nuclear magnetic resonance
s	singlet
d	doublet
dd	doublet of doublets
dt	doublet of triplets
t	triplet
m	multiplet
ODC	ornithine decarboxylase
PBS	phosphate buffer saline
Pht	phthaloyl
RP-HPLC	reverse phase high pressure liquid chromatography
Rf	retention factor
R_t	retention time
SDS	sodium dodecylsulfate
SDS-PAGE	sodium dodecylsulfate-polyacrylamide gel electrophoresis
TA	thioanisole
T. cruzi	*Trypanosoma cruzi*
***tert* (*t*)**	tertiary
TFA	trifluoroacetic acid
Tfa	trifluoroacetyl
TG	TentaGel

THF	tetrahydrofuran
TIS	triisopropylsilane
TLC	thin layer chromatography
TR	trypanothione reductase
Tris	*tris*(hydroxymethyl)aminomethane
$T[S]_2$ or TSST	oxidised trypanothione
UV	ultraviolet

Amino acids are abbreviated using standard codes

Abu (Ab)	α-aminobutyric acid	**Leu (L)**	leucine
Ahx (Ah)	α-aminohexanoic acid	**Lys (K)**	lysine
Ala (A)	alanine	**Met (M)**	methionine
β-Ala (bA)	β-alanine	**Nva (Nv)**	norvaline
Arg (R)	arginine	**Phe (F)**	phenylalanine
Asn (N)	asparagine	**Phg (Pg)**	phenylglycine
Asp (D)	aspartic acid	**Pro (P)**	proline
Glu (E)	glutamic acid	**Ser (S)**	serine
Gln (Q)	glutamine	**Thr (T)**	threonine
Gly (G)	glycine	**Trp (W)**	tryptophan
His (H)	histidine	**Tyr (Y)**	tyrosine
Ile (I)	isoleucine	**Val (V)**	valine

To Grandmother, Mother and Father with all my love

Chapter 1 Introduction

1.1 Naturally occurring polyamines and polyamine conjugates

1.1.1 Polyamines

The polyamines such as putrescine, cadaverine, 1,3-diaminopropane, spermidine and spermine are natural products discovered and characterized by 1930[1]. Putrecine and cadavarine are primary diamines and are well known as products of bacterial metabolism. Spermidine and spermine are triamines and tetraamines, respectively, that contain both primary and secondary amines (Figure 1.1). These compounds occur in cells at micromolar concentration and may rise to millimolar levels in certain cancer cells[2]. Both spermidine and spermine can be thought of as derivatives of putrescine.

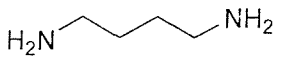

1 Putrescine

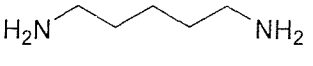

2 Cadaverine

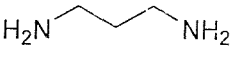

3 (1,3-diaminopropane)

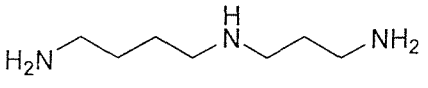

4 Spermidine

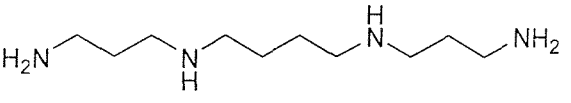

5 Spermine

Figure 1.1 Some early known polyamines

Two natural polyamines have been found that contain one carbon unit more than spermidine so called *homo*spermidine. Symmetrical *homo*spermidine, *bis*(aminobutylamine), is found in some plants and bacteria whereas an asymmetric *homo*spermidine, aminopropylcadaverine, was found in Syrian hamster epididymis cells relatively rich in cadaverine, but not in other tissues of this animal. The compounds may also be present in the epididymis of Chinese hamsters and the guinea pig[3]. This was the first report of tetraamines other than spermine in mammals. Other natural polyamines that contain moieties with one carbon atom less than spermidine and spermine are designated as *nor*spermidine and *nor*spermine.

1.1.2 Biosynthesis of polyamines

As the ubiquity and metabolic activities of the polyamines became clearer, the biogenesis of these bases was explored, with appropriate attention placed on the synthesis of possible precursors. The derivation of putrescine from L-ornithine and L-arginine and of cadaverine from L-lysine was recognised. The biosynthetic pathway of polyamines is shown in Figure 1.2.

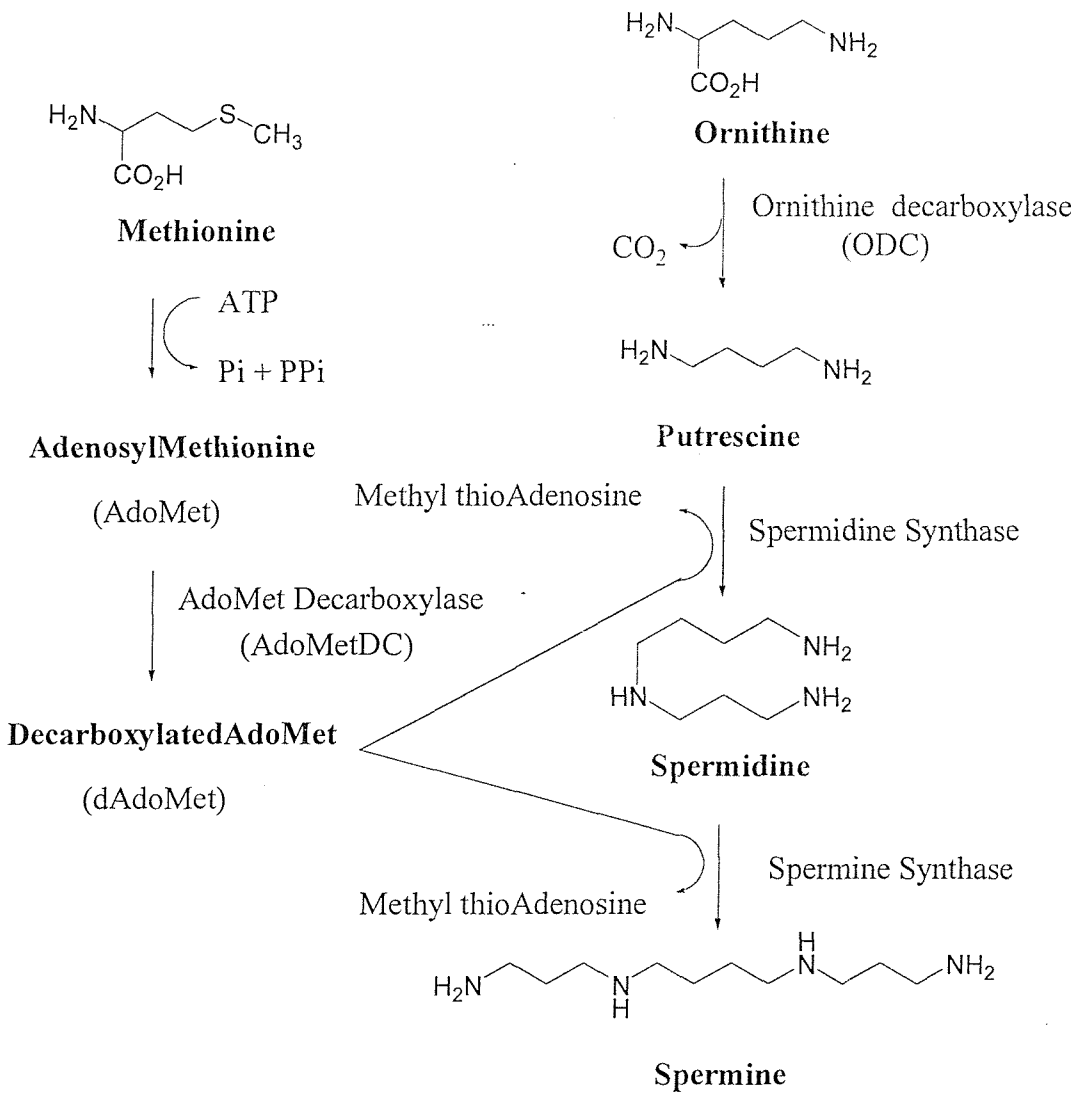

Figure 1.2 Biosynthetic pathway of polyamines

Investigations into the biochemistry of the polyamines began with studies on the decarboxylation of amino acids by the use of intact bacteria and their extracts[4]. An enzyme ornithine decarboxylase (ODC) was distinguished, which produced putrescine. In addition, an enzyme was identified, named lysine decarboxylase (LDC) which formed

cadaverine and was synthesised most actively toward the end of the growth cycle of the cells. The earliest assays of catabolic decarboxylation using ODC, LDC and arginine decarboxylate (ADC) were conducted by CO_2 analysis in Warburg respirometers. ODC and LDC rapidly approached, but did not exceed 1.0 mole of CO_2 per mole of substrate. In a study on crude ODC, using [U-^{14}C]-ornithine as a substrate, 1.0 mole CO_2 was produced per mole of substrate. In this assay, radioactive CO_2 was trapped on filter paper moistened with alkali. The paper was then added to scintilation fluid and radioactivity counted. Simple and direct methods were developed for the rapid isolation of radioactive putrecine by cation exchange paper or resin[5]. As the assay for ODC became a matter of increasing interest, methods were devised to improve the speed and recovery of crucial products. For example, CO_2 selective electrodes were devised for the study of decarboxylation. These were shown to be rapid, potentially continuous, and sufficiently precise for the study of partially purified bacteria LDC.

S-Adenosylmethionine (AdoMet) was discovered during studies on the origin of the methyl groups of creatine and *N'*-methylnicotinamide[6]. A liver extract, supplemented with ATP and methionine, gave rise to "active methionine" containing adenosine and methionine and was capable of transferring a methyl group to guanidoacetic acid. The biosynthetic pathway to spermidine and spermine is controlled by S-adenosyldecarboxylase (AdoMetDC). The aminopropyl moiety is transferred to one or both of the amino groups of putrecine affording spermidine or spermine. The activity of AdoMetDC is controlled by the natural polyamines and is independent of the metabolic status of the appropriate tissue. The enzyme increases in rapidly growing and neoplastic cells.

1.1.3 Biological activity of polyamines

Polyamines interact strongly with nucleic acids and play an important role in their biosynthesis and metabolism. The interaction of polyamines with DNA results in stabilisation of their conformation. This stabilisation occurs through electrostatic attraction between the polycationic polyamine molecules and negatively charged phosphate groups on the DNA molecules.[7] The DNA-polyamine complex also accounts for protection of DNA from denaturation which can be caused by heat, chemical reagents or radiation[8]. Polyamines also affect protein synthesis in several ways.[9] Furthermore, they are essential for normal growth and are even involved in the differentiation of

mammalian cells. Polyamines are directly responsible for the increase in the rate of macromolecular syntheses which takes place during development or tumour growth.[10] Polyamines are also involved in modulation of the NMDA receptor[11] and attempts have been made to exploit this interaction for therapy or prevention of neurotoxicology, epilepsy and neurodegenerative diseases.[12]

1.2 Polyamine conjugates

Polyamine conjugates display a wide range of biological functions, including antibacterial, glutamate receptor antagonists and anti-cancer effects. For example, the tetracyclic spermidine alkaloid (-)-hispidospermidine (**6**) from a fungal culture was discovered to be an inhibitor of phospholipase C (PLC),[13] while pseudoceratidine (**7**), a derivative of the polyamine spermidine, and isolated from a marine sponge, showed promising properties as an antifouling compound.[14] The antibiotic edeine A (**8**) and edeine B (**9**) are polyamines conjugated to peptides.[15] These compounds produced by *Bacillus brevis* have a broad spectrum of anti-microbial activity and little or no cytotoxicity against normal cells[16]. Recently a polyaminosteroidal antibiotic squalamine (**10**) was isolated from tissues of the dogfish shark.[17] This compound was shown to consist of a sulfate bile acid fused to the aminopropyl primary amine of spermidine. The antibiotic is not only bacteriacidal to many Gram-negative and Gram-positive bacteria, but also fungicidal and lytic to some protozoa. It is assumed that the compound is lethal as a result of its action on the cell membrane. Bile acids containing basic groups possess antibiotic activity, which is enhanced when this modification occurs at the C-3 position.

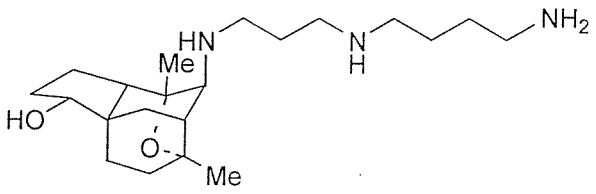

6 (-)-hispidospermidine

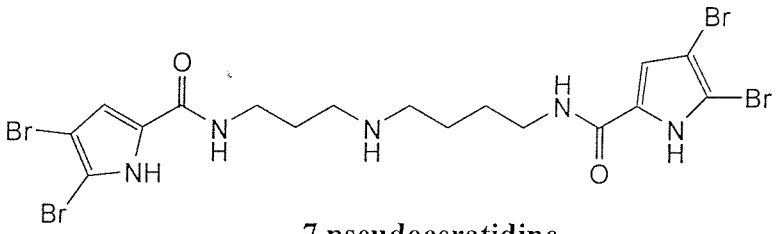

7 pseudoceratidine

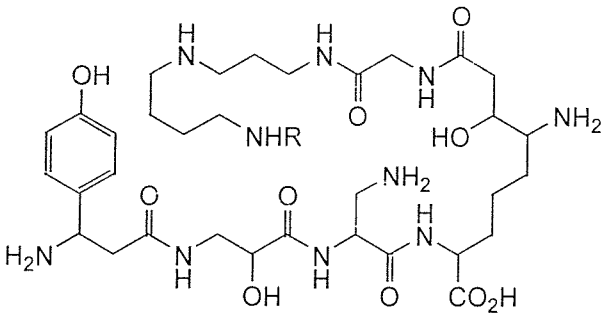

8 edeine A R=H

9 edeine B R= C(NH)NH_2

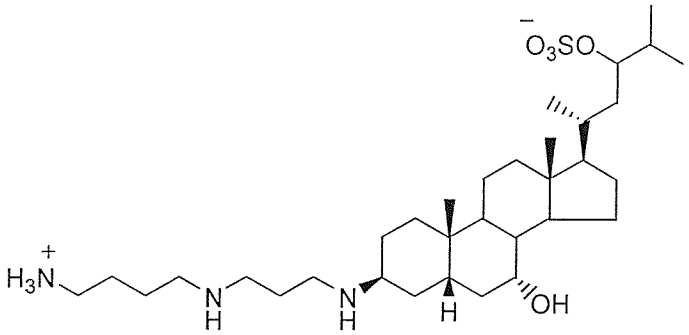

10 squalamine

Figure 1.3 Biologically active polyamine conjugates

1.2.1 Polyamine conjugates from spiders and wasps

A variety of amino acids conjugated to polyamines have been isolated from the venoms of spiders and wasps (see Figure 1.4).[18,19] The venom of the parasitic wasp philathotoxin PhTX-4.3.3 (**11**) is a potent blocker of cation channels. This toxin is believed to act both pre-and postsynaptically on the glutamate neuromuscular junction. Argiotoxin 636 (**12**) is one of the numerous polyamines isolated from spider venoms. This compound is a selective antagonist of the glutamate receptor, and therefore, they are potential pharmacological probes and lead compounds for the design of drugs to treat neurodegeneration. The similar funnel spider toxins FTX-3.3 (**13**) and sFTX-3.3 (**14**) have also potent paralytic properties as a result of their ability to inhibit voltage activated calcium channels.[20]

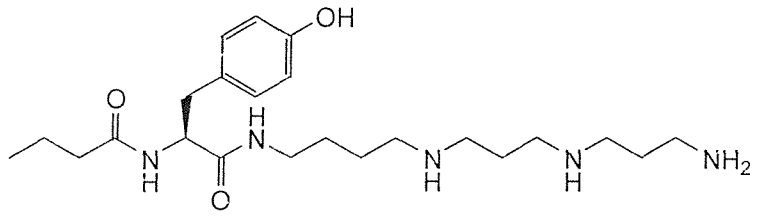

11 PhTX 433

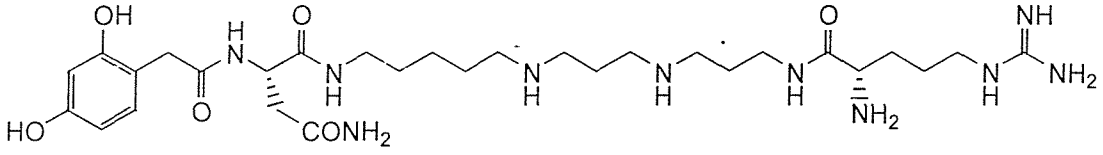

12 Agiotoxin 636

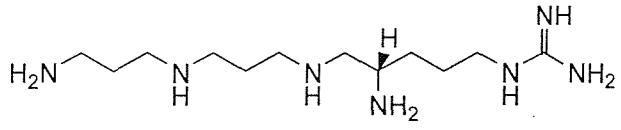

13 FTX-3.3

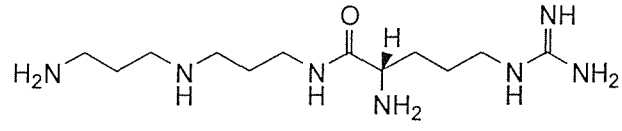

14 sFTX-3.3

Figure 1.4 Structures of some polyamine wasp and spider toxins

1.2.2 Polyamine conjugates from plants

Plants also contain a variety of polyamine conjugate alkaloids. Classic examples include the spermidine alkaloid meytenine (**15**) Figure 1.5.[21]

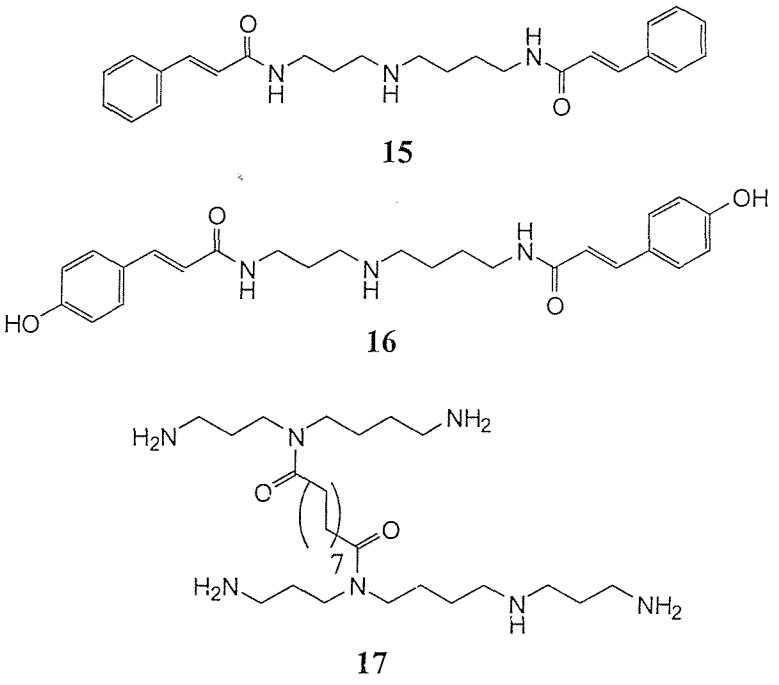

Figure 1.5 Polyamine conjugates from plants

A variety of other polyamine alkaloids have been isolated and characterised from the reproductive organs of many higher plants. These include spermidine amides of various hydroxycinnamic acids (HCA), such as caffeic acid or sinapic acid. Polyamine alkaloids often contain one HCA unit usually at N^4 or two HCA units at the N^1 and N^4, N^4 and N^8 or N^1 and N^8 position e.g. the alkaloid (**16**).[22] Recently, tenuilobine (**17**), the first polyamine alkaloid containing both spermine and spermidine, cross-conjugated through a long aliphatic chain was isolated.

Other examples of a naturally occurring spermine conjugate are kukoamine A (**18**) and B (**19**) (shown in Figure 1.6).[23] These compounds have been isolated from the root bark of *Lycium chinesse*. Kukoamine A has been used for centuries to treat hypertension and stress ulcers. Furthermore, it has been shown to inhibit trypanothione reductase (TR).[24] Although kukoamine A displays inhibition of TR as a mixed inhibitor with K_i = 1.8 μM and K_{ii} = 13 μM, it is devoid of human glutathione reductase inhibition activity (K_i > 10

mM). Structure-activity studies indicated that the *bis*-acyl compounds were more active than the mono-acylated compound while spermidine analogues were also still active.

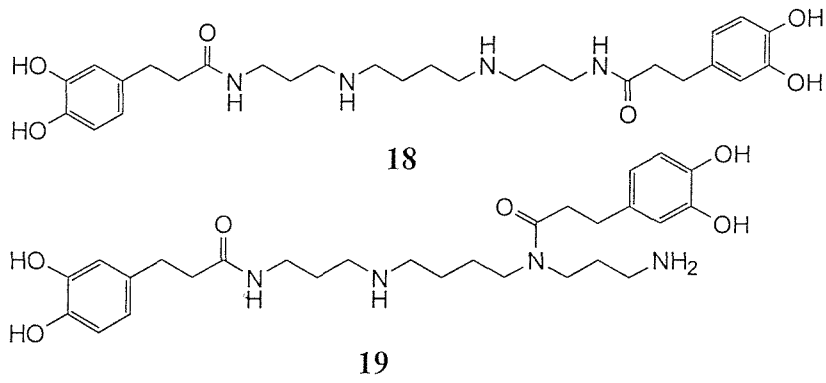

Figure 1.6 Spermine conjugates kukoamine A **(18)** and B **(19)**

Macrocyclic alkaloids are another group of spermidine and spermine conjugates produced by plants (Figure 1.7). Representative examples are the macrolactam spermidine alkaloid oncinotines, such as **(20)**.[25] Other examples of macrocyclic spermidine alkaloids are the loesenerines **(23)**. These alkaloids contain a thirteen-membered lactam ring made up of spermidine and part of a C_{10} fatty acid. Protoverbine and verbasitrine **(25)** containing a seventeen-membered ring are other classes of spermine alkaloids. These groups of alkaloids have been shown to have antibacterial and cytotoxic activities.

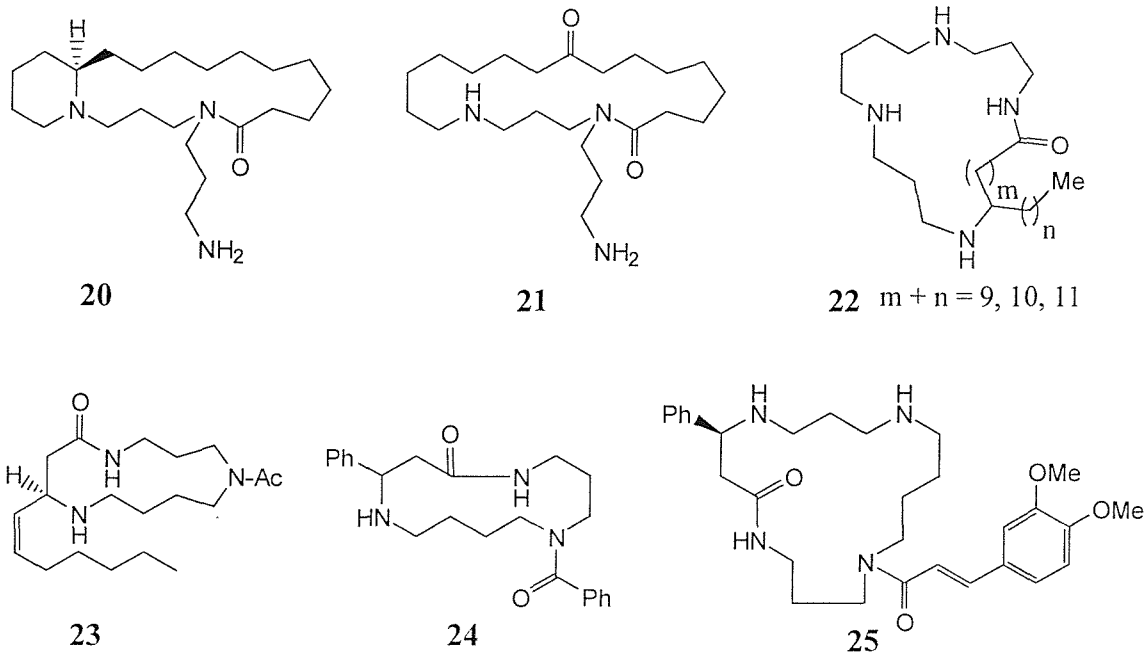

Figure 1.7 Examples of macroclactam spemidine and spermine alkaloids

1.2.3 Polyamine conjugates from parasites

Parasites such as *Leishmania* and *Trypanosomes* use endogenous antioxidant molecules to confront the oxidation stress caused by various active oxygen species. These parasites are responsible for the infection of several million people and animals worldwide, causing widespread disease and fatalities. The spermidine glutathione conjugate $T(SH)_2$ known as trypanothione is the key antioxidant molecule of the parasites.[26] This compound is oxidised by oxygen reactive species with the formation of a disulfide bridge, giving rise to the cyclic disulfide conjugate $T(S)_2$. The survival of the parasite depends on the enzyme Trypanothione reductase (TR) which reduces $T(S)_2$ back to $T(SH)_2$ (Figure 1.8).

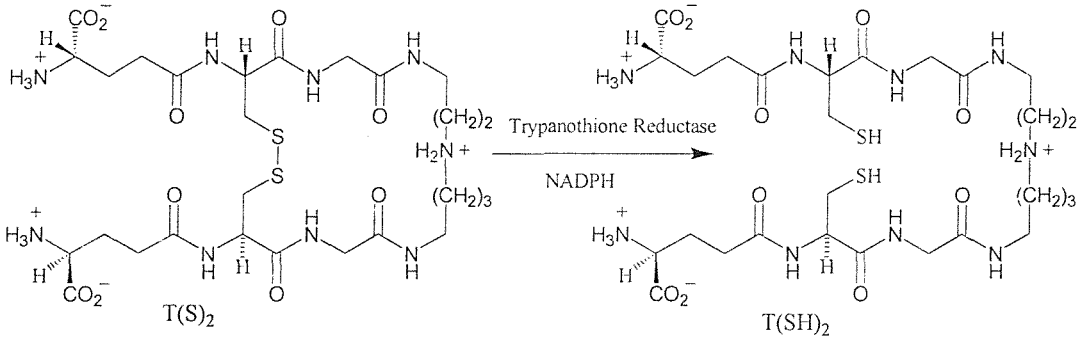

Figure 1.8 Trypanothione reductase mediated transformation of trypanothione disulfide to the reduced form

1.3. Synthetic polyamines and polyamine conjugates

1.3.1 Synthetic polyamines

Based on the fact that in tumour cells there is a high concentration of polyamines and a higher activity of the anabolic enzymes, inhibitors for all the enzymes involved in the biosynthesis of polyamines have been developed for use as anticancer agents.[10] Some of the simplest and most effective synthetic polyamines to show anticancer activity have been developed such as the derivative DENSPM (**26**) DESPM (**27**) and DEHSPM (**28**) (Figure 1.9).[27] These compounds are recognised and taken into the cell by active polyamine transport. Moreover, $(OH)_2$DEHSPM (**29**) has been found to show anti-diarrhoeal activity and has potential in HIV-related diarrhoea, either as a result of infection or as a side effect of drugs.

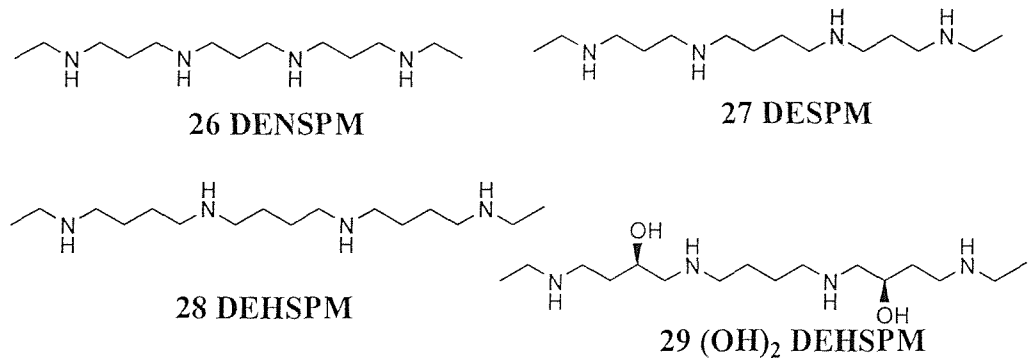

Figure 1.9 Structures of synthetic anticancer polyamines

Other polyamine conjugates, shown in Figure 1.10, have been shown to have anti-tumour activity.[28] The activity of these compounds is due to their ability to bind to DNA resulting in disruption of DNA transcription. Structure-activity studies on a series of analogues (**30-34**) have shown that the best activity is achieved by attaching spermine to acridine. The most potent cytotoxin in this series is compound (**33**) which confers a region of flexibility between the two bonding regions.

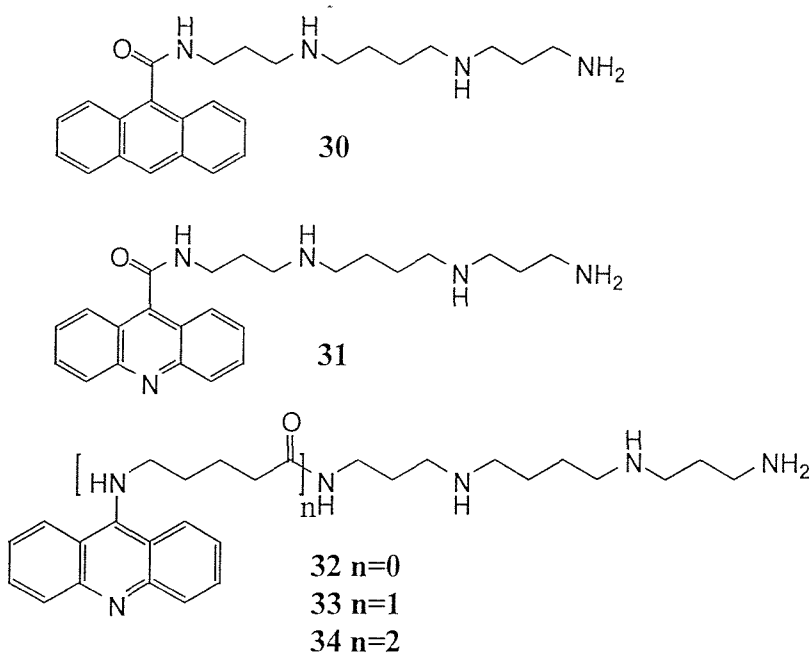

Figure 1.10 Structures of cytotoxic synthetic conjugates of polyamines with tricyclic aromatics

Carboranyl analogues of natural polyamines such as (**35**) and (**36**) incorporating ^{10}B have been prepared for possible use in boron neuron capture therapy (Figure 1.11).[29]

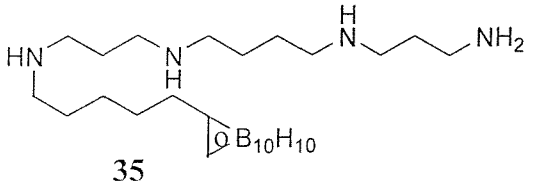

35

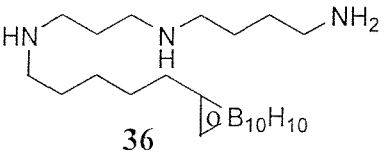

36

Figure 1.11 Natural polyamine incorporating ^{10}B atoms

1.3.2 Some recent synthetic polyamine conjugates

Polyamine conjugates result from the anchoring of a polyamine onto other organic or bioorganic molecules. These compounds are designed to show improved biological activity against particular targets, compared to the parent molecules, or to combine the activities of constituent molecules. Polyamine conjugates with nucleosides are a new class of inhibitors of polyamine biosynthesis. For example, adenosyl spermidine (**37**) was found to be a potent inhibitor of the anabolic enzyme spermidine aminopropyl transferase (Figure 1.12).[30] Conjugates of macrocyclic polyamines with AZT have also been synthesised and their anti-HIV properties evaluated.[31]

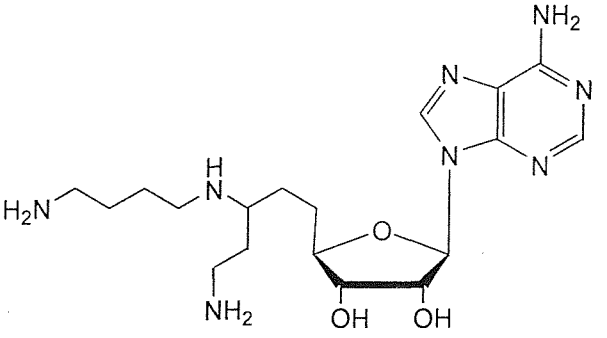

37 adenosyl spermidine

Figure 1.12 Polyamine conjugates with nucleoside

Conjugates of polyamines with cholesterol (**38**),[32] biles acid (**39**),[33] or long aliphatic chains (**40**)[34] have been recently developed as potent agents for the introduction of DNA into cells (see more detail in chapter 4 of this thesis). This methodology is known as transfection and has a role for gene delivery and possible gene therapy. This method may

be useful in the correction of a variety of disorders in humans ranging from cancer, inflammation and neurodegeneration (Figure 1.13).

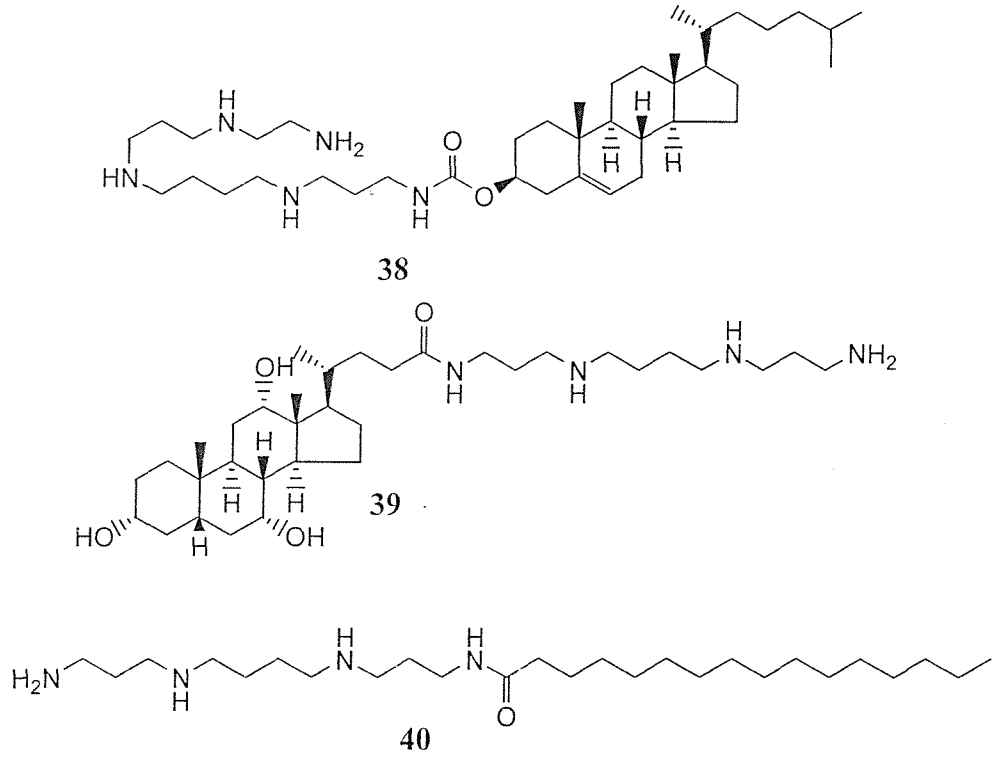

Figure 1.13 Polyamine conjugates with steroids and bile acids

1.4 Combinatorial chemistry

Combinatorial chemistry has developed not only for discovering new drugs, but also, more recently, for making catalysts and many other target molecules. This is a method for rapid synthesis of a large number of molecules with a driving need for compounds to satisfy high throughput screening. The purpose of combinatorial chemistry is twofold. Firstly to assemble as quickly as possible compounds for screening with the objective of finding a "lead" compound with the desired properties. Secondly once the lead compound has been found combinatorial chemistry can help to focus analogue synthesis in order to improve the potency, efficiency and selectively of a compound as a potential drug. Traditionally drug discovery has involved the optimisation of a lead structure, usually derived from biological sources, through a painstaking process of serial synthesis and screening. A new active compound is obtained by trial and error. Many thousand of molecules must be synthesised before a marketable product is found. This is one of the main factors that make the development of new pharmaceuticals a lengthy, and thus expensive, process.

Rapid progress in molecular biology and gene technology has brought about fundamental changes in biomedical research in the last decade. Use of molecular biological methods to identify and prepare proteins (enzymes, receptors) that are directly associated with medical symptoms is very important in drug research. Determination of the structure of these molecules has made it possible to understand diseases at the molecular level. In addition, and of great importance is the use of biological targets to design efficient test systems to enable thousands of compounds to be screened per day. The biological activity can be reliably ascertained even with minute amounts of substance. This approach is called **high-throughput screening (HTS)** for the identification of new lead structures. So, the traditional concept of synthesising one molecule after another soon reaches its limit since using these methods a medicinal chemist might be expected to synthesise at best 100 compounds a year. The need to find a more effective method of drug development has led to the pharmaceutical companies to examine combinatorial synthetic strategies. The speeds of synthesis methods known as high-throughput synthesis are staggering. This is a new dimension in organic synthesis, which can accelerate drug discovery programmes and increase the chemical diversity of compound libraries. The technique of combinatorial synthesis initially involved the preparation of large numbers of structurally related compounds as mixtures in the same reaction vessel, but now implies individual compound synthesis by parallel semi-automated synthesis. In this manner hundreds to millions of compounds can be synthesised.

In principle, combinatorial synthesis can be performed both in solution and on solid-phase. However, the majority of the compound libraries that have been synthesised to date have been synthesised on a solid support. There are two advantages to solid-phase synthesis strategies. First, using an excess of reagent accelerates the reaction and complete conversion can be achieved. Complex work-up and purification steps are replaced by washing away reagents at the end of each reaction. Second, innovative methods are available for the manipulation of discrete compounds and for "tracking" the identity of compounds when compounds are attached to a solid support. A number of general strategies have been developed for the synthesis and evaluation of compound libraries synthesised on the solid support. Although most of these strategies were demonstrated with peptide libraries, many of these approaches have now been applied to other compound classes. The following discussion will employ mainly techniques using solid phase synthesis.

1.4.1 Spatially separate synthesis

The most straightforward method for the preparation of a compound library is to synthesise many compounds in parallel. For example, n substances are synthesised in n reaction vessels and each compound kept in a separate reaction vessel. When the final compounds are spatially separate, the identity of a compound at a particular location is known and can be confirmed by analytical methods. A number of approaches for the parallel synthesis of organic compounds have been reported.[35] The first method was originally developed by Geysen for peptide epitope mapping.[36] In this method, 96 polyethylene pins are placed into a supporting block so that each pin fits into a separate well of a 96-well microtiter plate. Each pin is coated with a polymeric material that is amenable to solid-phase synthesis. The polymeric material is derivatised with aminoalkyl groups to provide sites for substance attachment. During a synthesis sequence each pin is placed in a separate well of the microtiter place so that each well serves as a distinct reaction vessel. Currently, pin loading levels range from 100 nmol to 50 μmol of material per pin. Even 100 nmol of material is sufficient for multiple biological assays, as well as for analytical evaluation of the purity and chemical integrity of the individual compounds.

1.4.2 The split and mix method

Furka and co-workers introduced the split and mix method in combinatorial chemistry for the first time in 1988.[37] This simple process of splitting, coupling and combining of the resin has given scientists the ability to generate libraries of millions of compounds on just a few grams of the resin. This technique is shown in Figure 1.14, which outlines the preparation of a library containing all possible trimers that can be constructed from 3 different monomer units. A quantity of resin is split into equal sized portions that are placed into separate reaction vessels. Excess of each building block is employed to ensure that all of the reactions are driven to completion. The resin from all of the vessels is then recombined, mixed thoroughly, and reapportioned into the requisite number of reaction vessels to carry out the second synthesis step. The second reaction provides compounds that incorporate all possible combination of the two sets of building blocks. By repeating the spit, react, and mix operations compounds incorporating all possible combinations of the set of different building blocks are generated. The obvious advantage is that 27 products are obtained in nine reaction steps with nine synthetic building blocks (in three mixtures of the nine compounds each), whereas their synthesis as separate compounds would require 81 reaction steps. At the end of the synthesis the libraries can either be

screened directly attached to the solid support or cleaved from the support and screened in solution with the active compound being found through the deconvolution of the active pool.

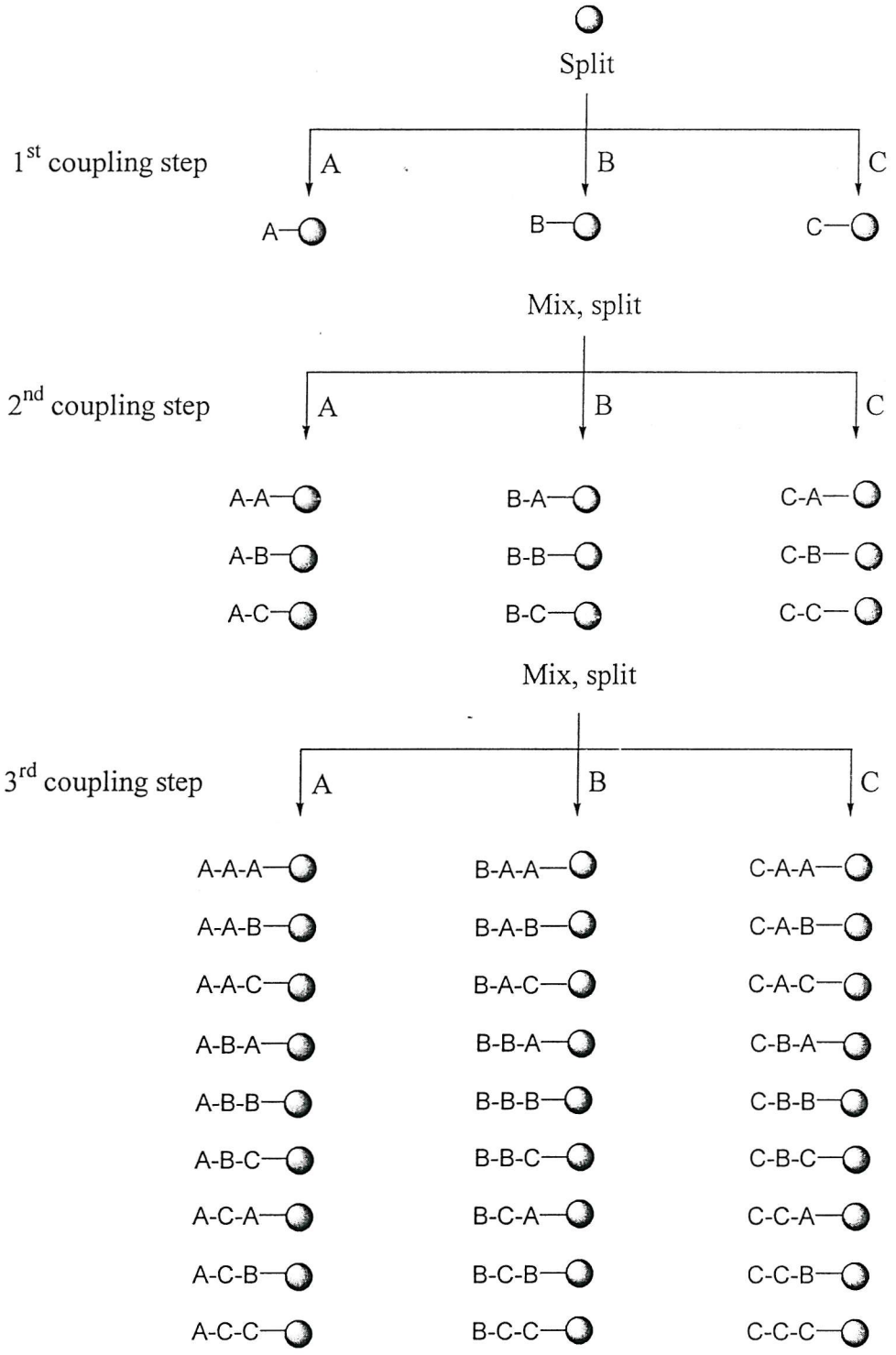

Figure 1.14 Split and mix method

A number of different strategies have been developed for evaluating libraries that are prepared by the split and mix synthesis procedure. This is because of the considerable challenge of correct structural elucidation of the molecules having the greatest biological activity. These strategies are described in the subsequent sections.

1.4.3 Deconvolution

Deconvolution is one of the most popular strategies and was developed by Houghten *et al.*[38] In this method (Figure 1.15), groups of related compounds are prepared such that separate pools have defined building blocks at one position and at the remaining positions all combinations of building blocks are incorporated. The optimal building block at the defined position is selected by determining which pool has the greatest biological activity. The most active compound in each sub-library in a given assay is selected and followed by re-synthesis and screening. This process is repeated until all positions are defined.

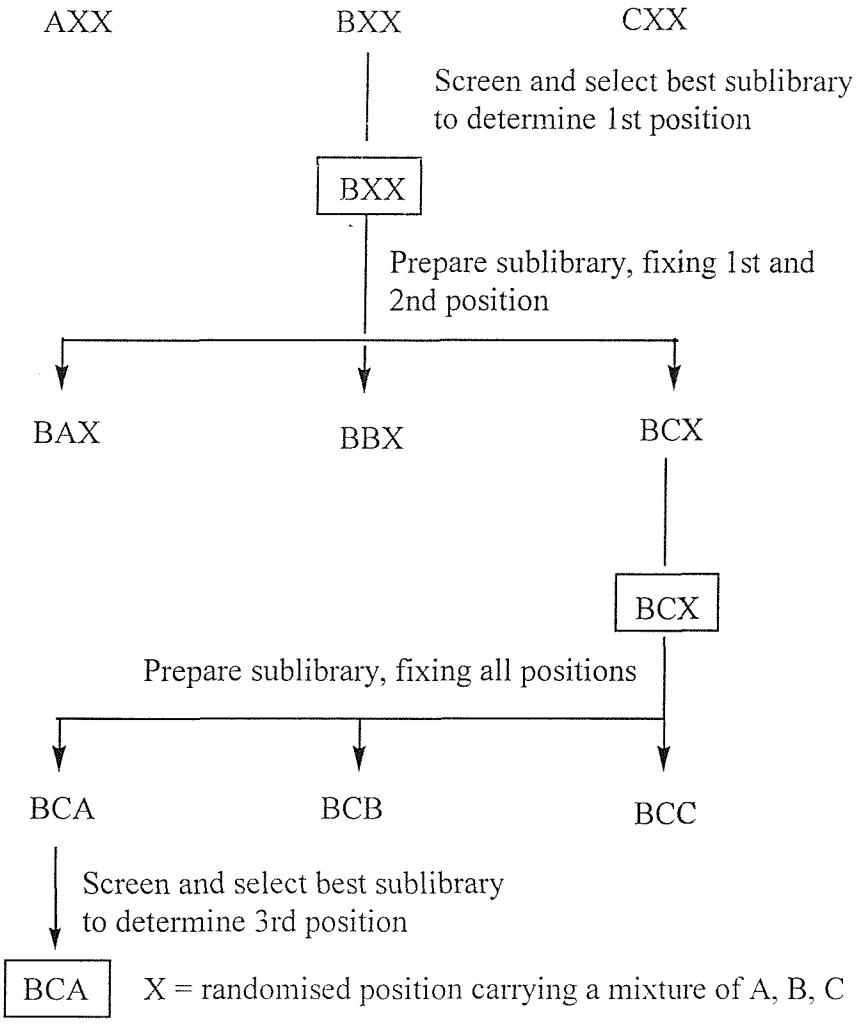

Figure 1.15 Synthetic combinatorial libraries deconvolution

For example, in the deconvolution sequence illustrated in Figure 1.15, three pots are produced that each contain a defined building block at the first position (A, B, C) and all possible combinations of building blocks at the second and third positions. For deconvolution, the pots are assayed and building block B is selected at the first position since the pot with B has the greatest activity. Three pots are now prepared in the second round of synthesis that incorporate building block mixture at the third position, a defined building block at the second position (A,B,C) and selected building block B at the first position. Each pot is evaluated for biological activity and building block C is selected for the second position. Three final pots are synthesised with defined building blocks at each position; building blocks B at the first position, building block C at the second position and A, B, or C at the last position. Evaluation of these pots results in the identification of compound BCA.

Although the devolution process described above has been applied successfully to identify high-affinity ligands, the major disadvantage of this method is the time consuming and laborious process. A number of modifications have been reported in order to overcome these problems including the positional scanning method of Houghten *et al*[39] and the "orthogonal" library of Tartar.[40]

1.4.4 Positional scanning method

In the positional scanning approach, separate positional libraries are prepared, each of which contain a single defined building block. For example, if a library was prepared from a three building block set, three positional libraries would be prepared (Figure 1.16). This may be denoted as OXX, XOX, and XXO, where O corresponds to the defined position and X corresponds to a random position.

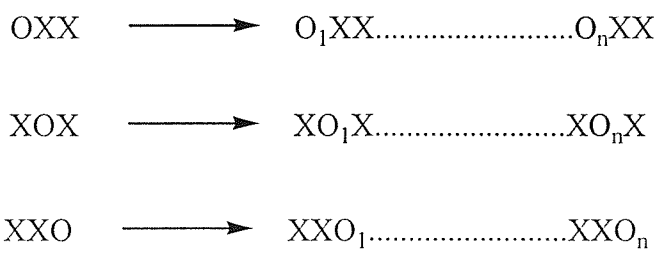

Figure 1.16 Positional scanning method

An advantage of this method is that only one round synthesis and screening is required. The most active residues at each position are combined into one compound to give the

optimum combination of libraries. However, this method has been shown to be less effective than deconvolution strategies, especially when multiple active compounds are present due to the interaction between residues.

1.4.5 Orthogonal library approach

Tartar demonstrated the orthogonal library method by the co-synthesis of two libraries containing orthogonal pot (subsets). Using this method, any of the subsets of the first library will have only one compound in common with any of the subsets of the second library. During an assay, any highly active compound will cause a signal in only one pot in each library. The active compound can immediately be identified without re-synthesis by examining which two pots are active. This method was demonstrated preparing two different 3-residue peptide libraries using 25 amino acids in the following manner. The 25 residues were grouped in 5 batches of 5 and coupled to resin. For the first libraries, these 5 batches of resin were each split into 5 pots and coupled to all 5 sets of residues giving 25 sub-libraries of 25 compounds each. This step was repeated to give 125 sublibraries of 125 compounds (15625 in total). The second library was made in an identical fashion except the original grouping into 5 was different; no two residues were kept with each other from the first library. This mean that one tripeptide appeared only once in either library.

1.5 Solid phase chemistry

1.5.1 Solid support

The origins of solid phase methodology can be traced back to 1963 with R.B. Merrifield's method of peptide synthesis on the solid support.[41] The solid support is generally a polymeric resin (an insoluble polymer that swells in the presence of the reaction solvent, but which is inert to the reaction conditions). One of the most widely used is polystyrene which is crosslinked with 1 percent divinyl benzene to give the polymer its structural rigidity and to render it insoluble (see Figure 1.17). The chemistry handle is typically a chloromethyl functionality, incorporated by co-polymerisation with chloromethyl styrene.

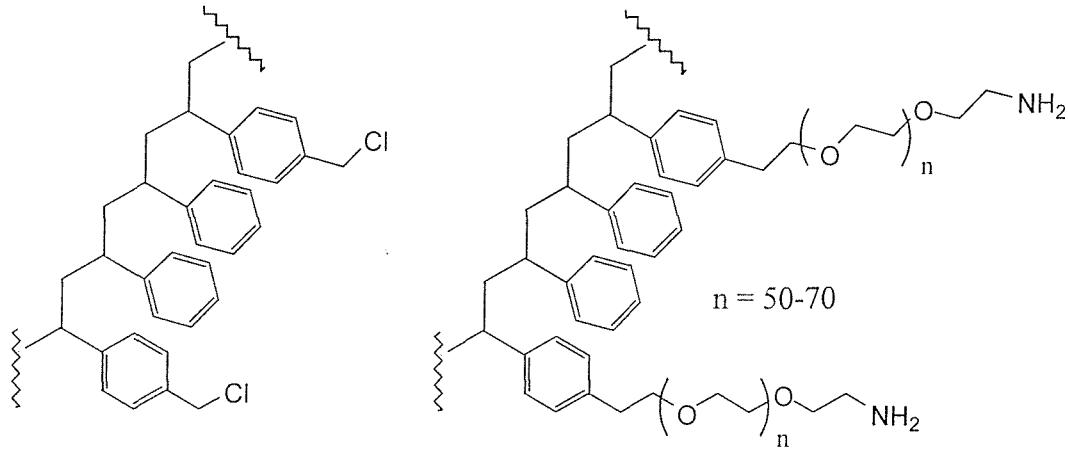

41 Polystyrene resin **42 TentaGel resin**

Figure 1.17 Structures of Polystyrene and TentaGel linkers

Another common type of solid support is TentaGel resin (**42**), which consists of polyethylene glycol attached to polystyrene through an ether linkage.[42] This resin is particularly useful for reactions which occur in water, since the hydrophilic nature of the support allows solvation to occur in aqueous solvent co-mixtures. The ability of the resin to swell in both organic and aqueous media is especially important when on-bead binding assays are used for screening. PS-PEG resin developed by Barany[43] has a similar composition and properties as TentaGel. However, the major difference is the placement of the chemically reactive groups (amino groups) in relation to the polystyrene matrix. TentaGel has the functionalisable group at the end of polyethylene chains, therefore far from the hydrophobic polystyrene chain. In contrast, PS-PEG has the functional group next to the polystyrene chain, and the polyoxyethylene chain in this case does not serve as the "spacer" connecting the synthesis compound to polymer, but rather as a "modifier" of the polymer properties. NovaGel™ (**43**) is a new type of PS-PEG resin that has been designed to meet the requirements of organic chemists for resins of high substitution with broad solvent compatibility. It was prepared from MeO-PEG_{2000}-*p*-nitrophenylcarbonate[44] (Figure 1.18), similar to the resin of Barany. The urethane linkage between the PEG and the base resin was stable under strongly acidic and basic conditions ensuring minimal loss of PEG chains during synthesis.

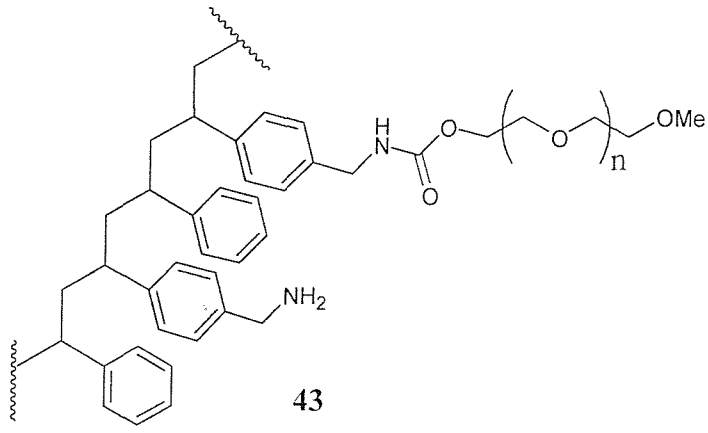

43

Figure 1.18 Structure of NovaGel^{TM} resin

A new polymeric carrier (PEGA **44**) described by Meldal *et al.*,[45] based on copolymerisation of acrylamide and a PEG based cross-linker is a cross-linked hydrophilic type polymer[46] (Figure 1.19).

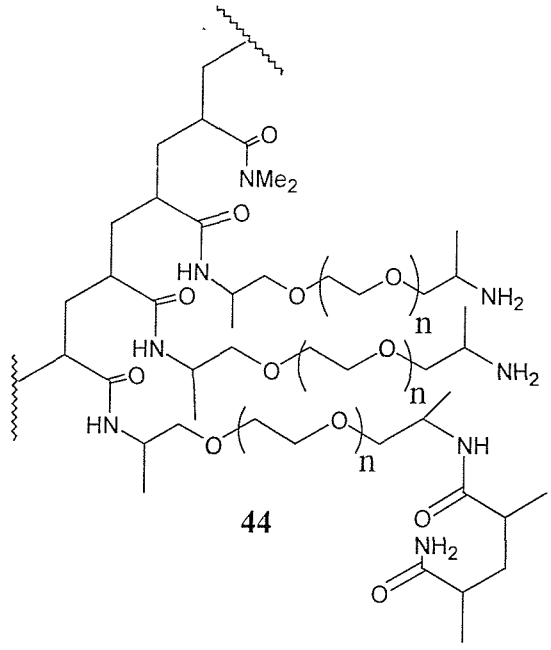

44

Figure 1.19 Structure of PEGA resin

1.5.2 Linkers

A linker joins the compound to the resin bead and is an essential part of solid phase synthesis, as the linker will determine both the methods used for cleavage from the solid

support and the terminal functionality of the compound. Thus, the linker is placed between the growing compound and the supporting resin. In many cases libraries are screened after cleavage from solid support. Thus, the synthesis of combinatorial libraries requires immobilisation of the first building block to the resin bead *via* the linker and cleavage of the compound once the library synthesis is complete. Therefore, the linker has to have certain properties. (i) The linker has to be stable to all chemical reactions performed during the library synthesis. (ii) The products must be readily cleaved from the resin beads (ideally quantitatively). (iii) The cleavage conditions should not degrade the library compounds. (iv) The cleavage condition should be user friendly and preferably provide the released compounds ready for screening. Two strategies have been applied to provide the first building block attached to the resin *via* a suitable linker. Typically the linker-resin construct can be derivatised with building blocks. Alternatively, the first building block plus linker is synthesised in solution and then attached to functionalised resin.[47] A number of different linkers have been used to attach synthesised compounds to the insoluble support. The structures of the most commonly used linker-resin constructs (**45-50**) are summarised in Figure 1.20.

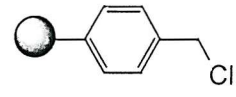

45 Merifield resin

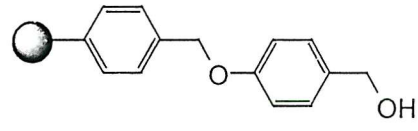

46 PS-Wang linker

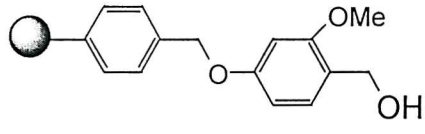

47 PS-Sasrin linker

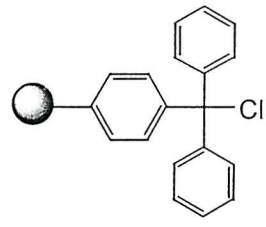

48 Trityl chloride linker

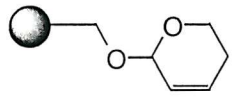

49 Tetrahydropyranyl Linker

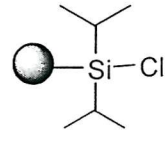

50 Silyl Linker

Figure 1.20 Commonly used linkers for solid phase chemistry

Merrifield resin usually comprises of approximately 1% cross-linked polystyrene that has been functionalised by chloromethylation, thus providing a handle for anchoring carboxylic acids during peptide synthesis. After synthesis, the peptide is detached by exposure to hydrogen fluoride. However, this cleavage method is not suitable for sensitive organic molecules. This linker has been replaced by other linkers which are more labile towards milder acidic conditions. S. S. Wang made the first major advance in 1973, [48] using a 4-phenoxybenzylalcohol linker. The significant difference between the Merrifield linkage and the Wang linker is in the cleavage step. The mesomeric effect of the oxygen atom at the *para* position of benzene ring results in an increase in electron density at the carbonyl group of the acid, allowing this to be cleaved with 50 percent TFA in dichloromethane rather than HF. This theme of modulating the electron density of the phenyl ring was later extended by Monika Mergler in 1988 to provide a super acid labile Sasrin linker.[49] In this case, an additional *ortho* methoxy substituent in the phenyl ring further increased the electron density such that cleavage can be effected with just 1 percent TFA. The evolution of linker technology has meant that the chemist can now perform a wider variety of chemistries on solid supports. The most common linkers like the Wang and Rink linkers[50] provide molecules with specific functional groups such as carboxylic acids or carboxamides after cleavage. This does not cause a problem if the target molecule requires this functionality, but sometimes the group is not desirable. This problem was overcome using silicon based linkers, sometimes known as traceless linkers.[51] The silyl linkers can be cleaved with TFA or fluoride ions and only leave a H-C bond behind in the target molecule.

Crucial to the success of any solid phase synthesis is the careful choice of a linker for attaching the organic molecule to the polymeric support. Linker design is a challenging area of research and modifications of these special protecting groups have greatly extended the combinatorial chemists arsenal. Like a protecting group in synthesis, the linker must survive the conditions of the synthesis, and the compound must be readily cleaved from the linker without destroying the synthesised molecule once the reaction is complete. Monitoring the progress of reactions on solid supports presents new challenges for chemists who are more usually reliant on thin layer chromatography for following reactions in solution. One option is to cleave quantities of resin at various stages during

the reaction and use standard methods to assess the amounts of intermediate and/or products formed.

1.5.3 Solid phase synthesis of polyamine conjugates

The first example of applying a solid phase synthesis technique to the synthesis of polyamine conjugates was the natural product spider toxin nephilatoxins (NPTX) reported by Bycroft *et al.* (Figure 1.21).[52]

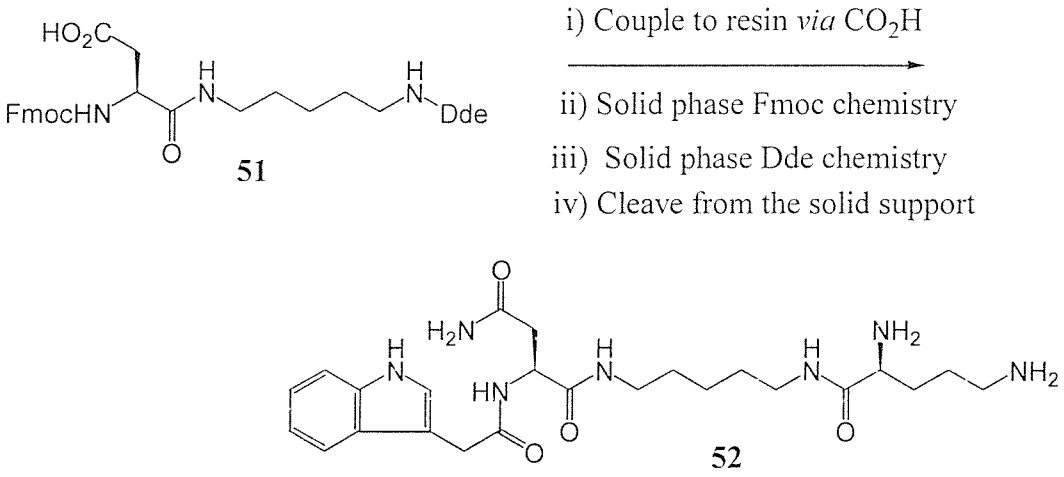

Figure 1.21 Solid phase synthesis of spider toxins nephilatoxins (NPTX)

Cadaverine derivative (**51**) was anchored on a Fmoc-Untrasyn C or Fmoc-PAL-PS/PEG amide resin and the amino protecting groups were then selectively removed to allow for the stepwise assembly of NPTX from both ends.

Later 2-chlorotrityl spermine resin (**53**) was used to synthesise potent philanthotoxin analogues PhTX-343.[53]

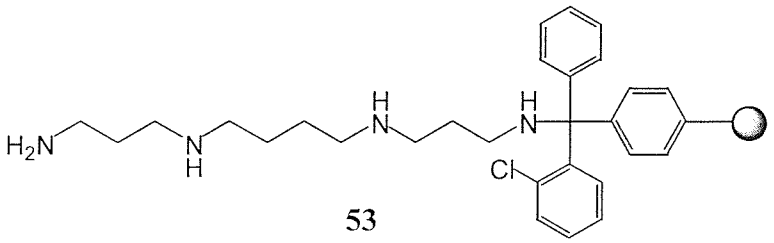

Figure 1.22 2-chlorotrityl spermine resin

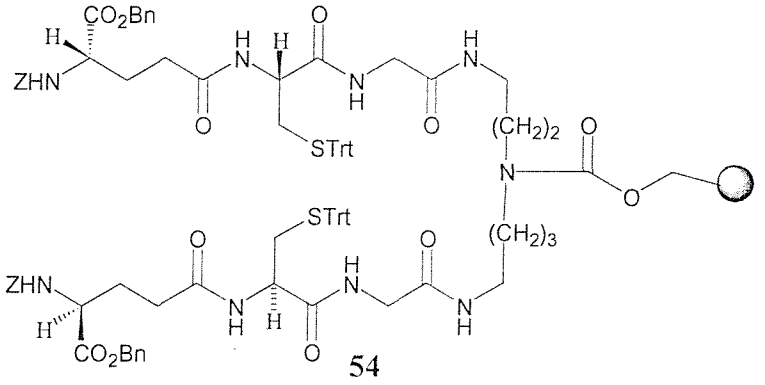

54

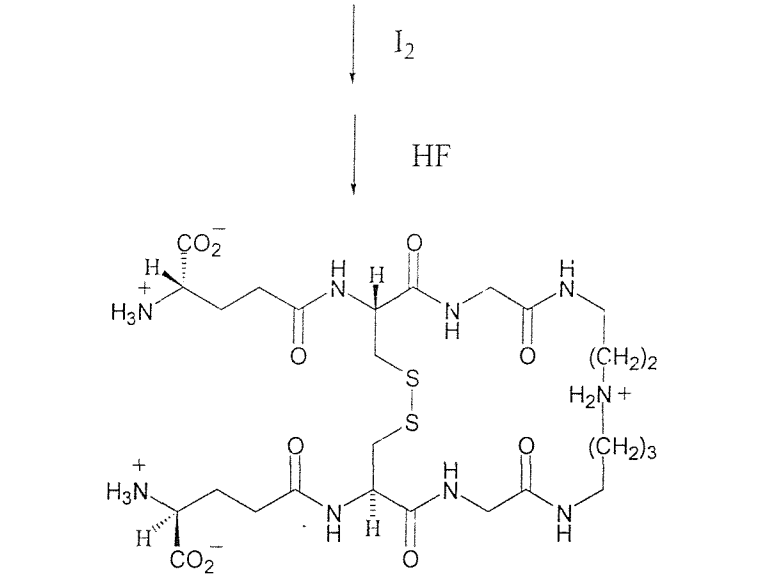

55 Trypanothione $T(SH)_2$

Figure 1.23 The first solid phase synthesis of trypanothione $T(S)_2$

The first solid phase synthesis of trypanothione $T(S)_2$ was reported by Sergheraert *et al.*, who used the novel derivative N^1,N^8-$TBDPS_2$-spermidine functionalised on Merrifield resin (Figure 1.23).[54] The fully protected $T(SH)_2$ (**54**) was assembled. However, simultaneous deprotection and cleavage from the resin to obtain $T(SH)_2$ (**55**) required the use of strong acid (HF), a destructive and inconvenient acid to handle.

Byk *et al.* recently exploited the extremely mild acidic conditions, trifluoroethanol (TFE), to detach from the 2-chlorotrityl linker a carboxyl functionality, in a series of linear transfection agents (Figure 1.24).[55]

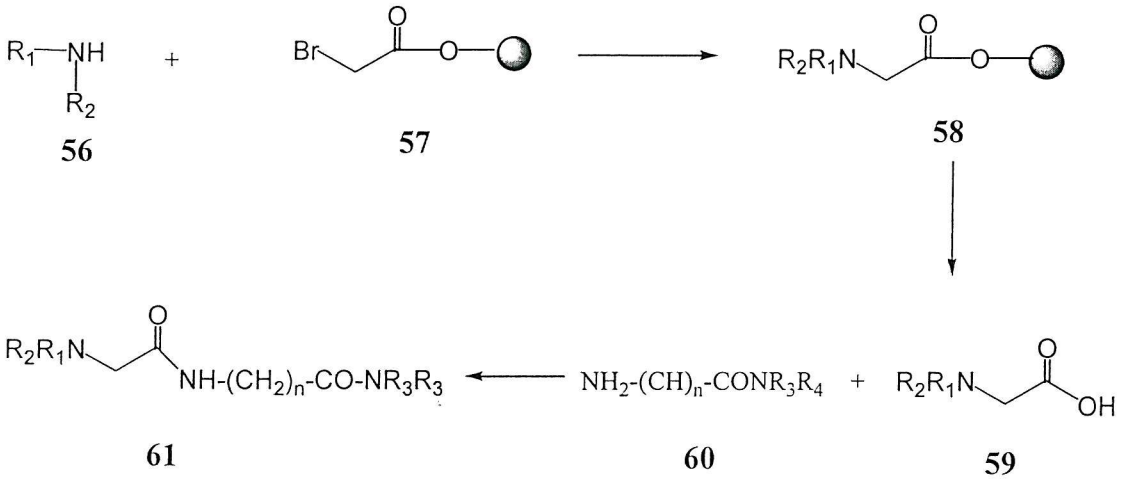

Figure 1.24 Solid phase synthesis of lipopolyamines

This methodology was successfully applied to the synthesis of novel lipo-polyamines as non-viral vectors for gene delivery. The geometrical diversity of mono-functionalised polyamines obtained using this method allowed extensive structure-activity relationship studies within the geometrically differing lipo-polyamines and lead to the identification of potent candidates for gene therapy studies such as RPR-120535 (**62**) (Figure 1.25).

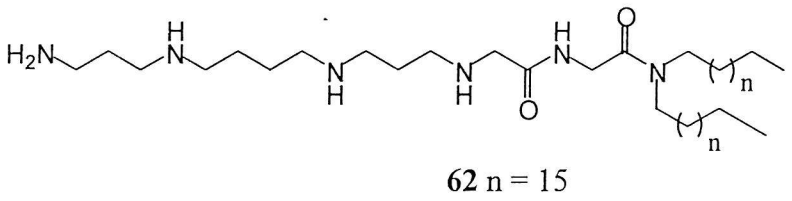

62 n = 15

Figure 1.25 The potent transfection agent RPR-120535

The synthesis of lipopolyamino-guanidines for gene delivery was also described by the same group.[56] In this method, a secondary generation library was generated using the concept of libraries from libraries. The primary amines in the first generation were transformed to guanidines using solid phase synthesis (Figure 1.26). This one-pot method allowed the easy and quick access to mono-functionalised guanidine (**63**), bis-guanidine (**64**) and tris-guanidines (**65**).

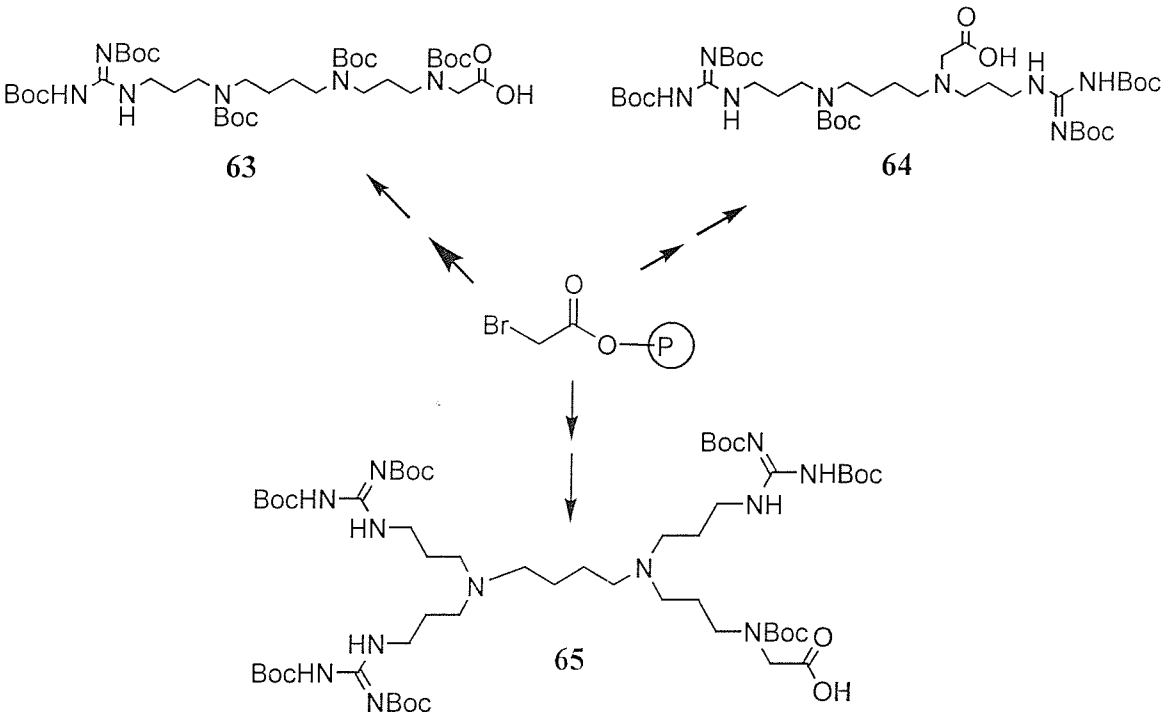

Figure 1.26 Synthesis of guanidine functionalised polyamines by a solid phase strategy

The building blocks mentioned above were subsequently introduced into cationic lipids to obtain products (**66-68**) (Figure 1.27).

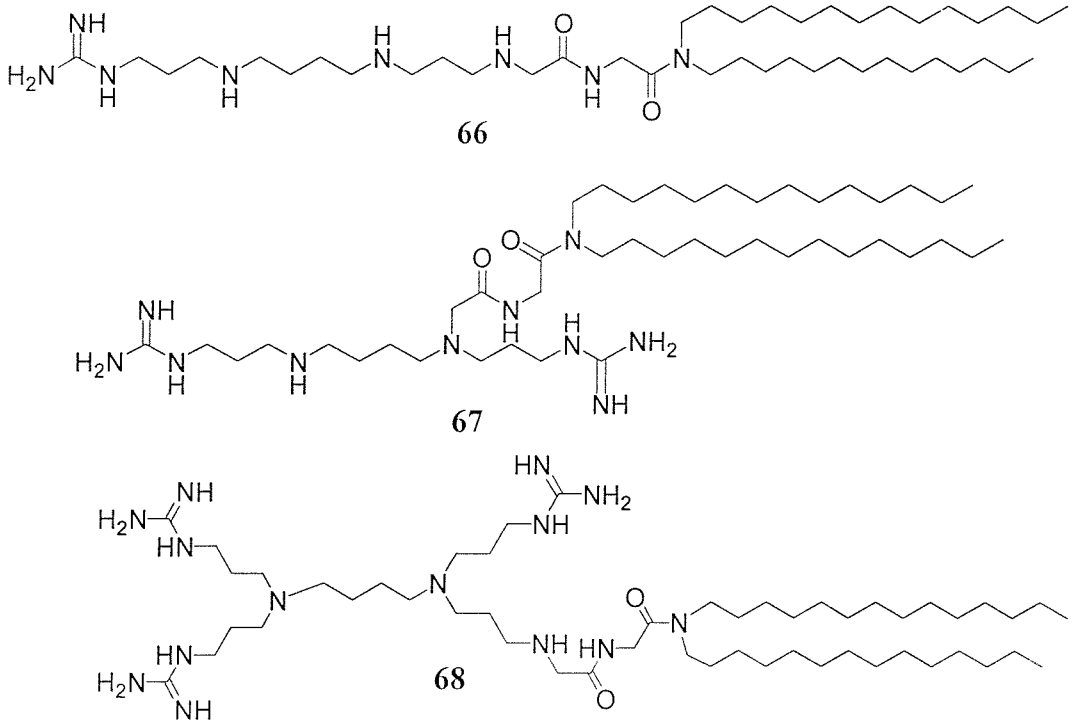

Figure 1.27 Some poly-(guanidinium) amines

This approach implies a significant extension of solid-phase organic synthesis to polyamines and to the synthesis of poly-(guanidium)-amines.

Chapter 2:

Solid phase synthesis of polyamine conjugates in the search for new inhibitors of trypanothione reductase

2.1 Parasitic diseases

The *Kinetoplastida* family of protozoa contain several pathogenic members, two of which are the trypanosomes and leishmanias. These parasites are the causative agents of many tropical diseases of humans and domestic animals in developing countries such as Africa and South America. The parasitic trypanosomes are the causative agents of diseases such as African sleeping sickness and Chagas' disease. African sleeping sickness is caused by *Trypanosomia brucei* and transmitted to humans through the bite of the tsetse fly (genus *Glossina spp*). The disease derives its name from the neurological disorders that result during the second stage of the disease, where the parasite invades and begins to destroy the central nervous system after an initial infection of the bloodstream. This disease is found over vast areas of tropical Africa and exists in two main forms which are caused by two different parasites. *Trypanosoma brucei gambiense* causes a chronic infection lasting years and affects countries of western and central Africa. Whereas *Trypanosoma brucei rhodesiense* causes acute illness lasting several weeks in countries of eastern and southern Africa. If untreated, the disease is inevitably fatal, due to invasion and destruction of the central nervous system.[57] Sumamin and pentamidine (both toxic) are used in the treatment of early stage of the disease, but the more toxic aromatic arsenicals or nitrofurazone are used when there is CNS involvement, as the former drugs do not cross the 'blood-brain barrier'. About 25-50,000 new cases of human sleeping sickness are estimated by the World Health Organisation to occur each year.

Chagas' disease is a parasitic infection caused by the protozoa *Trypanosoma cruzi* and it is endemic in South America. According to an estimate by the World Health Organisation more than 20 million people from lower socio-economic groups are infected with *T. cruzi.*[58] In the USA about 100,000 people are infected, probably due to transfusion of blood and blood products originating from South America. Blood-sucking bugs are responsible for transmission of the disease. It multiplies in the insect gut as an

epimastigote form and is spread as a nondividing metacycle trypomastigote by the insect faeces by contamination of mucous or wounds produced by the blood-sucking activity of the vector. In the mammalian host, *T. cruzi* multiplies intracellularly in the amastigote form and is subsequently released into the blood steam as a non-dividing trypomastigote.[58] The parasite targets are the muscle of the heart, the smooth muscle of the digestive tract and the autonomic nerve ganglia. In many patients the disease becomes chronic, leading to complete destruction of the heart. After years or decades, sudden death can occur due to disorders and rupture of the heart. It has been estimated that 55-60 million people are exposed to the risk of becoming infected with trypanosomes, however only four million of them are under surveillance.[59]

2.2 Chemotherapy against trypanosomaisis

The treatment of human African trypanosomes such as African sleeping sickness is still reliant upon drugs which originated from the early half of the century (Figure 1). Pentamidine (**69**) and suramin (**70**) are recommended for the early haemolymphatic stages of the disease and melarsoprol (**71**) for later CNS stages of the infection. Melarsoprol requires parental administration and is toxic, causing reactive encephalopathy in up to 10% of patients treated with a mortality rate of up to 5%.[60] Alternative treatments include two other trypanosomal drugs, nifurtimox (**72**) and berenil (**73**). Recently a re-examination of the clinical pharmacokinetics of melarsoprol has led to a proposal for a dose regime that could reduce toxicity.[61] The only new drug to be developed for the treatment of human African trypanosomaisia has been eflornithine (**74**) (Ornidyl ®). This is a selective and irreversible inhibitor of ornithine decarboxylase, a key enzyme in polyamine biosynthesis in *Trypanosoma brucei.* This drug was first shown to have activity against CNS infection of *T. brucei* in rodents. Eflornithine has proven to be an effective treatment for late stage infection caused by *T. b. gambienese* in West and Central Africa. However, due to rapid excretion of the drug, the compound has to be given in very large quantities. A full treatment takes 400 grams of eflornithine over a total period of two weeks. This drug is also called the "resurrection" drug, since comatose patients treated with eflornithine may wake up rapidly and resume their activities. There are side effects in up to 40% of patients, and, most importantly, the drug is ineffective as a monotherapy against *T. b. gambienese.*[61] A combination of

eflornithine (**74**) and suramin (**70**) is on trial for the treatment of late stage *T. b. gambienese* sleeping sickness.[62]

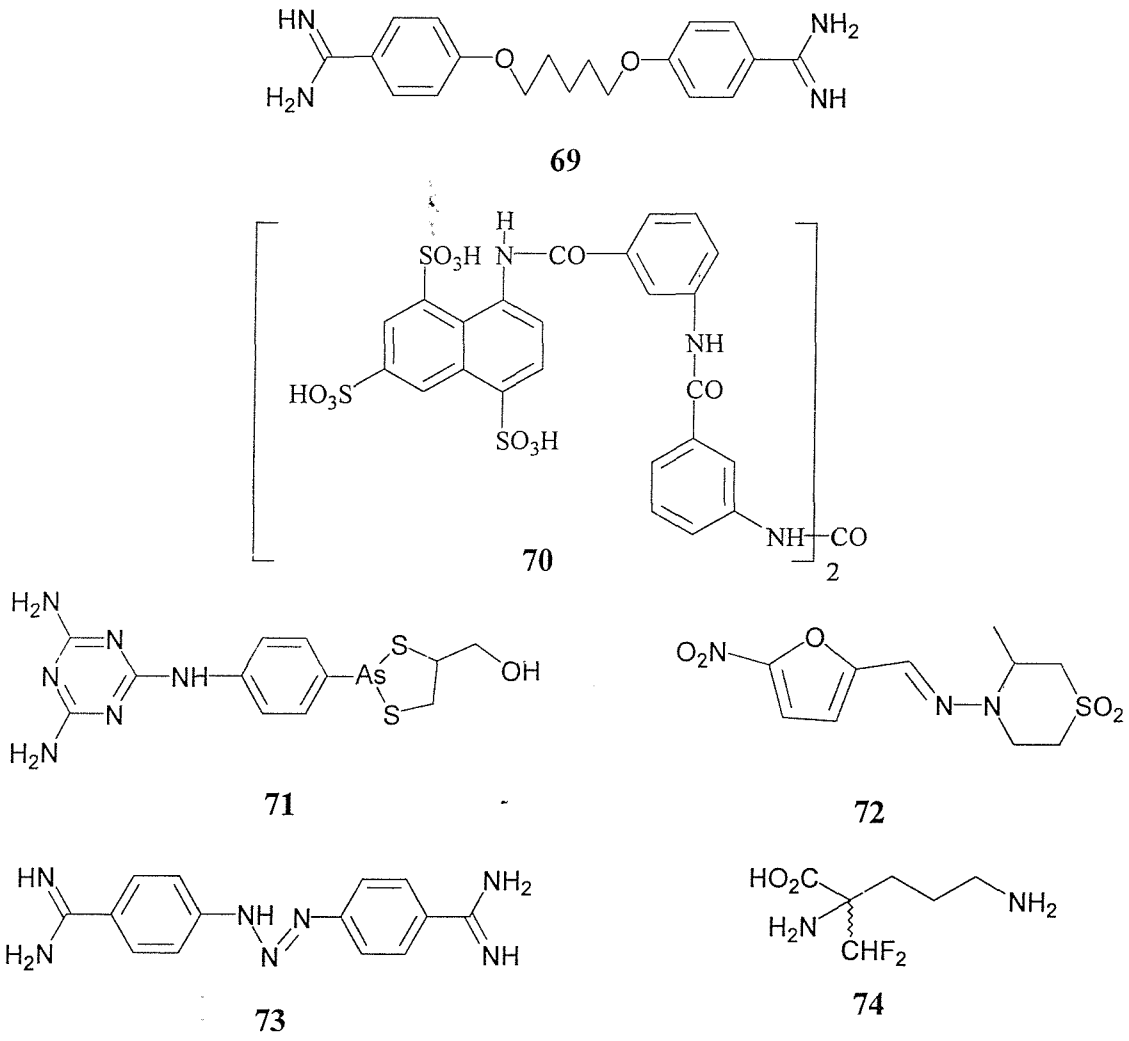

Figure 2.1 Some chemotherapies against trypanosomes

The situation for the treatment of South American trypanosomaisis (Chagas' disease) is no more promising. Current treatment is dependent upon two drugs, nifurtimox (**72**) and benznidazole (**75**). These drugs have been shown to cure at least 50% of recent infections as demonstrated by the disappearance of symptoms and negativization of parasitemia and serology.[63] However, results of treatment trials for acute infections have not been homogeneous in different countries, probably because of the different drug sensitivities of the distinct *T. cruzi* strains. Gentian violet (**76**) is the only drug available as a chemopropylactic agent to prevent blood transmission of Chagas' desease.[64]

However, this drug is carcinogenic in animals and safety concerns have been raised about its use.[65]

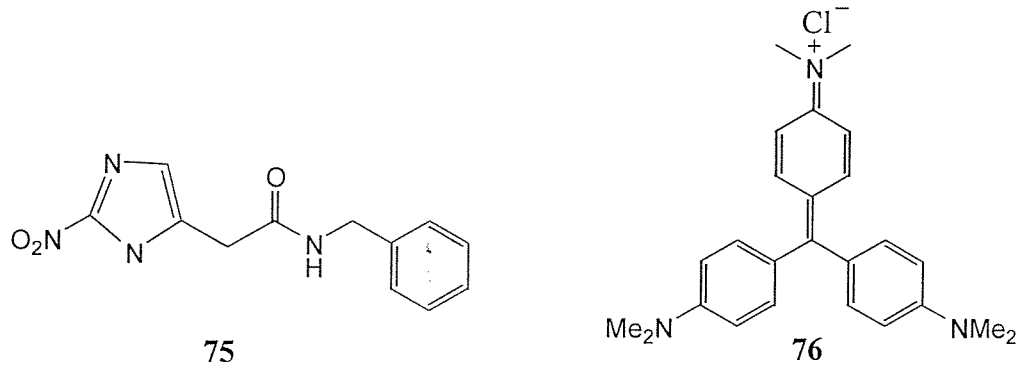

Figure 2.2 Current drugs for the treatment of Chagas' disease and blood sterilisation

2.3 The design of drugs for trypanosomiasis

The majority of anti-parasite drugs were developed for chemotherapy without knowledge of their mode of action. Even for some well known drugs, like pentamidine (**69**), the precise mechanisms of action are still not clear. In the past two decades, the strategy has been reversed[66] and the imperative has been to define metabolic differences between the parasite and host in order to design specific inhibitors. This rational approach to chemotherapy has not been fully exploited yet, but this chapter contains many examples of the characterisations of molecular, biochemical and physiological drug targets.[67]

Drugs design applies bio-molecular recognition mechanisms to the chemotherapeutic problem.[68] The first step is the determination of the three-dimensional structure of a protein or another macromolecule that plays an important role for the particular pathogen or disease process. Then inhibitors of this target molecule can be proposed using computer modeling.[69] These molecules are synthesised, tested for their chemotherapeutic activity and if promising, improved further. In order to deal with the need to develop novel compounds to combat parasitic diseases, a disulfide reductase, the antioxidative enzyme trypanothione reductase (TR), was chosen as a target for the design of antiparasitic drugs.

2.3.1 Oxidative stress as a chemotherapeutic strategy

Humans consumes 800 litres of oxygen per day, 5% of which is converted by side reactions into reactive oxygen species such as $O^{\cdot}_2^-$, $HO^{\cdot}$, $ONOO^-$, $HO^{\cdot}$ and H_2O_2.[70] These

compounds are cytotoxic because of their ability to modify nucleic acids, thiol-containing proteins and membrane lipids. There are numerous pathways for the detoxication of reactive oxygen species; when these antioxidative systems are challenged, the cells are regarded as being under "oxidative stress".

Most living organisms contain high levels of a low-molecular weight compound known as glutathione. Glutathione is a thiol containing metabolite which has numerous roles including heavy metal sequestering, protein folding and the maintaince of a reducing environment within cells. In order to maintain its active free thiol state, oxidised glutathione (GSSG) requires an NADPH dependent enzyme called glutathione reductase (GR) Figure 2.3.

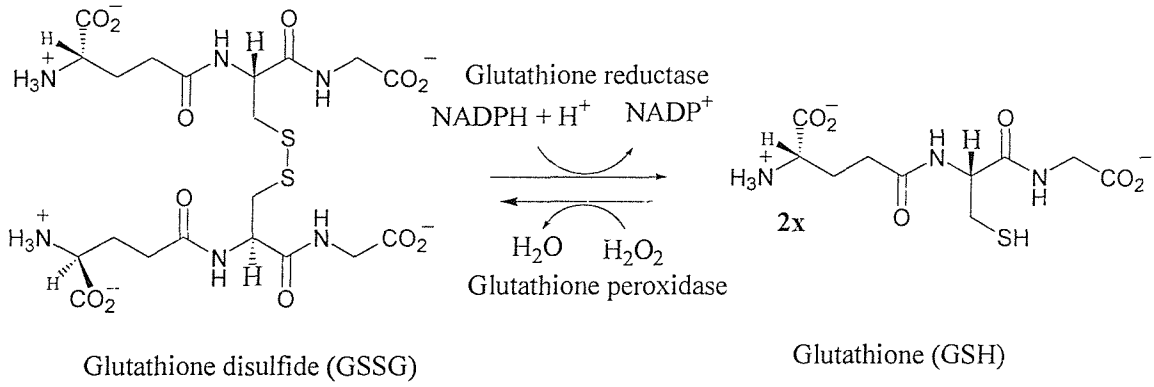

Figure 2.3 Reaction catalysed by human glutathione reductase

The main defence system against reactive oxygen species is the glutathione redox cycle, which involves the enzyme (GR) and glutathione peroxidase (Figure 2.3). The flavoenzyme gluthathione reductase catalyses the NADPH-dependent reduction of glutathione disulfide (GSSG, oxidised glutathione) to glutathione (GSH). Thus, GR is the link between the pyrimidine nucleotide redox system and the thiol disulfide redox system in the cell.[71]

Clinical and epidemiological observations have provided further evidence that oxidative stress is an important mechanism for the destruction of parasites and tumour cells.[70] The best known example is glucose-6-phosphate dehydrogenase deficiency (G6PDH$^-$). This functional defect limits availability of NADPH. In erythrocytes (red blood cells) this leads to an impairment of the glutathione redox system (see Figure 2.3) with a consequent marked increase in oxidative stress due to the reactive oxygen species. The

additional oxidative load due to the parasite probably explains the premature liberation of immature nonviable parasites in this population set.

Many intracellular parasites lack important oxygen-detoxifying enzymes such as superoxide dismutase and catalase which confer protection against oxidative stress,[72] Therefore, the glutathione-based antioxidant capabilities are often very important for survival.[73] However, protozoa parasites such as trypanosomes and leishmanias are protected against oxidative damage by a glutathione-like system involving trypanothione ($T(SH)_2$ c.f. to GSH) which is synthesised from glutathione and spermidine. These compounds are maintained in the reduced state by the NADPH dependent enzyme trypanothione reductase Figure 2.4.[74]

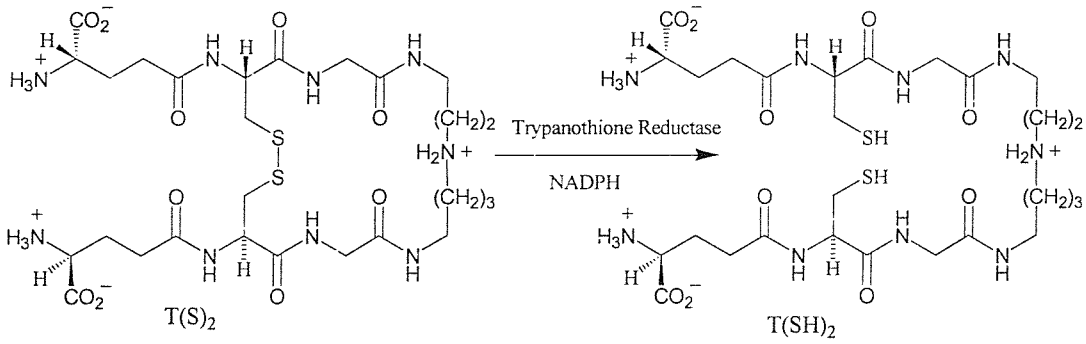

Figure 2.4 Reaction catalysed by parasite trypanothione reductase

2.3.2 The three-dimensional structures of glutathione and trypanothione reductases

Human glutathione reductase (GR) is one of the most thoroughly studied of enzymes. The amino acid sequence[75] and the three-dimensional structures at 1.5 Å resolution are known.[76] The binding of substrate,[77] substrate analogues, and inhibitors,[78] as well as the stereochemistry of catalysis have been studied in great detail.[79] The gene for human glutathione reductase has been cloned and sequenced with the result that more detailed structure-mechanism analysis of the enzyme has become possible by site-directed mutagenesis.[80] GR is a homodimer consisting of two subunits with a M_r of 52 kDa. Amino acids of both protein sub-units are involved in both catalytic sites. As shown in Scheme 2.1,[77, 79] NADPH binds to a pocket that is in close proximity to the prosthetic FAD isoalloxazine ring (2). Hydride ions are transferred from the *re* side of FAD through to the *si* side where the second substrate pocket is situated for glutathione binding. This is also the site of the redox active cysteine residues (Cys58-Cys63) which exists as a

linked disulfide in the oxidised enzyme (E_{ox}). This sulfur-sulfur bond is reduced by $FADH_2$, releasing a nucleophilic thiolate. Upon oxidised glutathione binding, this free thiolate performs a displacement reaction freeing one molecule of glutathione and forming an enzyme-substrate covalent bond (3). The released glutathione removes a proton from nearby His467. The second molecule of glutathione is liberated upon reformation of the Cys58-Cys63 disulfide bond (4).

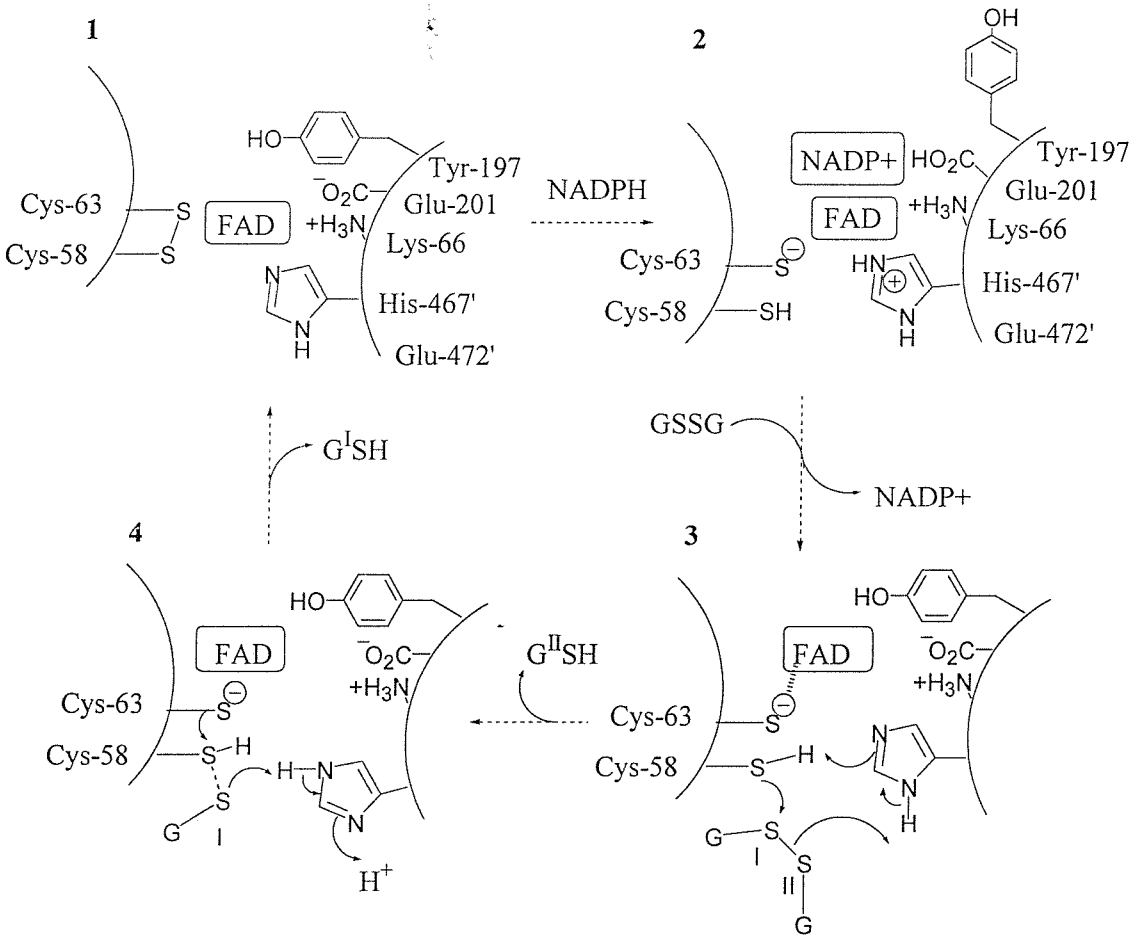

Scheme 2.1 Catalytic cycle of glutathione reductase

The three-dimensional structures of trypanothione reductase (TR) from *Crithidia fasciculata*[81] and *Trypanosoma cruzi*[82] have recently been elucidated. TR is an FAD- and NADPH-dependent disulfide reductase and hence shares many physical and chemical properties with GR, the closely related host enzyme. The most important difference between two enzymes is the mutually exclusive specificity for the disulfide substrate. GR is specific for glutathione, while TR reduces only the glutathionylspermidine conjugate (trypanothione, TSST) with a K_m of 45 μM.[72] The

active site of TR with the redox-active disulfide/dithiol and the flavin ring is very similar to that of GR (Figure 2.5).

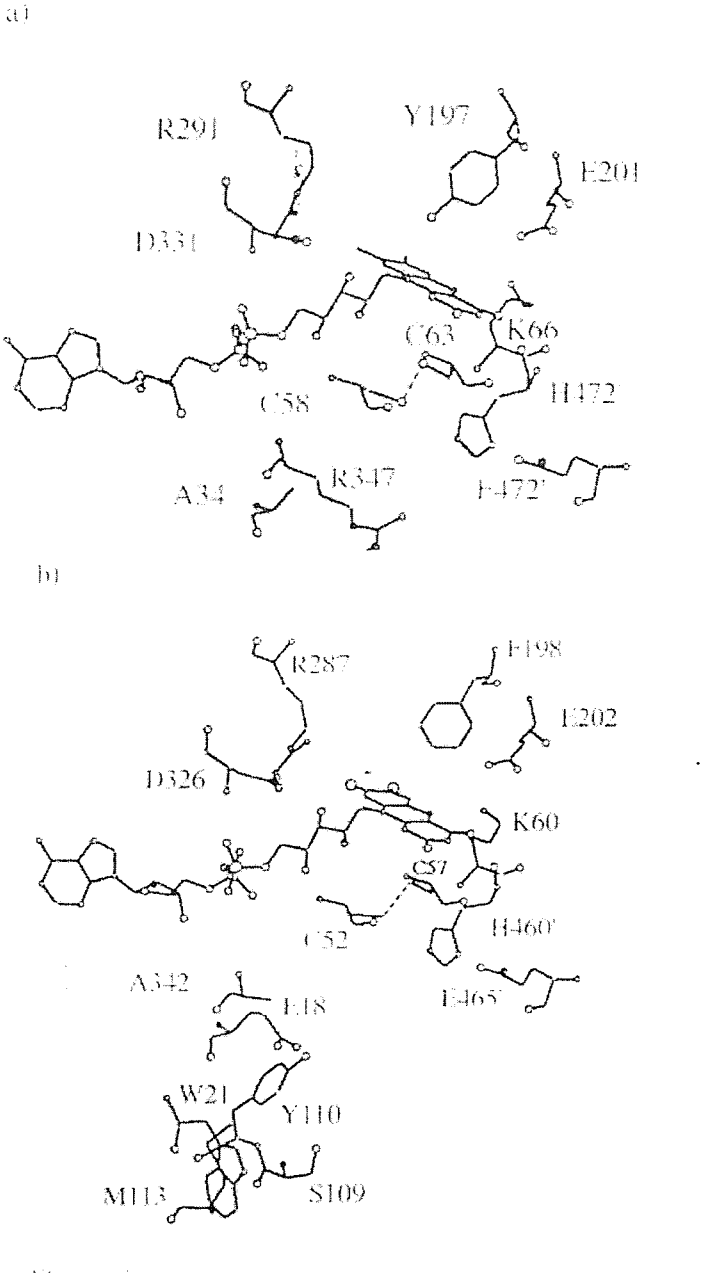

Figure 2.5 View into active site of a) human GR[76] b) TR from *C. fasciculata*[81]

The isoalloxazine of FAD forms the centre of the active site. The redox-active disulfide bridge of the protein is represented by a broken line (C 58-C 63 and C 52-C 57). Of the

19 residues which in GR participate in the binding of glutathione substrate (GSSG), only five are not conserved in TR (Figure 2.5). Thus TR from *Trypanosoma cruzi* and human GR contain different amino acids such as Glu 18 (corresponding to Ala 34 in GR), Tyr 21 (Arg 37), Ser 109 (Ile 113), Met 113 (Asn 117) and Ala 342 (Arg 347) (the numbering is different for the two enzymes because of amino acid insertions and/or deletions along the polypeptide chains). Most significant and remarkable is that two arginine residues at the active site of GR are replaced by neutral residues in TR, while there is also an additional negatively charged residue in TR (Glu 18). This exchange reflects the different charges on the substrates. Whereas GSSG has an overall charge state of –2 (the two carboxylate groups of the glycine residues), the TR substrate TS_2 (see Figure 2.4) has an overall charge of +1 in the corresponding region. Site-directed mutagensis of TR and GR have confirmed the importance of certain amino acid residues, a few changes are sufficient to convert a TR into GR and vice versa.

Overall GR has a much more closed, positively charged active site (to accommodate the glycine carboxylates), whereas the active site of TR is more open and has greater hydrophobic character. This hydrophobic character in turn allows the binding of the polyamine component of trypanothione, probably *via* aromatic π stacking interactions between the ammonium ion and the Trp residue, as well as more general hydrophobic interactions with the methylene bridges of the polyamine. Indeed this difference probably explains the selectivity of many existing inhibitors, but also suggests that the polyamine component is an ideal place to gain selectivity.

2.3.3 Tricyclic compound based TR inhibitors

The discovery of hydrophobic niches within the active site of TR has proven important for the design of potential TR binding compounds. A molecular modelling study of the active site of TR suggested that certain tricyclic compounds might bind selectively to TR without inhibiting host GR. This was confirmed by testing thirty known drugs including phenothiazine and some tricyclic antidepressants, the most potent of these compounds being clomipramine (**77**) with K_i value of 6 μM (Figure 2.6).[83]

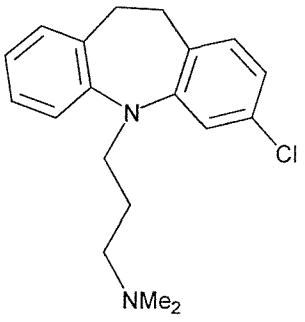

77

Figure 2.6 Tricyclic TR inhibitors

Another tricyclic compound with trypanocidal properties was the acridine derivative mepacrine (**78**) which had a K_i of 15 μM and was a competitive inhibitor of TR, but not of GR.[84] The examples of clomipramine (**77**) and mepacrine (**78**) show that a rigid ring system fits into the enzyme pocket.[85]

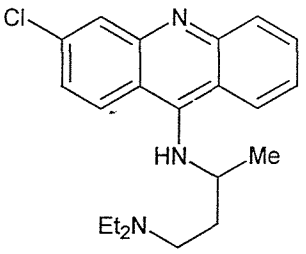

78

Figure 2.7 Mepacrine an acridine containing tricyclic TR inhibitor

Tricyclic compounds containing the saturated dibenzazepine (imipramine) nucleus have been found to inhibit with K_i values in the low micromolar range (Figure 2.8).[86] The lead structure was designed by molecular graphics analysis using a three-dimentional homology model, concentrating on the active site region. Hansch QSAR analysis showed inhibitory strength to depend on terms in π, π^2 and σ_m indicating dependence on both lipophilicity and inductive effects for ring-substituted analogues of imipramine.

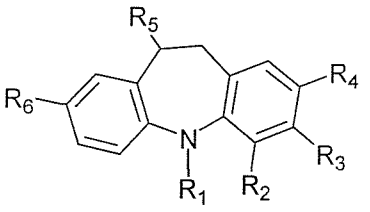

79

Figure 2.8 Structure of dibenzazepenes based on imipramine

The side ω-aminoalkyl chain should be longer than 2-carbon units for inhibition. The effect of substitution at the ω-amino position of the side-chain of the central ring nitrogen depends very much on the detailed substitution pattern of the rest of the molecule. This provides kinetic evidence for multiple binding modes within a single, blanket binding site for the inhibitor with the tricyclic ring system in the general region of the hydrophobic pocket lined by Trp21, Tyr110, Met113 and Phe114. Quaternary alkylammonium phenothiazines are a new class of TR inhibitor. These compounds were designed based on the use of an additional hydrophobic binding site. A major contribution to improving K_i values and inhibitor strength was the hydrophobic nature and structures of the *N*-benzyl substituents (Figure 2.9).[87]

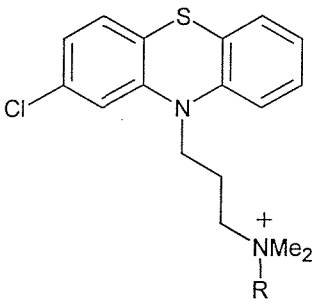

80

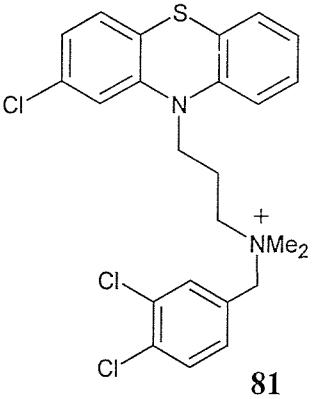

81

Figure 2.9 Structures of quaternary alkylammonium phenothiazines

The strongest inhibitor, the [3-(2-chloro-4a,10a-dihydro-phenothiazin-10-yl)-propyl]-(3,4-dichlorobenzyl)-dimethylammonium derivative (**81**), (K_i 0.12 μM), was ~ 2 orders of magnitude more inhibitory than the parent chloropromazine. Several of these quaternary phenothiazines completely inhibited *T. brucei* parasite growth *in vitro* at < 1

μM. Anti-parasite activity was not solely determined by inhibition strength against trypanothione reductase, there being a strong contribution from hydrophobicity (for example, benzhydryl-quaternized chlorpromazime had ED_{50} < 1 μM). Although active against *Leishmania donovani*, none of the analogues showed major improvement in this activity relative to chloropromazine or other non-quarternized phenothiazines. The *p-tert*-butylbenzyl-quaternized analogues very strongly inhibited (ED_{50} < 1 μM) growth of the amastigote stage of *T. cruzi*.

2.3.4 Peptide based TR inhibitors

A peptide based TR inhibitor with the aim of occluding both hydrophobic niches and the acidic glutamate region was designed by Douglas *et. al.* (see Figure 2.10).[88] Molecular modelling showed that the napthyl region contacted the W21, M113 hydrophobic wall, the *N*-terminal arginine linked to D105 whilst the other arginine residue formed a salt bridge with E466' and E467' as predicted. The leucine residue fitted the L399, P462 and V58 surface and the *N*-terminal blocking benzoyl group interacted with F-396' of the enzyme. The binding conferred high specificity of this compound for TR over GR, inhibiting TR competitively with a K_i of 13.8 μM. However, the strongest peptide inhibitor to date was found to be *N*-benzyloxycarbonyl-Ala-Arg-Arg-4-methoxy-β-naphthylamide (**83**) with a K_i value of 2.4 μM.

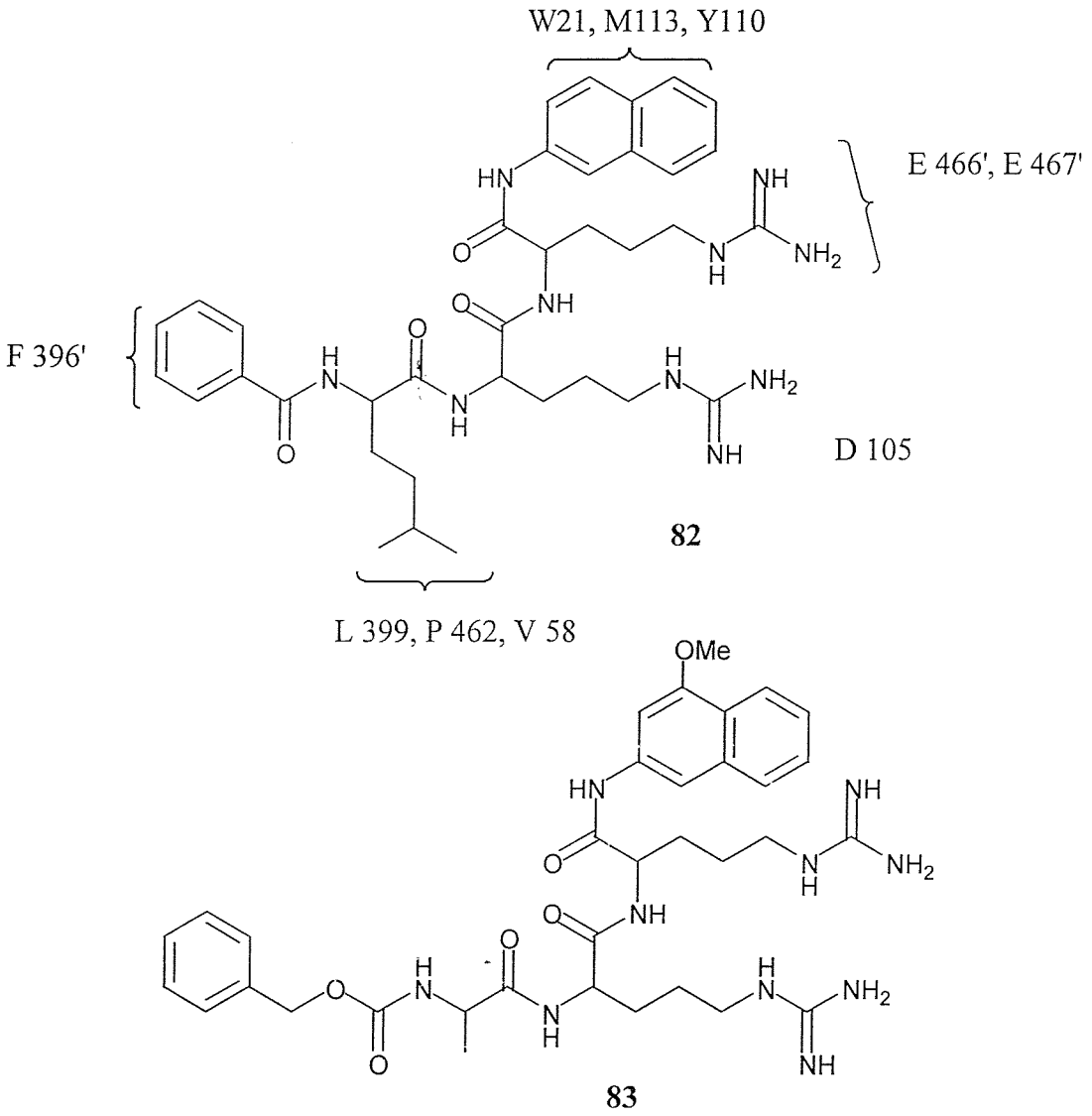

Figure 2.10 Peptide based TR inhibitors (all amino acids have the L-configuration).

2.3.5 Polyamine based inhibitors

Antiparasitic activity has been observed for several polyamine based compounds. For example, *N*, *N'-bis*(benzyl)-substituted polyamine analogues such as MDL 27695 (**84**) and MDL27699 (**85**) were found to be the most active showing inhibition of *T cruzi* infection (Figure 2.11).[89]

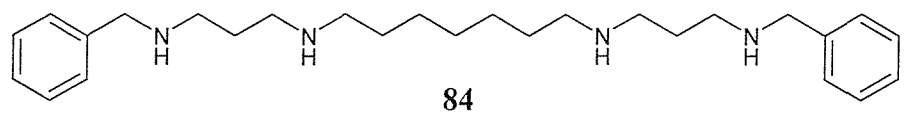

84

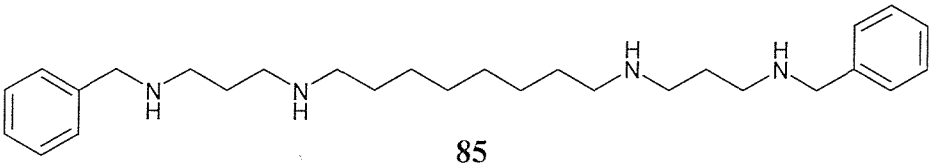

85

Figure 2.11 Anti-trypanosomal polyamine conjugates

Recently, polyamine derivatives of spermidine and spermine were reported as potent and selective TR inhibitors. In one series, synthesis was based on a convenient procedure for the selective trifluoroacetylation of the primary amino groups of the polyamines.[90] The most potent inhibitor (K_i = 3.5 μM) was obtained by substituting the secondary amino groups of spermine with 3-phenylpropyl moieties (see Figure 2.12).

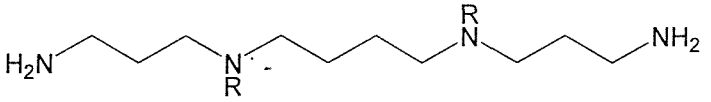

86 R = $CH_2CH_2CH_2Ph$ (K_i = 3.5 μM)

87 R = CH_2-Naphthyl (K_i = 5.5 μM)

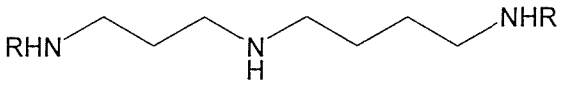

88 R = CH_2-Naphthyl (K_i = 9.5 μM)

Figure 2.12 Structures of potent TR inhibitors based on spermine and spermidine conjugates

Polyamine derivatives containing 2-amino diphenylsulfide (**89**) and phenothiazine (**90**) have been prepared and tested for their inhibiting effects on TR using a high-throughput assay.[91] The most active were compounds (**91**) and (**92**) (Figure 2.13).

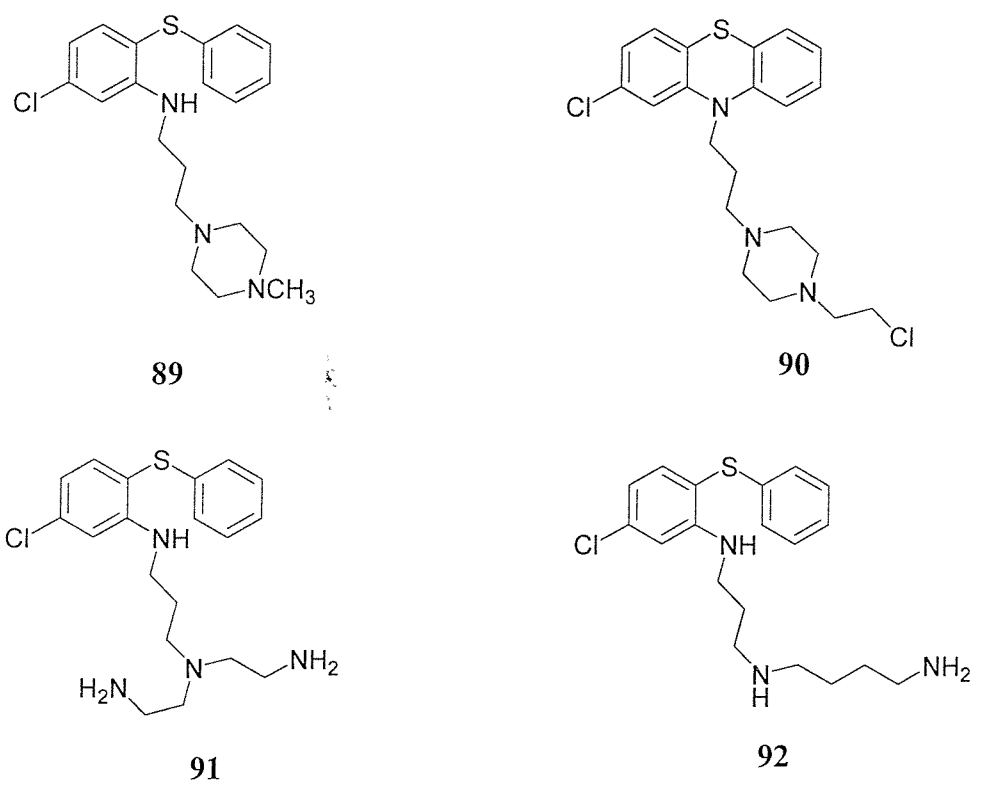

Figure 2.13 Structure of some TR inhibitors

The introduction of spermine and spermidine moieties in the side chain of compound (**89**) led to potent inhibitors of *Trypanosoma cruzi* trypanothione reductase. IC_{50} values were assessed between 0.3 and 3 μM.[92] Compound (**93**) was the most potent TR inhibitor (K_i = 1.8 μM) (Figure 2.14).

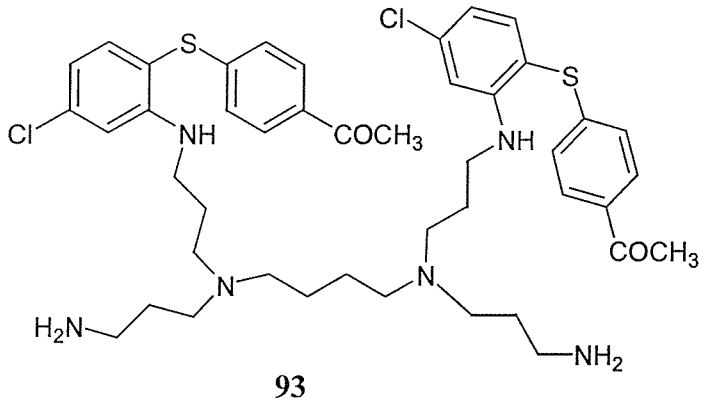

Figure 2.14 Structures of TR inhibitors

Another promising polyamine was the natural product kukoamine A (**18**) which was first isolated from the root bark of *Lycium chinese* and has potent anti-hypotensive and anti-stress ulcer properties. The compound acts as a TR inhibitor with a K_i of 1.8 μM and is devoid of any effect upon glutathione reductase (see Figure 2.15).[24]

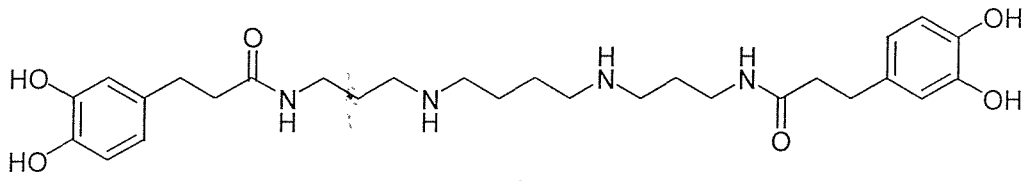

18

Figure 2.15 Kukoamine A

It can be seen that the crucial factor in determining the selectivity of trypanothione reductase inhibitors lies in the parasite enzymes' ability to discriminate the polyamine bridge found in its natural substrate. For this reason, polyamine chemistry is central to the production of potential anti-trypanosomal therapeutics.

2.4 Synthetic methods for the preparation of polyamine analogues and conjugates

Various synthetic methods have been used for synthesising polyamine analogues and conjugates. These methods all involve the selective functionalisation or protection of the amino functionalities of the polyamine.

2.4.1 Methods of direct selective functionalisation of primary amino groups

These methods involve the reaction of polyamines with reagents that selectively deliver protecting groups onto the primary amino functions. The reagents which have been used for this purpose include PhtN-CO_2Et,[93] Z-Cl,[94] Boc-ON,[95] Tfa-OEt,[96] Trt-Cl,[97] and Dde-OH.[98] These protecting groups are introduced onto the polyamines in high yield and can be removed under mild deprotection conditions including hydrazinolysis, acidolysis and catalytic hydrogenation. For example, the Pht and Dde protecting groups can be removed using hydrazinolysis while Z, Boc and Trt protecting groups are removed by

acidolysis. Useful intermediates prepared *via* this method are the polyamine derivatives (**94-98**) (Figure 2.16).

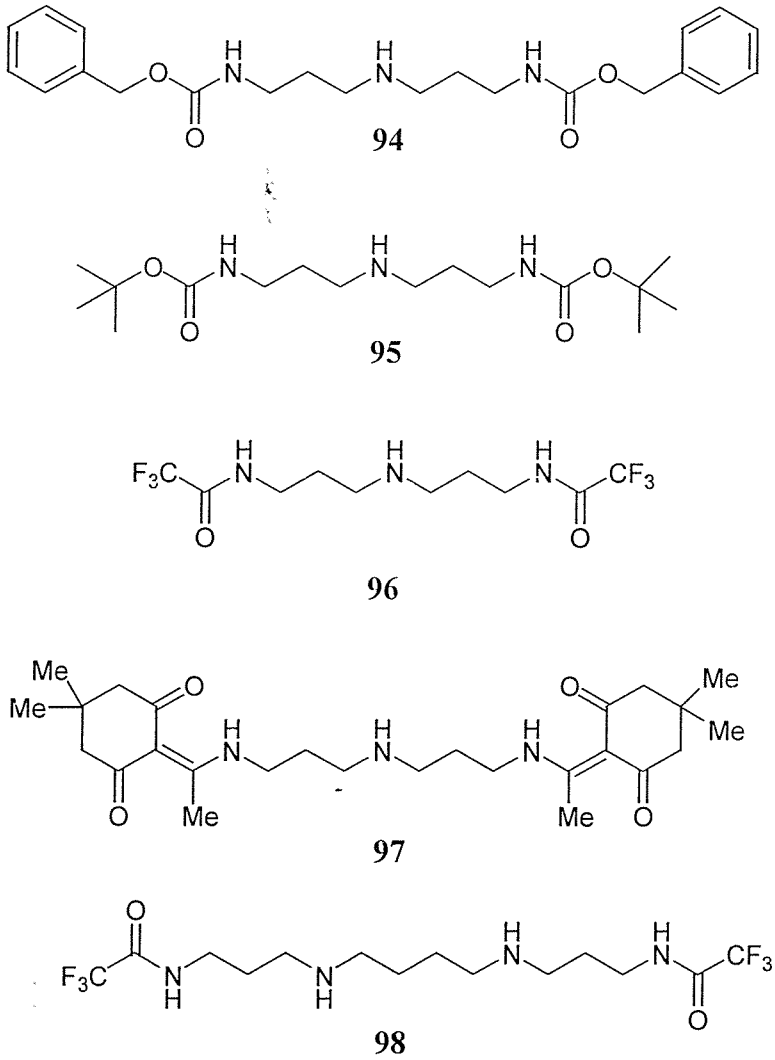

Figure 2.16 Synthetically useful primary amine functionalised polyamines

2.4.2 Methods of selective functionalisation of secondary amines

The methods previously described, which allow the selective protection/modification of the primary amino functions of polyamines, can give access to a variety of derivatives of polyamines functionalised at the secondary amino group. One such recent example can be found in the synthesis of the branched alkaloid tenuilobine (**17**) by Hesse *et al.*,[99] which involved the use of N^1,N^8-*bis-(Z)*-spermidine (**99**) and N^1, N^4, N^{12}*tris-(Z)*-spermine (**100**) (Figure 2.17) for the assembly of the alkaloid skeleton.

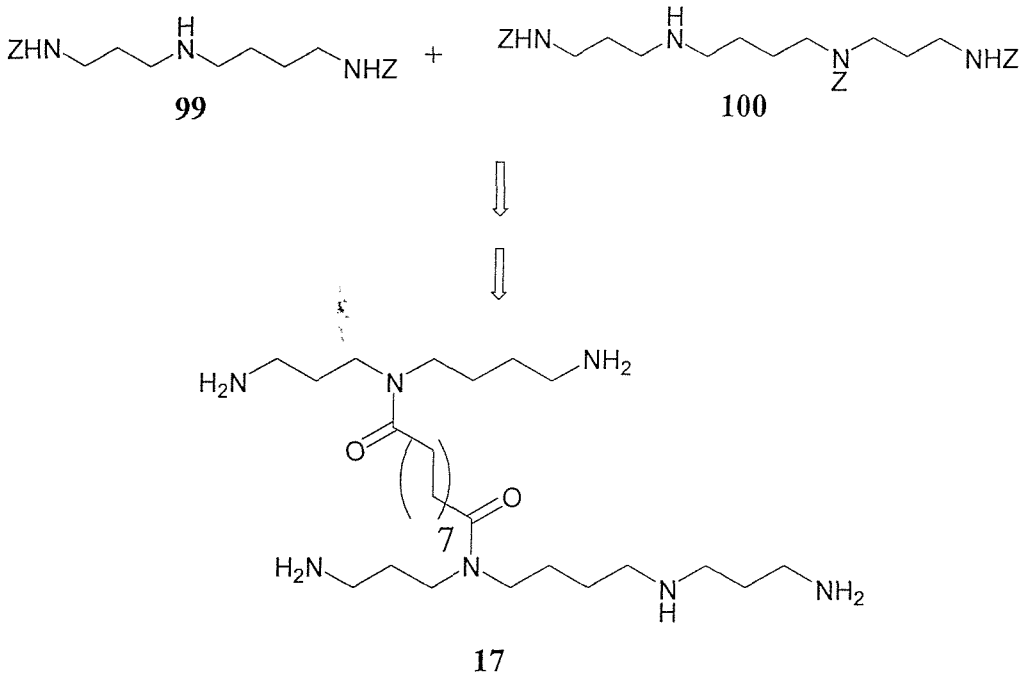

Figure 2.17 Synthesis of the branched alkaloid tenuilobine (**17**)

With few exceptions, protection of the secondary amino group of polyamines is usually effected though indirect methods. For example, in the synthesis of hirudomine (**103**) Golding *et. al.* used the trifluoroacetyl group for the temporary protection of the primary amino functions.[100] This allowed the preparation of the synthetic intermediate N^4-Acbz-spermidine (**102**) (Figure 2.18). The Acbz protecting group was removed *via* reduction with DTT in the presence of Et_3N.

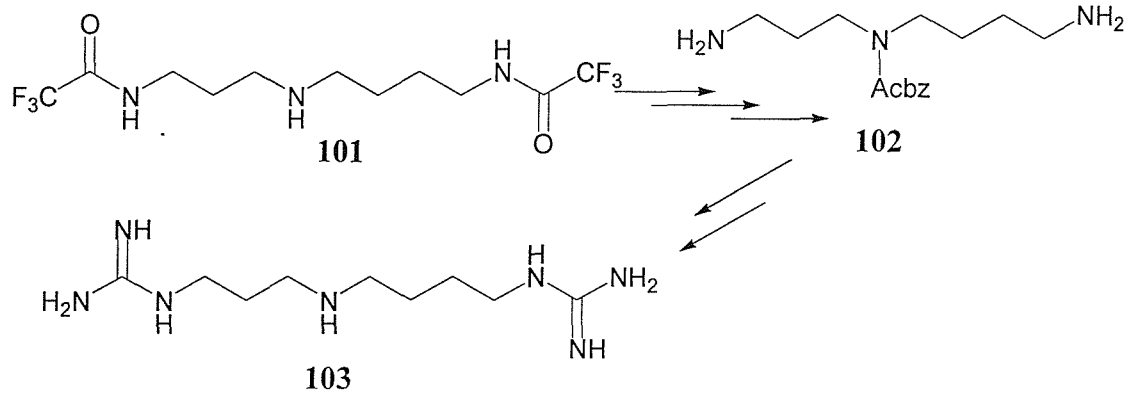

Figure 2.18 Synthesis of hirudomine (**103**) using the Acbz protecting group for secondary amines

2.5 Solid phase synthesis of polyamine conjugates

The synthesis of polyamine conjugates has been mostly concerned with solution phase chemistry. This process is tedious and time consuming due to the high polarity of these molecules. Therefore, solid-phase synthesis offers many advantages over solution phase reaction including increased yields and speed of synthesis, due to the ability to use excess reagents driving reactions to completion, the elimination of purification processes but most importantly the elimination of the handing issues with these highly polar materials. Using solid phase combinatorial chemistry and a defined polyamine template, it is possible to selectively target the unique parasitic enzyme trypanothione reductase over the human counterpart gluthathione reductase and to make large libraries of novel polyamine conjugates.[101] A number of efficient polyamine templates that incorporate a protected polyamine have been designed within our research group for the solid phase synthesis of trypanothione analogues are shown in Schemes 2.2 and 2.3.

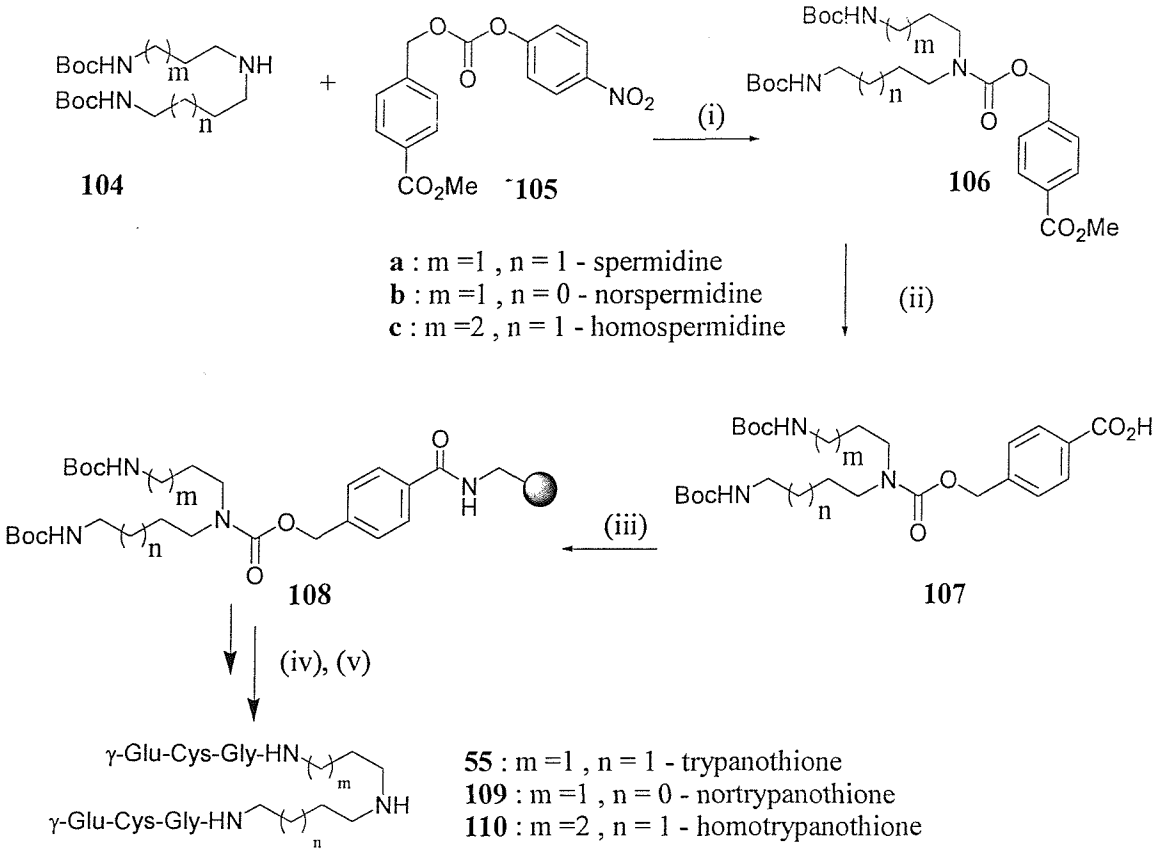

Scheme 2.2 (i) NEt_3, DMF 40°C, 96% (ii) aq. NaOH, dioxane, (iii) aminomethyl resin DIC, HOBt, DMF, (iv) solid phase Boc peptide synthesis, (v) HF or TFMSA

Linkage agents (**108 a,b,c**) were used to prepared the polyamine/glutathione conjugates trypanothione (**55**), nortrypanothione (**109**) and homotrypanothione (**110**) respectively.[102] In order to incorporate an orthogonally protected spermidine, the synthetic strategy was modified as shown in Scheme 2.3, the central goal being to prepare a range of linkage agents that incorporate protected polyamines, with the secondary amine of spermidine providing the ideal opportunity to act as the link to the solid support. The protecting groups on the primary amines Boc or Fmoc groups enabled the use of existing solid phase peptide synthesis protocols.

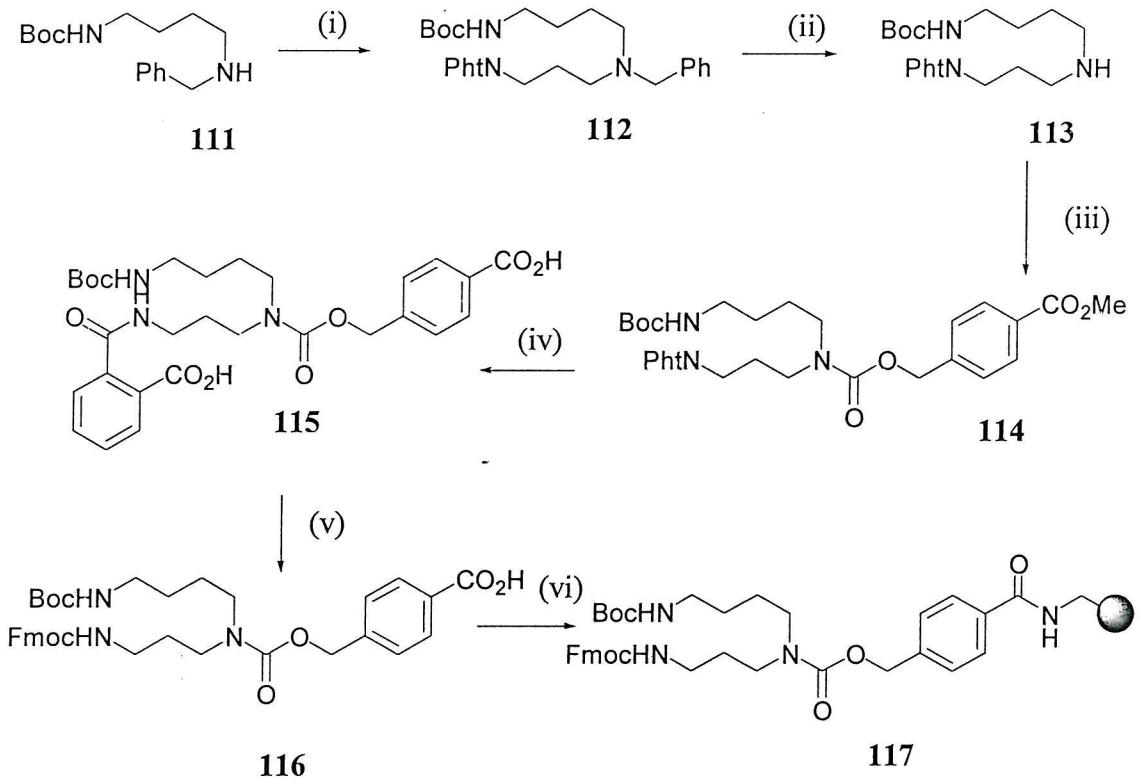

Scheme 2.3 (i) 3-bromopropylphthalimide, Na_2CO_3, KI, n-BuOH, 63% (ii) H_2, palladium/C, 83% (iii) methyl 4-[(4-nitrophenoxycarbonyloxy)methyl]benzoate (**105**), NEt_3, DMF 97% (iv) aq. NaOH, dioxane, 91% (v) $N_2H_4.H_2O$, EtOH; then Fmoc-succinimide, aq. $NaHCO_3$, dioxane, 75% (vi) aminomethyl resin, DIC, HOBt, DMAP, DMF.

The urethane linkers (**108**) and (**117**) are stable to TFA but cleavage can occur using stronger acid conditions such as TFMSA. These linkers are suitable for preparing libraries for screening on the solid phase as the compound does not need to be removed

from the polymeric support. A more electron rich urethane is required to increase the acid lability of the linker if screening a large number of compounds (library) has to be performed in solution. This led to the use of the urethane linker and Fmoc protected polyamine (**118**) (Figure 2.19) which also allows Fmoc chemistry to now be carried out. Differentiation of the primary amines has also been achieved as in (**119**).

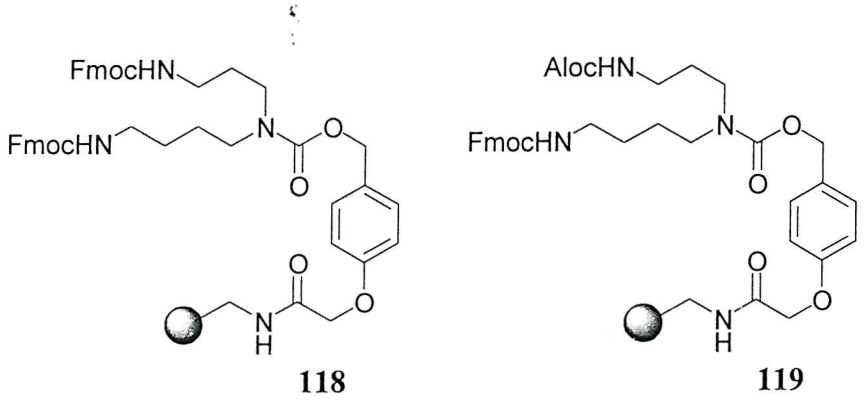

118 **119**

Figure 2.19 Fmoc protected spermidines with a TFA labile linker

2.6 Aims of this chapter

The aim of this chapter was to exploit solid phase technology for the synthesis of polyamine conjugates in the search for new inhibitors of trypanothione reductase. The solid phase immobilisation of phthaloyl protected spermine (**120**) and spermidine (**121**) were designed for synthesising these libraries (Figure 2.20).

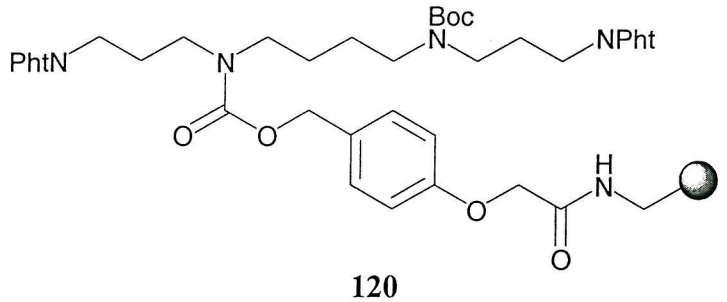

120

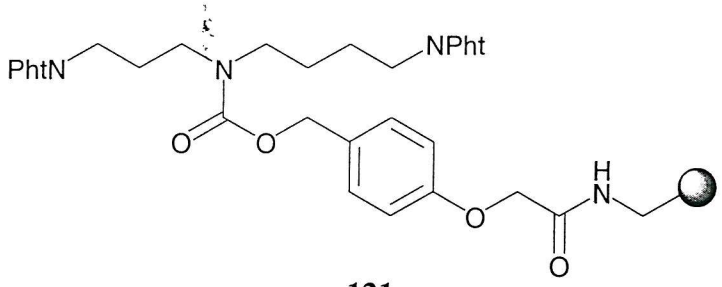

121

Figure 2.20 Phthaloyl protected spermine and spermidine scafolds

The first series of compounds synthesised were based on the natural product kukoamine A, a known inhibitor of trypanothione reductase which shows no significant inhibition of human glutathione reductase (K_i > 10 mM) and thus provides a novel, selective lead. Our first objective was the synthesis of a number of polyamine derivatives followed by a lead optimisation process, preparing a series of new derivatives structurally related to kukoamine A, and evaluation of their biological activity.

2.7 Result and discussion

Kukoamine A contains the symmetrical polyamine spermine (3.4.3), regioselectively diacylated on the primary amino functional groups of the spermine moiety with 3,4-dihydroxyphenylpropionic acid (**122**). Taking spermine as the key structural unit of kukoamine A, the synthesis of analogues of this compound could be achieved by varying the terminal carboxylic acids (Figure 2.21).

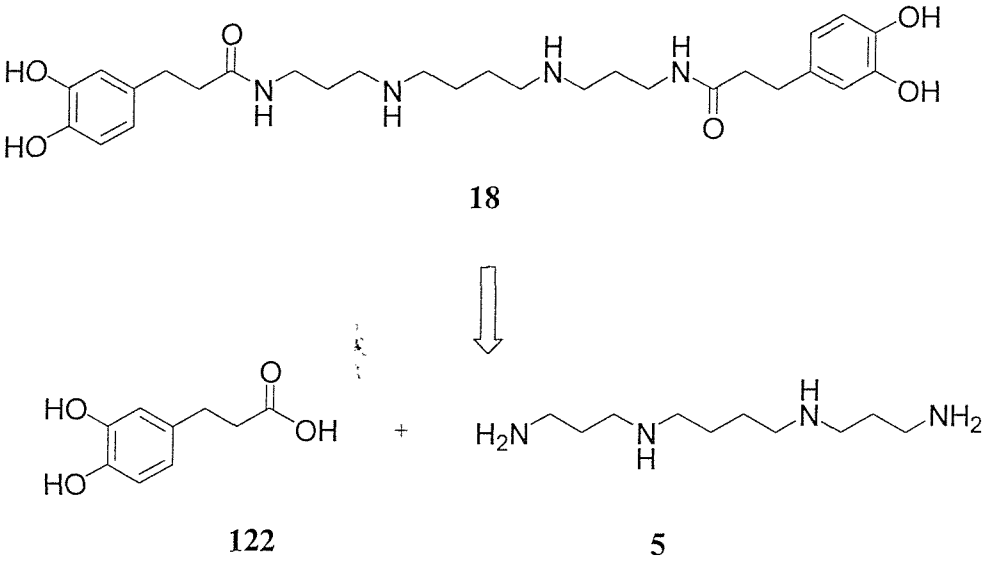

Figure 2.21 Retrosynthesis of kukoamine A

The solid phase synthesis of kukoamine A and analogues involved resin bound polyamine (**123**) readily accessible from the *N*-protected spermine derivative (**124**) and various aminomethylated resins (**125**) (Scheme 2.4). Based on experiences in the polyamine area, the phthaloyl protection of the primary amines was used. This protecting group was easily removed by refluxing with hydrazine in ethanol. However, in order to avoid base catalysed ring opening of the phthaloyl group, it was necessary to protect the carboxylic acid of the linker with an allyl group rather than an ethyl or methyl ester. This protecting group was specifically removed by reaction with palladium ($Pd(PPh_3)_4$) which was compatible with the phthaloyl methodology.

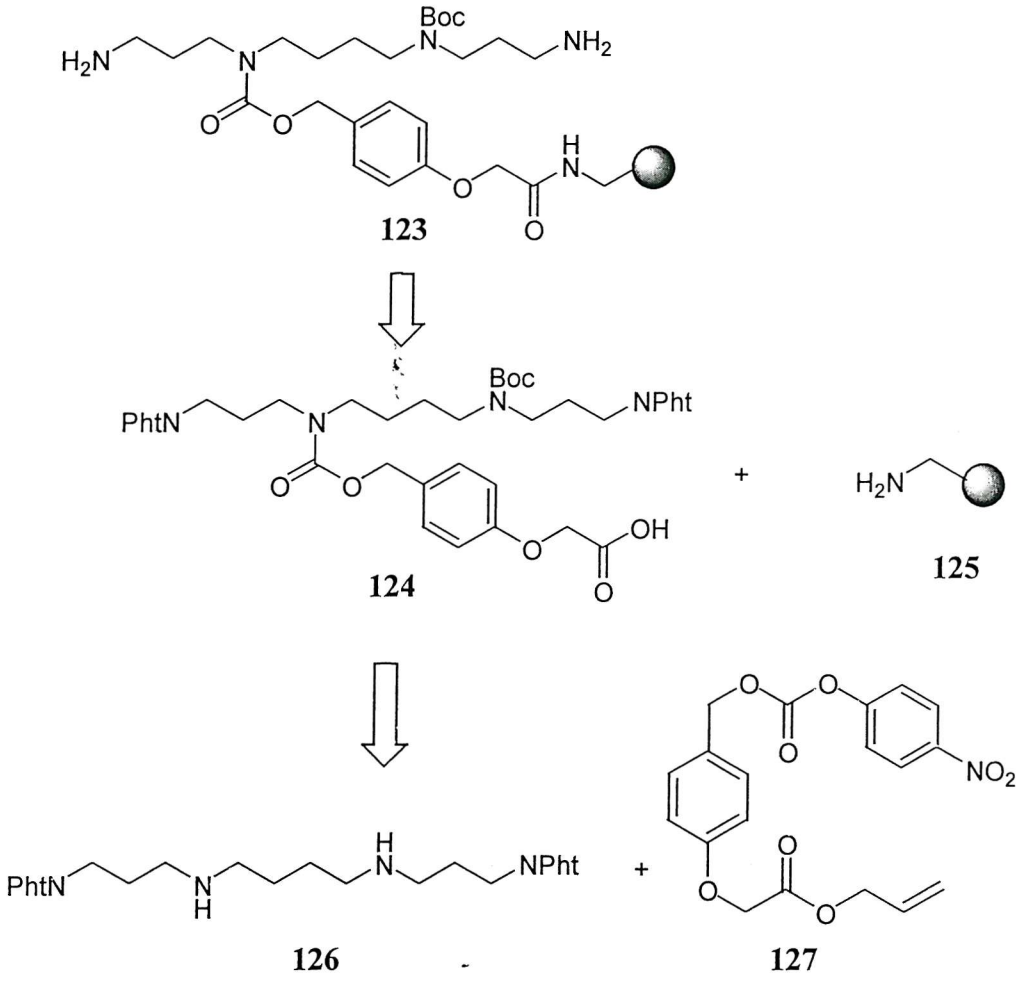

Scheme 2.4 Retro-synthesis of the spermine scaffold for solid phase synthesis

2.7.1 Synthesis of the modified carbonate linker

For the synthesis of the carbonate linker (**127**), 4-hydroxybenzadehyde (**128**) was first o-alkylated using K_2CO_3 and allyl chloroacetate to give (**129**) in 95% yield as shown in Scheme 2.5. The aldehyde (**129**) was converted into the benzyl alcohol (**130**) with sodium cyanobororhydride. In order to optimise this step, it proved necessary to use a solvent mixture of THF/water (1:1) which avoided the by-product (**133**) formed when ethanol used as a solvent alone (see Scheme 2.6). Carbonate formation occurred between alcohol (**130**) and *p*-nitrophenyl chloroformate to give (**127**) in 90% yield after recrystalization.

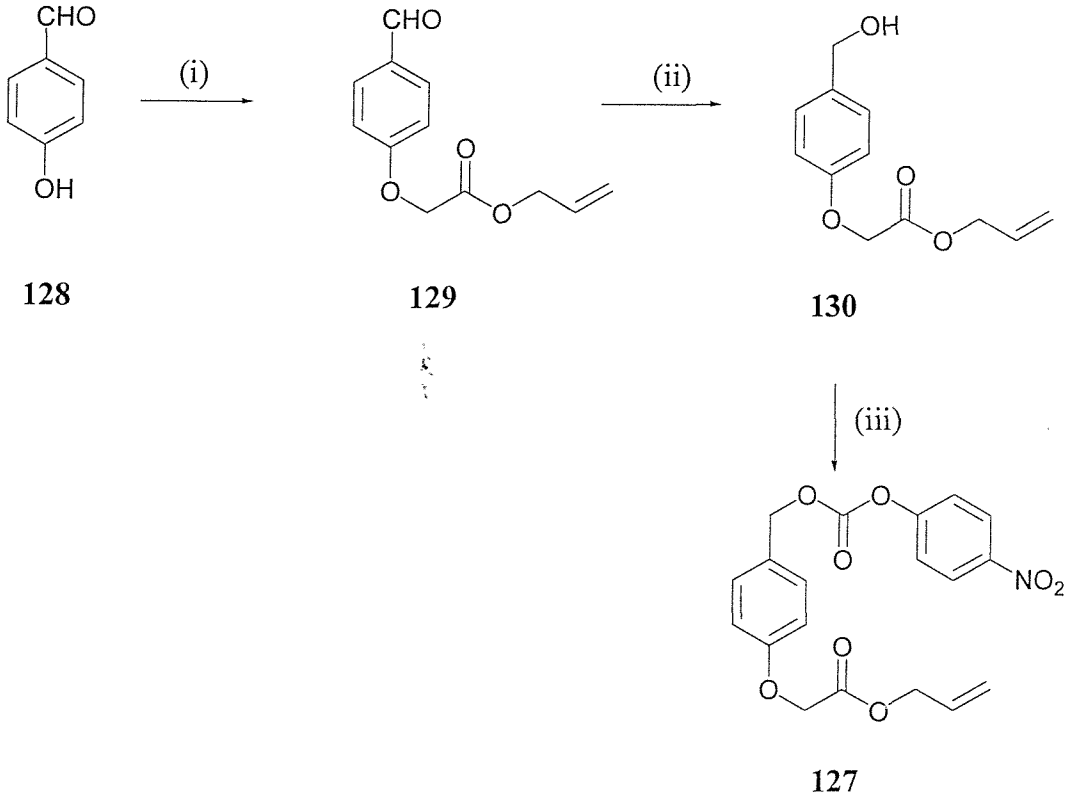

128 **129** **130**

127

Scheme 2.5 (i) K_2CO_3, allyl chloroacetate KI, CH_3CN 95% (ii) $NaBH_3CN$, THF/H_2O (1:1), 95%, (iii) *p*-nitrophenyl chloroformate, pyridine, $CH_2Cl_2/0^oC$, 90%

The mechanism of side-product (**133**) formation probably involved an acid-catalysed dehydration as shown in Scheme 2.6. Since the reaction with $NaBH_3CN$ was carried out under acidic conditions, the benzylic alcohol loses water to give intermediate (**132**). Ethanol acts as a nucleophile to give side-product (**133**). In order to overcome this problem the reaction was carried out in a mixed solvent system with THF/water (1:1), as a result of poor solubility of the aldehyde in water alone.

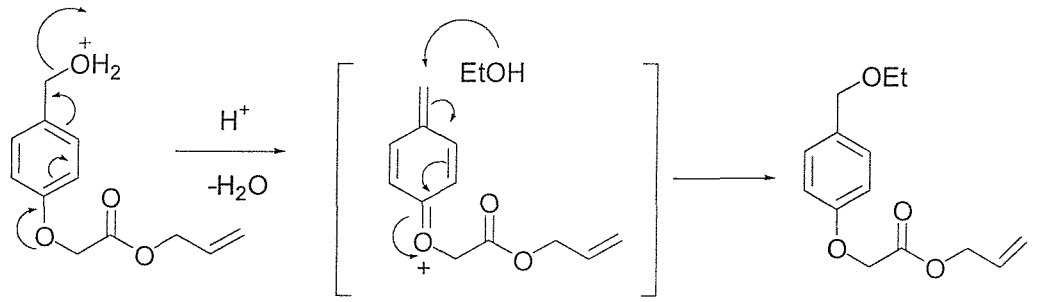

131 132 133

Scheme 2.6 Possible side reaction during reduction

2.7.2 Synthesis of linkage agents containing protected spermine

Selective phthaloyl *bis*-protection of spermine (**5**) to give *bis*-phthaloyl spermine dihydrochloride (**134**) was first achieved following a procedure reported by Jentgens *et al.*,[103] using 2 equivalents of ethoxycarbonylphthalimide in chloroform at room temperature, followed by addition of HCl to give the salt (Scheme 2.7). This product was easy to purify by recrystallisation from methanol. However, an attempt to couple (**134**) with linker (**127**) gave the required product (**135**) in only 22% yield. Several reaction conditions were investigated including excess of base, change of solvents and heating, but these did not significantly improve the yield. The problem was a result of the poor solubility of spermine salt (**134**) and the poor mono-selectivity of the Boc protecting group for the two secondary amines. In order to overcome this, the spermine salt (**134**) was converted into the free base (**126**) by dissolving in 10% $NaHCO_3$ and extraction into dichloromethane. Alternatively (**126**) could be synthesised directly from spermine (**5**) without purification as the HCl salt. Spermine derivative (**126**) was treated sequentially with 1 equiv. of Boc_2O and 1.1 equiv. of linker (**127**) to give (**135**) in 44 % yield.

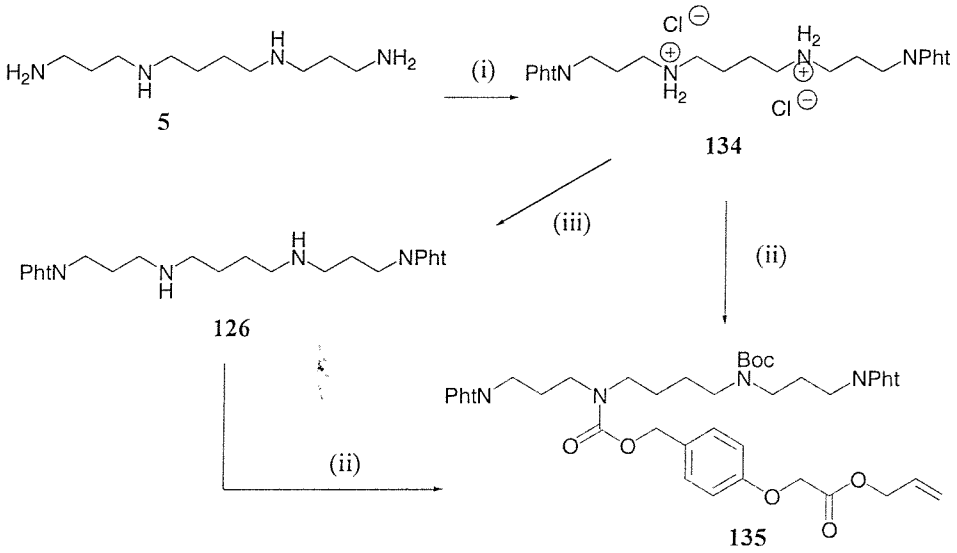

Scheme 2.7 (i) Phthalimido-*N*-ethoxycarbonyl, $CHCl_3$, followed by HCl, 84%, (ii) activated linker (**127**), NEt_3, DMAP, DMF, (iii) 10% $NaHCO_3/CH_2Cl_2$

Allyl ester (**135**) was converted to the corresponding carboxylic acid (**124**) using $Pd(PPh_3)_4$ and dimedone in CH_2Cl_2/THF (1:1).[104] However, purification of acid (**124**) was problematic as dimedone and triphenylphosphine oxide contaminated the product and were difficult to remove. Furthermore, the by-product (**136**) was found under these conditions. These problems were solved using mercaptobenzoic acid[105] as an allyl group scavenger (Scheme 2.8).

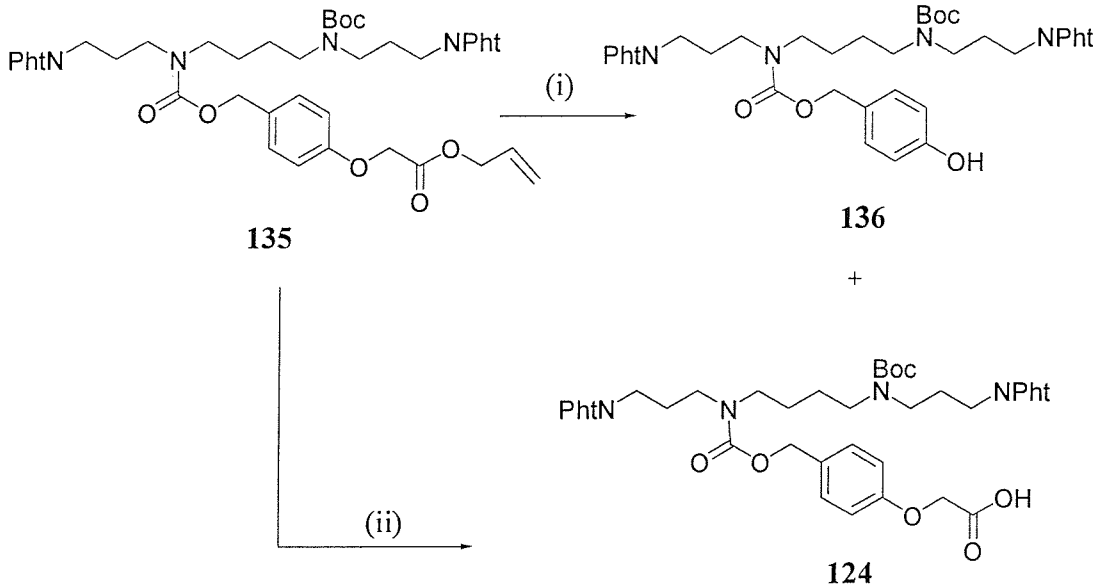

Scheme 2.8 Optimised allyl ester deprotection using mercaptobenzoic acid (i) $Pd(PPh_3)_4$/dimedone, THF:CH_2Cl_2 (1:1), 42 %, (ii) $Pd(PPh_3)_4$/ mercaptobenzoic acid, THF:CH_2Cl_2 (1:1) 72 %.

2.7.3 The synthesis of aminomethyl resin

Aminomethyl resin was prepared from Merrifield resin as shown in Scheme 2.9.[106] The starting Merrifield resin was treated with potassium phthalimide in DMF to yield phthalimidomethyl resin (**138**) which was subjected to hydrazinolysis to convert the phthalimide group to an amine, giving the aminomethyl resin (**125**).

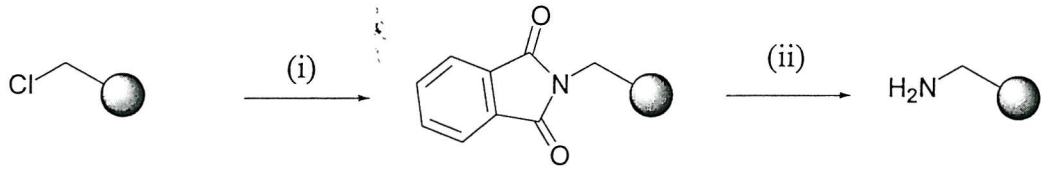

137 **138** **125**

Scheme 2.9 (i) KI, DMF, potassium phthalimide, 100°C, 5h (ii) EtOH reflux, N_2H_4, overnight.

The spermine template (**124**) was first coupled to aminomethyl resin (**125**) using the coupling reagents DIC and HOBt in dichloromethane. A trace of DMAP was found to help the rate of reaction. The coupling was monitored using the quantitative ninhydrin test[107] to indicate complete reaction of primary amino groups. The phthaloyl group was removed using hydrazine in refluxing ethanol to give (**123**) in 90% yield (Scheme 2.10).

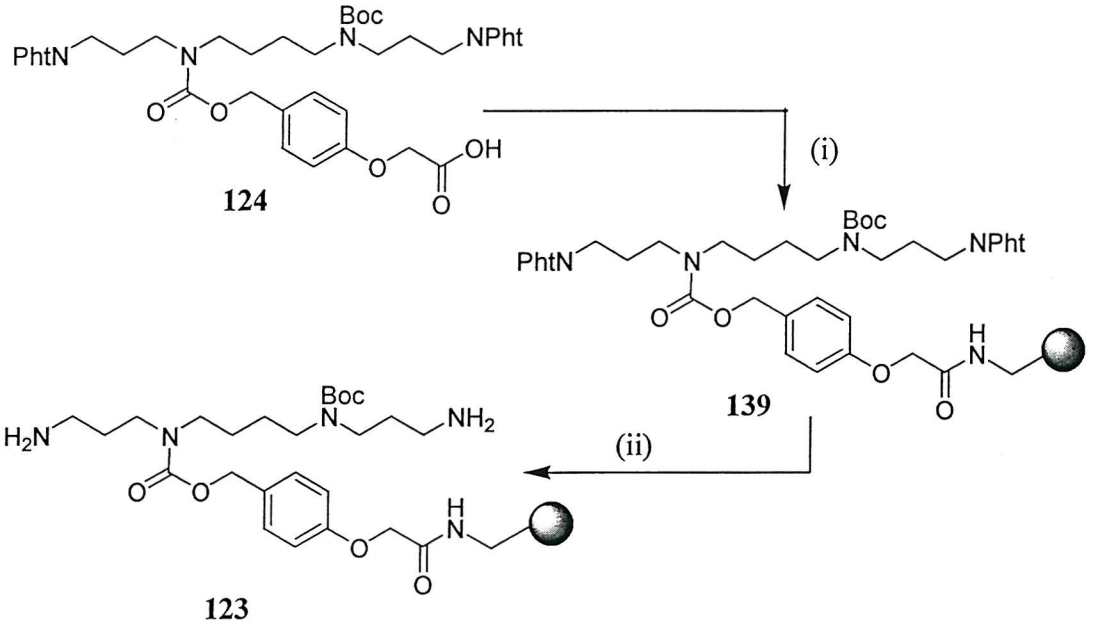

Scheme 2.10 (i) Aminomethyl resin (**125**), DIC/HOBt/CH_2Cl_2: DMF (3:1), (ii) EtOH reflux, N_2H_4, overnight

2.7.4 Synthesis of kukoamine A

The resin bound template (**123**) was first used for the synthesis of kukoamine A as shown in Scheme 2.11. 3,4-Dihydroxyphenylpropionic acid was coupled with DIC and HOBt in dichloromethane. After three hours, washing of the sample and analysis using the ninhydrin test showed that the reaction had reached completion. In order to release kukoamine A from the resin, the sample was treated with a cleavage cocktail using trifluoroacetic acid/triisopropylsilane/phenol/thioanisole/dichloromethane/water (15:1:1:1:1:1). This broad scavenger cocktail was suitable for kukoamine A and prevented the alkylation of the electron rich phenols, a serious problem with compounds of this type.

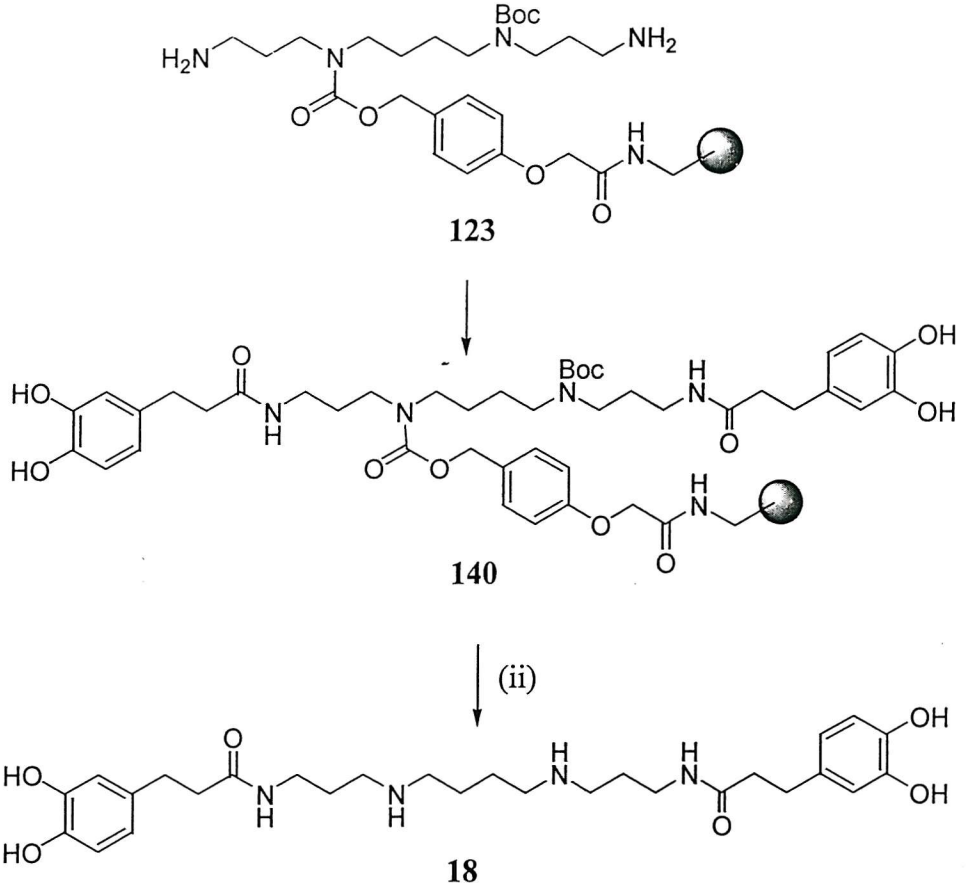

Scheme 2.11 (i) 3,4-dihydroxyhydrocinnamic acid/DIC/HOBt/CH_2Cl_2 : DMF (3:1), (ii) TFA/TIS/thioanisole/phenol/H_2O/DCM (15:1:1:1:1:1).

Kukoamine A was purified by reverse-phase HPLC. Figure 2.22 shows the RP-HPLC of the crude mixture upon cleavage from the solid support and the purified compound. The major peak at 8.0 min corresponds to the product kukoamine A. The ^{1}H-NMR spectrum of the purified compound is shown in Figure 2.23.

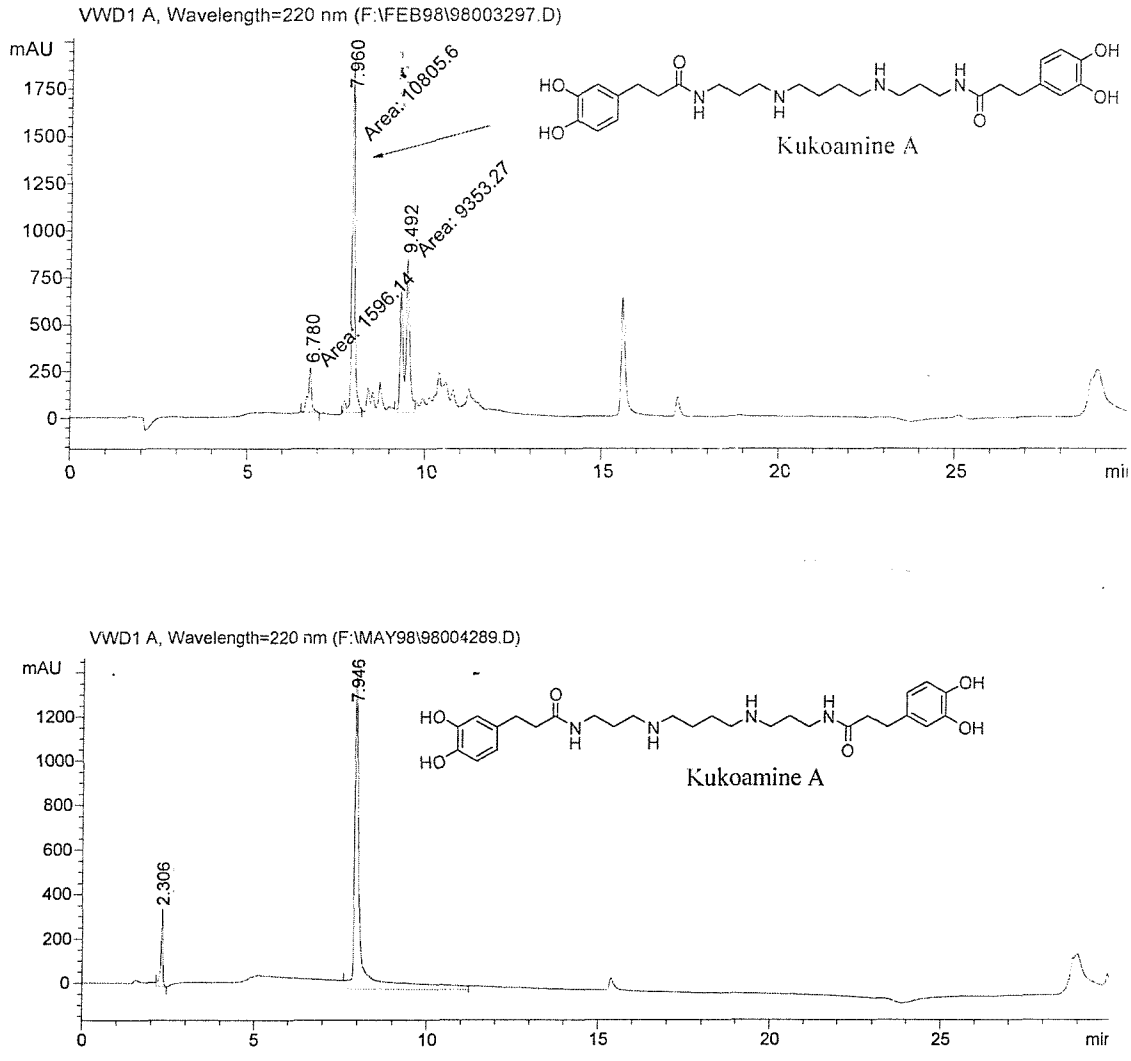

Figure 2.22 Analytical RP-HPLC of (A) crude and (B) purified kukoamine A

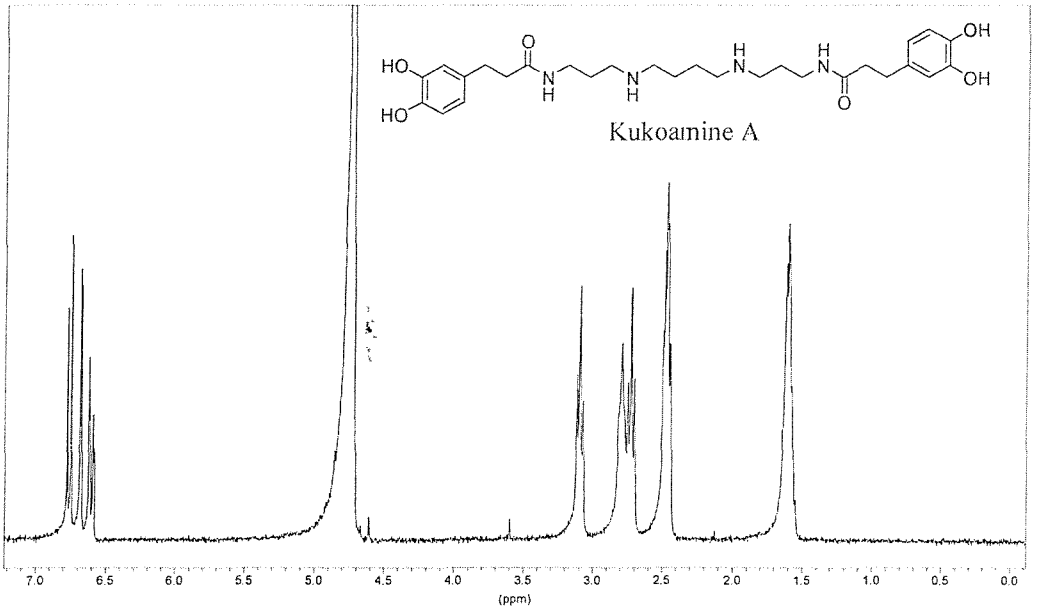

Figure 2.23 The ^{1}HNMR spectrum of purified kukoamine A

2.7.5 Synthesis of kukoamine A analogues

Using the template (**123**), several spermine conjugates with different carboxylic acids were prepared as described for the synthesis of kukoamine A (see Scheme 2.12). The synthesis was performed using a Supelco 24 syringe-reservoir, which enables the simultaneous coupling, washing and up to 24 separate samples. The products were cleaved from the resin with the cleavage cocktail previously described. However, this cocktail containing triisopropylsilane (TIS) not only cleaved the desired compounds from resin but caused the reduction of molecules containing conjugated double bonds. In fact, the reduction of tryptophan residues using trialkylsilane has been reported to convert the side-chain indole moiety to an indoleine group.[108] As a result another cocktail consisting of TFA/thioanisole/phenol/dichloromethane/water in a ratio of (16:1:1:1:1) was found to be effective for the cleavage of all compounds from the solid support and compounds were purified using reverse-phase HPLC prior to screening against TR (*T. cruzi*). The carboxylic acid capping groups used in these libraries are shown Table 2.1.

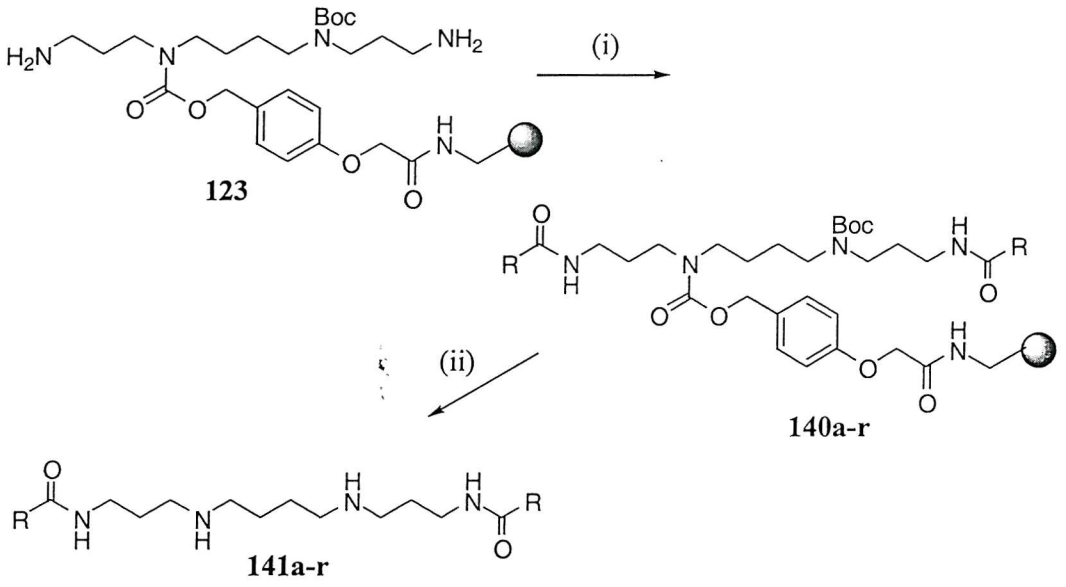

Scheme 2.12 (i) Capping acid/DIC/HOBt/CH_2Cl_2: DMF (3:1), (ii) TFA/thioanisole/ phenol/H_2O/DCM (16:1:1:1:1).

Capping acid	Capping acid	Capping acid
a = 3,4-dihydroxyhydro cinnamic acid	**h** = 2,5-dihydroxyphenyl acetic acid	**m** = 4-hydroxy-7-trifluoro methyl 3-quinoline carboxylic acid
b= 2,3-dimethoxyhydro cinnamic acid	**i** = 2-hydroxyphenyl acetic acid	**n** = 2-pyrimidylthioacetic acid
c = 4-hydroxy-3, 5-dimetho-xycinnamic acid	**j** = 3-hydroxyphenyl acetic acid	**o** = pyrrole-2-carboxylic acid
d = 4-methoxycinnamic acid	**k** = 4-hydroxyphenyl acetic acid	**p** = thiophene-2-acetic acid
e = 3-methoxycinnamic acid	**l** = 2-quinoxaline carboxylic acid	**q** = 2-thiophenecarboxylic acid
f = 4-hydroxycinnamic acid		**r** = 5-bromofuroic acid
g = 3,4-dihydroxyphenyl acetic acid		

Table 2.1 Capping acids used in the synthesis kukoamine A analogues

Following the successful preparation and isolation of kukoamine A analogues, the screening of the compounds for inhibitory properties of trypanothione reductase (TR)

could be undertaken. In order to screen for inhibition, the substrate and enzyme were required.

2.7.6 Trypanothione synthesis

Trypanothione is a natural substrate of trypanothione reductase and was used as a reference compound to monitor enzyme inhibition. This compound is commercially available but is quite expensive costing about £ 10,000g^{-1}. Enough trypanothione could be prepared by solid phase for many thousand of inhibition assays, easily and reproducibly.

The solid phase synthesis of trypanothione involved resin bound spemidine (**121**) which was readily accessible from the *bis*-phthaloyl protected spermidine derivative (**142**) (Scheme 2.13).

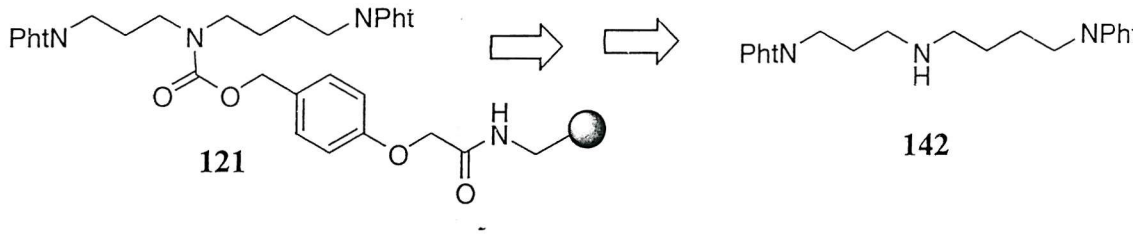

Scheme 2.13 Key intermediates in the solid-phase synthesis of trypanothione (TSST)

Polyamine spermidine scaffold (**145**) was prepared following the procedure described for the spemine based template. The polyamine unit in (**142**) was prepared from spermidine (**4**) by treatment with phthalimido-*N*-ethoxycarbonyl (Scheme 2.14). Although the method of synthesis of the spermidine scaffold (**145**) is similar to spermine, this template is much simpler and easier to prepare, furthermore, all of the processes gave higher yields compared to the spermine analogue.

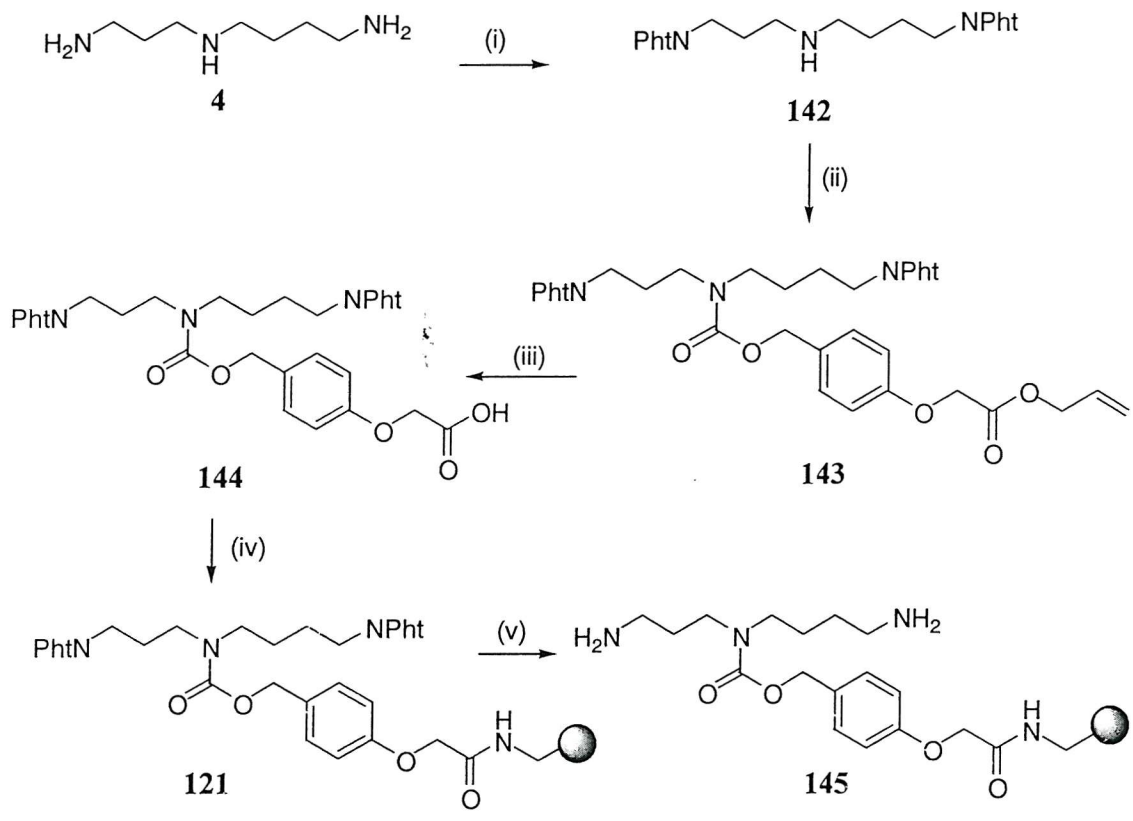

Scheme 2.14 (i) Phthalimido-*N*-ethoxycarbonyl, $CHCl_3$, 84%, (ii) activated linker (**127**), NEt_3, DMAP, DMF, 80%, (iii) $Pd(PPh_3)_4$, mercaptobenzoic acid, THF:CH_2Cl_2 (1:1), 96%, (iv) Aminomethyl polystyrene resin (**125**), DIC/HOBt/CH_2Cl_2: DMF (3:1), (ii) N_2H_4, EtOH reflux.

The synthesis of trypanothione disulphide was accomplished *via* standard peptide chemistry, involving sequential addition of Fmoc-Gly-OH, Fmoc-Cys(Trt)-OH and Boc–Glu(OH)O^{t}Bu onto both the N^1,N^8-amino groups of resin bound spermidine as shown in Scheme 2.15.

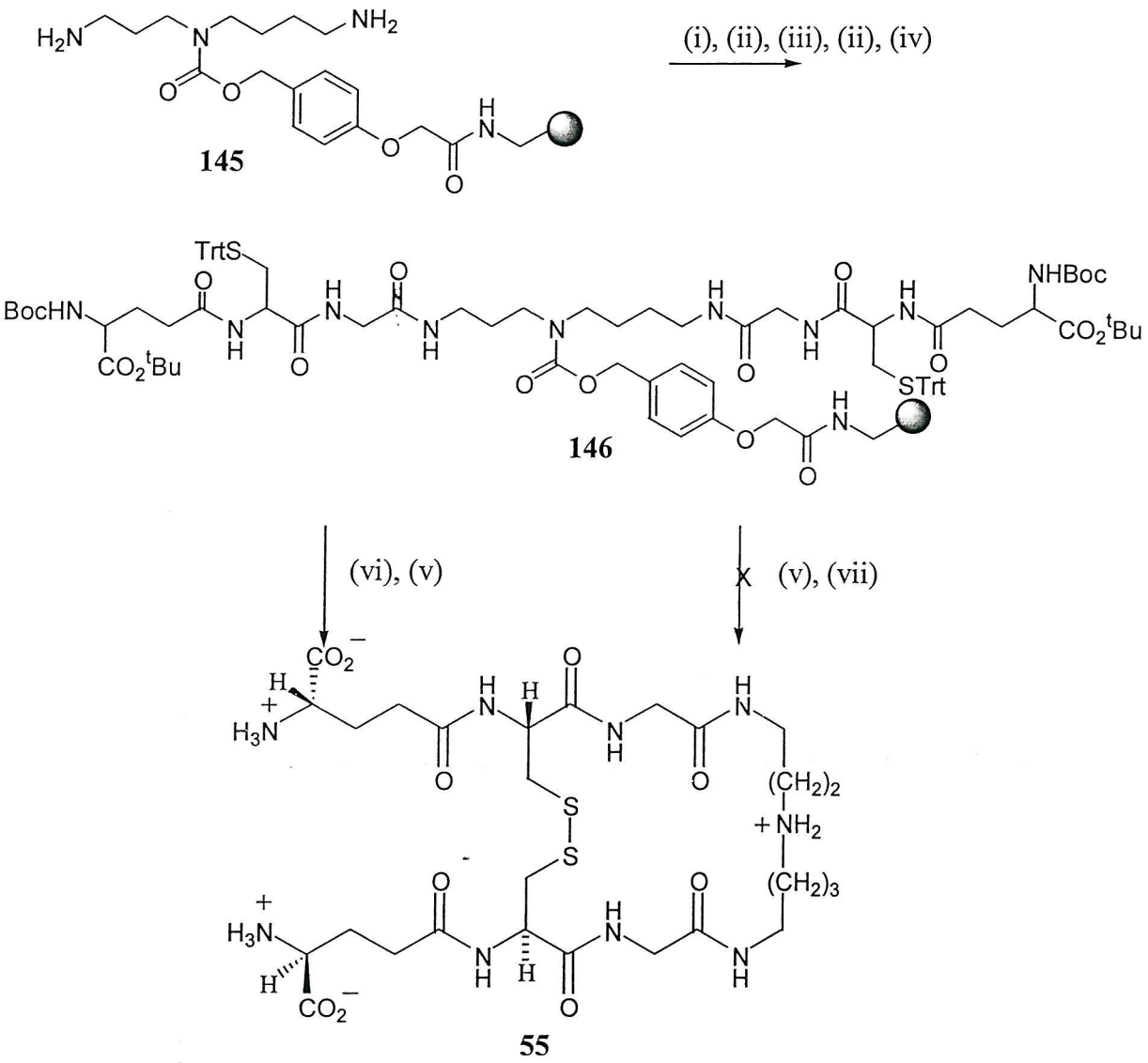

Scheme 2.15 Solid phase synthesis of trypanothione disulfide: (i) Fmoc-Gly-OH, DIC, HOBt, (ii) 20% piperidine in DMF, (iii) Fmoc-Cys(Trt)-OH, DIC, HOBt, (iv) Boc-Glu(OH)-^{t}Bu, DIC, HOBt, (v) TFA/thioanisole/H_2O, (vi) I_2 in DMF, (vii) I_2 in MeOH.

Fmoc deprotection was achieved using 20 % piperidine in DMF and each acylation reaction was accomplished using the DIC/HOBt coupling strategy. The reaction was monitored using the ninhydrin test after Fmoc deprotection. TFA and scavengers (thioanisole/dichloromethane/water) effected the cleavage of side chain protecting groups and urethane bound linker. The filtrate was first evaporated and the compound isolated by precipitation. Finally, the precipitate was dissolved in a large volume of methanol and

stirred vigorously while a methanolic solution of 0.1 M I_2 was added dropwise. When the orange colour persisted, addition was stopped and the solvent was removed *in vacuo* to give crude trypanothione disulfide. The product was analysed by analytical RP-HPLC but was found to contain a mixture of by-products and was difficult to purify. However, the oxidation reaction on solid-phase, with concomitant removal of the trity protecting groups from cysteine, which has reported by Nishino *et. al.*[109] was achieved cleanly (see Scheme 2.15). Thus the resin was suspended in DMF and treated with I_2 (10 equiv.) for 1 hour at room temperature. After washing in DMF, MeOH, CH_2Cl_2 and Et_2O, the product was cleaved from the resin using TFA. The product was analysed by analytical RP-HPLC and purified by preparative RP-HPLC to give the desired product in 30-40% yield.

2.7.7. Purification of *T. cruzi* Trypanothione Reductase

Plasmid pIBITczTR containing the *T. cruzi* TR gene was used[110] with a transcription promotor specific for T7-RNA polymerase and also contained the gene for ampicillin resistance[111]. This was introduced (transformed) into DE3 *E. coli*, ready for growing/expression. This strain contains a copy of the T7-RNA polymerase gene under the control of the *lac* promoter. T7-RNA polymerase is required to transcribe the TR gene starting at a specific T7 promoter, and is induced by the addition of IPTG (isopropyl-β-D-1-thiogalactopyranoside). The ampicillin resistance gene is present so that when the bacteria are grown in the presence of the antibiotic ampicillin, only the plasmid containing cells are able to survive. The transformed cells were first grown on agar plates containing ampicillin, and a single colony was selected for growth on a larger scale. The cells were first grown overnight in 5 ml of 2 x TY growth media (see experimental to Chapter 2) at 37°C. 1 ml of this broth was introduced into 50 ml of media and grown overnight followed by its addition to 2 l of media. At the end of log phase, IPTG was added to induce the T7 RNA polymerase and hence the expression of TR. After 3 hours, the cells were harvested by centrifugation and cell lysis was achieved by sonication. The desired protein was purified from the cell supernatant by ammonium sulfate precipitation followed by affinity chromatography. This involved passing the crude cell lysate over an affinity column of adenine-2, 5-diphosphate-agarose. These ligands have an affinity for the vacant NADPH binding sites within TR, binding the enzyme to the column. Proteins were eluted using a salt gradient. Upon isolation, TR has a yellow appearance characteristic of flavin proteins. This provided a means with which

to determine the protein concentration by measuring the absorbance at 458 nm (ε_{458}= 11.2 $mM^{-1}cm^{-1}$)[110], alternatively, a Bradford assay could be performed.[112]

2.7.8 Initial screening of kukoamine A and analogues

A method similar to that used for the kinetic analysis of trypanothione was adapted for the screening process. The main modification was necessitated by the poor aqueous solubility of some of the compounds. All were found to be soluble in water containing 20% DMSO. An aqueous buffer system containing 50 mM K_2HPO_4, 1 mM EDTA and 20% DMSO at pH 7.5 was employed for the initial screening of the library mixtures. This buffer did not affect the function of trypanothione reductase in its ability to reduce its natural substrate, indeed the DMSO re-oxidises trypanothione dithiol thus maintaining the initial concentration of trypanothione disulfide. Each kukoamine A analogue was dissolved in a volume of water/DMSO that resulted in a concentration of each compound in the mixture being present at a concentration of 1mM so that identical volumes of each solution could be added in the assaying process. A competitive assay was used, where the ability of a particular compound to inhibit the reduction of trypanothione by TR was measured by a decrease in the consumption of NADPH (absorbance at 340 nm) in a 1 ml total assay volume containing NADPH (100 μM) concentration, trypanothione reductase (recombinant *T.cruzi* TR), trypanothione (100 μM) and the inhibitor at 100 μM per constituent compound. The initial rate of consumption of NADPH was monitored at 340 nm and compared to a control assay containing no library compounds. The initial rate data were compared and used to calculate the percentage inhibition for each compound. The percentage inhibition is shown in Figure 2.24.

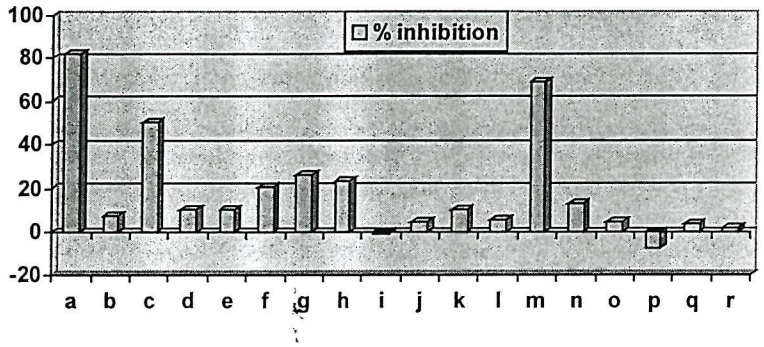

Figure 2.24 The inhibition of TR with spermine derivatives (**141a-r**) (100μM).

From this initial library of spermine derivatives, three inhibitors of trypanothione reductase were found (**141a**) (**141c**) and (**141m**). Unfortunately, the percentage of inhibition of all the analogues was less than that of kukoamine A (**141a**). Therefore, other polyamines were investigated.

2.7.9 Synthesis of spermidine analogues

The spermidine scaffold (**145**) was chosen (see Scheme 2.16), because the spermidine analogue of kukoamine A was nearly as potent an inhibitor of TR as kukoamine A itself.[24] The comparable activity of this compound may indicate that either end of the polyamine backbone is sufficiently long and flexible to interact with the active site of the enzyme. Polyamine spermidine derivatives (**148a-y**) were prepared, and screened as shown in Scheme 2.16 and Figure 2.25.

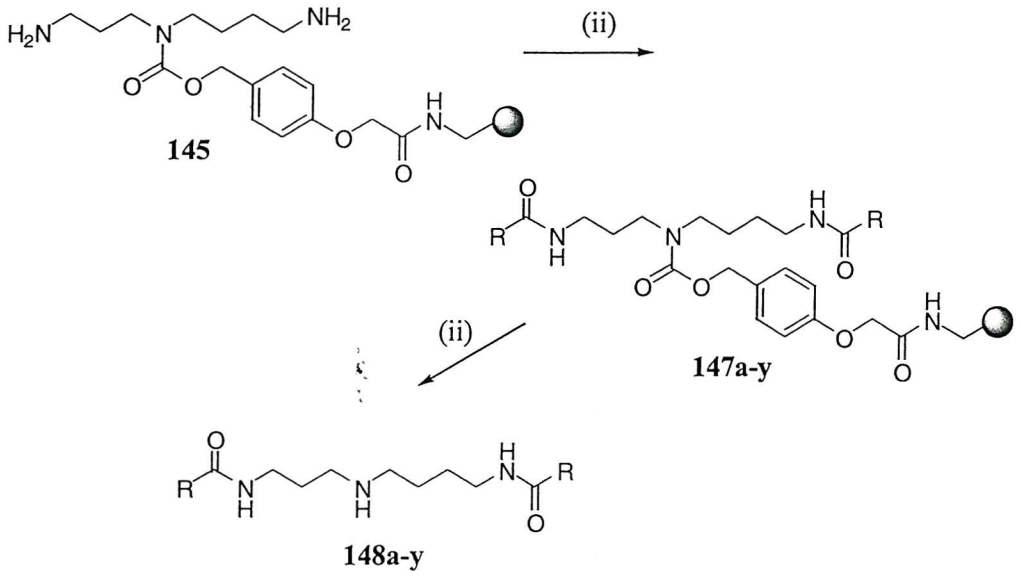

Scheme 2.16 (i) Capping acid/DIC/HOBt/CH_2Cl_2: DMF (3:1), (ii) TFA/thioanisole/ phenol/H_2O/DCM (16:1:1:1:1).

Capping acid	Capping acid	Capping acid
a = 3,4-dihydroxyhydro cinnamic acid	**j** = 3-hydroxyphenyl acetic acid	**q** = 2-thiopheneacetic acid
b= 2,3-dimethoxyhydro cinnamic acid	**k** = 2-quinoxaline carboxylic acid	**r** = 5-bromofuroic acid
c = 4-hydroxy-3,5-dimethoxy cinnamic acid	**l** = 3-hydroxy-2-quinoxaline carboxylic acid	**s** = 2-methoxy-4-hydroxy phenylacetic acid
d = 4-methoxycinnamic acid	**m** = 4-hydroxy-7-trifluoro methyl 3-quinoline carboxylic acid	**t** = 3,4-dihydroxy phenylacetic acid
e = 3-methoxycinnamic acid	**n** = 2-hydroxyphenyl acetic acid	**u** = benzoic acid
f = 4-hydroxycinnamic acid	**o** = pyrrole-2-carboxylic acid	**v** = 3,4-(methylenedioxy) carboxylic acid
g = 2, 4-dihydroxyhydro cinnamic acid	**p** = 2-thiophenecarboxylic acid	**w** = 4-chlorobenzoic acid
h = 3.4-(methylenedioxy) cinnamic acid		**x** = 6-chloro-3-pyridine-carboxylic acid
i = 2,5-dihydroxyphenyl acetic acid		**y** = 3-indole acetic acid

Table 2.2 Capping acids used in the synthesis of spermidine analogues

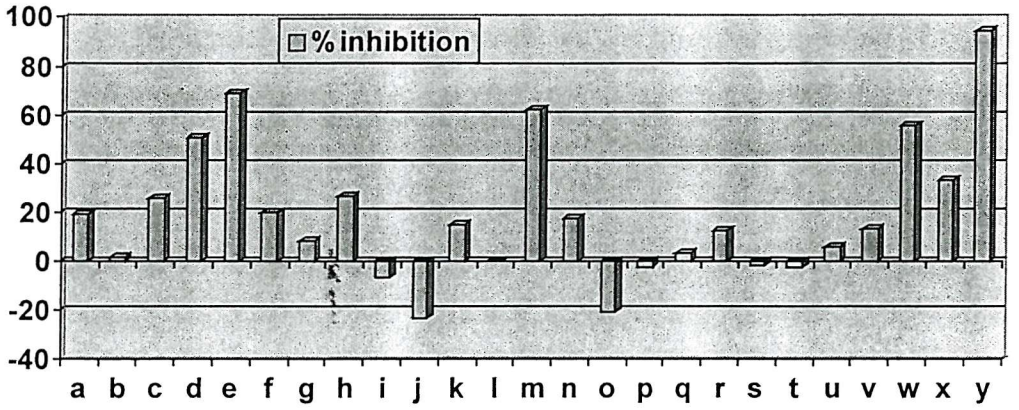

Figure 2.25 Inhibition of TR with spermidine derivatives (**148a-y**) (100 μM)

2.7.10 Enzyme kinetics

Clearly some highly potent compounds were identified and required further analysis. Full inhibition kinetic studies require enzyme assays at different inhibitor and substrate concentrations. These concentrations were chosen by estimating the amount of compound required to reduce the maximum rate by 50% and then evaluation at $0K_i$, $0.5K_i$, K_i and $2K_i$. Keeping the inhibitor concentrations ([I]) constant, the concentrations of substrate should vary between 0.5-5x K_m and the initial rate (V) of each assay measured. These assays were performed in triplicate and the average rates used in the kinetic plots. Plots of V versus V/[S] were linear with the slope being $-K_m$. The intercept on the V axis gives V_{max}.[133] However a series of parallel lines were obtained. The most potent inhibitors reported in this experiment were analysed using the commercial Erithacus software (GraFit Version 4). The kinetic data fitted the equation given in Eq. 1, for non-competitive inhibition, with the assays being carried out at six concentrations of substrate (oxidised trypanothione).

$$v = \frac{Vmax\,[S]/(1+[I]/Ki)}{Km+[S]} \qquad \text{Eq. 1}$$

The kinetic data of the four most potent inhibitions based on the spermine and spermidine derivatives is given in Table 2.3. All the inhibitors were shown to be non-competitive Figure 2.26.

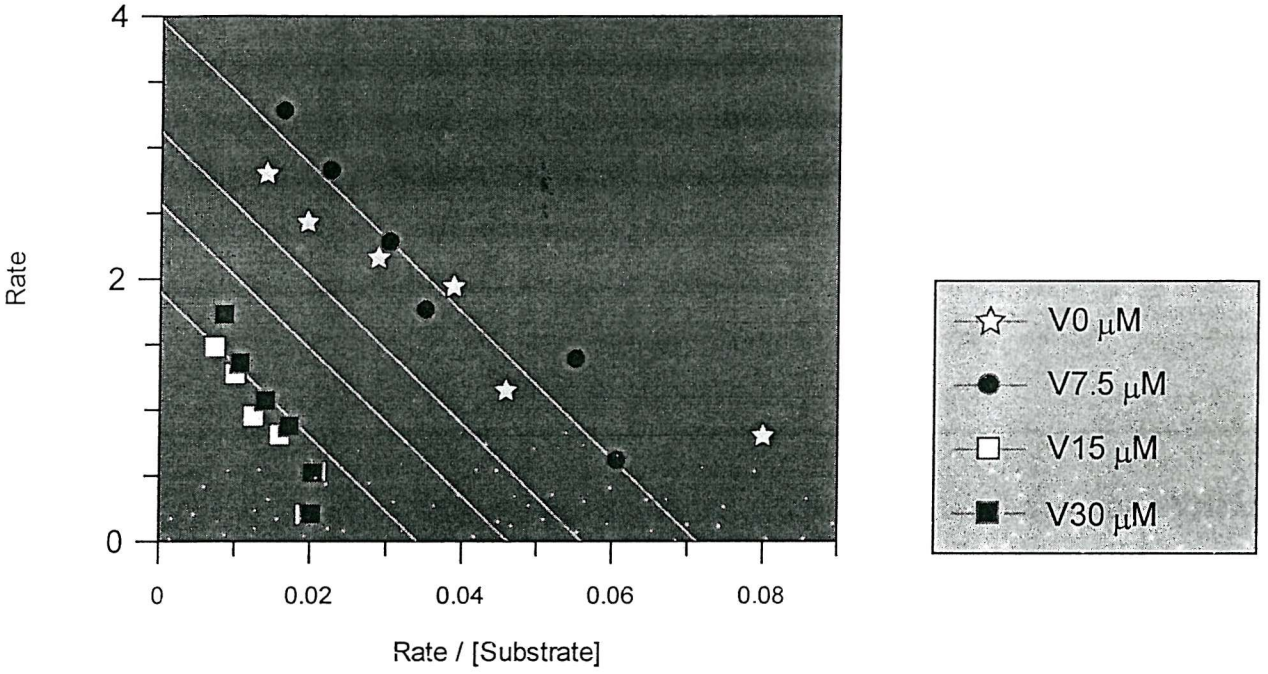

Figure 2.26 The full kinetic characterisation of compound (**148y**)

	Capping acid	Polyamine	Ki (μM) ±SD
(**141a**)	3,4-Dihydroxyhydocinnamic acid	Spermine	1.39 ±0.41
(**141m**)	4-Hydroxy-7-trifluoromethyl-3-quinoline-carboxylic acid	Spermine	0.75± 0.22
(**148m**)	4-Hydroxy-7-trifluoromethyl-3-quinoline-carboxylic acid	Spermidine	0.85±0.22
(**148y**)	3-Indole acetic acid	Spermidine	0.39±0.06

Table 2.3 The four most potent inhibitors in the initial library, K_i values were determined in triplicate and analysed using the commercial program GraFit.

Preliminary biological assays indicated that the most active compound was the indole-3-acetic acid conjugate of spermidine (**148y**). This compound was some 3 fold more potent than the natural product kukoamine A (**141a**). It was therefore decided to prepare a set of closely related compounds in order to find an optimal structure, to assess the influence of both substitutions on the indole ring and the aliphatic chain length on biological activity. A series of compounds based on the indole derivative and spermine (**148y**) were prepared (see Table 2.4) and screened against trypanothione reductase (see Figure 2.27).

Capping acid	Capping acid
(**148I**) 5-hydroxy-3-indole acetic acid	(**148VIII**) tryptophan
(**148II**) 3-indole propanoic acid	(**148IX**) 2-methyl-5-methoxy-3-indole acetic acid
(**148III**) 2-methyl-3-indole acetic acid	(**148X**) 3-indolecarboxylic acid
(**148IV**) 5-hydroxy-2-indole carboxylic acid	(**148XI**) 3-indole-butanoic acid
(**148V**) E-3-indole-acrylic acid	(**148XII**) 5-bromo-3-indole acetic acid
(**148VI**) 5-methoxy-3-indole acetic acid	(**148XIII**)2,3-dihydro-2-indole carboxylic acid.
(**148VII**) 2-indole carboxylic acid	

Table 2.4 A series of compounds based on the indole nucleus

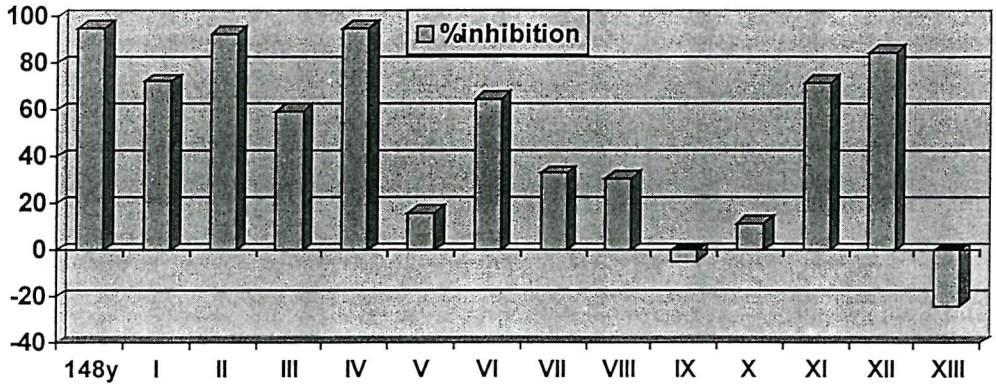

Figure 2.27 Inhibition of TR by spermidine conjugates of 3-indole-acetic acid (100 μM).

From the data, it can be see that the presence of a methyl group at C-2 gave a large decrease in activity. For example, compound (**148III**) shows 60 % inhibition compared to (**148y**) (97% inhibition). This effect was also found in compound (**148IX**) which exhibited very low activity compared with compound (**148VI**). Compound (**148VI**) gave as much as 65 % inhibition, while compound (**148IX**) had no effect. The second group consisted of methoxy, hydroxy and bromine substitution at the C-5 position of the indole ring. These analogues had considerably lower activities than the lead compound itself but substantially higher activity than the C-2 methyl compounds. The next group was the indole-2 and 3-carboxyl analogues. The percentage inhibition in these groups was significantly lower than for the indole-3-acetyl lead compound (**148y**) except for compound (**148IV**) (5-hydroxy-2-carboxyl analogues) which showed the same degree of inhibition..

The last group contained an extended aliphatic chain such as indole-3-propyl and indole-3-butyl analogues (**148II, 148XI**). Approximately the same percentage of inhibition was found when the chain contained one or two carbons' more than the lead compounds. In these groups, the range was from 72 % inhibition for compound (**148XI**) to 93 % for compound (**148II**). However, the introduction of a double bond or an amino group in the chain resulted in a marked decrease of activity. For example (**148V**) was a 6 fold weaker TR inhibitor than compound (**148II**). The results indicate that the conformational freedom of the acyl polyamines is important. The five most active compounds of this series were fully characterised kinetically and the data is given in Table 2.5.

Compound	Capping acid	Ki (μM) ±SD
(**141y**)	3-Indole acetic acid	0.39±0.06
(**141II**)	3-Indole propanoic acid	0.35±0.05
(**141VI**)	5-Methoxy-3-indole acetic acid	0.28±0.02
(**141XI**)	3-Indole butanoic acid	1.26±0.23
(**141XII**)	5-Bromo-3-indole acetic acid	0.076±0.01

Table 2.5 The most potent inhibitors from the indole series. K_i values were determined in triplicate and analysed using the commercial program GraFit.

In summary, a new series of trypanothione reductase inhibitors have been identified from lead compound (**141a** and **148y**). The structure-activity relationships of these compounds show a high preference for compounds containing substituent groups at C-5 whereas those at the C-2 position have reduced activity. The most potent compound to date is compound (**141XII**) with a K_I of 76 nM.

Based on the fact that the indole moiety constituted the central core of numerous potent inhibitors prompted us to carry out an extensive investigation of the series looking at the polyamine component. Thus the activity of the active indole analogues was assessed using spermine, spermidine and norspermidine as backbones. The solid phase synthesis required immobilised of polyamine *nor*spermidine (**149**), which was prepared from the *nor*spermidine derivative (**150**) (Scheme 2.17, 2.18).

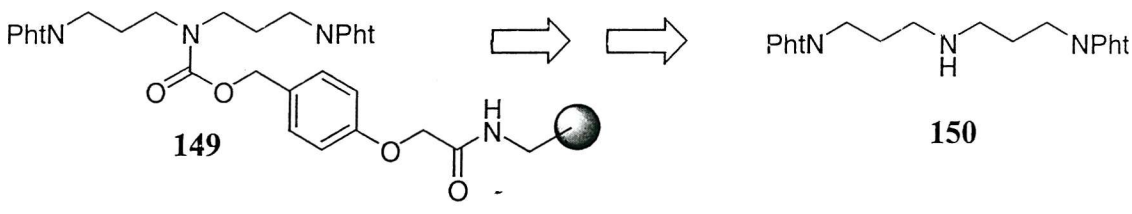

Scheme 2.17 Key intermediates for immobilisation of *nor*spermidine.

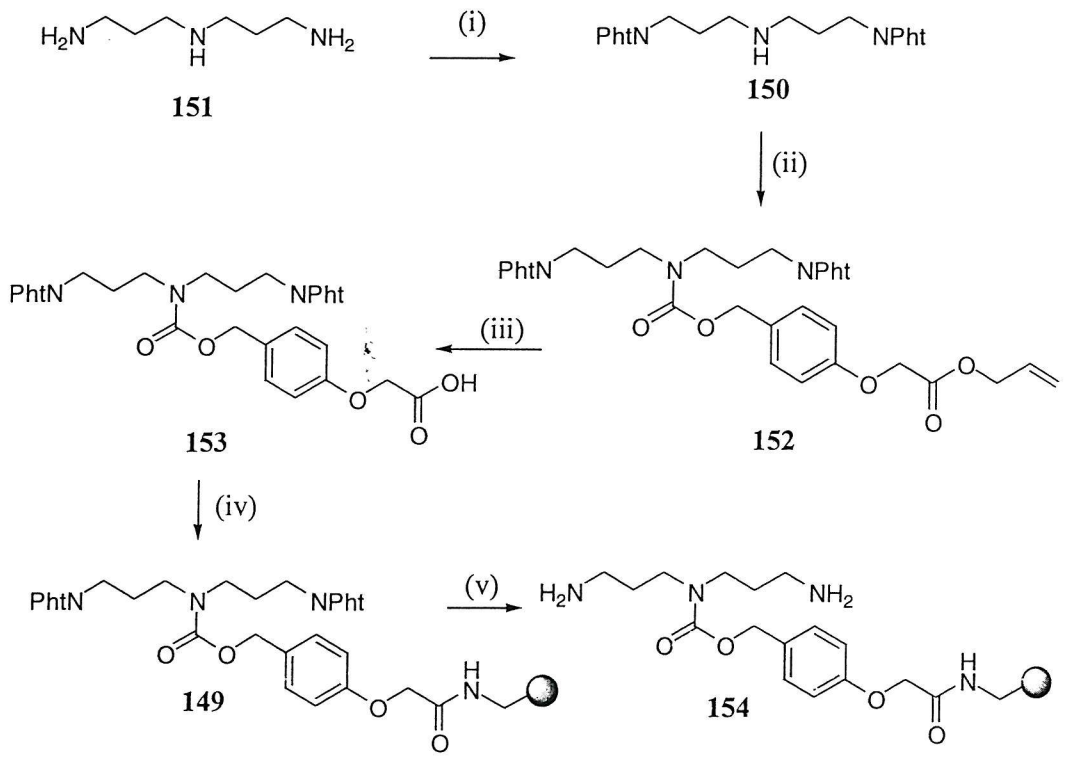

Scheme 2.18 (i) Phthalimido-*N*-ethoxycarbonyl, $CHCl_3$, 63%, (ii) activated linker (**127**), NEt_3, DMAP, DMF, 88%, (iii) $Pd(PPh_3)_4$, mercaptobenzoic acid, THF:CH_2Cl_2 (1:1), 96%, (iv) Aminomethyl polystyrene-resin (**125**), DIC/HOBt/CH_2Cl_2: DMF (3:1), (ii) N_2H_4, EtOH reflux, overnight.

The norspermidine conjugates (**156**) were prepared as shown in Scheme 2.19.

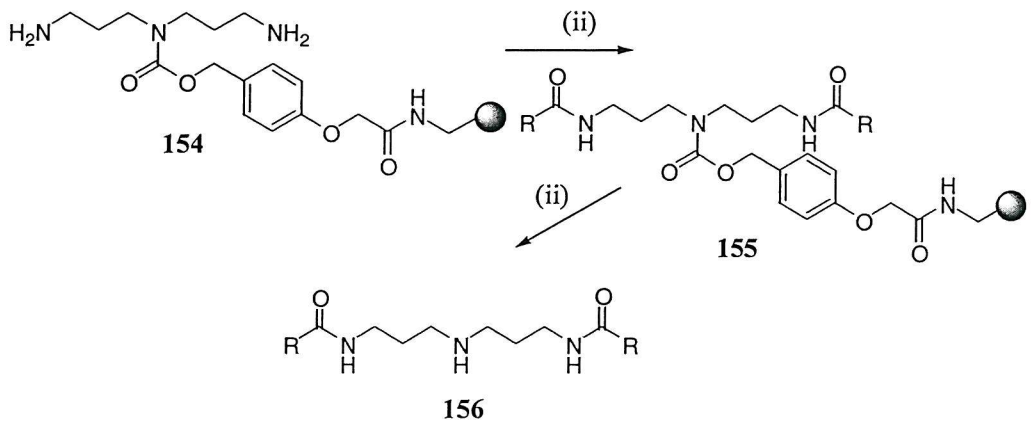

Scheme 2.19 (i) Capping acid/DIC/HOBt/CH_2Cl_2/DMF (3:1), (ii) TFA/thioanisole/ phenol/H_2O/DCM (16:1:1:1:1).

All compounds were screened at a single concentration of 100 μM and gave the data shown in Table 2.6.

	Capping acid	Norspermidine	Spermidine	Spermine
(a)	3,4-dihydroxyhydrocinnamic acid	38%	20%	82%
(m)	4-hydroxy-7-trifluoromethyl-3-quinoline carboxylic acid	85%	62%	69%
(y)	3-indole acetic acid	97%	95%	97%
(I)	5-hydroxy-3-indole acetic acid	24%	65%	95%
(II)	3-indole propanoic acid	60%	72%	96%
(VI)	5-methoxy-3-indole acetic acid	96%	85%	96%
(XI)	3-indole butanoic acid	63%	93%	97%
(XII)	5-bromo-3-indole acetic acid	54%	72%	98%

Table 2.6 Screening of the three polyamine conjugates with the most potent capping groups

Although there is undoubtedly some levelling of activity for the most potent compounds of the series, the data shows quite clearly the important influence of the polyamine moiety. Thus although the natural polyamine spermidine is found in oxidized trypanothione (the presumed natural substrate for trypanothione reductase) this is not observed to be the basis of the most potent inhibitors, with the tetra-amine spermine being by far the most active. The subtle differences between spermidine and norspermidine are also of interest, with a large variation being observed between the two compounds although not in a consistent manner. With the indole series the natural polyamine spermidine is generally the more active of the two, although this is reversed with the capping groups (a and m). Interestingly, it was one of these compounds that was more active than the spermine analogue, the only example where this is the case across the whole series.

2.8 Conclusion

A number of immobilised polyamines were prepared which were derivatised with a range of aromatic carboxylates. The most potent compound of the series had a K_i of 76 nM.

The effectiveness of the indole functionality fits with other inhibitors reported elsewhere[101,102] and suggests that despite the natural substrate of trypanothione reductase lacking aromatic residues the active site is able to accommodate electron rich aromatics. The kinetic behaviour of all these inhibitors was not simple competitive inhibition, but non-competitive and thus the possibility exists that binding is taking place at an alternative active site, perhaps that of the co-factor NADPH. It is even possible that it is competing with the reduced product.

Chapter 3

A New Bio-Compatible pH Cleavable Linker

3.1 Introduction

Linkers play a dominant role in solid phase organic synthesis, determining not only the method of compound cleavage and attachment, but also placing restraints on the necessary nature of library synthesis.[114] The attachment point of the linker to the solid-support should be chemically stable during the synthesis and cleavage. A great number of linkers have been developed over the past fifteen years in order to allow many multi-step organic syntheses to be performed. The use of a broad range of reagents allows cleavages in a very selective manner. Although a linker should ideally enable a selective cleavage to take place under a defined set of conditions, these conditions are not only dependant on the linker but also on the compound attached to the linker, the resin type, its loading and bead size. For example, smaller beads have a much greater efficiency of cleavage under photolysis conditions, whereas lack of resin pre-swelling in CH_2Cl_2 prior to cleavage with TFA can cause a dramatic reduction in yield. Many different parameters are thus involved in the cleavage of compounds from the solid support not just the linker and all issues need to be considered.

Linkers can be classified into one of two types: (i) *Integral linkers* in which part of the solid support core forms part or all of the linker. (ii) *Grafted linkers* in which the linker is attached to the resin core (having been prepared in solution). Many examples of integral linkers were used in the early period of solid-phase synthesis. The original chloromethylated polystyrene resin used by Merrifield is a classical example of an integral linker. This allowed Merrifield to anchor *N*-protected amino acids onto solid supports by formation of immobilised benzyl esters. The disadvantage with any integral linker is the control of synthesis, taking place as it does directly on the resin, with the whole range of steric and electronic effects having influence over synthetic outcome. The exact degree of loading and functionalisation can be difficult to control. The majority of linkers used in solid-phase synthesis are thus of the grafted type. These can be loaded onto the resin then derivatised or pre-loaded prior to attachment. The choice of which method is the most suitable for use in solid-phase synthesis is not clear-cut. The pre-loading method usually ensures much higher loading levels and that only purified material is coupled onto the solid support and also reduces the number of solid-phase steps. The direct loading method is usually less efficient since excess materials are often

used in the coupling step, a problem if valuable templates are being used but is faster since no solution steps or purification are needed (Figure 3.1).

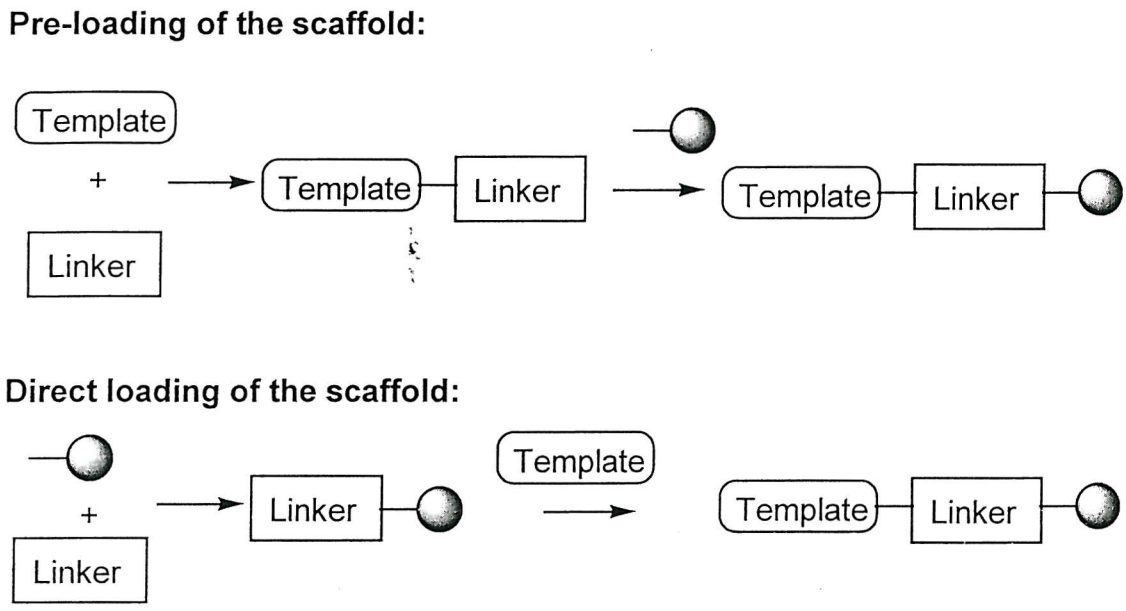

Figure 3.1 Principle of solid phase synthesis by pre-loading and direct loading

A huge number of linkers are now known,[115] falling predominately into electrophilically (such as the Wang, Rink and Trityl linkers) [116]and nucleophilically cleavable linkers (such as the Kenner, Marshal and ester based linkers),[117] however other categories include photo-cleavable[118] and enzyme-labile linkers.[119]

3.2 Safety-catch linkers

Linkers that can be cleaved directly within a biological assay offer some advantages over traditional linkers in a range of screening applications. One type of linker that has been relatively little used in the area of solid phase organic synthesis (SPOS) is the "**safety catch linker**". These linkers require some form of pre-activation prior to compound cleavage, often requiring two orthogonal steps to necessitate cleavage (Figure 3.2).[120]

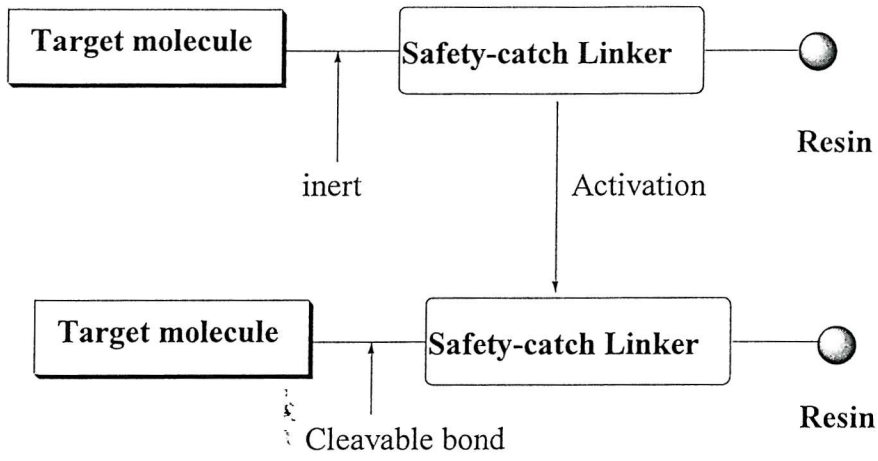

Figure 3.2 Schematic of a safety-catch linker

Some of these linkers potentially allow compound cleavage to take place under mild and bio-compatible conditions, either within assay wells or within agarose gels for zone diffusion based screens. Such linkers seem to be particularly promising for SPOC because they are compatible with many reaction conditions. A number of such linkers have been developed and are briefly described in the following sections.

3.2.1 Kenner's alkylation based safety-catch linker

The first linkers used to demonstrate the safety-catch principle were the acyl sulfonamides (**157**) proposed by Kenner and co-workers (Figure 3.3).[121] It was based on the acyl sulfonamide functionality, which is stable to both strong acid and base. *N*-methylation activates the linker and renders it susceptible to cleavage by NaOH, ammonia, amine or hydrazine.

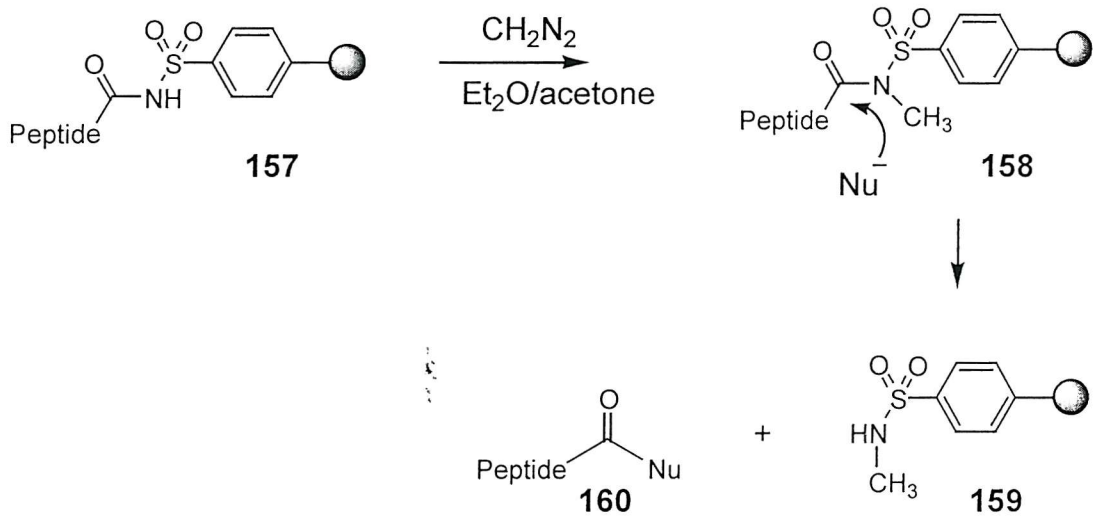

Figure 3.3 Kenner's safety-catch linker

More recently, Backes and Ellman have adapted the original Kenner's safety-catch linker for the synthesis of phenylacetic acid derivatives.[122] However, the reactivity of the *N*-methyl acylsulfonamide (**158**) is so poor that weak nucleophiles such as anilines do not react at all, while for the more nucleophilic alkylamines an excess of reagent is required to ensure complete cleavage. To overcome this problem, haloacetonitrile was used to give (**161**). This activated linker was dramatically more reactive toward a large variety of nucleophiles than compound (**158**) (Figure 3.4).

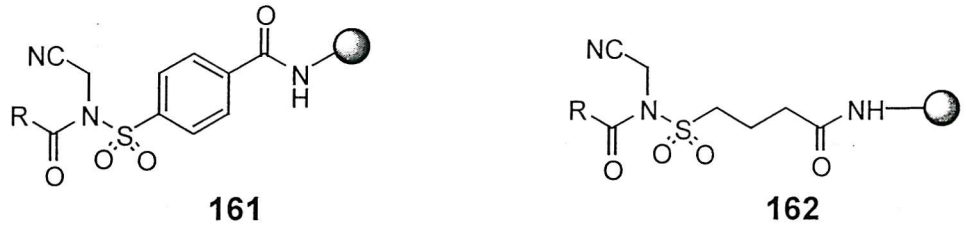

Figure 3.4 Haloacetonitrile and alkylsulfonamide safety-catch linker

This linker was also compatible with common peptide coupling reagents, enolate alkylation and Suzuki reaction conditions.[122] However, one limitation of this linker was the incomplete alkylation of the acyl sulfonamide when carboxylic acids possessing α-electron withdrawing groups were used. To overcome this limitation, alkyl sulfonamide (**162**) was synthesised.[123] This compound was more readily cleaved than (**161**). The overall improvement from the original aryl sulfonamide linker (**157**) was shown by the

high cleavage yield in a comparative experiment. However, certain limitations of these linkers, such as incomplete and racemisation-free acylation with protected amino acids, still remain to be solved.

3.2.2 Oxidative safety-catch linker

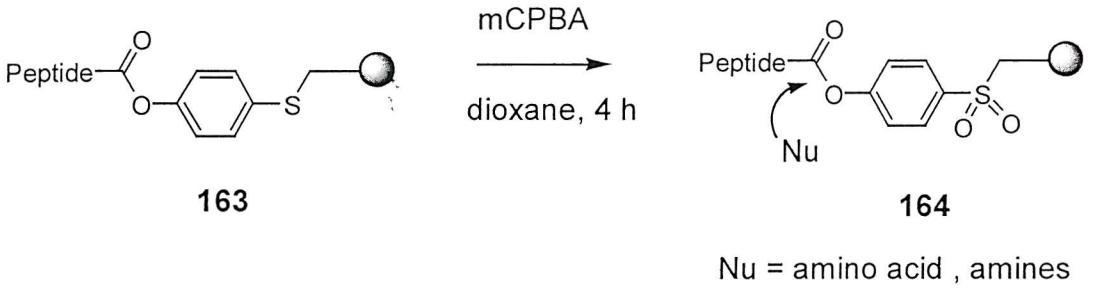

Figure 3.5 Oxidative safety-catch linker

The oxidative safety catch linker (**163**) was originally employed to provide protected peptide fragments (Figure 3.5).[124] The attractive feature of this linker is its facile conversion to the activated alkylsulfonyl ester (**164**). Investigation of the corresponding sulfoxides as active esters revealed only mild activation toward aminolysis. The utility of this linker has been reported for the synthesis of both linear and cyclic peptides. However, the limitation preventing practical application is related to the oxidation step, which means that oxidation-sensitive amino acids such as tryptophan can not be used in the peptide sequence.

3.2.3 Base labile safety-catch linkers

This novel linker strategy was designed for the clean synthesis of tertiary amines on solid phase[125] (Figure 3.6). Michael addition of a secondary amine onto the acrylate (**165**) generated a resin bound tertiary amine (**166**).

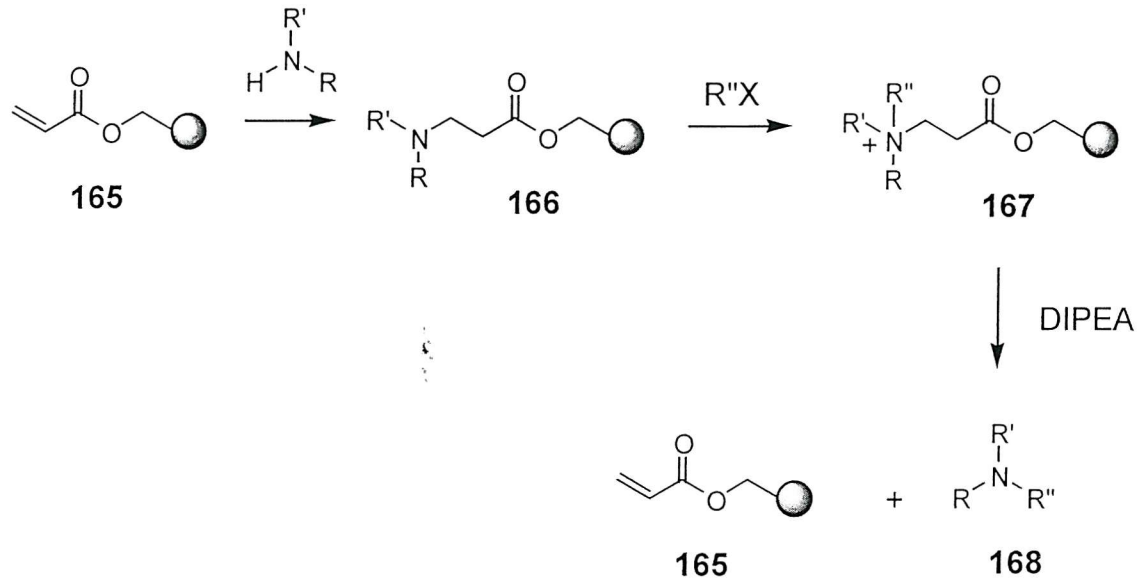

165 166 167 165 168

Figure 3.6 Base labile safety-catch linkers

Quaternisation of this amine with an alkyl halide is the activation step. Hoffman elimination with a base regenerated the original linker and released the tertiary amine product from the resin. The synthesis of an array of amines demonstrated the utility of the linker.

3.2.4 Acid labile safety-catch linkers

Based on the *p*-(methylsufinyl)benzyl protecting group[126] the SCAL (safety-catch acid labile linker) was developed for the synthesis of peptide amides, which are present in many naturally occurring peptides.[127] In the oxidised form the linker is stable to acids and bases and is amenable to peptide synthesis using either Fmoc or Boc protection strategies. The linker is activated by reductive acidolysis, with $PPh_3/Me_3SiCl/DCM$ converting the sulfoxide to a thioether, thus making the sulphur electron donating (Figure 3.7). Peptide amides are released from the linker in the presence of TFA/H_2O.

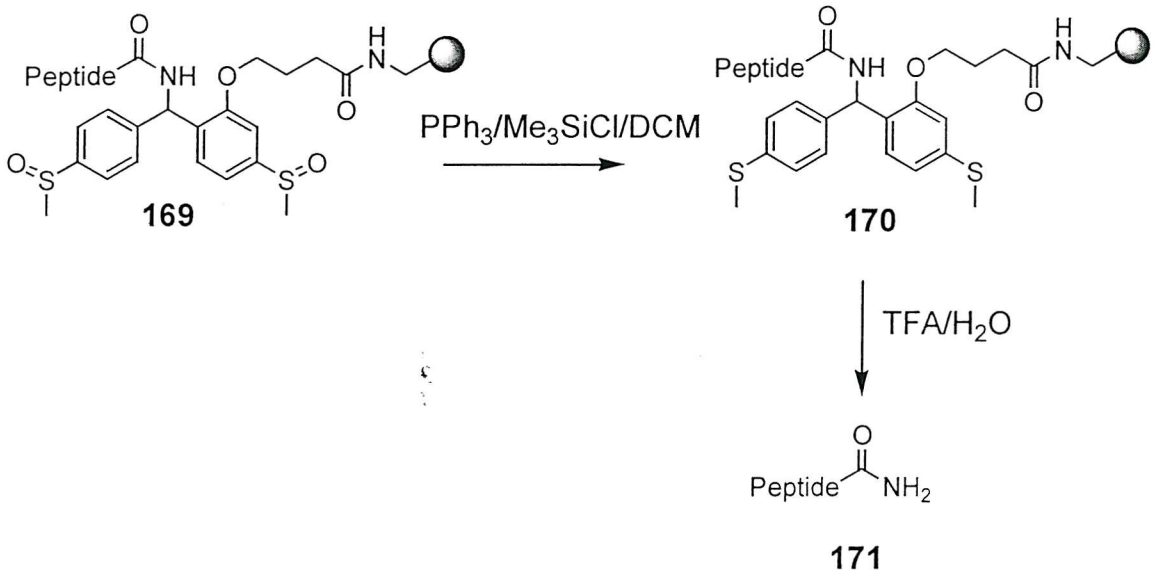

Figure 3.7 Acid labile safety-catch linkers

3.2.5 Safety-catch linkers which cleave in aqueous buffer

Hoffman[128] amended a previously documented glycolic acid linker[129] by incorporating an imidazole ring (Figure 3.8). The imidazole ring has significantly reduced basicity due to the Boc protection. Activation of this linker occurred under acidic conditions, removing the Boc group and other acid labile protection. On exposure to buffer the imidazole became deprotonated and assisted the hydrolysis of the ester by intramolecular catalysis.

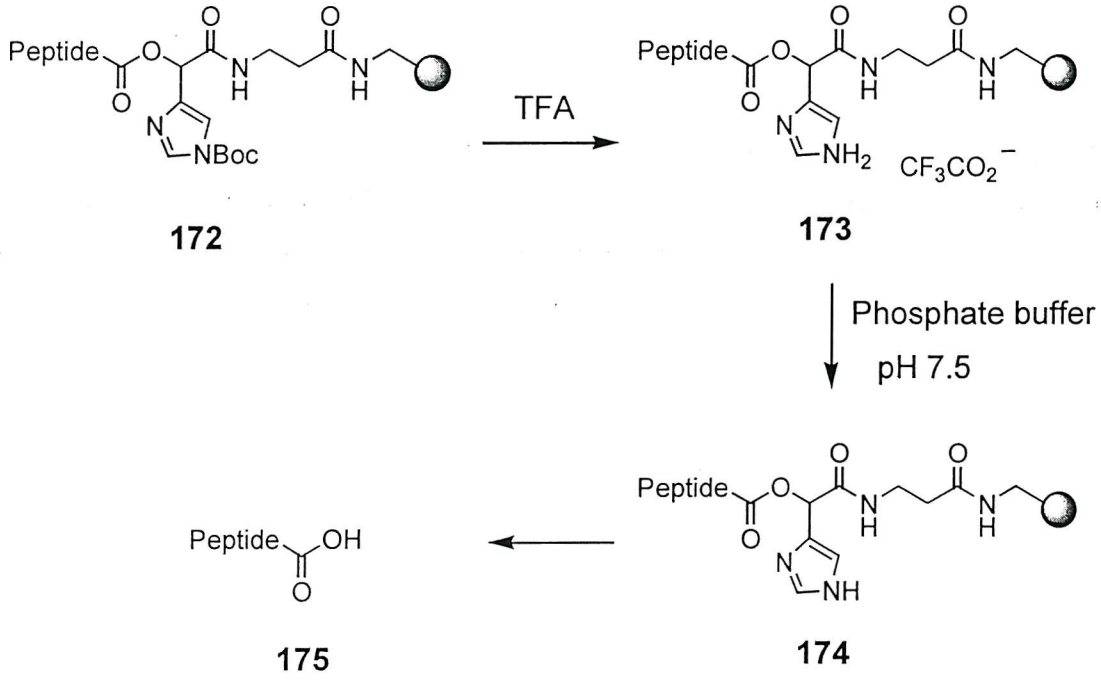

Figure 3.8 Imidazole based linker

3.2.6 Photolabile safety-catch linkers

Chan[130] described a safety-catch cleavage strategy based on the dithiane protected 3-alkoxy benzoin, and demonstrated the practicability of the strategy in solution. Balasubramanian[131] demonstrated the utility of this strategy on the solid phase (Figure 3.9). Activation of the linker was performed by exposure to mercury (II) perchlorate which removed the dithiane protection. Irradiation at 350 nm effected photolytic cleavage.

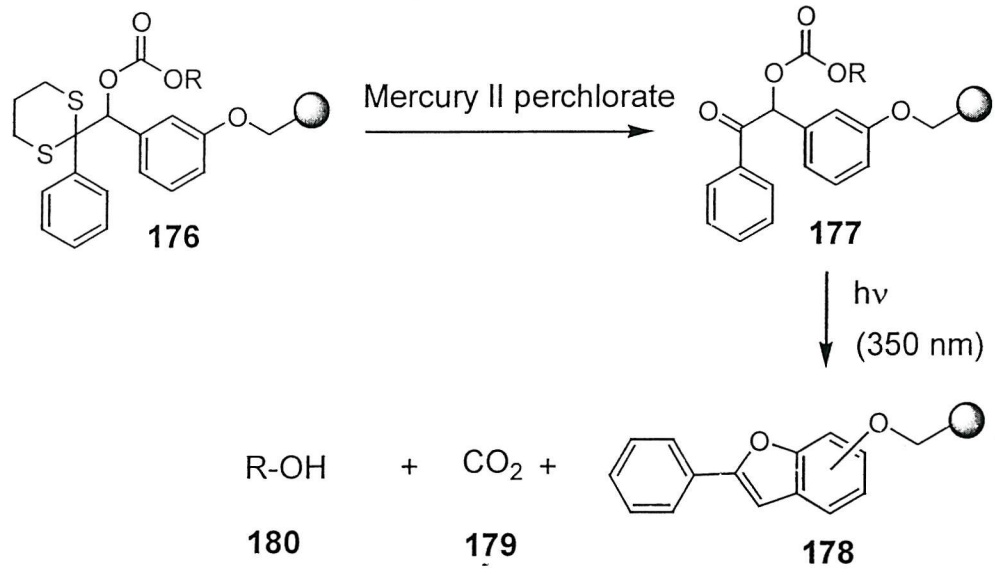

Figure 3.9 Photolabile safety-catch linker

3.2.7 Diketopiperazine based safety catch linkers

Safety-catch linkers acting by a cyclisation type process is a valuable approach to compound cleavage (Figure 3.10). The cleavage mechanism involves an intramolecular cyclisation, that provides a heterocyclic side product that can remain attached to the solid support, with the desired compound being released into solution. The formation of a five or six-membered ring provides the driving force for the final cleavage step.[132] Often activation takes place by *N*-deprotection of the linker such as in (**181**) which gives intermediate (**182**), which is stable to a protocol designed to remove contaminants from the solid-support before cleavage. Peptide cleavage is then achieved in good yield by treating (**182**) with a solution at pH 7.0 to give peptide (**184**)

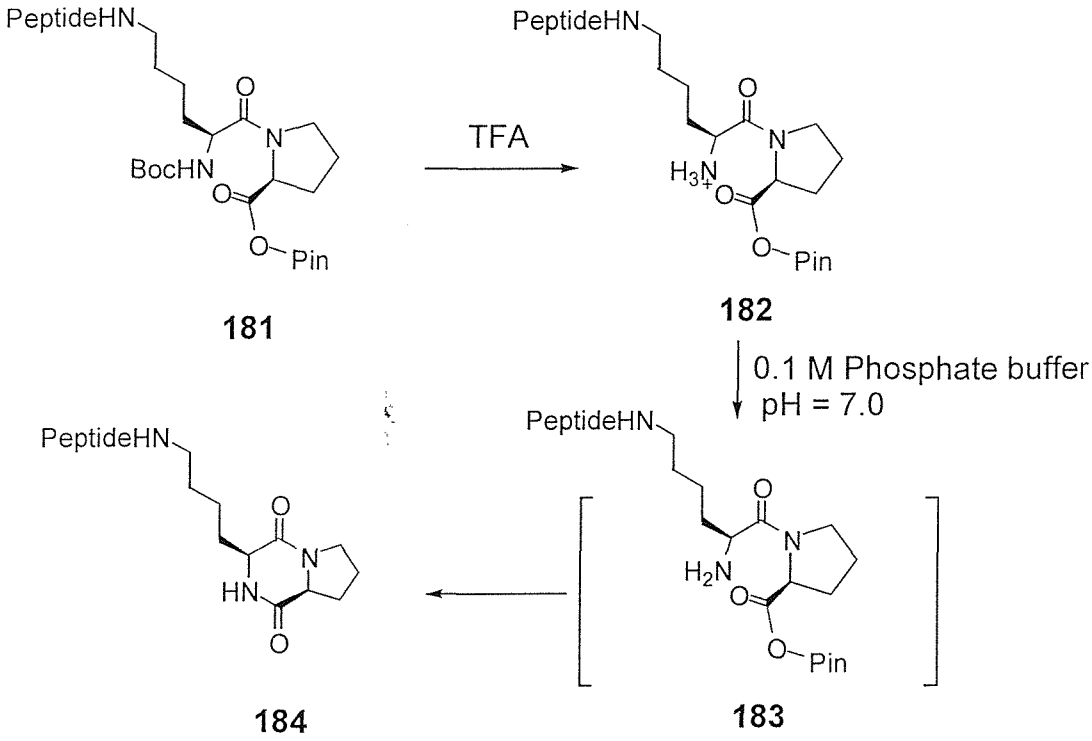

Figure 3.10 A diketopiperazine based safety-catch linker

Recently, our group[133] designed a similar diketopiperazine linker (**185**), which after acidic activation undergoes cleavage in aqueous buffer (pH 7-8). However the linker does not release a product that was linked to the diketopiperazine. This linker was stable to the base treatments required during Fmoc peptide chemistry and was efficiently cleaved in buffered aqueous solution following activation (Figure 3.11) and left no trace. This linker allowed compound cleavage under mild and bio-compatible conditions within agarose gels for zone diffusion based screening for biological activity.

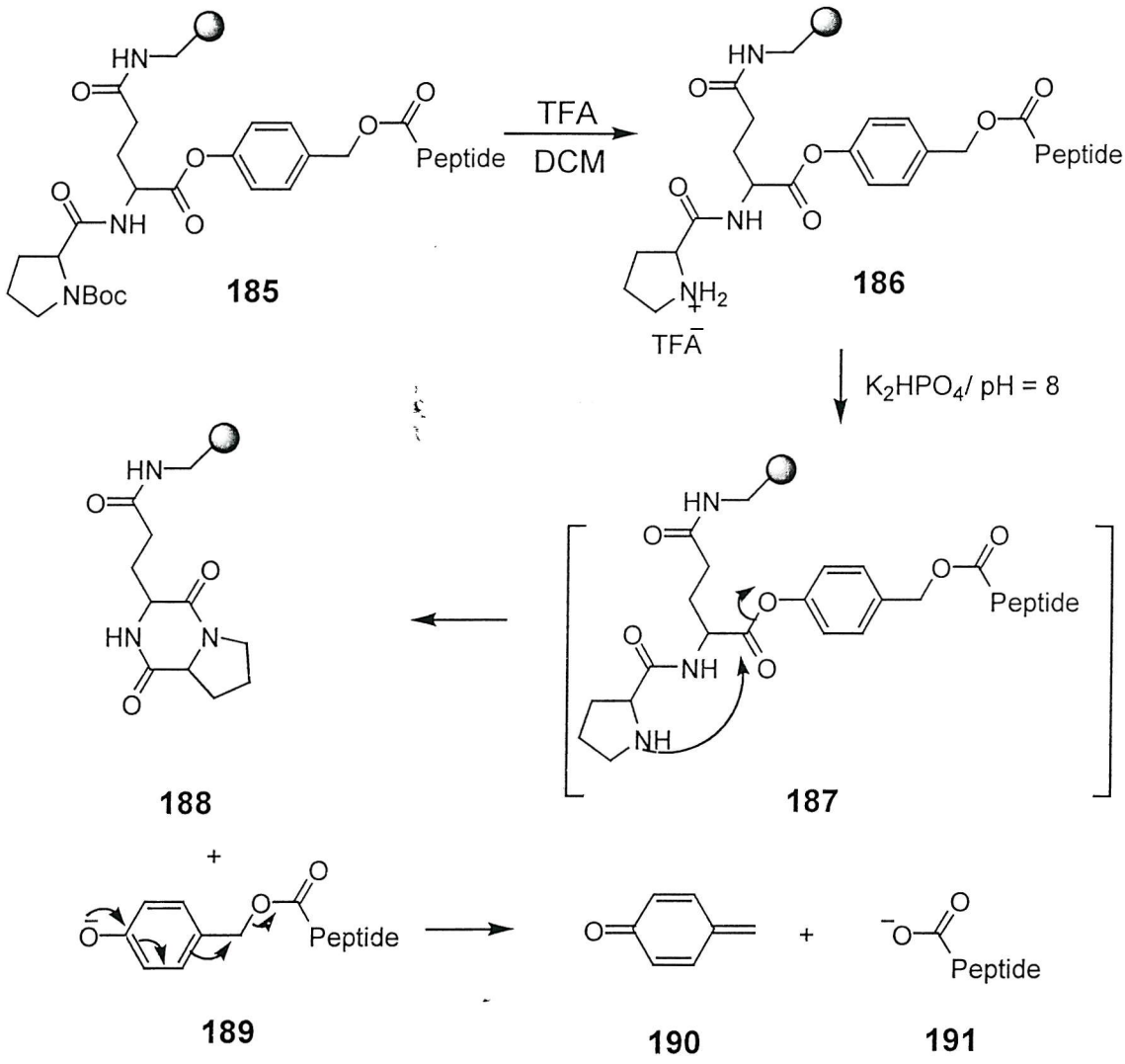

Figure 3.11 A modified diketopiperazine based safety-catch linker

A New Bio-Compatible Safety Catch Linker

Although many safety-catch linkers have been described, problems with these linkers have limited their application. To improve on previous results, this part of the project focussed on the development of a new pH cleavable linker system, based on the 1,6-elimination process of our previously described linker (**185**), but without the liberation of the reactive quinone methide by-product (**190**). This quinone methide (**190**) can cause damage to DNA and thereby contribute to inhibition of cellular replication.[134]

The safety catch linker (**192**) should be suitable for the direct biological evaluation of a compound cleaved from the solid support (Figure 3.12). The linker is attached through an amide bond to the solid support and contains an acyl group such as acetate which will be cleaved by an intramolecular acyl migration. The mechanism of the safety-catch requires

the Boc group to be cleaved from (**192**) under acidic conditions to give (**193**), which then undergoes an intramolecular acyl transfer from oxygen to nitrogen. A phenolate (**196**) is thus generated, which fragments to give quinone methide (**197**) and the required product (**198**). The quinone methide remains attached to the solid phase and is trapped by water.

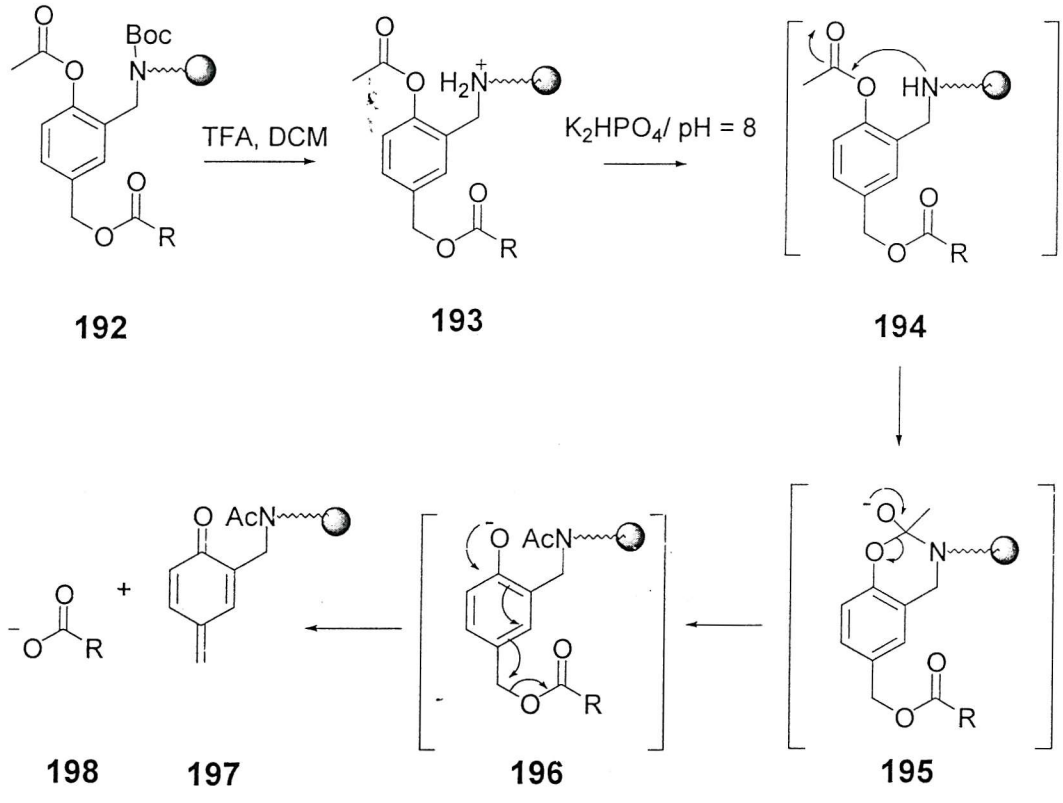

Figure 3.12 Principle for the development of a bio-compatible pH cleavable linker

3.3 Results and discussion

This chapter describes the synthesis of the new safety-catch linker for use in solid phase chemistry and utilised polystyrene and TentaGel resins to test linker viability. The synthesis focused on a number of peptides in order to test linker cleavage efficiency. The new linker model (**203a**) was initially prepared in solution, followed by solid phase synthesis

3.3.1 Synthesis of new linker in solution

The process was initially investigated in solution using (**203a**), which was synthesised as shown in Scheme 3.1,[135] from (**199**).

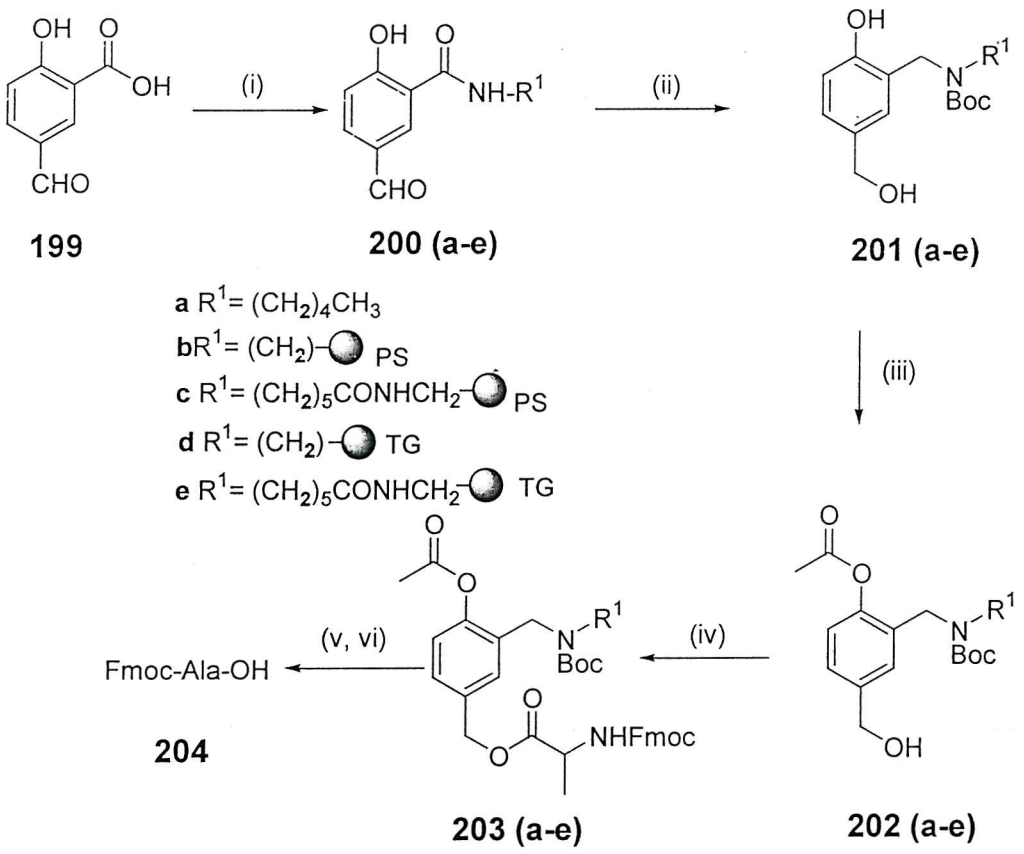

Scheme 3.1 Synthesis of pH cleavable linker (**203**) (i) R^1NH_2, DIC, HOBt, DCM, (ii) BH_3.THF/THF, 65°C, 48 h, Boc_2O, DCM, (iii) 1M NaOH (aq), 1-Acetyl-1*H*-1,2,3-triazolo[4,5-*b*]pyridine/THF, (iv) Fmoc-Ala-OH, DIC, HOBt, 4-DMAP, DCM, (v) 50%TFA/ DCM, 1h, (vi) K_2HPO_4 buffer 50 mM pH = 8

The synthesis started with 5-formylsalicylic acid (**199**), which was coupled to pentylamine to give (**200a**) (88%). This was then reduced with borane using the procedure described by Hall *et al.*[136] The amine was then protected without isolation with Boc_2O to give (**201a**), followed by selective acetylation[137] of the phenol using 1-acetyl-1*H*-1,2,3-triazolo[4,5-*b*]pyridine to give (**202a**) (90%). Esterification of the hydroxymethyl entity with Fmoc-Ala-OH using DIC/DMAP gave (**203a**) (86%). This was then used as a solution model for subsequent resin based chemistries.

The kinetics of linker cleavage in solution was monitored using RP-HPLC. The Boc protecting group was first removed by treatment with a 50% solution of TFA in DCM followed by removal of any volatiles. K_2HPO_4 buffer (50 mM, pH = 8) was then added. Samples were removed and quenched with 0.1 % TFA before injection and quantification using internal standards. The cleavage rate of Fmoc-Ala-OH was then followed as shown in Figure 3.13. The half-life of cleavage was 12 minutes and Fmoc-Ala-OH was recovered in 96% yield.

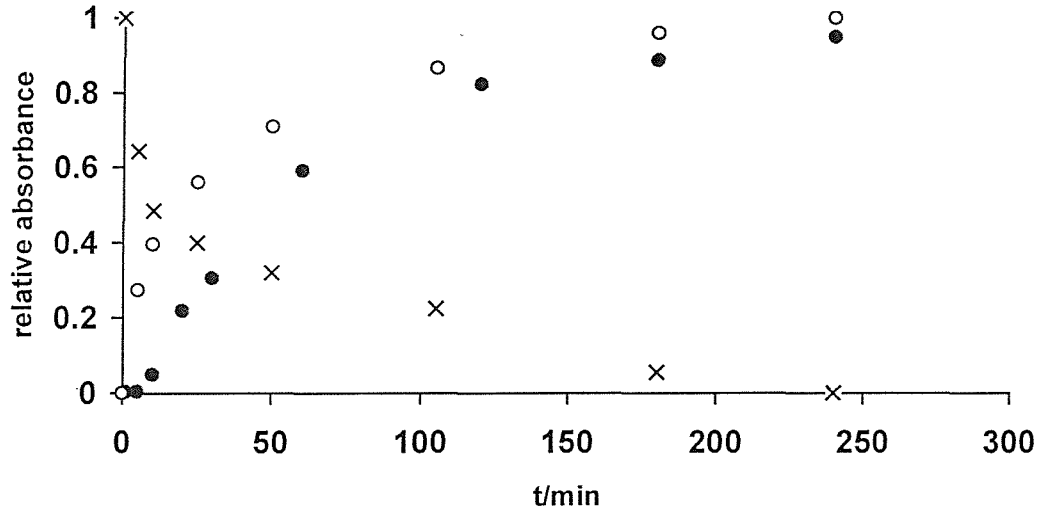

Figure 3.13 Kinetics of compound release from (**203a**) and (**203b**):
(x) disappearance of (**203a**); (○) production of Fmoc-Ala-OH from (**203a**); (●) production of Fmoc-Ala-OH from (**203b**).

3.3.2 Synthesis of new linker on solid support

The linker was synthesised directly onto the solid phase using both polystyrene and TentaGel resins (Scheme 3.1). Aminomethyl polystryrene resin was first coupled to 5-formylsalicylic acid (**199**) under standard reaction conditions to give the desired product (**200b**). The amide resin was converted to the secondary amine using a procedure described in the literature by Hall.[136] A mild and highly practical workup procedure was employed using iodine to promote the fast oxidative cleavage of the borane-amine adducts. When performed on the solid support, this mild method prevented premature release of products from the acid sensitive linker. After the reduction step and extensive washing, the resin was swollen in a THF-MeOH-$^{i}Pr_2EtN$ mixture (7:2:1). Iodine (2 equivalents in THF) was then added and the mixture was shaken for 1 h during which time the purple solution became discoloured as the iodine was consumed. The resin-bound amine was then treated with 2 equivalents of Boc_2O in dichloromethane at room temperature. Selective acetylation of the phenolic position was performed using the triazolide reagent 1-acetyl-1*H*-1,2,3-triazolo[4,5-*b*]pyridine.[137] The literature method was adapted for use on solid phase by using a large amount of THF as solvent, due to the poor swelling properties of the resin in aqueous NaOH.

In order to optimise the synthesis of a new linker on the solid phase, the spacer between the linker and polymeric support was varied, as it may be important in reducing the steric effect between the bulky polystyrene matrix and linker. A 6-aminohexanoic acid was the unit of choice for the spacer (Scheme 3.2).

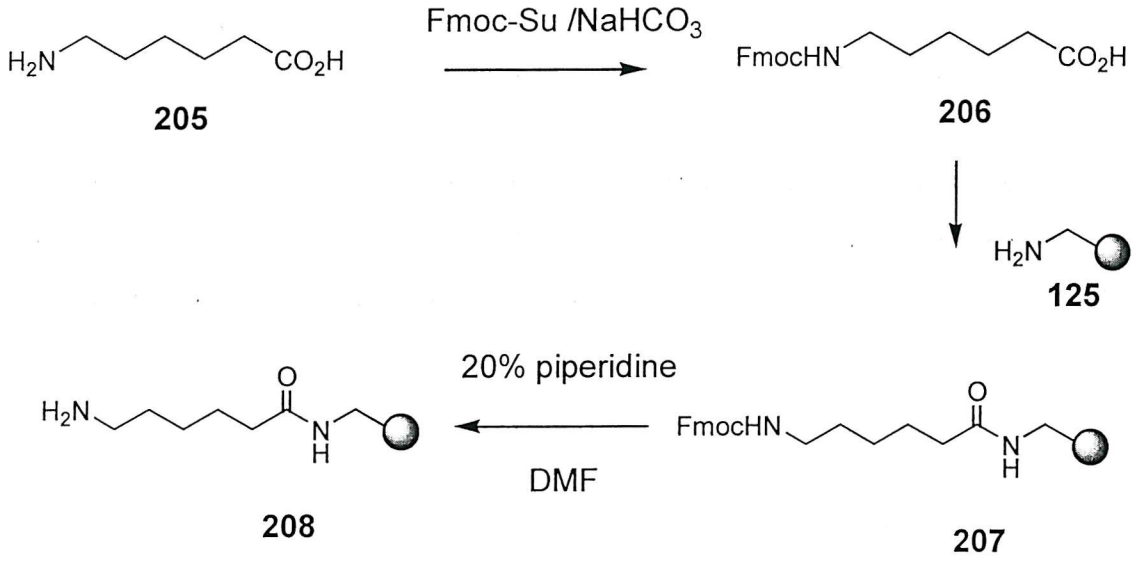

Scheme 3.2 Synthesis of spacer bond amino methyl resin

6-Aminohexanoic acid (**205**) was selectively protected with Fmoc succinimide and followed by coupling to aminomethyl resin (**125**). After treatment of the resin with 20% piperidine in DMF this gave a substitution of 0.41 $mmol.g^{-1}$ of (**208**). This resin was coupled to 5-formylsalicylic acid (**199**) under standard reaction conditions to give the desired product (**200c**). The amide resin was converted to the secondary amine using the procedure described above. With the linkers now available, it was possible to use them in synthesis and test linker cleavage efficiency.

The kinetics of the release of Fmoc-Ala-OH from compound (**203b**) was then carried out in the same manner as described above. As expected, product release was slower than that obtained in solution and a half-life of 40 minutes was observed (Figure 3.13). The kinetics of Fmoc-Ala-OH release from compound (**203c**) was identical to that of (**203b**). Hence the small hydrophobic spacer attached to the resin had no effect on the kinetics of cleavage. Other compounds released from the linker immobilised on PS included Fmoc-Phe-Ala-OH, Fmoc-Gly-Phe-Ala-OH, and 4-hydroxy-7-trifluoromethyl-3-quinoline carboxylic acid. In all cases a quantitative recovery of the compounds released was achieved.

The linkers attached to TentaGel (compounds **203d** and **203e**) were found to cleave substantially upon treatment with the acid used to remove the amino protecting group. Use of various percentages of TFA (5–50%) and reaction times (1–30 min) to remove the Boc group still resulted in substantial cleavage of Fmoc-Ala-OH. An analogous structure to that of (**203d**) was synthesised, but using Bpoc instead of Boc as the amino protecting group. Here, after deprotection with acetic acid, most of the Fmoc-Ala-OH was released.

Following the demonstration that the linkers were effectively cleaved from PS resin under phosphate buffer (pH = 8) conditions, intermediate (**202c**) was used in the synthesis of the antibacterial squalamine analogue (**213**) (Scheme 3.3).

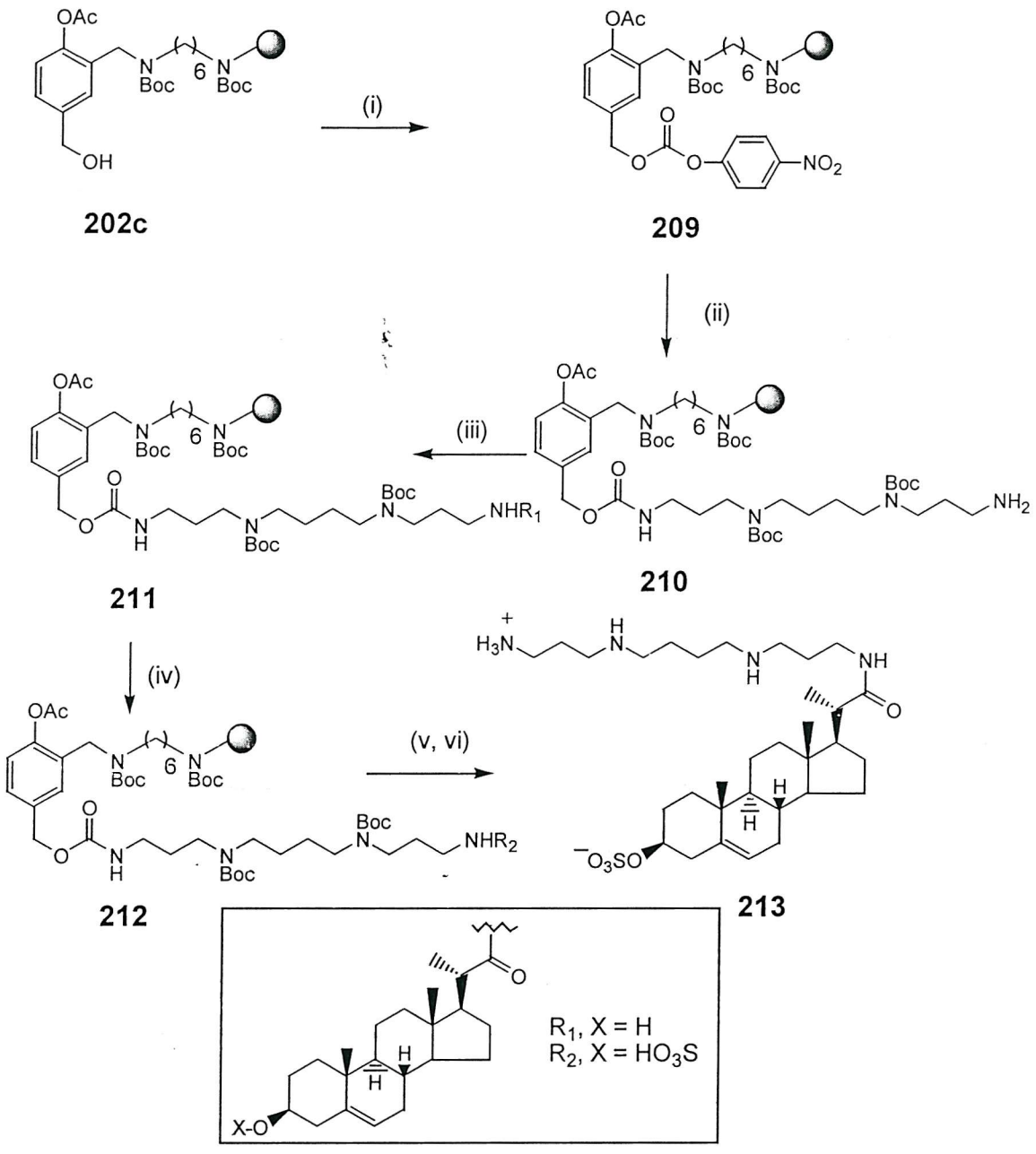

Scheme 3.3: Reagents and conditions: (i) *p*-O_2N-PhO-COCl, pyridine, DCM, RT (ii) $NH_2(CH_2)_3NBoc(CH_2)_4NBoc(CH_2)_3NH_2$ (iii) 3β-acetoxybisnor-5-cholenic acid/ DIC/HOBt DCM: DMF (3:1) (iv) $Pyr.SO_3$, $CHCl_3$ (v) 50%TFA/DCM, RT, 1h, (vi) 50 mM K_2HPO_4, pH = 8.0, 24 h.

Linker (**202c**) was transformed into an active carbonate using *p*-nitrophenyl chloroformate. The linker was then functionalised using diBoc-protected spermine to give compound (**210**). The spermine template was coupled to 3β-acetoxybisnor-5-cholenic acid and compound (**211**) was converted into the sulfate derivative using sulfur

trioxide in pyridine.[138] This compound was cleaved from the resin by activating with 50% TFA/DCM followed by treatment with pH 8.0 phosphate buffer (60% yield).

3.4 Conclusion

In summary, the synthesis of a new safety catch linker was achieved on the solid phase. It was used for the first solid phase synthesis of an analogue of the shark derived antibacterial agent squalamine, and these linkers are suitable for cleaving directly within a biological assay.

Chapter 4

Synthesis and evaluation of transfection agents using a safety-catch linker

4.1 Introduction

The introduction of DNA into cells is a necessity in molecular biology. It has been used for genetically engineering microoganisms, plants and animals. Interest in this research area has also dramatically increased with the arrival of **gene therapy**. This therapeutic approach is based on systems that provide efficient *in vivo* transfer and expression of genetic information in the target cell. Gene therapy can be defined as the use of genes as medicines to treat disease or the delivery of nucleic acid to patients for some therapeutic purpose.[139] For example, if a patient is suffering form a disease caused by a known genetic defect, delivery of a correct copy of the defective genes to the diseased cell could be expected to correct directly for the genetic defect and therefore treat the disease. In the case of a patient suffering from a disease for which there is not a clear genetic cause but pathophysiology is well understood, the vector might be used to deliver a gene to the disease cells and hence disrupt the known disease pathophysiolgy in some way. Although gene therapy has the potential to correct a variety of diseases such as inflammation, cancer or neurodegeneration, there are still some problems which need to be solved. One major problem is the vector that carries the DNA into the cell. Both viral and non-viral vectors have been investigated but viral vectors have limited use since many viruses only infect dividing cells while viruses are of fixed sizes which sometimes limit the amount of DNA they can carry. Moreover, viral genes integrate randomly and may disrupt host genes. The main limitation of viral vectors is immunlogical problems as a function of high dose or repeated use.[140] Consequently, there has been increasing attention focused on synthetic non-viral vectors. These vectors are based on cationic compounds such as cationic liposomes, which are heterogeneous lipid vesicles. These vesicles are made up of a cationic head group attached by a linker to a hydrophobic moiety and are known as **cytofectins**; cyto-for cell and-fectin for transfection. They mediate gene delivery by interacting electrostatically with negatively charged DNA to form complexes, which are capable of entering a cell.

This process of introducing nucleic acids into cells by a non-viral method is defined as **transfection.** This process is distinct from infection, which is a viral method of nucleic acids introduction into the cells. Progress in transfection technology was relatively slow until the advent of molecular biology for cloning plasmid DNA. This technique provided the means to prepare and manipulate DNA sequences and enabled the ability to prepare virtually unlimited amounts of relatively pure DNA for transfection experiments. As the ability to prepare DNA for transfection became easier, additional methods, such as electroporation and liposome-mediated transfer, were developed to enable more efficient transfer of the nucleic acids into a broad range of cultured mammalian cells.[141]

4.2 Transfection technologies

Many transfection techniques have been developed. Desirable features include high efficiency transfer of nucleic acid into the appropriate cellular organelle such as DNA into the nucleus, minimal interference with normal cell physiology, low toxicity, ease of use, reproducibility, successful generation of stable transfectants, and *in vivo* efficiency. The techniques developed for non-viral gene transfer can be broadly classified as either being chemical reagents or physical in nature.

4.2.1 Chemical reagents

4.2.1.1 Calcium phosphate became a popular transfection technique following the systematic examination of this method by Graham and Van der Eb.[142] Their study examined the effect of different cations, phosphate concentrations and pH on the parameters of transfection. Although the mechanism remains obscure, it is believed that the transfected DNA enters the cytoplasm of the cells by endocytosis and is transferred to the nucleus.

4.2.1.2 DEAE-dextran is one of the chemical reagents used for the transfer of nucleic acids into cultured mammalian cells.[143] DEAE-dextran is a cationic polymer that associates with negatively charged nucleic acids. An excess of positive charge, contributed by the polymer in the DNA/polymer complex, allows the complex to come into closer association with negatively charged cell membranes. Uptake of this complex is presumably by endocytosis. This technique is generally useful for stable transfection studies that rely upon the integration of transferred DNA into the chromosome.[144] Other

synthetic cationic polymers that have been used for the transfer of DNA into cells, includes polybrene.[145], polyethyleneimine[146] and PAMAM dendrimers.[147]

4.2.1.3 Liposomes (artificial membrane vesicles) have been used to deliver DNA into cells.[141] Liposome-mediated delivery offers advantages such as relatively high efficiency of gene transfer, ability to transfect certain cell types that are intransigent to calcium phosphate or DEAE-dextran, successful delivery of DNA of all sizes from synthetic oligonucleotides to yeast chromosomes. Cells transfected by liposome techniques can be also used for transient and longer term experiments that rely upon integration of the DNA into chromosomes.

4.2.2 Physical methods

4.2.2.1 Directed microinjection

Direct microinjection onto cultured cells or nuclei is an effective, although laborious technique to deliver nucleic acids into cells. This method has been used to transfer DNA into embryonic stem cells that are used to produce transgenic organisms.[148] However, this technique is not appropriate for studies that require a large number of tranfected cells.

4.2.2.2 Electroporation

The use of pulsed electric fields to introduce DNA into cells in culture has been termed electroporation.[141] This method has been used to introduce DNA into a variety of animal cells, plant cells and bacteria. The mechanism for entry into the cell is based upon perturbation of the cell membrane by an electrical pulse, which forms pores that allows the passage of nucleic acids into the cell.[149] Electroporation works well with cell lines that are refractive to other techniques such as calcium phosphate. However, this technique requires fine-tuning and optimisation of duration and strength of the pulse for each type of cell used. Furthermore, the conditions established in one laboratory do not necessarily work well in another!

4.2.2.3 Biolistic particle delivery

Another physical method of gene delivery is biolistic particle delivery. This method relies upon high velocity delivery of nucleic acids on microprojectiles into recipient cells.[150] This method has been successfully employed to deliver DNA into cultured cells, as well as into cells *in vivo*.[151]

4.3 Structures of cationic liposomes

The use of cationic liposomes in gene delivery was first reported by Felgner and co-workers[152] who developed the cationic liposome now available commercially as Lipofectin (Figure 4.1). Lipofectin consists of a 1:1 mixture of bis-ether (2,3-dioleyloxy) propyl-*N,N,N*-trimethylammonium chloride (DOTMA) (**214**) and the diester dioleoylphosphatidyl ethanolamine (DOPE) (**215**).

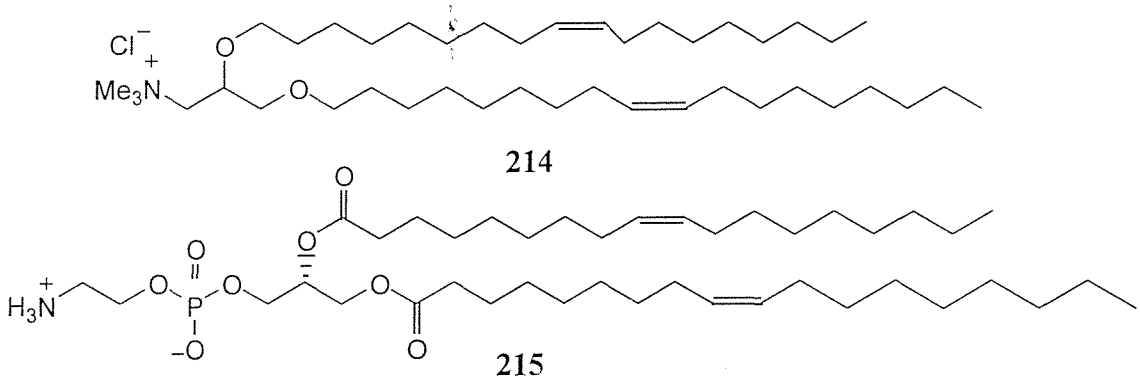

Figure 4.1 Cationic liposome now available commercially as Lipofectin

Dioctadecylamidoglycylspermine (DOGS), (*Transfectam* **216**) and dipalmitoyl-phosphatidyl ethanolamine spermine (DPPES) (**217**)[153] were the first polyamine based lipid gene delivery vectors. These molecules contain a polyamine covalently bound to two hydrophobic chains (Figure 4.2). When mixed with DNA, these polyamines cause condensation and formation of self-organised nuclear particles with an excess of cationic lipid.

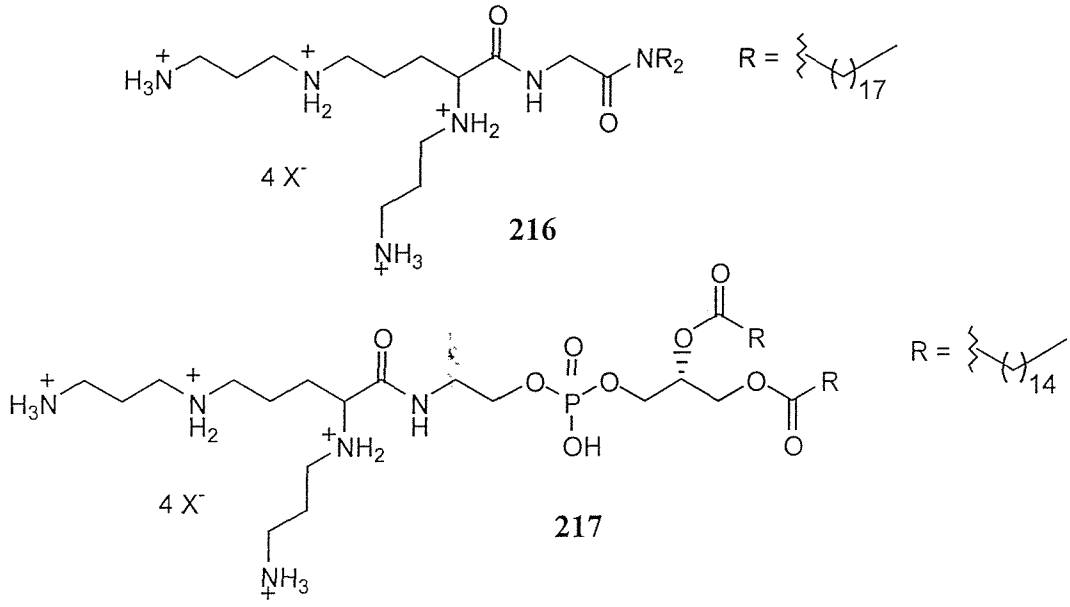

Figure 4.2 The first polyamine based lipid gene delivery vectors

Cationic facial amphiphiles are another polyamine based system showing promise for gene delivery. For example, spermine, tetraethylenepentamine and pentaethylenehexamine have been conjugated to bile acid based amphiphiles and then mixed with DOPE (1:1) to facilitate transfection.[154] Although most tranfection agents contain a cationic head group attached to a hydrophobic tail such as cholic and lithocholic acid derivatives (**218**) and (**219**), the more hydrophilic bile acid conjugate (**220**) had the greatest tranfection activity (Figure 4.3).

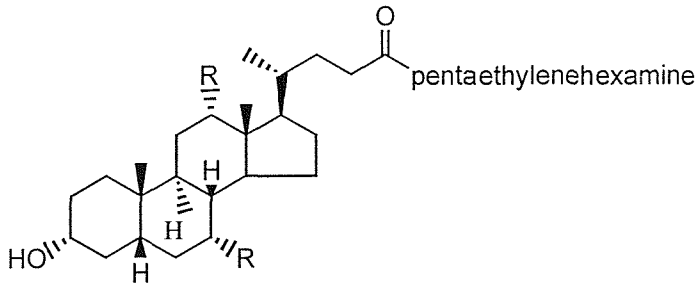

218 R = OH
219 R = H
220 R = α-glucose

Figure 4.3 Polyamines conjugated to cholic acid derivatives

The first reported cholesterol derivative was 3β-[*N*-(*N'*,*N'*-dimethyl aminoethane)-carbamoylcholesterol (DC-Chol **221**) and is still widely used. This compound can be used in combination with DOPE **215** to prepare liposomes that have been shown to efficiently transfect mammalian cells (Figure 4.4).[155]

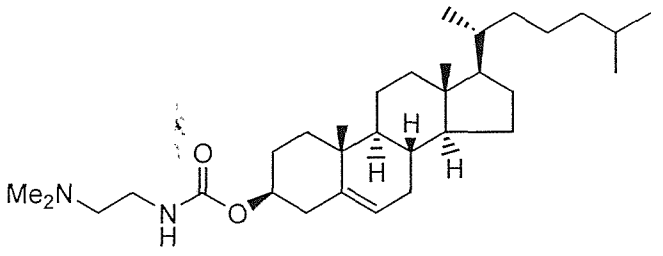

221

Figure 4.4

Moreover, polyamines DC-Chol analogues (**222**), (**223**) and (**224**) showed significant improvements on gene delivery efficiency over DC-Chol/DOPE liposomes formulated in a similar way (Figure 4.5).[156]

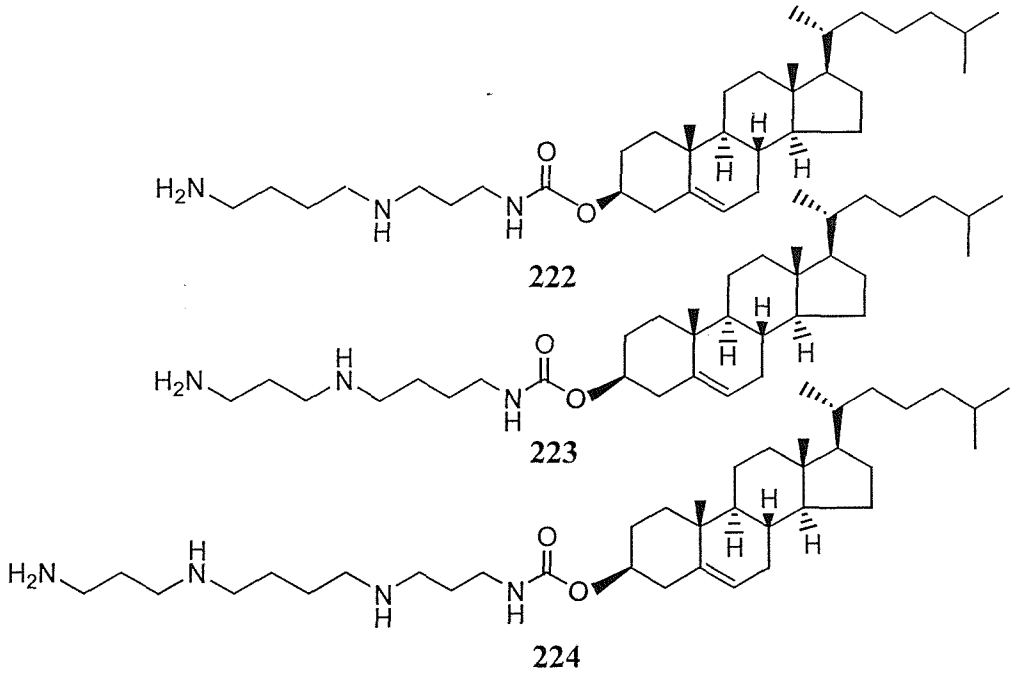

222

223

224

Figure 4.5 Polyamine containing DC-Chol analogues

Two of the most potent liposomes reported to date are polyamine CTAP (**38**)[32] and lipid 67 (**225**). Liposomes formed from CTAP (**38**) delivered genes 100 times more efficiently

in mouse lung than DC-Chol/DOPE liposomes. Only liposomes containing a T-shaped spermine analogue lipid 67 (**225**) have been reported to function at this level of efficiency *in vivo* (Figure 4.6).

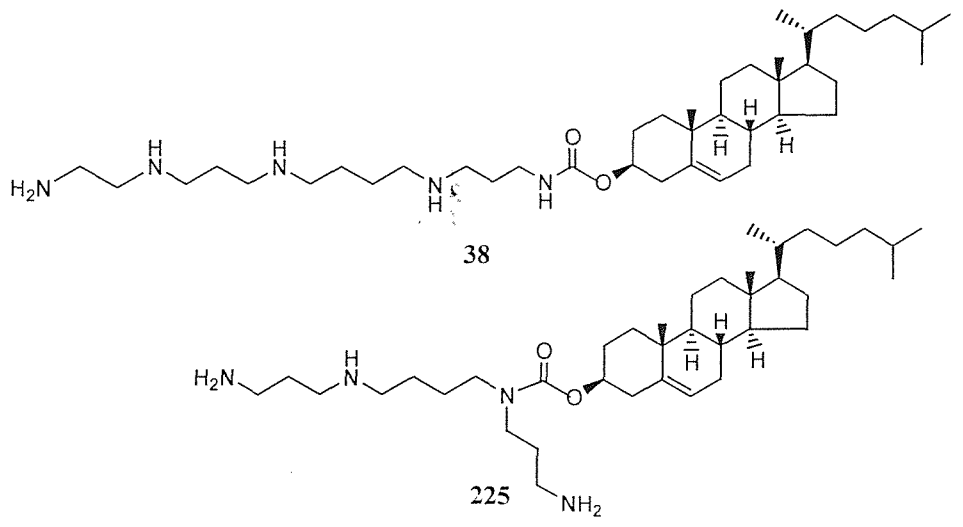

Figure 4.6 The most potent liposomes

Other polyamine derivatives have also been described including cholesteryl-spermidine (**226**)[157] and bis-guanidinium-trencholesterol BGTC (**227**).[158] BGTC (**227**) is very efficient for transfection into a variety of mammalian cell lines (Figure 4.7) when used as a micellar solution. This result revealed the usefulness of cholesterol derivatives bearing guanidinium groups for gene transfer.

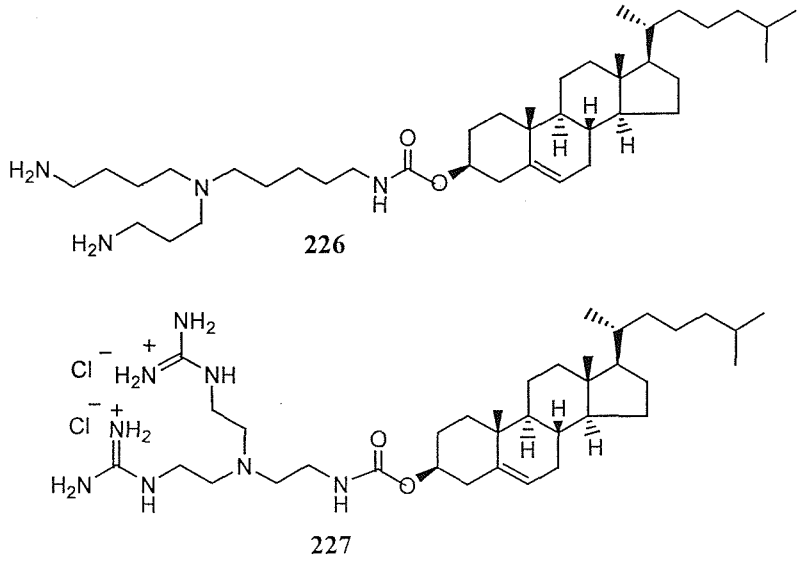

Figure 4.7

4.4 Methods for cationic liposome formation

The formulation of transfection agents into cationic liposomes, with or without a neutral co-lipid, has involved a number of different procedures. These include sonication and/or vortex-mixing of an aqueous dilution of an ethanolic stock solution. The method of formulation is undoubtedly important, but the extent to which this affects the efficiency of nucleic acid transfer has yet to be properly evaluated. DOTMA and its analogues are usually formulated into cationic liposomes with the neutral co-lipid DOPE (**215**). Liposomes are prepared by vortex-mixing equimolar amounts of transfection agent and DOPE (**215**) at room temperature to produce large multilamellar vesicles (MLVs). Sonication produces smaller unilamellar vesicles (SUVs) suitable for gene transfection.[159] Cationic liposomes with DOSPA are available commercially as LipofectAMINE. It contains DOSPA and DOPE in a 3:1 ratio. Cationic liposome DOTAP is also available without neutral co-lipid. Transfectam is formulated simply by tenfold dilution of an aqueous ethanol stock solution of DOGS.[153] Cholesterol derivatives are usually formulated into liposomes with DOPE (**215**) but in a number of different ways. For example, DC-Chol (**221**) is usually combined with DOPE (**215**) in a 3:2 molar ratio and the liposomes are generated either by sonication alone[155] or vortex-mixing followed by sonication.[160] Polyamine lipid 67 (**225**) and CTAP (**38**) have been transformed into liposomes, in combination with DOPE (**215**) in a 1:2 molar ratio by vortex-mixing alone.[32]

4.5 Mechanism of nucleic acid delivery

The mechanism of cationic liposome mediated DNA delivery is complicated. This process will be discussed in three stages. Firstly, the structure of complexes between liposomes and nucleic acids will be described. Nucleic acid delivery appears to be most efficient when the complexes are formed under conditions where the ratio of liposome positive charges to nucleic acids negative charges lies around 1 and above. Secondly, the mechanism involved in the entry of cationic liposome/nucleic acid complexes into cells will be discussed. The predominant mechanism now appears to be endocytosis, irrespective of the type of cationic liposome involved. Therefore, the evidence for this will be presented together with some other possible mechanisms for cell entry. Finally, the fate of nucleic acids will be described with special emphasis on the trafficking of nucleic acids to the nucleus where in most cases is their potential therapeutic site of action.

4.5.1 Structure of complexes between liposomes and nucleic acids

Felgner and Ringold have shown that cationic liposomes electrostatically bind DNA.[161] Experimental evidence shows that cationic liposomes/DNA complexes are very heterogenous and dynamic, varying in size and shape depending upon the molar ratio of cationic liposome to nucleic acid. The most dramatic changes in structure appear to occur when the charge ratio is around 1. The first experiments were carried out by Gershon *et al.*, using ethidium bromide as a fluorescent probe for exposed DNA pairs,[162] titrating fixed concentrations of DNA with liposome. They observed that DNA was generally accessible until the positive/negative charge ratio approached 1, at which point extensive DNA masking was diagnosed as shown by a rapid decline in fluorescence intensity.

4.5.2 Entry of cationic liposome/nucleic acid complexes into cells

The first step of cationic liposome mediated DNA delivery is the entry of the complex into cells. It was initially thought that membrane fusion between liposome and cell membrane was the primary means of cell entry.[152,163] However, cationic liposome/DNA complexes fuse much less readily with negatively charge membranes, indicating that cell entry by membrane fusion may not apply.[164] Instead, evidence now suggests that slow endocytosis of intact complexes is the primary method[165] and it is mediated by proteoglycan interactions.[166] Proteoglycans are a fundamental component of basement membranes and the extracellular matrix. They play a pivotal role in cellular proliferation, migration and differentiation. Sulfated proteoglycans are among the most negatively charged components of the cells. They consist of a core protein covalently linked to one or more sulfated glycosaminoglycans such as heparin, heparan sulfate, dermatan sulfate and keratan sulfate. This process was first suggested by Behr *et. al.*[167] and has been beautifully observed by Zabner *et al.* who used electron microscopy to follow the cell entry of gold-labeled DNA liposomes (Figure 4.8).[168]

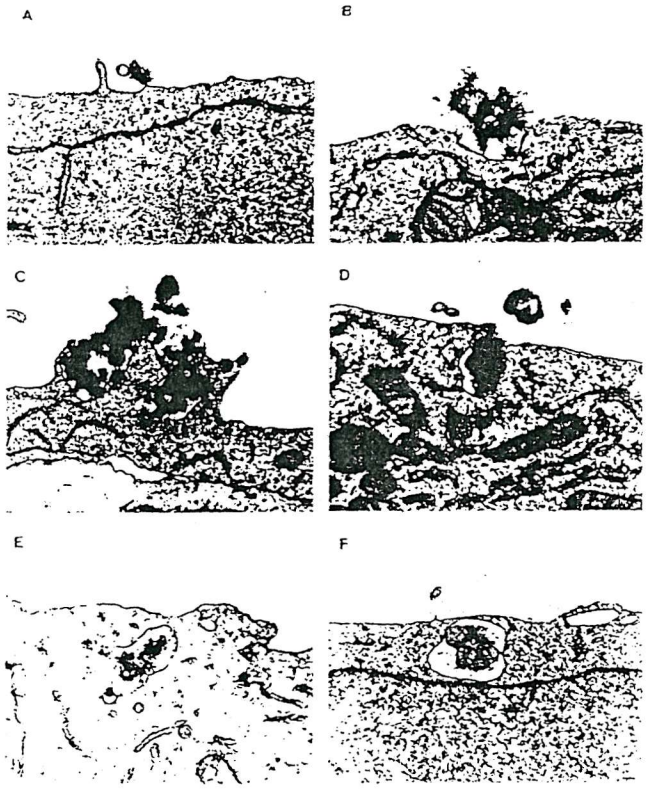

Figure 4.8: Electron photomicrographs of COS cells transfected with gold-labeled DNA complexed with liposomes. Cells were exposed to DMRIE/DOPE/DNA complexes and then removed for electron microscopy at the following times: *panel A*, 5 min; *panel B*, 30 min; *panel C*, 1 h; *panel D*, 6 h; *panel E*, 24 h; *panel F*, 24 h. Cells transfected with plasmid that had not been labelled with gold are shown in *panel F* (reproduced with permission from Zabner *et al*).[168]

After an initial association to the cell surface, complexes enter by endocytosis and remain localised within a vesicle or endosome. The subsequent intracellular fate of the endosome-trapped complex was then monitored. Upwards of 24h after internalisation, complexes were found to accumulate in the perinuclear region. This was interpreted to be the result of endosome fusion, thereby allowing enclosed complexes to coalesce and form macromolecular lipid/DNA structures. These structures are highly ordered and comprise an array of regularly packed tubes in which DNA is surrounded by bilayers or tubular monolayers of lipid.

4.5.3 Trafficking of DNA into the nucleus

After liposome/DNA complex entry into the cells, not all nucleic acids will be functional. This point has been shown by Zabner *et al.*[168] They found that gene expression occurred in less than 50% of cells, even though endocytosis was determined to have an efficiency of at least 80%. Unfortunately, a large proportion of delivered nucleic acids are usually unable to escape from the endosomal compartments into the cells cytoplasm after entry. As a result, cationic liposome mediated delivery actually appears to be a very wasteful and inefficient way to deliver DNA into cells. When DNA does succeed in escaping from endosomes, most recent evidence indicates that it does so at an early stage after endocytosis has taken place. The mechanism of early endosome escape is not well understood, but when DOPE forms part of the cationic liposome, escape may aided by the tendency of DOPE to promote significant polymorphic charges in the lipid phase under physiologically relevant conditions. Therefore, DOPE could provide the means for endosome disruption by promoting membrane fusion. Xu and Szoka proposed a model for early endosome breakout in which complexes destabilise the endosome allowing the DNA to escape (see Figure 4.9).[169] Electrostatic interaction between cationic liposome and endosome membrane induces the flip-flop of anionic lipids from the monolayer of the endosome membrane that face the cytoplasm.

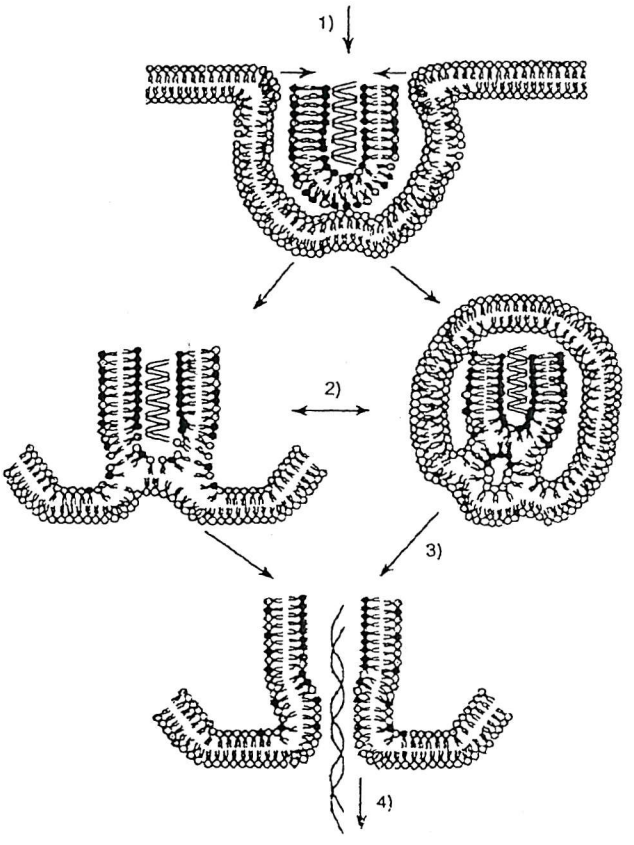

Figure 4.9. Mechanism of uptake and release of plasmid DNA from the complex. (Step 1) After electrostatic interaction with the cell membrane, cationic liposome/DNA complexes are endocytosed. (Step 2) In the early endosome, membrane destabilization results in anionic phospholipid flip-flop. (Step 3) The anionic lipids diffuse into the complex and form a charge neutral ion pair with cationic lipids. (Step 4) The DNA dissociates from the complex and is released into the cytoplasm (reproduced with permission from Xu and Szoka).[169]

4.6 Genetic reporter systems[170]

Genetic reporter systems have contributed greatly to the study of eukaryotic gene expression and regulation. Reporter genes have played a significant role in numerous applications,[171] and are frequently used as an indicator of transcriptional activity in cells.[172] Typically, a reporter gene is joined to a promoter sequence in an expression vector that is to be transfected. Following transfer, the cells are assayed for the presence of the reporter by directly measuring the amount of mRNA or the reporter protein itself or the enzymatic activity of the reporter protein. An ideal reporter gene is not endogenously

expressed in the cell type of interest, and is amenable to assays that are sensitive, quantitative, rapid, easy, reproducible and safe.

The availability of a wide variety of naturally occurring and genetically engineered reporter genes allows an extensive number of reporter proteins to be monitored by a variety of detection systems, such as electrochemical, fluorescence, and bio and chemi-luminescence. Researchers also have at their disposal, among the several luminescence-based reporter gene systems, a wide range of reporter proteins emitting at different wavelengths. Thus, there exists a palette of colours to choose from, depending on application. Additional reporter proteins with different emission wavelengths are continuously becoming available, further extending the applicability of these methods. For instance, many organisms, including single cell algae, sea walnuts, jellyfish, fireflies, and even some mushrooms are bioluminescent because certain photoproteins, or enzymes, are present or some possess substrates that cause chemo-illuminescence. Hence, all these organisms, could be a source of reporter proteins/systems.

Desirable characteristics in a reporter protein include detection with high sensitivity, wide dynamic range of response, and ease of use. Moreover, the ideal reporter protein should be environmentally safe, give rise to an easily discernible signal from the background. Sensitivity can be a function of several factors, including the detection method, efficiency of expression and reporter protein turnover number if the reporter is an enzyme.

One of the first proteins to be used as a reporter was chloramphenicol acetyltransferase (CAT) from *E. coli*. This protein, like other nonluminescent reporter proteins, used synthetic substrates that generated products that could be monitored by different detection systems.[173] CAT catalyses the transfer of an acetyl group from acetylcoenzyme A (acetyl-CoA) to the antimicrobial drug chloramphenicol. The system originally developed used ^{14}C-labeled chloramphenicol or ^{14}C-labeled acetyl-CoA to from a radioactive product that was monitored after extraction. It is now possible to use fluorescent chloramphenicol substrates which, upon action of CAT, form the corresponding acetylated fluorescent product. It is still necessary, however, to separate the product from the substrate. This poses a disadvantage in CAT-based methods. The reason that the CAT system is still used as a reporter is that its activities are not native to eukaryotic cells.

Alkaline phosphate (AP), β-galatosidase and β-glucuronidase are well-studied enzymes that have been used as reporter proteins. The common feature of these enzymes is that they are phosphohydrolases that function optimally at alkaline pH. A drawback is that some form of alkaline phosphatase activity is present in practically all cell types. On the other hand, alkaline phosphatases are versatile because a wide range of substrates can be detected with different methods, depending on the desired application.[174] Bacterial β-galatosidase encoded by the gene l*acZ* of *E. coli* catalyses the hydrolysis of β-galatosides. The β-galatosidase gene can be successfully used in prokaryotic and eukaryotic cells. The level of endogenous β-galatosidase activity varies greatly within cells; however, it is possible to distinguish between mammalian and bacterial enzymatic activity by altering the pH. β-glucuronidase is one of most popular reporter proteins for use in plants. Many plants lack endogenous β-glucuronidase activity.[175] This enzyme is a hydrolase, catalysing the cleavage of β-glucuronide. Alkaline phosphatase (AP), β-galatosidase, β-glucuronidase are all enzymes that have a high turnover number and can generate a strong signal using any one of a number of fluorescence, electrochemical, and chemiluminescence substrates, many of which are sold as part of commercially available kits.

The use of luminescent reporter proteins has grown in recent years because of the proteins' low detection limits and low, if any, endogenous activity in most cells. The most commonly used luminescent reporter proteins include luciferase (bacterial and firefly) and aequorin.[176] The genes encoding each of these proteins have been isolated. Other luminescent protein exists and research continues to discover new light-emitting proteins and their corresponding genes. Efforts also continue to modify known genes to alter excitation and emission wavelengths, increase luminescence quantum yields, and enhance stabilities.

Firefly luciferase was first isolated from the North American firefly *Photnus pyralis* and differs from the bacterial luciferases in the structure and light-emitting reaction. Firefly luciferase is encoded by the *luc* gene. In the presence of adenosine triphospate (ATP) and molecular oxygen, firefly luciferase catalyses the oxidation of its substrate luciferin to oxyluciferin yielding CO_2 and light (λ_{max} = 560 nm, quantum yield = 0.88). The bioluminescence signal is linear over 8 orders of magnitude of luciferase concentration, and enzyme can be detected at subatomolar level, making this luciferase an attractive choice for quantitative analytical applications.[177]

4.7 Application of green fluorescent protein

Green fluorescent protein (GFP) has become a versatile tool for monitoring mammalian expression and protein localisation in the field of biochemistry, molecular and cell biology, high-throughput screening and gene discovery.[178] GFP was originally isolated from the jellyfish *Aequorea Victoria*. Following the cloning of the GFP gene,[179] the protein has been used extensively as an *in vivo* marker and as a monitor of dynamic processes inside living organisms.[180] Native GFP has excitation maxima at 395 nm and 470 nm and emits light at 509 nm with a shoulder at 540 nm. The quantum yield of GFP (0.85) is comparable to that of fluorescein. The fluorescence of GFP is the result of an internal chromophore formed by post-translational cyclisation of three amino acids, Ser65-Tyr66-Gly67.[181] The unique three-dimensional structure of GFP, a series of β-sheets, protects the internal chromophore from the surrounding environment.[182]

GFP has several characteristics that make it an excellent reporter protein. Unlike other bioluminescent proteins and enzymes, GFP does not require substrates or co-factors to emit light. Because of the protected location of the chromophore inside the β-barrel of the protein, GFP retains its fluorescence capability under mild denaturants, heat, detergents, and most common proteases. The fluorescence is also stable at pH 7-12.[179] In addition, GFP is non-lethal when expressed at high levels in various cells. Most importantly, mutation of the gene has allowed proteins with different spectral properties to be created, such as increased fluorescence intensity and shifted wavelengths of excitation and emission.

Typically, the control reporter gene is driven by a strong, constitutive promoter and is co-transfected within experimental vectors. The regulatory sequences are linked to a second reporter gene so that the relative activities of the two reporter gene products can be assayed individually. Control vectors can also be used to optimise transfection methods. Gene transfer efficiency is monitored by assaying reporter activity in cell lysates or by staining the cell *in situ* to estimate the percentage of cells expressing the transfected gene.

4.8 Aims

The aims of this part of the project were to use a solid phase polyamine scaffold to synthesise delivery vehicles for transfection using a linker which should allow cleavage directly within the assay vehicle. The compounds were to be based on spermine conjugated to cholesterol or other lipids which would be characterised by their cationic

moieties and by their solubility behaviour in the aqueous phase. The strategy was first to focus on ***Green fluorescent protein (GFP)*** as a reporter gene to monitor the transfection efficiency in *E. coli.* and the ND7 cell line.

4.9 Results and discussions

As an extension to solid phase polyamine chemistry a new safety catch linker was designed (see Chapter 3). Here the synthesis of a variety of transfection agents was investigated using this linker. The design of the transfection agents was based upon the known behaviour of cholesterol in the membrane bilayer and the liposome model for DC-Chol/DOPE liposomes proposed by Felgner *et al.* (Figure 4.10).[159]

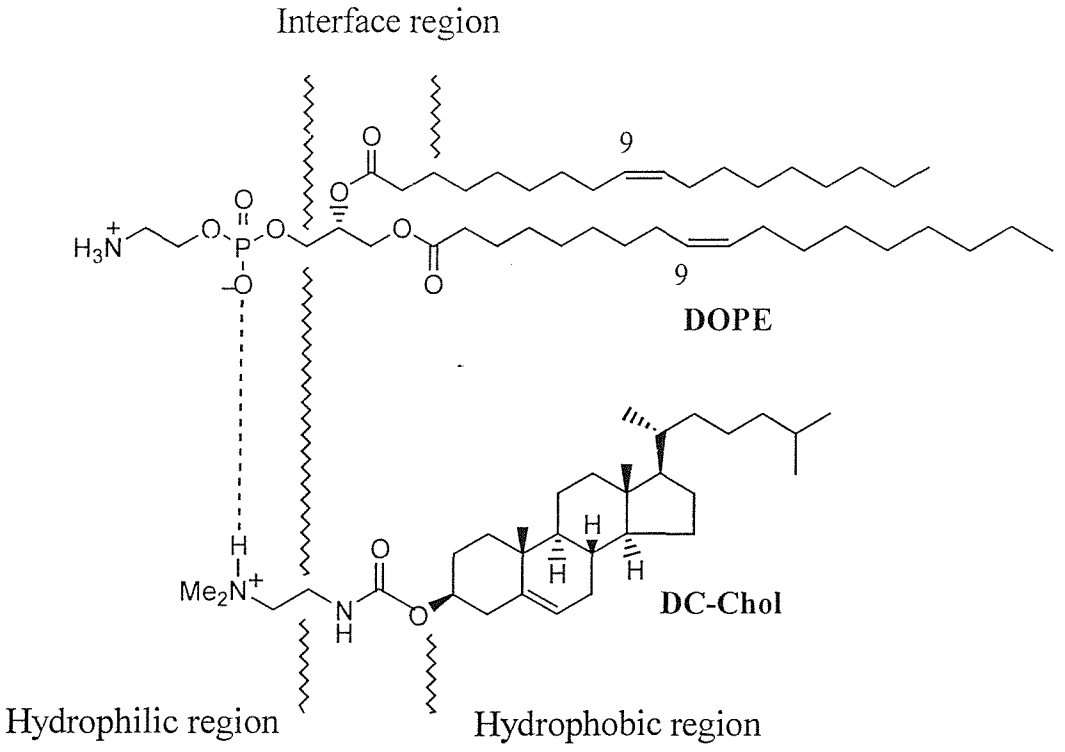

Figure 4.10 Putative alignment of DC-Chol and DOPE in cationic liposome bilayer.

According to this model, carbon atoms C-1 to C-9 of the oleoyl side chains of DOPE pack against the four fused chlolesterol rings of DC-Chol so that the phosphate ester group of DOPE and protonated tertiary amine functionality of DC-Chol are aligned and neutralise each other. The positive charge of the liposome then derives from the protonated ethanolamine side chain of DC-Chol. The model indicates that the methylene spacer between the carbamoyl and the first amine functional group of a given DC-Chol

polyamine analogue should be two or three carbon atoms to maintain charge complementation with DOPE.

Spermine derivatives were first planed as a series of model compounds. In order to avoid the difficulties in handing polyamine compounds, a solid phase synthesis allowed rapid preparation of a great number of differing monofunctionalised polyamines. Cationic lipids are composed of three elements as shown in Figure 4.11. The strategy including structure-activity relationship (SAR) studies focused on a spermine linker which modified the cationic moiety and allowed variation in the length of the lipid chains.

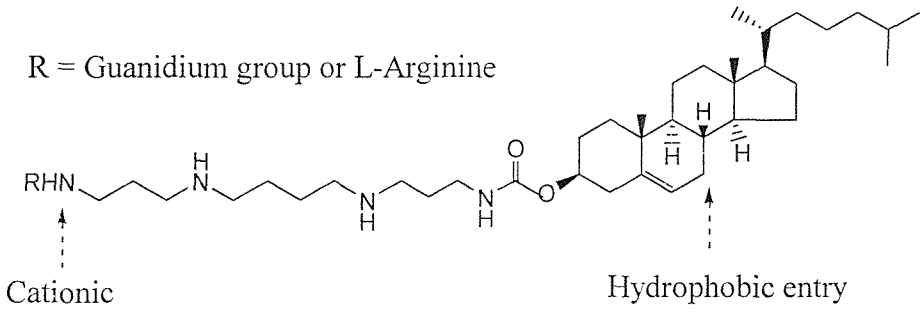

Figure 4.11 General composition of cationic lipid for DNA delivery

In order to release the compounds directly into aqueous solution for biological screening, it was necessary to use a linker allowing for selective cleavage of the product from the polymer support under mild conditions. Linkers which provide high stability during the synthesis of a variety of compounds but which allow for the mild cleavage of products from the solid phase are known as **safety catch linkers** (see details in Chapter 3). The linker used was the one described in detail in Chapter 3.

4.9.1 Synthesis a series of transfection agents using the novel safety-catch linker

The series of spermine-based amphiphiles were constructed via solid phase parallel synthesis as depicted in Scheme 4.1 using the novel safety-catch linker. Selective phenolic acylation of resin bound (**228**) was performed using acetic anhydride in THF leaving the benzylic alcohol of (**202**) to be transformed into active ester (**209**) using *p*-nitrophenyl chloroformate. The linker was then functionalised using *bis*-Boc-protected spermine to furnish resin (**210**). The free amino group of (**210**) was then coupled to a series of lipid carboxylic acid derivatives (Figure 4.12) under standard peptide coupling conditions. Compounds (**230a-i**) were generated by activation of resin bound intermediates (**229**) with

50% TFA in dichloromethane followed by phosphate buffer (pH 8.0) assisted release into solution.

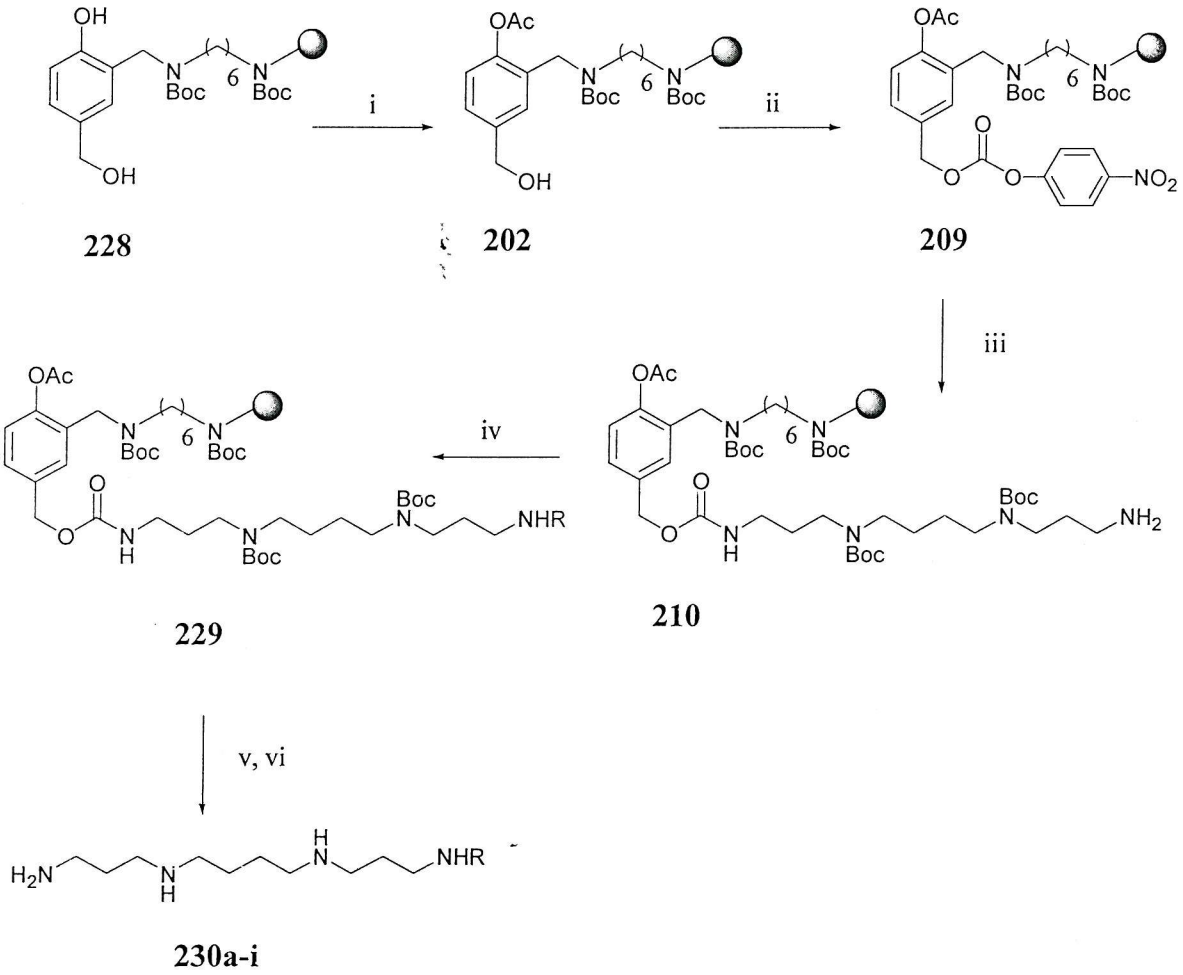

Scheme 4.1 Synthesis of transfection agents using the pH cleavable linker (i) 1N NaOH (aq), Ac_2O/THF, (ii) *p*-O_2N-PhO-COCl, pyridine, DCM, (iii) $H_2N(CH_2)_3NBoc(CH_2)_4NBoc(CH_2)_3NH_2$, (iv) RCO_2H/DIC/HOBt DCM: DMF (3:1), (v) 50%TFA/DCM, RT, 1h, (vi) K_2HPO_4 50 mM pH = 8.0, 24 h.

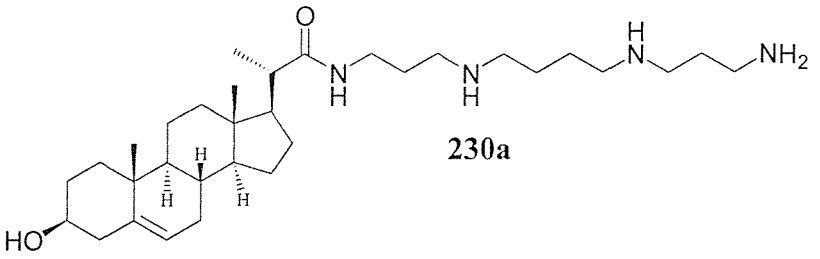

230a

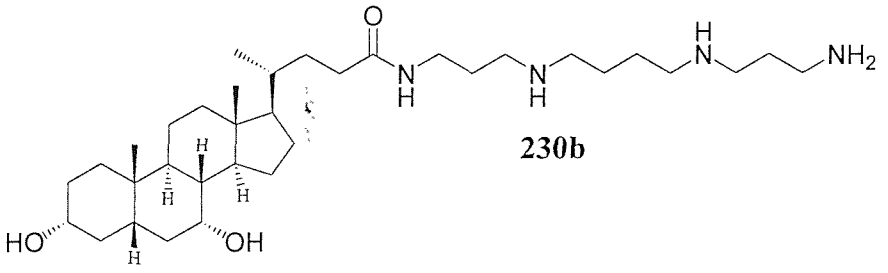

230b

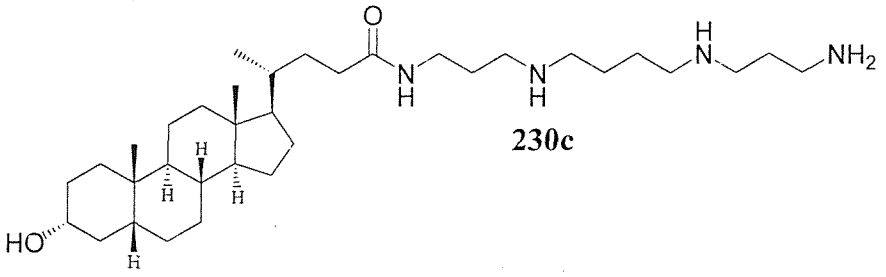

230c

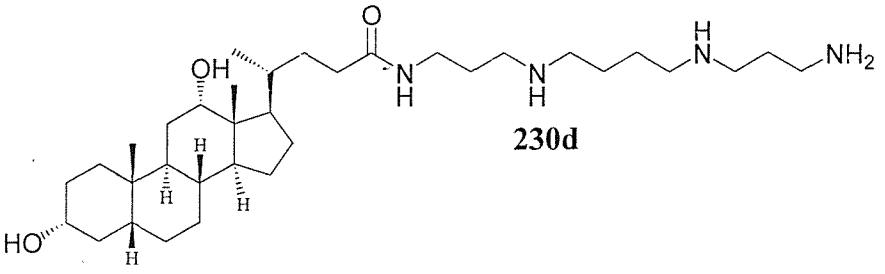

230d

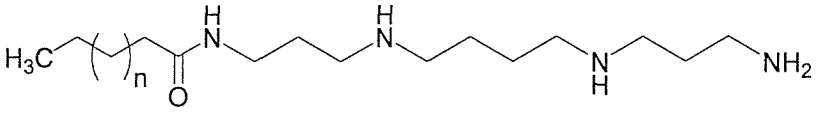

230e n = 16
230f n = 18
230g n = 20

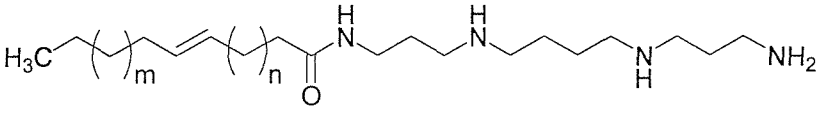

230h m = 5 n = 8
230i m = 5 n = 10

Figure 4.12 Transfection agents synthesised

4.10 Biological assays

With variety of transfection agents in hand, it was now possible to begin assaying their utility as transfection agents. One possible technique for screening transfection agents involved the use of bacterial cells as a host. It was initiated by considering simple bacteria cells because many principles of transcription control that operate in bacteria apply to more complex transcription process in eukaryotic or human cells. The bacteria, (e.g. *E. coli.*), were also used to prepare large amounts of relatively pure DNA for transfection experiments.

4.10.1 Expression plasmids

Two types of plasmid DNA were used in these studys: pGLO, a plasmid containing the arabinose (araC) promoter (obtained from Bio-Rad). This plasmid carried a gene encoding for the Green Fluorescent Protein (GFP), while the arabinose promoter precisely controls expression of the GFP in transformed cells. The second plasmid used was pEGFPLuc which encodes a fusion of enhanced green fluorescent protein and luciferase. Protein expression is under the control of the human cytomegatovirus (CMV) promoter. pEGFPLuc is a co-transfection marker that allows determination of transfection efficiencies in mammalian cells by fluorescence microscopy or a standard luciferase assay.

4.10.2 Preparation of DNA for transfection

The quality of the DNA used for transfection is critical. Purified plasmid DNA should be free from protein, RNA and chemical contamination. DNA may be purified using a plasmid preparation protocol, a CsCl gradient or chromatography. One measure of DNA purity is the ratio of absorbance at 260 to 280 nm; for transfection the A_{260}:A_{280} ratio should be at or above 1.8. The purified DNA should be ethanol precipitated and resuspended in sterile TE buffer to a final concentration of 1 mg/mL. The optimal amount of DNA to use for transfection depends on both the cell type and the reagent used.

4.10.3 Preparation of pGLO plasmid

The transformed cells were streaked out on agar plates containing ampicillin. A single colony from a plate was grown overnight a 37 °C in 5 ml of LB broth medium containing 100 $\mu g ml^{-1}$ ampicillin (see experimental to chapter 4). 1 ml of this culture was used for preparing plasmid DNA using a commercially available kit from Promega. Briefly, an overnight culture of bacteria was centrifuged and the pellet resuspended in 50 mM

glucose, 25 mM Tris.HCl, pH 7.5, 10 mM EDTA with lysozyme (40 mg/mL) and incubated at room temperature for 10 min. The solution was then lysed by alkaline lysis and plasmid DNA was isolated using a development of the silica binding method. In this method the DNA-binding matrix is diatomaceous earth (a cheap and convenient source of silica particles).[183] It was found that DNA prepared in this way was suitable for transfection of eukaryotic cells using our synthetic transfection agents.

4.10.4 Transformation efficiency

In order to calculate the transformation efficiency of bacteria, the transformed cells were grown on agar plates containing ampicillin and 0.2 % of arabinose. Each single colony assumed to be obtained from single cell and the total number of green fluorescent cells was determined under the UV light (366 nm). The transformed *E. coli* (HB101) cells are shown in Figures 4.13 and 4.14.

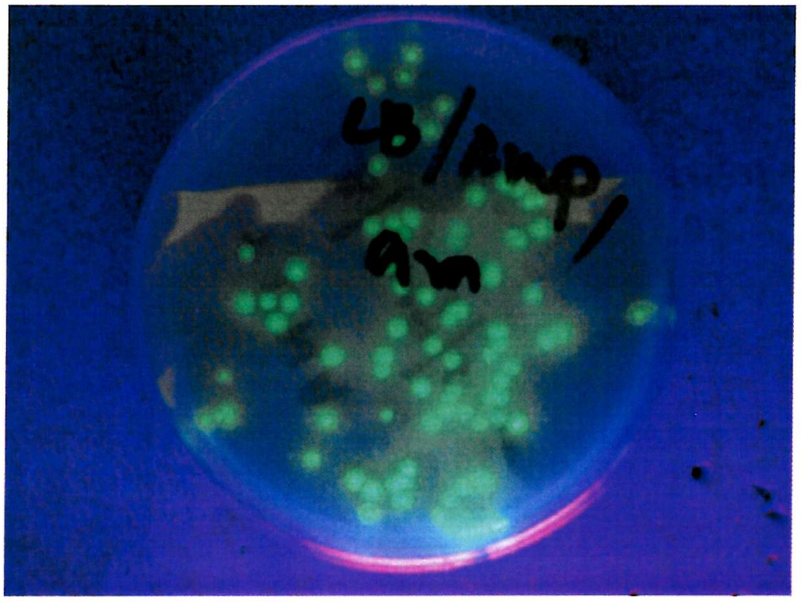

Figure 4.13 Transformation of *E. coli* (HB101) using pGLO plasmid DNA

Figure 4.14 GFP in *E. coli*

4.10.5 Quantitative fluorometric assay

GFP can also be used in fluorometric assays to confirm and measure GFP fluorescence. Furthermore, using known amounts of purified recombinant GFP or GFP variant, fluorometric assays can be used to quantify the expression of GFP or GFP variants. After generating a standard curve using known amounts of recombinant protein, the fluorescence intensity of experimental samples can be measured and compared to the standard curve to determine the amount of GFP expressed in the sample.

4.10.6 Preparation of cell lysates

The assessment of GFP fluorescence in cell lysates was performed as described in the Living Colours User Manual (Clontech). For cell extract studies, lysis was achieved using sonication. Following centrifugation for 5 mins, the supernatant was transferred to a clean tube. The excitation and emission wavelengths were set to 360 nm and 510 nm respectively, with a slit width of 5 nm. The fluorescence values obtained from the fluorimeter (readings in an arbitrary units) are shown in Figure 4.15.

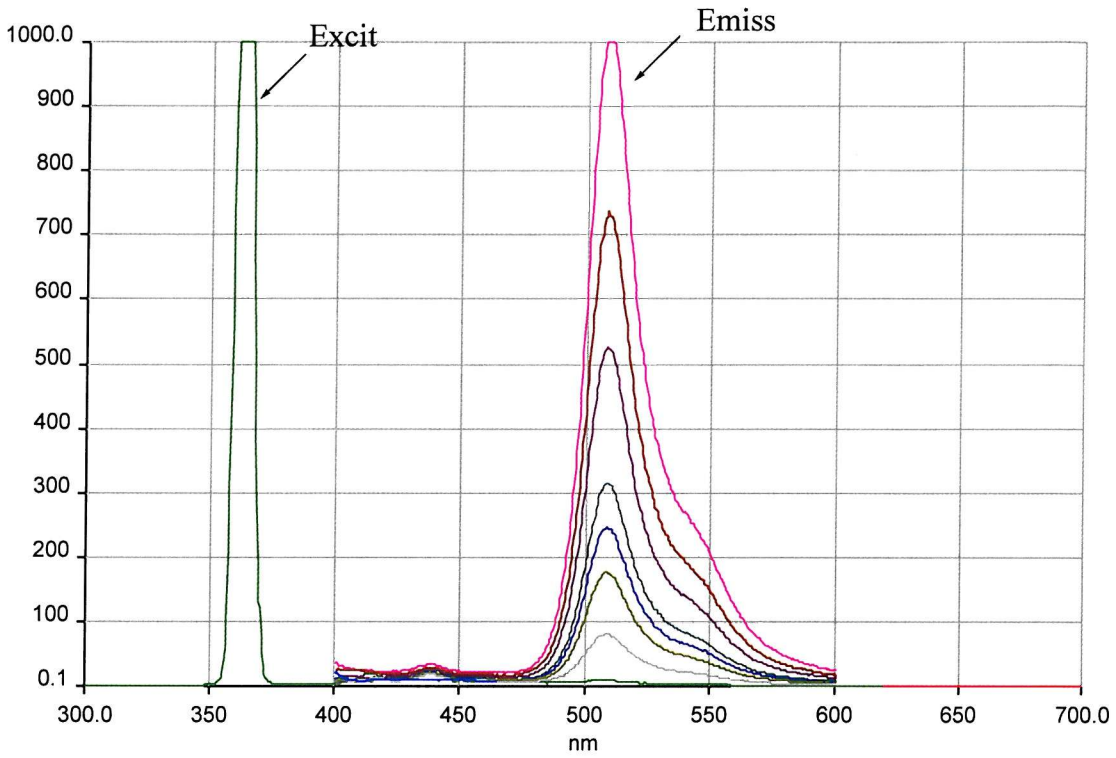

Figure 4.15 Fluorescence intensity of GFP in sonication buffer

The fluorescence values obtained from the fluorimeter were then plotted as a function of concentration for each sample using the standard curve shown in Figure 4.16, showing the linear nature of the assay.

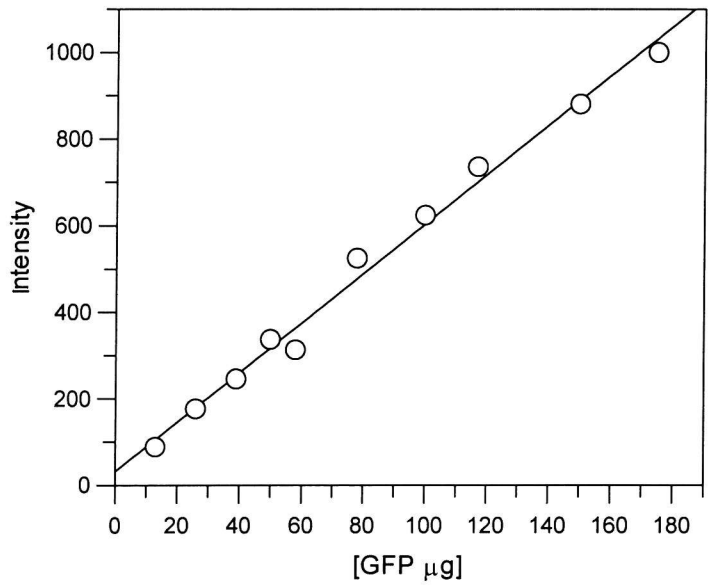

Figure 4.16 Relative fluorescence intensity of GFP in sonication buffer

4.10.7 Initial transfection using *E. coli* (HB 101)

E. coli (HB 101 cells) were first used for the transfection assay. The cells were grown on plates and a single colony was selected for growth. The cells were resuspended in LB medium at $2x10^7$ cells/mL (O.D. 600 nm *ca* 1.0). Liposome complexes were prepared by mixing 5 μg of pGLO plasmid DNA in 100 μl of LB medium and 10-40 μl of transfection agent (2 mM) in 100 μl of LB medium. The liposome complexes were incubated for 20 minutes followed by gentle application of the liposome complexes to the cells. After 1 h incubation at 37°C, 0.8 mL of complete medium was added to the cells. 100μl of the mixture were plated onto the agar plate containing 100μg/mL ampicillin, 0.2 % arabinose and the remaining cells were grown in a tube containing 0.2 % arabinose and 100μg/ mL ampicillin. After 24 hours incubation at 37°C, the cells were assayed for transfection efficiency. Unfortunately, the results showed no activity, although the compounds were used at the high concentrations showing bacterial cells were not suitable for transfection using this method. The transfection agents used in these experiments including DC-Chol, Transfectam, ESCORT and compound (**230c**). After the lack of success in the transfection of bacterial cells, attention was directed towards the more normal mammalian cell lines.

4.10.8 Transfection using the ND7 cell line

ND7 cells (Mouse neuroblastoma x rat neurone hybrid cell line) were used for the transfection assay. After several passages and subsequent growth, the cells were plated out at a concentration of $5x10^4$ cells/well in one mL of medium. They were allowed to grow for 24 hours to 60-80% confluence. The degree of confluency on the day of transfection is a parameter that needs to be optimized for each individual cell line. The transfection "vector" consisted of transfection agent/DOPE vesicles (2 mM) prepared in filtered water by vortexing the mixture 2-3 min at room temperature. Plasmid DNA (pEGFPLuc, Clontech Laboratories) contained the gene for green fluorescent protein (GFP) and luciferase as a co-transfection marker. Liposome complexes were prepared by mixing 1 μg of plasmid DNA and 5-10 μl of transfection agent (2 mM) in 200 μl of serum free medium. These complexes were incubated for 15-20 minutes at room temperature. The cells were then rinsed with 1 mL of serum free medium followed by gentle application of the liposome complexes. After 1 hour incubation at 37°C in 5% CO_2, 0.8 mL of complete medium was added to the cells. After 24 hours incubation, the cells were assayed for transfection efficiency. The fraction of fluorescent cells was determined under

a fluorescecne microscope by cell counting. The percentage transfection was calculated by comparison with non-transfected cells and the results are shown in Figure 4.17.

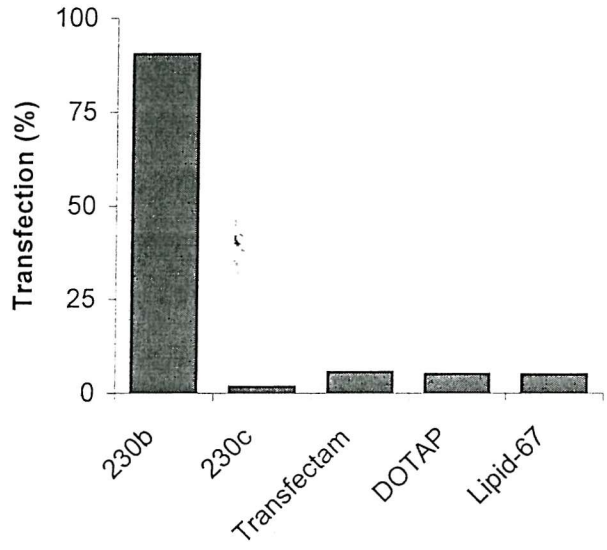

Figure 4.17 Initial screen of transfection library **230a-i**

The first compound to be tested was the squalamine analogue (**230a**). Disappointingly the results indicated no transfection activity at all. The bile acid derivatives (**230b and 230c**) proved more successful (Figure 4.17). Of this series of compounds, (**230b**) was found to be the most potent mediator of gene delivery, compound (**230c**) showing only modest activity comparable to the commercially available agents such as Transfectam, DOTAP and Lipid-67. Liposome complexes derived from the long chain fatty acids showed little activity. The results of cells transfected with pEGFP DNA using the bile acid derivative (**230b**) are shown in Figure 4.18.

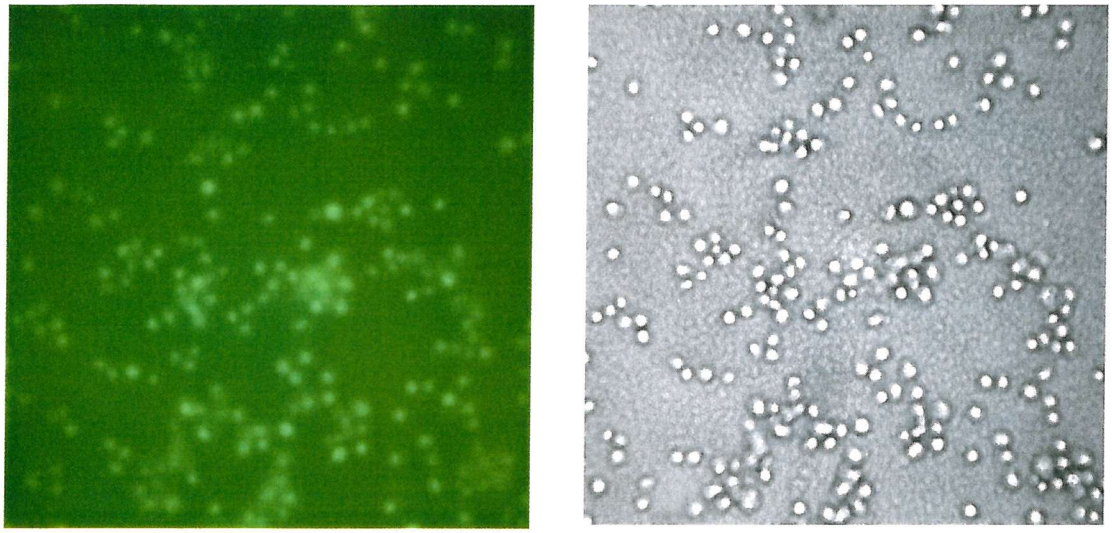

A B

Figure 4.18 ND7 cells were treated with transfection agent (**230b**) and green fluorescent protein (GFP) reporter gene. (A) cells analysed under a fluorescein filter and (B) represents cells under normal light

Analysis of our results indicate that conjugate (**230b**) was the most potent transfection agent, as evidenced by the greater population of GFP positive cells. This result differs from the structurally related steroidal analogues (**230c** and **230d**). A possible explanation for this dissimilarity between the series may be partly attributable to the ability of the respective compounds to bind DNA. It has been suggested that DNA binding is affected not only by the polyamine moiety (in our case spermine), which is constant in all the conjugates but also the lipid anchor group.[185] Compound (**230b**) has a charge ratio (CR_{50}) of 2.3 whilst the CR_{50} values for (**230c**) and (**230d**) are 0.7 and 1.6, respectively, indicating that DNA is most tightly bound by (**230c**). (The binding affinities for DNA are expressed as the charge ratio at which 50% (CR_{50}) of ethidium bromide fluorescence was quenched.) (Their relative binding affinity for calf thymus DNA were determined using an ethidium bromide displacement assay). The proposed mechanism of DNA delivery into cells is via endocytosis,[165] however effective transfection also requires the release of the DNA inside the cell. The lack of activity of compounds (**230c**) and (**230d**) may be related to the reduced propensity of DNA to escape from the endosomal compartment as compared to (**230b**) due to the greater affinity for DNA. Finally, none of the conjugates alone (in the absence of DOPE) showed any significant degree of transfection, indicating that the polyamine conjugates alone do not facilitate the uptake of DNA and the neutral co-lipid

DOPE[159] is required. This supports the argument that DOPE may help to promote endosome escape resulting in increased transfection.[159]

4.10.9 Optimisation parameters

To achieve maximum transfection efficiency of the ND7 cells, it was essential to optimise the lipid-DNA ratio. The optimal amount of DNA per transfection was the first critical parameter to determine, although this will vary among cell types. It can be seen that increasing the amount of DNA may not necessarily result in higher transfection levels of the GFP reporter gene. For ND7 cells, the DNA to charge ratio of 3:4 was optimal (Figure 4.19).

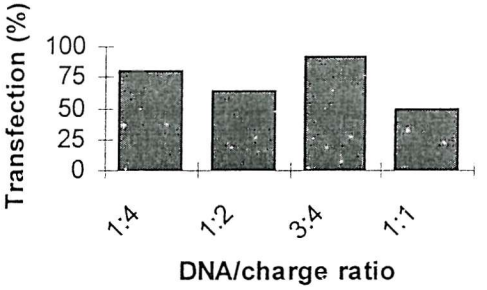

Figure 4.19. Optimisation of the amount of DNA required using compound (**230b**)

Transfection efficiency

Percentages of transfected cells were determined using a fluorescence microscope. ND7 cells were transfected with plasmid DNA containing GFP and luciferase genes under transcriptional control of the CMV promoter. High transfection efficiencies were obtained, as evidenced by the result that 50 to > 95% of the cell populations were positive for green fluorescence.

4.11 Conclusions

In conclusion, we have described the development of a safety-catch linker for the solid phase synthesis of some cholesterol based ampiphiles. These cationic liposomes displayed a highly efficient capability to transfect rat neuronal cells *in vitro*. This method is simple and quick for finding lead compounds. The transfection activity of cationic liposomes formulated with DOPE as a co-lipid compared well with commercially available DC-Chol transfectam, DOTAP and ESCORT.™ These results suggest that a bile acid based cationic lipid is more effective than those commercially available. The transfection

efficiency, relatively low toxicity and ease of preparation makes them promising candidates for general gene therapy in the future.

Chapter 5 Experimental

5.1 General Experimental Information

^{1}H-NMR and ^{13}C-NMR spectra were recorded on a Bruker DPX400 (400 and 100 MHz, respectively) or with a Bruker AC300 (300 and 75 MHz, respectively) at 298 K unless otherwise stated. All chemical shifts are quoted in ppm on the δ scale using the residual protonated solvent as the internal standard. Coupling constants (*J* values) were measured in Hz. C-13 shifts are listed and not assigned (according to the policy of the journal of organic chemistry) unless a full correlation had been obtained.

Mass spectra were obtained on a VG Platform single quadrupole mass spectrometer in electrospray ionisation (ES+ or ES-) mode or atmospheric pressure chemical ionisation (APCI+) mode. High resolution accurate mass (HRMS) measurements were carried out on a VG Analytical 70-250-SE normal geometry double focusing mass spectrometer, fitted with an Ion-Tech saddle-field gun (for FAB), using mixtures of polyethylene glycols and/or polyethylene glycomethyl ethers (FAB) or perfluorokerosene (EI) as mass calibrants.

Thin layer chromatography (TLC) plates were visualised by ultra-violet light and/or ninhydrin solution (0.3% ninhydrin in 1-butanol and 3% acetic acid) with heating unless otherwise stated. Other stains used were: Permanganate stain ($KMnO_4$ (3 g), K_2CO_3 (20 g), 5% aq. NaOH (5 mL), H_2O (300 mL)) and iodine (solid I_2 in sand, left to sublime onto the plate). Enzyme assays were performed using a Hewlett-Packard 8452A Diode array spectrophotometer, with a 1 mL cell volume.

LC/MS was carried out on a HP1050 HPLC connected to a Micromass Series II mass spectrometer. The spectrometer operated in both positive (ES+) and negative (ES-) modes, switching between the two modes automatically during sample analysis. The HPLC system was equipped with a 3 μm ABZ+PLUS column (3.3 cm x 4.6 mm ID) and a gradient from 0.1% formic acid in H_2O (+ 10 mM ammonium acetate) to 0.05% formic acid in acetonitrile/H_2O 95:5 over 5 min. was run.

Analytical RP-HPLC was performed on a HP1100 system equipped with a Phenomenex Prodigy C_{18} reverse phase column (150 x 4.6 mm i.d.) with a flow rate of 1 mL/min monitoring at either 220 nm or 254 nm and eluting with (A) 0.1% TFA in H_2O and (B) 0.042% TFA in acetonitrile using a gradient of 0% (B) to 100% (B) over 20 minutes.

Semi-preparative RP-HPLC were performed on a HP1100 system equipped with a Phenomenex Prodigy C_{18} reverse phase column (250 × 10 mm i.d., flow rate 2.5

mL/min), monitoring at either 220 nm or 254 nm and eluting with (A) 0.1% TFA in H_2O and (B) 0.042% TFA in acetonitrile using a gradient 0% (B) to 100% (B) over 40 minutes. When compounds were prepared by TFA cleavage from the solid phase or purified by HPLC the yields are quoted for the TFA salts. IR spectra were obtained on a BioRad FTS 135 spectrometer with a Goldengate ATR accessed with neat compounds, only strong bands are given. UV-VIS spectra were recorded using a HP 8452A Diode Array Spectrophotometer. Melting points were determined using a Gallenkamp melting point apparatus and are uncorrected. The integral naming programme of Chemdraw Ultra 5.0 was used as necessary. Polyamine conjugates were named based on a carbon skeleton.

5.2 General Experimental Methods

5.2.1 Ninhydrin analysis[107]

Quantitative test:

Samples for analysis were prepared as described below:[107]

Two samples of dry resin (2-5 mg; W mg) were weighed into 10 x 75 mm test tubes. Reagent A (6 drops) and reagent B (2 drops) (see below) were added, mixed well and placed in an oil bath at 100°C for 10 min. As a control, the reagents were heated in another test tube without resin. The tubes were placed in cold water and 60% ethanol in H_2O (2 mL) was added and mixed thoroughly. The solutions were filtered through a pasteur pipette containing a tight plug of glass wool, washed twice with 0.5 M Et_4NCl in DCM (0.5 mL) and diluted to 50 mL (V mL) with 60% ethanol. The absorbance (A) of these solutions was recorded at 570 nm using the control as a blank. The following equation is used to calculate the amount of amine present on the resin beads ($mmol.g^{-1}$).

$(mol.g^{-1} = (Abs.\ at\ 570\ nm \times V\ mL / (\times W\ mg) \times 10^6$

$\varepsilon = 1.5 \times 10^4\ M^{-1}cm^{-1}$

Qualitative test:

A small sample of resin (<0.5 mg) is treated as above. After heating at 100°C for approximately 5 min, the degree of blue colour gives a qualitative indication of the amount of free amine present.

Reagent A

Solution 1 - Reagent grade phenol (40 g, 0.43 mol) was mixed with absolute ethanol (10 mL). The mixture was warmed until dissolved. IWT TMD-8 ion exchange resin (4g) was added and the mixture stirred for 45 min then filtered.

Solution 2 - KCN (65 mg, 1 mmol) was dissolved in water (100 mL). The KCN solution (2 mL) was then diluted to 100 mL with pyridine (freshly distilled from ninhydrin). IWT TMD-8 ion exchange resin (4 g) was added, stirred for 45 min and filtered. Solutions 1 and 2 were mixed.

Reagent B

Ninhydrin (2.5 g, 14 mmol) was dissolved in absolute ethanol (50 mL).

5.2.2 Quantitative Fmoc test[185]

Three aliquots of dry resin (3-6 mg) was weighed into volumetric flasks (50 mL or 1 mL) and treated with a solution of 20% piperidine in DMF (20 mL or 1 mL) for 20 min. The volume was made up to 50 mL (or 1 mL) with more 20% pieridine in DMF and the solutions mixed thoroughly. The absorbance at 302 nm was measured against a blank of 20% pieridine in DMF. The resin substitution was deduced from the following equation and calculated from the average value obtained from the three samples of resin:

$$\text{mmol/g (}\mu\text{mol/bead)} = [(A_{302} \times V) / (\varepsilon_{302} \times W)] \times 10^3$$

where A_{302} is the absorbance of the piperidyl-fulvene adduct, V is the total volume (mL), W is the weight of the resin (mg) or the exact number of beads and ε_{302} is the extinction coefficient of the adduct at 302 nm (7800 $M^{-1}cm^{-1}$).

5.2.3 Preparation of aminomethyl resin[106]

Chloromethyl resin (Merrifield resin) (15.5 g, 1.39 mmol/g, 20.7 mmol) was swollen in DMF (300 mL) for 20 min, then potassium phthalimide (6.14 g, 33.1 mmol) was added and the mixture heated at 120 °C overnight. The resin was cooled, filtered and then washed with hot DMF (2x100 mL), dioxane/water (1:1) (2x100 mL), dioxane (2x100 mL), EtOH (2x100 mL), MeOH (2x100 mL) and Et_2O (2x100 mL) and dried *in vacuo* to yield phthalimidomethyl resin (17.36 g). The phthalimidomethyl resin (15.0 g, 19.5 mmol) was suspended in EtOH (300 mL) and hydrazine hydrate (14.3 mL, 293 mmol) was added. The mixture was refluxed overnight. The resin was cooled, filtered and then washed with hot DMF (2x200 mL), hot water (2x200 mL), DCM (2x200 mL), hot water (2x200 mL), DMF (2x200 mL), EtOH (2x200 mL), MeOH (2x200 mL) and Et_2O (2x200 mL) and dried *in vacuo* to yield the title aminomethyl resin. A quantitative ninhydrin test gave the resin loading as (1.23 mmol/g) (87% yield).

5.2.4 SDS-PAGE: gel preparation and running[111]

SDS-PAGE gels were prepared as follows:

A separating gel contained the following:

30% acrylamide and 2.6% cross linking (C_{bis}) (2 mL), running gel buffer (see below) (1.5 mL), 10% SDS (60 µl), water (2.41 mL) 10% ammonium persulfate in water (30 µl) and TEMED (10 µl). This was poured between the two glass plates of a BioRad Mini-PROTEAN II and layered with 2-propanol (0.5 mL) added to the top and the gel left to set. After 45 min, the propanol was removed and the gel rinsed with water.

A stacking gel contained the following:

30% acrylamide, 2.6% cross linking (C_{bis}) (532 µL), Stacking gel buffer (see below) (1 mL), 10% SDS (40 µL), water (2.44 mL) 10% ammonium persulfate in water (20 µL) and TEMED (10 µL). This was poured between the plates with a comb in position. After 1 hour, the comb was removed and the wells rinsed with water.

Solutions of protein (approx. 1 µg and 10 µg) were added to an equal volume of treatment buffer, and boiled for approximately 5 min. Approximately 10 µL of each sample was loaded into the gel wells. A molecular weight marker set (Sigma) (Mr (x 10^3Da) = 66, 45, 35, 24, 18.4, 14.3) was used. The gel was run at 200 V for approximately 45 min in tank buffer. Upon completion, the gel was stained with Coomassie Blue stain for 30 seconds while heating in a microwave, followed by 25 min. at room temperature before immersion into destaining solution overnight.

Buffers and solutions used for gel preparation and running[111]

Running gel buffer: 1.5 M Tris (tris(hydroxymethyl)aminomethane), pH 8.8.

Stacking gel buffer: 0.5 M Tris, pH 6.8.

Treatment buffer: 125 mM Tris, 4% SDS, 20% glycerol, 10% β-mercaptoethanol, 0.05% bromophenol blue.

Tank buffer: 25 mM Tris, 192 mM glycine, 0.1% SDS, pH 8.3.

Coomassie Blue stain: 0.125% Coomassie blue R-250, 50% methanol, 10% acetic acid.

Destaining solution: 50% methanol, 40% water, 10% acetic acid.

5.2.5 Production of Trypanothione Reductase (TR):

A single colony of pIBI30TR/DE3 (BL21) was grown overnight at 37 °C in 5 mL of 2 x TY media containing 100 $\mu g.mL^{-1}$ ampicillin. 1 mL of this culture was grown overnight in 50 mL of media containing ampicilin 100 $\mu g.mL^{-1}$. Finally 2 litres of 2 x TY media containing 100 $\mu g.mL^{-1}$ ampicillin was inoculated with 10 ml of this overnight culture and the optical density (OD) was monitored at 600 nm. After 5 hours, cell growth IPTG was added to a final concentration of 0.1 mM. After 3 hours at 37 °C, the cells were harvested by centrifugation for 20 min at 5K rpm and resuspended in 50 mM potassium phosphate buffer with 1 mM EDTA and 0.1% BME, pH 7.5 (120 mL). The cells were lysed by sonification (6 x 3 min) with cooling on ice. The supernatant was retained after centrifugation for 20 min at 20K rpm and the pellets resuspended in buffer (20 mL) and resonicated (5 x 3 min). The combined supernatant (120 mL) was treated with ammonium sulfate (46.8 g) to 60% saturation and left to stir at 4 °C for 2 hours. Precipitated protein was collected by centrifugation at 10K rpm for 20 min and re-suspended/dissolved in approximately 40 mL of buffer. Dialysis was carried out twice against 50 mM phosphate buffer, 1 mM EDTA and 0.1% BME (2 L) (1 x overnight, 1 x 6 hours). The crude extract was spun at 10K rpm for 5 min to remove residual precipitate, and the supernatant loaded onto a column containing adenosine-2,5-diphosphate on agarose (Sigma). A NaCl concentration gradient (0-2 M) was used to elute the desired protein from the column using a flow rate of 0.5 $mL.min^{-1}$.

5.2.6 Determination of Kinetic Parameters of TR

For kinetic studies, trypanothione disulfide (TSST) was dissolved in phosphate buffer 50 mM K_2HPO_4, 1 mM EDTA, pH 7.5). The actual concentration of TSST was determined by titration by monitoring consumption of NADPH at 340 nm, using a 1 mL assay containing 100 µM NADPH and 0.1 µg of TR in phosphate buffer. Trypanothione (5, 10 and 20 µL) was added and the ΔA was calculated once complete consumption of the substrate had occurred. Using the Beer Lambert rule ($\Delta A=\varepsilon cl$, where $\varepsilon = 6.22 \times 10^{-3}$ M^{-1} cm^{-1} for NADPH), the average concentration was calculated.

Kinetic parameters were determined by running a series of assays using a total volume of 1 mL and consisted of potassium phosphate buffer (50mM), 100 µM NADPH, (10 µl of stock TR and various known concentrations of trypanothione, from approximately 10µM

to 200 μM. The initial rates of reduction were recorded at 340 nm, after addition of the substrate.

[Substrate] ([S]), (μM)	Rate (v) (Δ A sec^{-1} , x 10^{-3}
12.5	0.847
25	1.131
50	1.568
75	2.070
100	2.511
200	2.594

The data was analysed according to Michaelis- Menten kinetics:

$v = vmax\ [S] / ([S] + Km)$

v = rate, v_{max} = maximum rate, [S] = Substrate concentration

Using the rearrangement of Eadie and Hofstee v is plotted against v/[S] in accordance with the equation:

$v = v_{max} - Km\ (v / [S])$

$K_m = 44\ \mu M$ (lit[72] 45 μM)

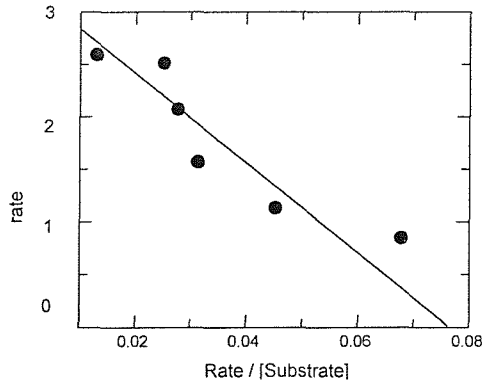

Eadie and Hofstee[113] plot to determine the K_m of *T. Cruzi* TR with $T(S)_2$

5.3 Experimental for Chapter 2

Synthesis of (4-Formyl-phenoxy) acetic acid allyl ester (129)

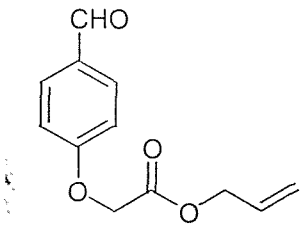

The title compound was prepared using a modification of the literature procedure. Allyl chloroacetate (9.1 g, 65.1mmol) was refluxed in acetonitrile (150 mL) with 4-hydroxybenzaldehyde (6.12g, 50.1 mmol), and potassium carbonate (9.0g, 65.1mmol), and potassium iodide (0.83g, 5.0mmol) for 3 hours. The mixture was filtered after cooling, and the residual solid was washed with ethyl acetate (2x100 mL). Following removal of the solvent *in vacuo*, the residue was purified by column chromatography on silica gel eluting with hexane/ethylacetate (3:1) to give the title compound as a colourless liquid. Spectroscopic data agreed with the literature.[186]

TLC: $R_f = 0.6$ (hexane / ethyl acetate) (3:1).

Yield: 10.48 g (95%).

IR (ν_{max}/ cm^{-1}) 1755 (C=O, ester), 1677 (C=O, aldehyde).

δ_H (300 MHz, $CDCl_3$): 4.71 (2H, d, *J* 6, $OC\underline{H}_2CH=CH_2$), 4.75 (2H, s, $OC\underline{H}_2$) 4.75 (2H, s, $OC\underline{H}_2CO$), 5.28 (1H, dd, *J* 10, 2, $OCH_2CH=C\underline{H}_{cis}$), 5.34 (1H, dd, *J* 17, 2, $OCH_2CH=C\underline{H}_{trans}$), 5.92 (1H, ddt, *J* 17, 10, 6, $OCH_2C\underline{H}=CH_2$), 7.01, (2H, d, *J* 9, Ar$\underline{H}$), 7.85 (2H, d, *J* 9, Ar$\underline{H}$), 9.90 (1H, s, C$\underline{H}$O).

δ_C (75MHz, $CDCl_3$): 65.3, 66.3 115.0, 119.6, 130.9, 131.3, 132.1, 162.7, 167.9, 190.9 (agreed with chemical shifts calculated by CS ChemNMR Pro).

(4-Hydroxymethyl-phenoxy)-acetic acid allyl ester (130)

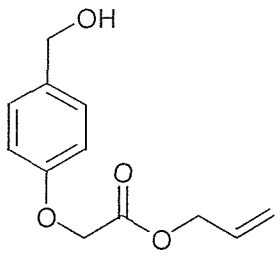

The title compound was prepared according to the literature procedure. 4-Formylphenoxy acetic acid allyl (10.0 g, 45.4 mmol) and a trace of bromocresol green (10 mg) were dissolved in ethanol/water (1:1) 500 mL, and sodium cyanoborohydride ($NaCNBH_3$) 3.14 g (50 mmol) was added. The solution immediately turned deep blue 2N HCl in ethanol was added dropwise with stirring to restore the yellow-green colour. The solution was stirred for an additional 2 hours, 1-2 drops of acid being added occasionally to restore the green-yellow colour. The residue was saturated with solid of sodium chloride, the ethanol was evaporated at reduced pressure and the aqueous solution was extracted with ethyl acetate (3x100 mL). The combined extracts were dried (Na_2SO_4) and evaporated *in vacuo*. The crude product was purified by column chromatography on silica gel (eluding with hexane / ethyl acetate 2:1) and gave the title product as a colourless oil. Spectroscopic data agreed with the literature.[186]

TLC: Rf = 0.25 (hexane/ethyl acetate (2:1)

Yield: 8.6 g (85%)

IR (ν_{max}/ cm^{-1}) 3388 (OH), 1759 (C=O)

δ_H (300 MHz, $CDCl_3$)**:** 4.59 (2H, d, *J* 4, Hz, $ArC\underline{H}_2OH$); 4.65 (2H, s, $OC\underline{H}_2CO$), 4.70 (dd, *J* 6, 2, $OC\underline{H}_2CH{=}CH_2$), 5.28 (1H, dd, *J* 10,2, $OCH_2CH{=}C\underline{H}_{cis}$), 5.34 (1H, dd, *J* 17, 2, $OCH_2CH{=}C\underline{H}_{trans}$), 5.93 (1H, ddt, *J* 17, 10, 6, $OCH_2C\underline{H}{=}CH_2$), 6.89, (2H, d, *J* 9, $Ar\underline{H}$), 7.28 (2H, d, *J* 9, $Ar\underline{H}$).

δ_C (75MHz, CDCl3): 64.9, 65.5, 66.1, 114.8, 119.3, 128.8, 131.5, 134.5, 157.4, 168.8. (agreed with chemical shifts calculated by CS ChemNMR Pro).

[4-(4-Nitro-phenoxycarbonyloxymethyl)-phenoxy]-acetic acid allyl ester (127)

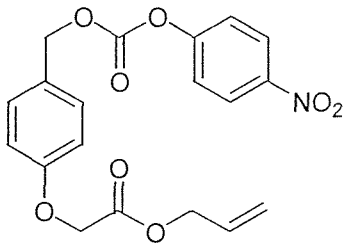

(4-Hydroxymethyl-phenoxy)-acetic acid allyl ester (4.8 g, 21.6 mmol) was dissolved in dichloromethane (50 mL) and pyridine (1.96 mL, 23.8 mmol) and cooled in an ice bath. A solution of *p*-nitrophenylchloroformate (4.79g, 23.8 mmol) in dichloromethane (20 mL) was added dropwise over 20 minutes with stirring and cooling maintained for a further 2 hours. The reaction mixture was poured into water (70 mL) and the organic phase separated. The aqueous phase was extracted with dichloromethane (2x50 mL), the organic extracts combined, dried ($MgSO_4$) and the solvent removed under reduced pressure. The crude product was crystallised from diethyl ether / dichloromethane to give the title compound as pale yellow crystals. Spectroscopic data was in agreement with the literature.[186]

TLC: Rf = 0.6: (hexane: ethyl acetate) (2:1).

Yield 5.97 g (69 %).

IR (ν_{max}/ cm^{-1}) 1753 (C=O, ester), 1728 (C=O, urethane).

δ_H (300 MHz, $CDCl_3$): 4.70 (2H, s, $OC\underline{H}_2CO$), 4.72 (2H, dd, *J* 2, 6, $C\underline{H}_2CH=CH_2$), 5.24 (2H, s, $ArC\underline{H}_2O$), 5.29 (1H, dd, *J* 10, 2, $OCH_2CH=C\underline{H}_{cis}$), 5.36 (1H, dd, *J* 17, 2, $OCH_2CH=C\underline{H}_{trans}$), 5.94 (1H, ddt, *J* =17 10, 6, $OCH_2C\underline{H}=CH_2$), 6.95, (2H, d, *J* 8, Ar<u>H</u>), 7.38, (2H, d, *J* 8, Ar<u>H</u>), 7.40 (2H, d, *J* 10, Ar<u>H</u>), 8.27, (2H, d, *J* 10, Ar<u>H</u>).

δ_C (75MHz, $CDCl_3$): 65.4, 66.1, 70.8, 115.0, 119.4, 122.0, 125.5, 127.6, 130.9, 131.5, 145.4, 152.6, 155.7, 158.6, 168.6 (agreed with chemical shifts calculated by CS ChemNMR Pro).

N^1,N^{14}-*bis*(Phthaloyl)-1,5,10,14-tetraazatetradecane dihydrochloride (121)[103]

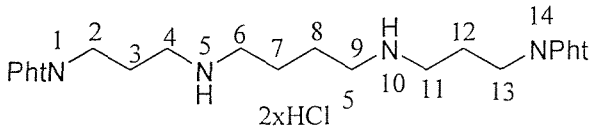

To a solution of spermine (10.0g, 49.4 mmol) in $CHCl_3$ (150 mL) was added a solution of *N*-(ethoxycarbonyl)-phathalimide (23.85 g, 108.8 mmol) in $CHCl_3$ (100 mL) at room temperature over in 30 min. After stirring for 2 hours, the solvent was evaporated *in vacuo* and the residue was converted into its dihydrochloride salt by the addition of 1 M HCl solution in methanol. The solid was collected by filtration and washed with diethyl ether (2x50 mL) and dried under vacuum to give N^1,N^{14}-*bis*(phthaloyl)-1,5,10,14-tetraazatetradecane dihydrochloride salt as a colourless solid.

TLC: Rf = 0.4: (CH_2Cl_2: MeOH: NH_4OH) (70:10:1).

Yield 20.2 g (76 %).

m.p.: >230°C

IR (ν_{max}/ cm^{-1}) 1753 (C=O).

δ_H (300MHz, D_2O): 1.65, (4H, br m, $C^{7+8}H_2$); 1.95 (4H, br m, $C^{3+12}H_2$), 3.00 (8H, m, $C^{4+6+9+11}H_2$), 3.60 (4H, t, *J* 6, $C^{2+13}H_2$), 7.65 (8H, s,Ar<u>H</u>).

δ_C (75MHz, D_2O): 25.3, 27.6, 37.2, 47.5, 49.5, 126.0, 133.7, 137.4, 173.0 (agrees with chemical shifts calculated by CS ChemNMR Pro).

ES-MS (+ve): m/z = 463.4 (100%, $M+H)^+$.

N^1,N^{14}-*bis* (Phthaloyl)-N^{10}-*tert*-butyloxycarbonyl-N^5-(4-benzyloxycarbonyl-oxyacetic acid allyl ester)-1,5,10,14-tetraazatetradecane (135)[186]

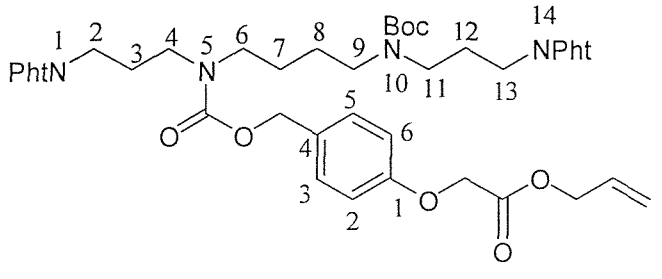

N^{1},N^{14}-*bis*(Phthaloyl)-1,5,10,14-tetraazatetradecane 0.94 g, 2.2 mmol) was dissolved in DMF (30 mL) and Et_3N (1.0 mL, 7.1mmol). The solution was cooled in an ice bath and a solution of di-t-butyl-dicarbonate (0.47g, 2.2 mmol) was added dropwise over 10 min followed by the addition of DMAP (~50 mg). After 1 hour [4-(4'-nitro-phenoxycarbonyloxymethyl)-phenoxy]-acetic acid allyl ester (0.86g, 2.2 mmol) in DMF (10 mL) was added dropwise over 10 min. After 30 min at 0 °C the mixture was allowed to warm to room temperature and was stirred overnight, before partitioning between 2M $KHSO_4$ (50 mL) and ethyl acetate (200 mL). The organic extract was washed with 10% sodium bicarbonate (2x50 mL) and saturated aqueous sodium chloride (50 mL), dried ($MgSO_4$) and the solvent evaporated *in vacuo* to give a yellow liquid. Purification by flash chromatography on silica gel (eluting with hexane: ethyl acetate; 1:1) provided the title compound as a colourless liquid.

TLC: Rf = 0.3: (hexane: EtOAc) (1:1).

Yield: 1.0 g (41 %)

IR (ν_{max}/ cm^{-1}) 1707 (C=O), 1690 (C=O).

δ_H (300MHz, $CDCl_3$): 1.38 (9H, s, CH_3), 1.47, (4H, br m, $C^{7+8}H_2$); 1.88 (4H, m, $C^{3+12}H_2$), 3.21 (8H, m, $C^{4+6+9+11}H_2$), 3.66 (4H, t, *J* 7, $C^{2+13}H_2$), 4.63 (2H, s, $OC\underline{H}_2CO$), 4.68 (2H, d, *J* 6, $C\underline{H}_2CH{=}CH_2$), 4.99 (2H, br s, $ArC\underline{H}_2O$), 5.25 (1H, d, *J* 10, $OCH_2CH{=}C\underline{H}_{cis}$), 5.32 (1H, d, *J* 17, $OCH_2CH{=}C\underline{H}_{trans}$), 5.91 (1H, ddt, *J* 17, 10, 6, $OCH_2C\underline{H}{=}CH_2$), 6.80, (2H, dd, *J* 7, Ar$\underline{H}$), 7.20, (2H, m, Ar$\underline{H}$), 7.71 (4H, m, Ar$\underline{H}$), 7.81 (4H, m Ar$\underline{H}$).

δ_C (75MHz, $CDCl_3$): 26.0, 28.0, 28.5, 35.9, 44.8, 46.9, 65.4, 66.0, 66.7, 79.5, 114.7, 119.3, 123.3, 129.8, 130.2, 131.6, 132.2, 134.1, 155.5, 156.1, 157.6, 168.4, 168.7, (agrees with chemical shifts calculated by CS ChemNMR Pro).

APCI ES-MS (+ve): m/z = 833.2 (20%, $M+Na)^+$, 711.2 (M^+-$C_5H_7O_2$, 100%).

N^1,N^{14}-*bis* (Phthaloyl)-N^{10}-*tert*-butyloxycarbonyl-N^5-(4-benzyloxycarbonyl-1-oxy acetic acid)-1,5,10,14-tetraazatetradecane (124)[186]

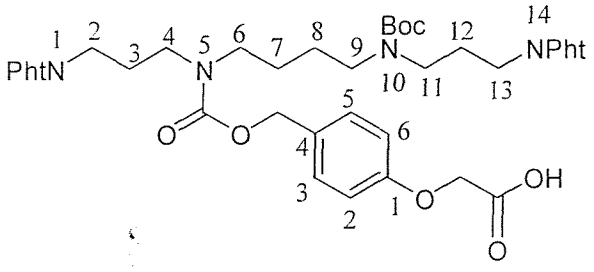

To a stirred the solution of N^1,N^{14}-*bis*(phthaloyl)-N^{10}-*tert*-Butyloxycarbonyl-N^5-(4-benzyl oxycarbonyl 1-oxy acetic acid allyl ester)-1,5,10,14-tetraazatetradecane (2.74 g, 3.4 mmol) in dry dichloromethane (15 mL) and tetrahydrofuran (15 mL) was added thiosalicylic acid (0.78g, 5.1 mmol) and $Pd(PPh_3)_4$ (0.51 g, 0.4 mmol) and the mixture stirred under nitrogen for 3 hours at room temperature. The solution was concentrated under reduced pressure and the residue redissoved in dichloromethane (200 mL). The organic layer was washed with 2M $KHSO_4$ (2x50 mL) and saturated sodium chloride (50 mL), dried ($MgSO_4$) and the solvent evaporated *in vacuo*. Purification by flash chromatography (eluting with hexane: ethyl acetate; 1:1 and then ethyl acetate: methanol; 9:1) provided the title compound as an orange foam. Spectroscopic data was in agreement with the literature.

TLC: Rf = 0.3: (hexane: EtOAc: MeOH) (9:9:2).

Yield: 1.9 g (72 %)

IR (ν_{max}/ cm^{-1}) 1772 (C=O, acid), 1711 (C=O, ester).

δ_H (300 MHz, $CDCl_3$)**:** 1.38 (9H, s, CH_3), 1.45 (4H, br m, $C^{7+8}H_2$); 1.87 (4H, br m, $C^{3+12}H_2$), 3.20 (8H, br m, $C^{4+6+9+11}H_2$), 3.65 (4H, t, *J* 7, $C^{2+13}H_2$), 4.62 (2H, s, $OC\underline{H}_2CO_2H$), 4.98 (2H, s, $ArC\underline{H}_2O$), 6.86 (2H, m, Ar$\underline{H}$), 7.23 (2H, m, Ar$\underline{H}$), 7.69 (4H, m, Ar$\underline{H}$), 7.82, (4H, m, Ar$\underline{H}$).

δ_C (75 MHz, $CDCl_3$): 25.7, 27.97, 28.5, 35.96, 44.8, 46.9, 65.1, 66.9, 79.5, 114.7, 123.4, 130.0, 132.6, 132.2, 134.1, 156.1, 157.6, 168.5, 171.8 (agrees with chemical shifts calculated by CS ChemNMR Pro).

N^1,N^{14}-*bis* (Phthaloyl)-N^{10}-*tert*-butyloxycarbonyl-N^5-(4-benzyloxycarbonyl-1-oxy acetamidomethyl resin)-1,5,10,14-tetraazatetradecane (139)[186]

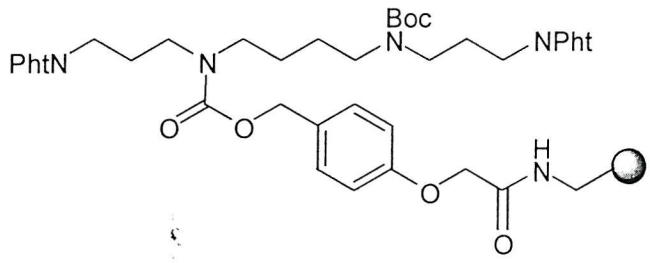

N^1,N^{14}-*bis*(Phthaloyl)-N^{10}-*tert*-butyloxycarbonyl-N^5-(4-benzyloxycarbonyl 1-oxy acetic acid)-1,5,10,14-tetraazatetradecane (1.9 g, 2.5 mmol) was dissolved in dichloromethane (15 mL) at room temperature and HOBt (0.5 g, 3.0 mmol) was added with DIC (0.5 mL, 3.0 mmol). After 10 min the solution was added to aminomethyl resin (pre-swollen in CH_2Cl_2 for 30 mims and filtered) (1.6 g, 2.0 mmol, 1.3 $mmolg^{-1}$) and the suspension was shaken at room temperature overnight. The resin was filtered and washed with CH_2Cl_2 (2x20 mL), DMF (2x20 mL), MeOH (2x20 mL), and diethyl ether (2x20 mL). The resin was dried under vacuum and gave a negative ninhydrin test.

N^{10}-*tert*-Butyloxycarbonyl-N^5-(4-benzyloxycarbonyl-1-oxy acetamidomethyl resin)-1,5,10,14-tetraazatetradecane (123)[186]

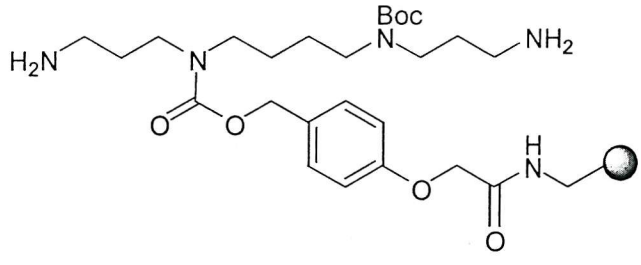

N^1,N^{14}-*bis*(Phthaloyl)-N^{10}-*tert*-butyloxycarbonyl-N^5-(4-benzyloxycarbonyl-1-oxy acetamidomethyl resin)-1,5,10,14-tetraazatetradecane (3.5 g) was added to absolute ethanol (50 mL) and hydrazine monohydrate (3 mL, 60 mmol). The solution was heated under reflux overnight. The resin was filtered and washed successively with hot water (2x20 mL), EtOH (2x20 mL), MeOH (2x20 mL), CH_2Cl_2 (2x20 mL) and diethyl ether (2x20 mL). The resin was dried under vacuum and the quantitative ninhydrin test gave a loading of 0.5 $mmol.g^{-1}$ (2.4 g).

N^1,N^{14}-*bis*(3,4-Dihydroxyhydrocinnamoyl)-N^{10}-*tert*-butyloxycarbonyl-N^5-(4-benzyl oxycarbonyl-1-oxy acetamidomethyl resin)-1,5,10,14-tetraazatetradecane (140)[186]

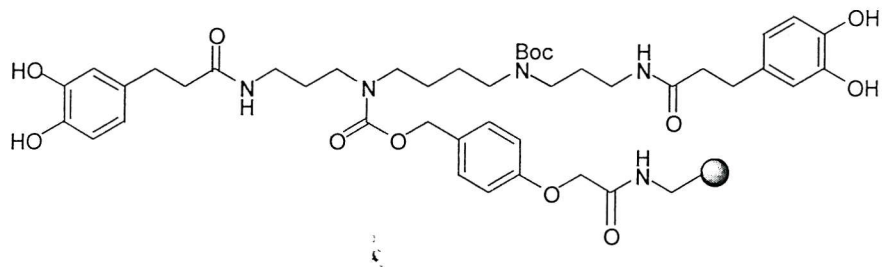

To a shaken suspension of N^{10}-*tert*-butyloxycarbonyl-N^5-(4-benzyloxycarbonyl 1-oxy acetamidomethyl resin)-1,5,10,14-tetraazatetradecane (0.22g, 0.1mmol, pre-swollen in CH_2Cl_2 and filtered) was added a solution of 3,4-dihydroxyhydrocinnamic acid (0.08 g, 0.4 mmol) dissolved in CH_2Cl_2 (3 mL) with a few drops of DMF, HOBt (0.063 g, 0.4 mmol) and DIC (0.04 mL, 0.4 mmol). The suspension was shaken at room temperature 3 hours. The resin was filtered and washed with CH_2Cl_2 (2x10 mL), DMF (2x10 mL), MeOH (2x10 mL), and diethyl ether (2x10 mL). The resin was dried under vacuum and gave a negative ninhydrin test.

N^1,N^{14}-*bis*(3,4-Dihydroxyhydrocinnamoyl)-1,5,10,14-tetraazatetradecane (141a)[186]

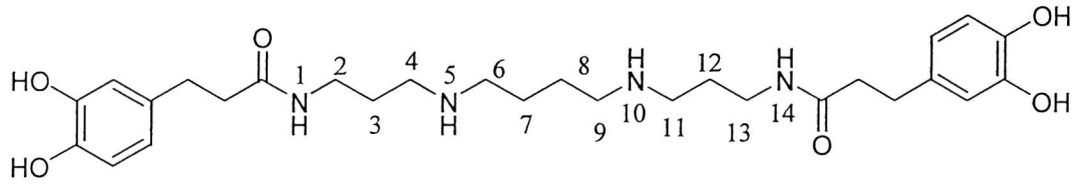

N^1,N^{14}-*bis*(3,4-Dihydroxyhydrocinnamoyl)-N^{10}-*tert*-butyloxycarbonyl-N^5-(4-benzyloxy carbonyl 1-oxy acetamidomethyl resin)-1,5,10,14-tetraazatetradecane (0.23 g) was pre-swollen in CH_2Cl_2 30 min and resin was filtered. The resin was treated with a cleavage cocktail of TFA/water/tri-isopropylsilane/CH_2Cl_2/thioanisole (15:1:1:1:1, 3 mL) and the suspension was shaken at room temperature for 3 hours. The resin was filtered and washed with CH_2Cl_2 (2 mL). The solution was concentrated under reduced pressure to a volume of approximately 1 mL. The product precipitated by dropping into cold ^{t}butylmethylether 25 mL. The precipitate was collected by centrifugation and washed with hexane before being re-dissolved in water with few drops of acetonitrile and freeze-dried. Data agreed with the literature.[23]

RP-HPLC: R_t = 8.0 min.

Yield 48 mg, (56%)

IR (ν_{max}/ cm^{-1}) 1676 (C=O).

δ_H (300 MHz, D_20): 1.60 (8H, m, $C^{3+7+8+12}H_2$), 2.48 (8H, m, $C^{4+6+9+11}H_2$), 2.72 (4H, t, *J* 7, $ArCH_2C\underline{H}_2$), 2.79 (4H, m, $C^{2+13}H_2$), 3.09 (4H, t, *J* 7, $ArC\underline{H}_2$), 6.60 (2H, dd, *J* 8, 2,Ar<u>H</u>), 6.68, (2H, d, *J* 2,Ar<u>H</u>), 6.76 (2H, d, *J* 8,Ar<u>H</u>).

δ_C (75 MHz, D_2O): 25.4, 28.1, 33.0, 38.2, 39.5, 47.3, 49.5, 118.8, 118.9, 123.3, 135.6, 145.0, 146.4, 178.9, (agrees with chemical shifts calculated by CS ChemNMR Pro).

ES-MS (+ve): m/z = 531.8 (100%, $M+H)^+$.

HRMS (FAB): $C_{28}H_{43}N_4O_6$ Calc. 531.3183, Found 531.3162.

General procedure for the preparation of kukoamine analogues

To a shaken suspension of N^1,N^{14}-*bis*(3,4-dihydroxyhydrocinnamoyl)-N^{10}-*tert*-butyloxycarbonyl-N^5-(4-benzyloxycarbonyl-1-oxy acetamidomethyl resin)-1,5,10,14-tetraazatetradecane (**123**) (1 equiv, pre-swollen in CH_2Cl_2 and filtered) was added a solution of the carboxylic acid (4 equiv.) dissolved in CH_2Cl_2 (2-3 mL) and a few drops of DMF, HOBt (4 equiv) and DIC (4 equiv). The suspension was shaken at room temperature for 3-5 hours. The resin was filtered and washed with CH_2Cl_2 (2x10 mL), DMF (2x10 mL), MeOH (2x10 mL), and diethyl ether (2x10 mL). The resin was dried under vacuum and gave a negative ninhydrin test. The resin was treated with a cleavage cocktail of TFA/water/CH_2Cl_2/thioanisole (8.0:0.5:0.5:1.0, 3 mL) and the suspension were shaken at room temperature for 2-3 hours. The resin was filtered and washed with CH_2Cl_2 (2 mL). The solution was concentrated under reduced pressure to a volume of approximately 1 mL. The product precipitated by dropping into cold *tert*-butylmethylether 25 mL. The precipitate was collected by centrifugation and washed with hexane before being re-dissolved in water with few drops of acetonitrile and freeze-dried.

The crude product was analysed using analytical reverse-phase HPLC (C-18 column 4.5 mm x 250 mm using a linear gradient from H_2O + 0.1 %TFA (solvent A) to acetonitrile + 0.1 % TFA (solvent B) with a flow rate of 1mL/min, monitored at 220 nm). The gradient condition used were t = 0, 100 % A t = 20 100% B. The crude product was purified by preparative RP-HPLC using a linear gradient from H_2O + 0.1 %TFA (solvent

A) to acetonitrile + 0.1 % TFA (solvent B) with a flow rate of 2.5 mL/min, monitoring at 220 nm. The gradient condition used were t = 0, 100 % A t = 40 100% B.

N^{1},N^{14}-*bis*(2,3-Dimethoxyhydrocinnamoyl)-1,5,10,14-tetraazatetradecane (141b)

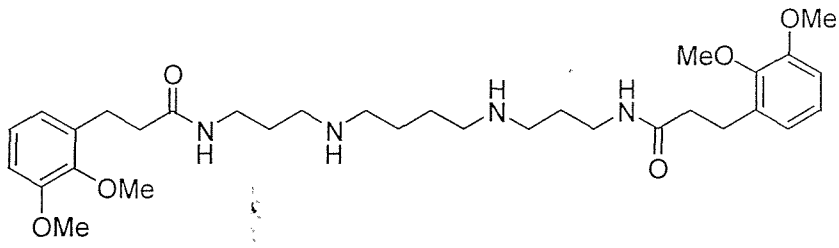

RP-HPLC: R_t = 10.7 min.

Yield: 11.7 mg (28%).

IR (ν_{max}/ cm^{-1}) 1679 (C=O).

δ_H (300 MHz, CD_3OD): 1.13 (8H, m, $C^{3+7+8+12}H_2$), 1.90 (4H, t, *J* 7, $ArC\underline{H}_2$), 2.12 (4H, m, $ArCH_2C\underline{H}_2$), 2.28 (8H, m, $C^{4+6+9+11}H_2$), 2.68 (4H, m, $C^{2+13}H_2$), 3.16 (6H, s,OCH_3), 3.20 (6H, s,OCH_3), 6.14, (2H, d, *J* 8,Ar$\underline{H}$), 6.21 (2H, d, *J* 7,Ar$\underline{H}$), 6.35 (2H, dd, *J* 8, 7,Ar$\underline{H}$)

ES-MS (+ve): m/z = 587.6 (100%, $M+H)^+$

N^{1},N^{14}-*bis*(4-Hydroxy-3,5-dimethoxycinnamoyl)-1,5,10,14-tetraazatetradecane (141c)

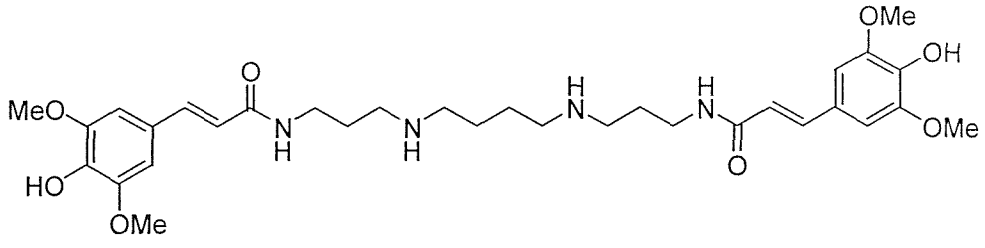

RP-HPLC: R_t = 8.8 min.

Yield 21 mg (25%).

δ_H (300 MHz, CD_3OD): 1.25 (8H, br m, $C^{3+7+8+12}H_2$); 2.40 (8H, br m, $C^{4+6+9+11}H_2$), 2.75 (4H, br m, $C^{2+13}H_2$), 3.15 (12 H, s, 4xOCH_3), 5.75 (2H, d, *J* 16, ArCH=C$\underline{H}$CO), 6.15 (4H, m,Ar$\underline{H}$), 7.1-7.3 (2H, m, ArC$\underline{H}$=CHCO).

ES-MS (+ve): 615.5 (100%, $M+H)^+$.

HRMS (FAB): $C_{32}H_{47}N_4O_8$ Calc. 615.3394, Found 615.3385.

N^1,N^{14}-*bis*(4-Methoxycinnamoyl)-1,5,10,14-tetraazatetradecane (141d)

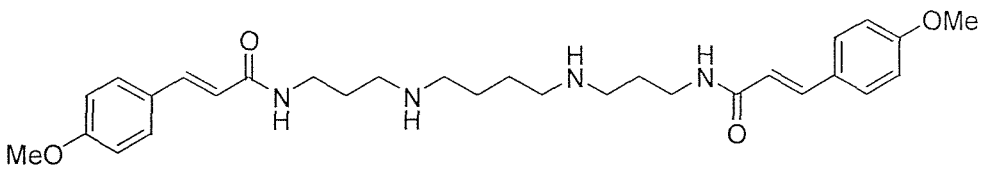

RP-HPLC: R_t = 10.8 min.

Yield 14 mg (26%).

IR (ν_{max}/ cm^{-1}) 1677 (C=O).

δ_H (300MHz, CD_3OD): 1.18 (4H, m, $C^{7+8}H_2$); 1.28 (4H, m, C^{3+12}), 2.38 (8H, m $C^{4+6+9+11}H_2$), 2.76 (4H, t, *J* 7, $C^{2+13}H_2$), 3.15 (6H, s, OCH_3), 5.79 (2H, d, *J* 16, C<u>H</u>=CHCO), 6.26, (4H, d, *J* 9, Ar<u>H</u>), 6.82 (4H, d, *J* 9, Ar<u>H</u>), 6.85 (2H, d, *J* 16, ArC<u>H</u>=CH).

δ_C (75MHz, CD_3OD): 24.3, 27.8, 36.8, 46.2, 55.8, 115.3, 118.3, 128.5, 130.5, 142.2, 162.7, 170.2.

ES-MS (+ve): m/z = 523.9 (100%, $M+H)^+$.

N^1,N^{14}-*bis*(3-Methoxycinnamoyl)-1,5,10,14-tetraazatetradecane (141e)

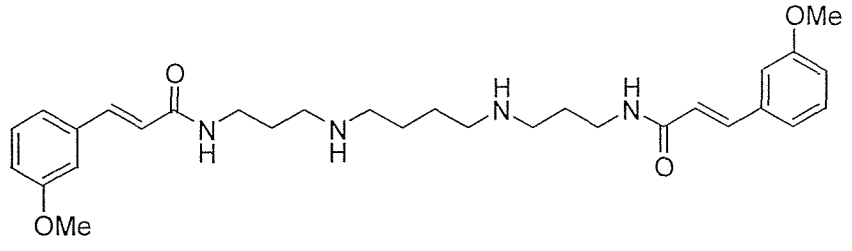

RP-HPLC: R_t = 10.3 min.

Yield 24 mg (49%).

IR (ν_{max}/ cm^{-1}) 1673 (C=O).

δ_H (300MHz, CD_3OD): 1.15, (4H, br m, $C^{7+8}H_2$); 1.27 (4H, m, C^{3+12}), 2.36 (8H, m $C^{4+6+9+11}H_2$), 2.74 (4H, t, *J* 7, $C^{2+13}H_2$), 3.10 (6H, s, OCH_3), 5.90 (2H, d, *J* 16, ArCH=C<u>H</u>CO), 6.24, (2H, dd, *J* 8, 2, Ar<u>H</u>), 6.38 (2H, d, *J* 2, Ar<u>H</u>), 6.42 (2H, d, *J* 8 Ar<u>H</u>), 6.59 (2H, t, *J* 8 Ar<u>H</u>), 6.83 (2H, d, *J* 16, ArC<u>H</u>=CHCO).

δ_C (75MHz, CD_3OD): 24.3, 27.7, 36.9, 46.3, 55.8, 113.9, 116.6,121.4, 131.0, 137.3, 142.4, 161.4, 169.6.

ES-MS (+ve): m/z = 523.9 (100%, $M+H)^+$

N^1,N^{14}-bis (4-Hydroxycinnamoyl)-1,5,10,14-tetraazatetradecane (141f)

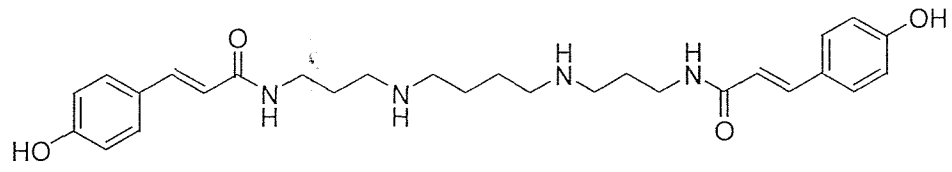

RP-HPLC: R_t = 8.9 min.

Yield 28 mg (77%).

IR (ν_{max}/ cm^{-1}) 1679 (C=O).

δ_H (300MHz, CD_3OD): 1.17, (8H, m, $C^{3+7+8+12}H_2$); 2.29 (8H, m $C^{4+6+9+11}H_2$), 2.70 (4H, m, $C^{2+13}H_2$), 5.13 (2H, br d, ArCH=C<u>H</u>CO), 5.68 (2H, d, *J* 15, ArC<u>H</u>=CHCO), 6.06 (4H, m, Ar<u>H</u>), 6.70 (4H, m, Ar<u>H</u>).

ES-MS (+ve): = 495.6 (100%, $M+H)^+$.

N^1,N^{14}-bis (3,4-Dihydroxyphenylacetyl)-1,5,10,14-tetraazatetradecane (141g)

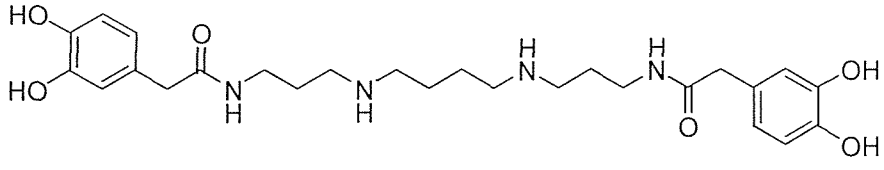

RP-HPLC: R_t = 7.6 min.

Yield 35 mg (37%).

IR (ν_{max}/ cm^{-1}) 1672 (C=O).

δ_H (300MHz, CD_3OD): 0.95 (4H, m, $C^{7+8}H_2$), 1.18 (4H, apparent quin, *J* 7, C^{3+12} H_2), 2.23 (8H, m, $C^{4+6+9+11}H_2$), 2.68 (4H, m, $C^{2+13}H_2$), 2.70 (4H, s, ArC<u>H</u>$_2$CO), 5.94 (2H, dd, *J* 8, 2,Ar<u>H</u>), 6.06 (2H, d, *J* 8,Ar<u>H</u>), 6.09 (2H, d, *J* 2,Ar<u>H</u>).

N^1,N^{14}-*bis* (2,5-Dihydroxyphenylacetyl)-1,5,10,14-tetraazatetradecane (141h)

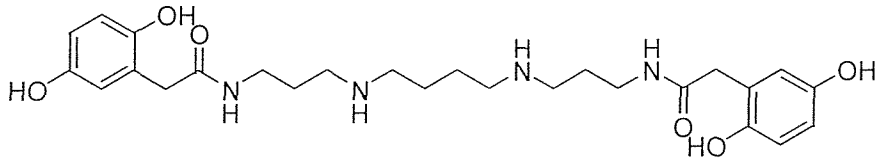

RP-HPLC: R_t = 7.2 min.

Yield 7 mg (10%).

δ_H (300MHz, CD_3OD): 0.98, (4H, m, $C^{7+8}H_2$); 1.17 (4H, m, C^{3+12}), 2.16 (4H, m $C^{6+9}H_2$), 2.25 (4H, t, *J* 7, $C^{4+11}H_2$), 2.66 (4H, m, $C^{2+13}H_2$), 2.80 (4H, s, $ArC\underline{H}_2CO$), 5.90 (2H, dd, *J* 9, 3, Ar<u>H</u>), 5.93 (2H,d, *J* 3, Ar<u>H</u> 5.99 (2H, d, *J* 9, Ar<u>H</u>).

ES-MS (+ve): m/z 503.8 (100%, $M+H)^+$

N^1,N^{14}-*bis*(2-Hydroxyphenylacetyl)-1,5,10,14-tetraazatetradecane (141i)

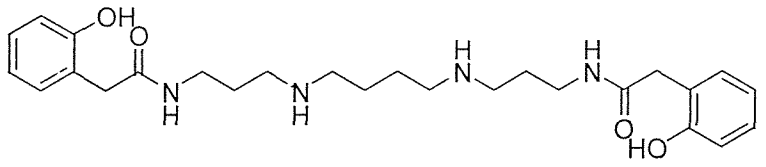

RP-HPLC: R_t = 7.6 min.

Yield 30 mg (38%).

IR (ν_{max}/ cm^{-1}) 1673 (C=O).

δ_H (300MHz, CD_3OD): 1.00 (4H, m, $C^{7+8}H_2$); 1.20 (4H, apparent quin, C^{3+12} H_2), 2.22 (4H, m, $C^{4+6}H_2$), 2.30 (4H, m, $C^{9+11}H_2$), 2.68 (4H, m, $C^{2+13}H_2$), 2.89 (4H, s, $ArC\underline{H}_2CO$), 6.15 (2H, d, *J* 7, Ar<u>H</u>), 6.17 (2H, dd, *J* 7, 2 Ar<u>H</u>), 6.47, (4H, dt, *J* 7,2 Ar<u>H</u>).

δ_C (75MHz, CD_3OD): 24.0, 27.6, 36.4, 39.0, 45.7, 47.9, 116.1, 120.8, 123.1, 129.6, 132.3, 156.7, 176.3.

N^1,N^{14}-*bis*(3-Hydroxyphenylacetyl)-1,5,10,14-tetraazatetradecane (141j)

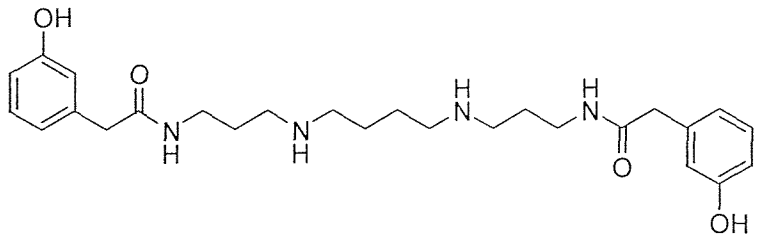

RP-HPLC: R_t = 10.1 min.

Yield 15 mg (18%).

IR (ν_{max}/ cm^{-1}) 1682 (C=O).

δ_H (300MHz, CD_3OD): 0.98 (4H, m, $C^{7+8}H_2$), 1.20 (4H, apparent quin, C^{3+12}), 2.25 (8H, m, $C^{4+6+9+11}H_2$), 2.65 (4H, m, $C^{2+13}H_2$), 2.80 (4H, s, $ArC\underline{H}_2CO$), 6.05 (2H, dd, *J* 7, 2 Ar<u>H</u>), 6.15 (4H, m, Ar<u>H</u>), 6.45 (2H, t, *J* 7 Ar<u>H</u>).

N^1,N^{14}-*bis*(4-Hydroxyphenylacetyl)-1,5,10,14-tetraazatetradecane (141k)

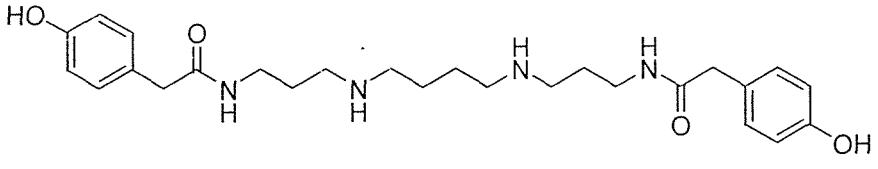

RP-HPLC: R_t = 9.8 min.

Yield 15 mg (23%).

IR (ν_{max}/ cm^{-1}) 1676 (C=O).

δ_H (300MHz, CD_3OD): 1.08 (4H, m, $C^{7+8}H_2$), 1.29 (4H, apparent quint, C^{3+12}), 2.28 (8H, br t, *J* 7, $C^{4+6+9+11}H_2$), 2.76 (4H, m, $ArC\underline{H}_2$), 2.88 (4H, m, $C^{2+13}H_2$), 6.21 (4H, d, *J* 8, Ar<u>H</u>), 6.56, (4H,d, *J* 8, Ar<u>H</u>).

N^1,N^{14}-*bis* (2-Quinoxaline-carboxyl)-1,5,10,14-tetraazatetradecane (141l)

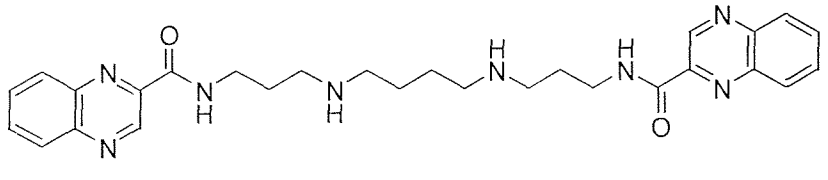

RP-HPLC: R_t = 9.5 min.

Yield 35 mg (54%).

IR (ν_{max}/ cm^{-1}) 1676 (C=O).

δ_H (300MHz, CD_3OD): 1.17 (4H, m, $C^{7+8}H_2$), 1.38 (4H, apparent quint, $C^{3+12}H_2$), 2.45 (8H, t, *J* 7, $C^{4+6+9+11}H_2$), 2.93 (4H, t, *J* 7, $C^{2+13}H_2$), 7.21 (4H, m, Ar<u>H</u>), 7.44 (2H, m, Ar<u>H</u>), 8.75 (2H, s, Ar<u>H</u>).

δ_C(75MHz, CD_3OD): 24.2, 27.7, 37.1, 46.4, 129.9, 130.8, 132.3, 133.2, 141.7, 144.4, 144.6, 144.9, 166.5.

ES-MS (+ve): m/z 515.3 (100%, $M+H)^+$.

***N*^{1},*N*^{14}-*bis*(4-Hydroxy-7-trifluoromethyl-3-quinolinecarboxyl)-1,5,10,14-tetraazatetradecane (141m)**

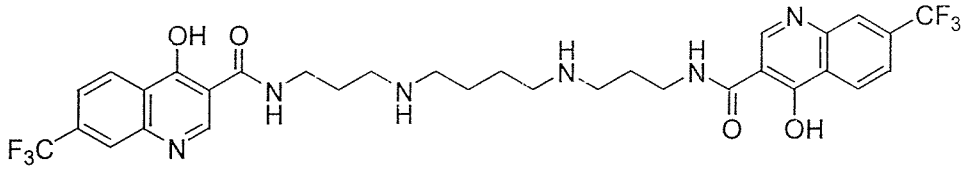

RP-HPLC: R_t = 11.5 min.

Yield 14 mg (25%).

IR (ν_{max}/ cm^{-1}) 1655 (C=O).

δ_H (300 MHz, CD_3OD): 1.25 (4H, m, $C^{7+8}H_2$), 1.39 (4H, apparent quint, $C^{3+12}H_2$), 2.46 (8H,br t, *J* 7, $C^{4+6+9+11}H_2$), 2.96 (4H, t, *J* 7, $C^{2+13}H_2$), 6.93 (2H, d, *J* 9, Ar<u>H</u>), 7.22, (2H, s, Ar<u>H</u>), 7.66 (2H, d, *J* 9, Ar<u>H</u>), 8.08 (2H, s, Ar<u>H</u>).

δ_C (75MHz, CD_3OD): 24.1, 28.0, 36.3, 46.1, 112.3, 117.4, 121.9, 128.3, 129.5, 140.1, 146.0, 168.2, 177.5 (one signal under DMSO)

ES-MS (+ve): m/z 681.6 (100%, $M+H)^+$

HRMS: $C_{32}H_{35}F_6N_6O_4$ Calc. 681.2624 Found 681.2620.

N^1,N^{14}-*bis*(2-Pyrimidylthioacetyl)-1,5,10,14-tetraazatetradecane (141n)

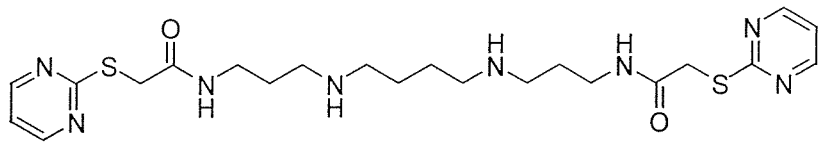

RP-HPLC: R_t = 7.6 min.

Yield 5 mg (4%).

IR (ν_{max}/ cm^{-1}) 1680 (C=O).

δ_H (300MHz, CD_3OD): 1.09 (4H, m, $C^{7+8}H_2$), 1.22 (4H, m, $C^{3+12}H_2$), 2.34 (4H, m, $SC\underline{H}_2$), 2.66 (8H, m, $C^{4+6+9+11}H_2$), 3.28 (4H, m, $C^{2+13}H_2$), 6.56 (2H, m, Ar$\underline{H}$), 7.96 (4H, m, Ar$\underline{H}$).

ES-MS (+ve): m/z 507.3 (100%, $M+H)^+$.

N^1,N^{14}-*bis*(Pyrrole-2-carboxyl)-1,5,10,14-tetraazatetradecane (141o)

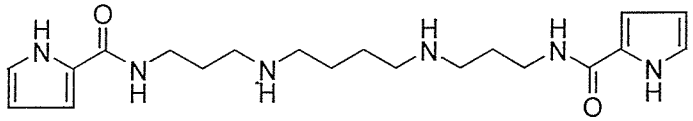

RP-HPLC: R_t = 10.2 min.

Yield 26 mg.(40%)

IR (ν_{max}/ cm^{-1}) 1676 (C=O).

δ_H (300 MHz, CD_3OD): 1.16 (4H, m, $C^{7+8}H_2$), 1.28 (4H, apparent quint, C^{3+12}), 2.37 (8H, t, *J* 7, $C^{4+6+9+11}H_2$), 2.78 (4H, t, *J* 7, $C^{2+13}H_2$), 5.49 (2H, dd, *J* 4, 2, Ar$\underline{H}$), 6.12, (2H, dd, *J* 4, 2, Ar$\underline{H}$), 6.24 (2H, dd, *J* 2, 2 Ar$\underline{H}$).

δ_C (75MHz, CD_3OD): 24.2 28.0 , 36.4, 46.1, 110.4 , 112.1, 123.3, 126.0 164.8 (plus one under DMSO signal).

ES-MS (+ve): m/z 389.4 (100%, $M+H)^+$.

N^1,N^{14}-*bis*(Thiophene-2-acetyl)-1,5,10,14-tetraazatetradecane (141p)

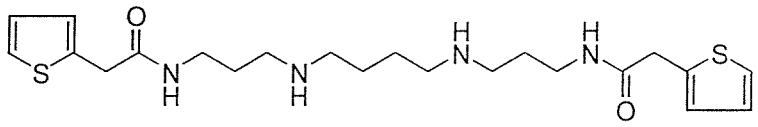

RP-HPLC: R_t = 8.7 min.

Yield 5 mg (16%).

IR (ν_{max}/ cm^{-1}) 1681 (C=O).

δ_H (300 MHz, CD_3OD)**:** 1.31 (4H, m, $C^{7+8}H_2$), 1.45 (4H, m, C^{3+12}), 2.53 (8H, m, $C^{4+6+9+11}H_2$), 2.74 (4H, m, $C^{2+13}H_2$), 2.95 (4H, d, *J* 6, $C\underline{H}_2CO$), 6.56 (4H, m, Ar$\underline{H}$), 7.10 (2H, m, Ar$\underline{H}$).

ES-MS (+ve): m/z 451.5 (100%, $M+H)^+$.

N^1,N^{14}-*bis* (2-Thiophenecarboxyl)-1,5,10,14-tetraazatetradecane (141q)

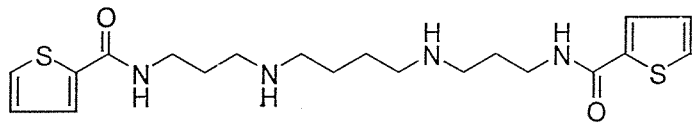

RP-HPLC: R_t = 8.9 min.

Yield 9 mg (32%).

IR (ν_{max}/ cm^{-1}) 1677 (C=O).

δ_H (300MHz, CD_3OD)**:** 1.18 (4H, m, $C^{7+8}H_2$), 1.31 (4H, m, C^{3+12}), 2.35 (8H, m, $C^{4+6+9+11}H_2$), 3.19 (4H, m, $C^{2+13}H_2$), 6.39 (2H, m, Ar$\underline{H}$), 6.68 (4H, m, Ar$\underline{H}$).

ES-MS (+ve): m/z 423.4 (100%, $M+H)^+$.

N^1,N^{14}-*bis*(5-Bromo-2-furoyl)-1,5,10,14-tetraazatetradecane (141r)

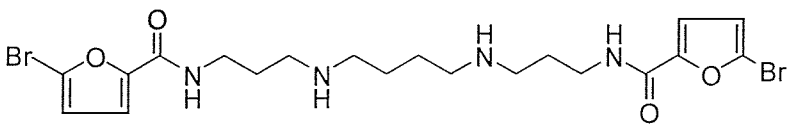

RP-HPLC: R_t = 10.0 min.

Yield 5 mg (15%).

IR (ν_{max}/ cm^{-1}) 1676 (C=O).

δ_H (300 MHz, CD_3OD): 1.21 (4H, m, $C^{7+8}H_2$), 1.36 (4H, m, C^{3+12}), 2.44 (8H, m, $C^{4+6+9+11}H_2$), 2.71 (4H,m, $C^{2+13}H_2$), 5.98 (2H, m, ArH), 6.50, (2H, m, ArH).

ES-MS (+ve): m/z 547.1, 549.1 and 550.9 (48%, 100%, 62%, M+H, bromine isotopes)$^+$.

N^1,*N*^{14}-*bis*(4-Hydroxyquinoneline carboxyl)-1,5,10,14-tetraaza tetradecane (141s)

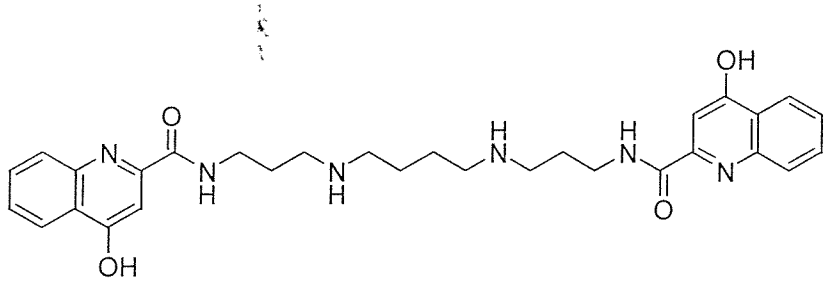

RP-HPLC: R_t = 8.8 min.

Yield 36 mg (63%).

IR (ν_{max}/ cm^{-1}) 1638 (C=O).

δ_H (300MHz, CD_3OD): 1.13 (4H, m, $C^{7+8}H_2$), 1.37 (4H, apparent quint, C^{3+12}), 2.43 (8H, m, $C^{4+6+9+11}H_2$), 2.87 (4H, t, *J* 7, $C^{2+13}H_2$), 6.23 (2H, s, ArH), 6.86 (2H, ddd, *J* 9,7,2,ArH), 7.16, (2H, ddd, *J* 9,7,2,ArH), 7.20 (2H, d, *J* 9,ArH), 7.54 (2H, d, *J* 9,ArH).

δ_C (75MHz, CD_3OD): 24.2 27.1, 38.2, 46.5, 49.7, 107.3, 120.7, 125.7, 127.0 135.2, 141.1, 144.0, 164.0, 180.2.

ES-MS (+ve): m/z 545.6 (100%, M+H)$^+$.

N^1,*N*^{14}-*bis* (Indole-3-acetyl)-1,5,10,14-tetraazatetradecane (141y)

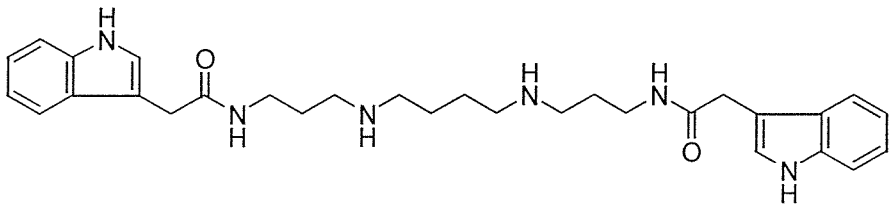

RP-HPLC: R_t = 9.9 min.

Yield 15 mg (60%).

IR (ν_{max}/ cm^{-1}) 1674 (C=O).

δ_H (300MHz, CD_3OD): 0.83 (4H, m, $C^{7+8}H_2$), 1.10 (4H, apparent quint, $C^{3+12}H_2$), 1.98 (4H, m, $C^{6+9}H_2$), 2.08 (4H, t, *J* 7, $C^{4+11}H_2$), 2.61 (4H, m, $C^{2+13}H_2$), 3.00 (2H, s, $ArC\underline{H}_2$), 6.34 (2H, d, *J* 8, Ar<u>H</u>), 6.43 (2H, dt, *J* 7, 1, Ar<u>H</u>), 6.51 (2H, s, Ar<u>H</u>), 6.68 (2H, d, *J* 8, Ar<u>H</u>), 6.87 (2H, d, *J* 7, Ar<u>H</u>).

δ_C (75MHz, CD_3OD): 23.9, 27.6, 33.8, 36.5, 45.8, 47.8, 109.3, 112.5, 119.2, 120.0, 122.7, 125.1, 128.3, 138.1, 176.5.

N^{1},*N*^{14}-*bis* (5-Hydroxyindole-3-acetyl)-1,5,10,14-tetraazatetradecane (141I)

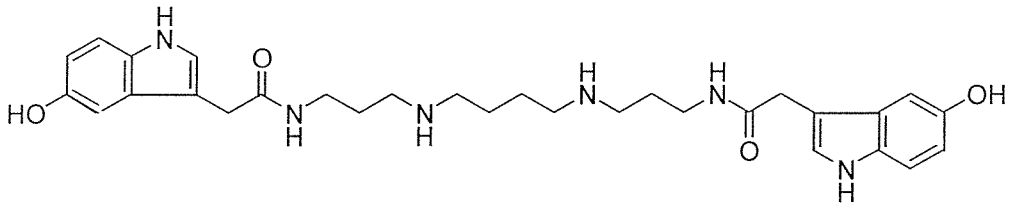

RP-HPLC: R_t = 9.9 min.

Yield 7 mg (35%).

IR (ν_{max}/ cm^{-1}) 1675 (C=O).

δ_H (300MHz, CD_3OD): 1.02 (8H, m, $C^{3+7+8+12}H_2$), 1.66 (2H, t, *J* 7, C^6H_2), 1.75 (2H, t, *J* 7, C^9H_2), 1.82 (2H, t, *J* 7, C^4H_2), 1.94 (2H, t, *J* 7, $C^{11}H_2$), 2.60 (4H, t, *J* 7, $C^{2+13}H_2$), 3.30 (4H, s, $ArC\underline{H}_2$), 6.37 (2H, d, *J* 2, Ar<u>H</u>), 6.43 (2H, s, Ar<u>H</u>), 6.50 (2H, dd, *J* 8, 2, Ar<u>H</u>), 6.66 (2H, d, *J* 8, Ar<u>H</u>).

ES-MS (+ve): m/z = 549.4 (10%, $M+H)^+$.

N^{1},*N*^{14}-*bis* (Indole-3-propionyl)-1,5,10,14-tetraazatetradecane (141II)

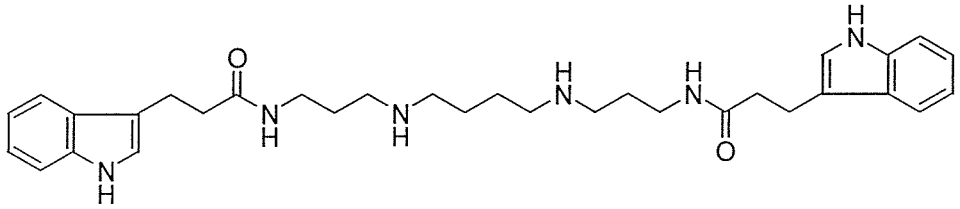

RP-HPLC: R_t = 10.5 min.

Yield 12 mg (32%).

δ_H (300MHz, CD_3OD): 0.91 (4H, m, $C^{7+8}H_2$); 1.09 (4H, apparent quint, $C^{3+12}H_2$), 1.88 (8H, t, *J* 7, $C^{4+6+9+11}H_2$), 2.05 (2H, t, *J* 7, indole $C^{\alpha}H_2$), 2.49 (2H, t, *J* 7, indole $C^{\beta}H_2$), 2.63 (2H, t, *J* 6, $C^{2+13}H_2$), 6.61 (1H, t, *J* 8, Ar<u>H</u>), 6.47 (1H, s, Ar<u>H</u>), 6.49 (1H, t, *J* 8, Ar<u>H</u>), 6.73 (1H, d, *J* 8, Ar<u>H</u>), 6.96 (1H, d, *J* 8, Ar<u>H</u>).

δ_C (75MHz, CD_3OD): 22.2, 24.1, 27.5, 36.2, 37.4, 45.5, 47.8, 112.3, 114.7, 119.4, 119.4, 119.7, 122.4, 123.1, 128.6, 137.9, 177.2.

ES-MS (+ve): m/z = 545.4 (40%, $M+H)^+$.

HRMS (EI): $C_{32}H_{45}N_6O_2$ Calc. 545.3598, Found 545.3597.

N^1,N^{14}-bis (5-Methoxyindole-3-acetyl)-1,5,10,14-tetraazatetradecane (141VI)

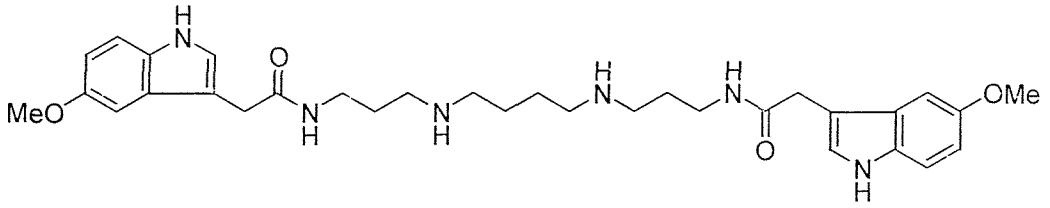

RP-HPLC: R_t = 12.1 min.

Yield 22 mg (50%).

IR (ν_{max}/ cm^{-1}) 1676 (C=O).

δ_H (300MHz, CD_3OD): 1.00 (4H, m, $C^{7+8}H_2$), 1.29 (4H, apparent quint, $C^{3+12}H_2$), 2.18 (4H, m, $C^{6+9}H_2$), 2.27 (4H t, *J* 7, $C^{4+11}H_2$), 2.79 (4H, m, $C^{2+13}H_2$), 3.14 (2H, s, Ar$C\underline{H}_2$), 3.29 (3H, s, OMe), 6.62 (1H, dd, *J* 9, 3 Ar<u>H</u>), 6.55 (1H, d, *J* 3, Ar<u>H</u>), 6.65 (1H, s, Ar<u>H</u>), 6.74 (1H, d, *J* 9, Ar<u>H</u>).

δ_C (75MHz, CD_3OD): 23.9, 27.6, 33.9, 36.5, 45.8, 47.8, 101.6, 109.1, 112.7, 113.2, 125.8, 128.7, 133.3, 155.2, 176.5.

ES-MS (+ve): m/z = 577.4 (70%, $M+H)^+$.

HRMS (EI): $C_{32}H_{45}N_6O_4$ Calc. 577.3497, Found 577.3497.

N^1,N^{14}-bis (Indole-3-buthyl)-1,5,10,14-tetraazatetradecane (141XI)

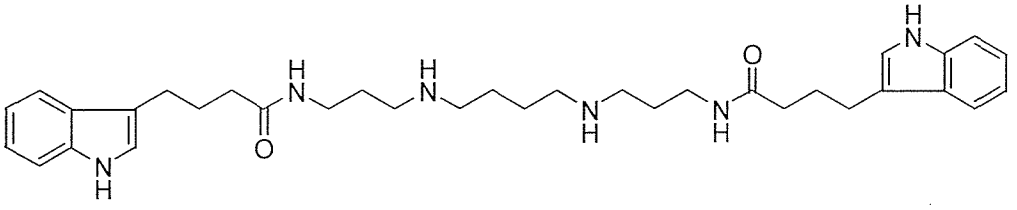

Material was very unstable and decomposed very rapidly after purification.

RP-HPLC: R_t = 10.6 min.

Yield 10 mg (36%).

IR (ν_{max}/ cm^{-1}) 1679 (C=O).

δ_H (400MHz, CD_3OD): 1.49 (4H, m, $C^{7+8}H_2$); 1.60 (4H, m, $C^{3+12}H_2$), 1.89 (4H, m, indole $C^{\beta}H_2$), 2.23 (4H, m, indole $C^{\alpha}H_2$), 2.44 (4H, m, $C^{4+6+9+11}H_2$), 2.76 (4H, m, indole $C^{\gamma}H_2$), 3.20 (4H, m, $C^{2+13}H_2$), 6.98 (2H, m, Ar<u>H</u>), 7.18 (2H, m, Ar<u>H</u>), 7.33 (2H, d, *J* 9, Ar<u>H</u>), 7.59 (2H, d, *J* 9, Ar<u>H</u>).

N^1,N^{14}-bis (5-Bromoindole-3-acetyl)-1,5,10,14-tetraazatetradecane (141XII)

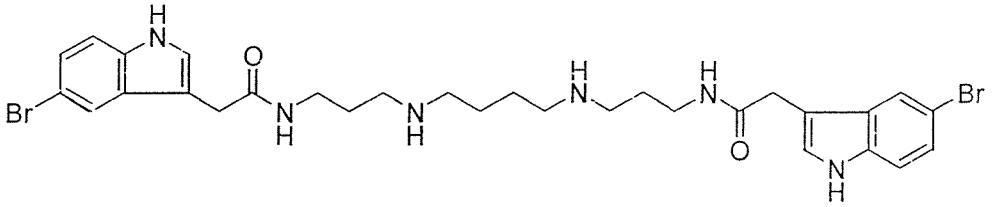

RP-HPLC: R_t = 11.4 min.

Yield 23 mg (55%).

IR (ν_{max}/ cm^{-1}) 1674 (C=O).

δ_H (300MHz, CD_3OD): 0.94 (4H, m, $C^{7+8}H_2$), 1.14 (4H, apparent quint, $C^{3+12}H_2$), 2.15 (8H, m, $C^{4+6+9+11}H_2$), 2.63 (4H, t, *J* 7, $C^{2+13}H_2$), 2.98 (2H, s, Ar$C\underline{H}_2$), 6.53 (1H, dd, *J* 9, 2, Ar<u>H</u>), 6.56 (1H, s, Ar<u>H</u>), 6.62 (1H, d, *J* 9, Ar<u>H</u>), 7.06 (1H, d, *J* 2, Ar<u>H</u>).

δ_C (75MHz, CD_3OD): 24.0, 27.6, 33.6, 36.6, 46.0, 47.9, 109.2, 113.1, 114.2, 122.0, 125.3, 126.6, 130.2, 136.7, 176.0.

ES-MS (+ve): m/z = 673.2, 675.2, 677.2 (20%, 45%, 20%, $M+H)^+$.

HRMS (EI): $C_{30}H_{39}N_6O_2Br_2$ Calc. 673.1496, Found 673.1491.

N^1, N^{10}- *bis*(Phthaloyl)-1,5,10-triazadecane (142)

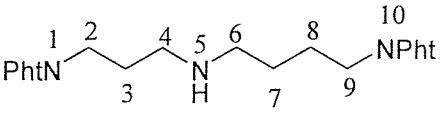

To a solution of spermidine (1.51g, 10.5 mmol) in $CHCl_3$ (20 mL) was added a solution of N-(ethoxycarbonyl)-phathalimide (5.27g, 24.1 mmol) in $CHCl_3$ (10 mL) at room temperature over in 30 min. After stirring for 3 hours, the solvent was evaporated *in vacuo* and the residue was recrystallized from methanol. The solid was collected by filtration and washed with diethyl ether (3x20 mL) and dried under vacuum to give N^1, N^{10}-(Phthaloyl)-1,5,10-triazadecane as a colorless solid.

TLC: $R_f = 0.7$ ($CHCl_2$ / MeOH / NH_4OH (70:10: 1)

Yield: 3.35 g (79%)

m.p. 138-140 ^{O}C.

IR (ν_{max}/ cm^{-1}) 1705 (C=O).

δ_H (300MHz, $CDCl_3$): 1.55 (2H, tt, *J* 7, 7, C^8H_2); 1.71 (2H, tt, *J* 7.4, 7, C^7H_2), 1.85 (2H, tt, *J* 7, C^3H_2), 2.62 (4H, tt, *J* 7, $C^{4+6}H_2$), 3.70 (2H, t, *J* 7, C^9H_2), 3.77 (2H, t, *J* 7, C^2H_2), 7.71 (4H, dd, *J* 6,4, ArH), 7.84 (4H, dd, *J* 6,4, ArH).

δ_C (75MHz, $CDCl_3$): 26.5, 27.5, 29.1, 36.0, 38.0, 47.0, 49.5, 123.3, 123.4, 132.3, 134.0, 168.6.

ES-MS (+ve): m/z = 406.2 (100%, $M+H)^+$.

N^1,N^{10}-*bis*(Phthaloyl)-N^5-(4-benzyloxycarbonyl-oxyacetic acid allyl ester)-1,5,10-triazadecane (143)[102]

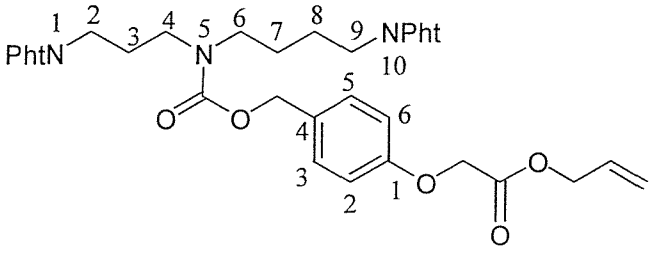

N^1, N^{10}-*bis*(Phthaloyl)-1,5,10-triazadecane (2.12g, 5.2 mmol) was dissolved in DMF (30 mL) and Et_3N (1.0 mL, 7.0 mmol). The solution was cooled in an ice bath to 0 °C and a solution of [4-(4'-nitro-phenoxycarbonyloxymethyl)-phenoxy]-acetic acid allyl ester

(2.73 g, 6.8 mmol) in DMF (10 mL) was added drop-wise over 10 min followed by the addition of DMAP (~50 mg). After 30 min at 0 °C the mixture was allowed to warm to room temperature and was stirred overnight, before partitioning between 2M $KHSO_4$ (50 mL) and ethyl acetate (100 mL). The organic extract was washed with 10% sodium bicarbonate (2x50 mL) and saturated aqueous sodium chloride (50 mL), dried ($MgSO_4$) and the solvent was evaporated *in vacuo* to give a yellow liquid. Purification by flash chromatography on silica gel (eluting with hexane: ethyl acetate; 1:1) provided the title compound as a colourless liquid.

TLC: R_f = 0.4 (hexane / ethyl acetate (1:1)

Yield: 2.72 g (80 %).

IR (ν_{max}/ cm^{-1}) 1769 (C=O, urethane), 1706 (C=O).

δ_H (300MHz, $CDCl_3$): 1.60 (4H, m, $C^{7+8}H_2$), 1.18 (2H, m, C^3H_2), 3.26 (4H, m, $C^{4+6}H_2$), 3.68 (4H, m, $C^{2+9}H_2$), 4.61 (2H, s, $OC\underline{H}_2CO$), 4.68 (2H, d, *J* 6, $C\underline{H}_2CH{=}CH_2$), 5.00 (2H, s, $ArC\underline{H}_2O$), 5.25 (1H, d, *J* 10, $OCH_2CH{=}C\underline{H}_{cis}$), 5.32 (1H, d, *J* 17, $OCH_2CH{=}C\underline{H}_{trans}$), 5.91 (1H, ddt, *J* 17, 10, 6, $OCH_2C\underline{H}{=}CH_2$), 6.85 (2H, m, $Ar\underline{H}$), 7.32 (2H, m, $Ar\underline{H}$), 7.70 (4H, m, $Ar\underline{H}$), 7.84 (4H, m, $Ar\underline{H}$).

δ_C (75MHz, $CDCl_3$) (rotameric forms observed), 26.0, 27.4, 27.9, 35.9, 37.6, 44.9, 45.4, 46.4 47.1, 65.5, 66.0, 66.8, 114.8, 119.3, 123.4, 129.8, 130.2, 131.6, 132.2, 134.1, 157.6, 168.4, 168.5, 168.7.

ES-MS (+ve): m/z = 654.9 (10%, $M+H)^+$, 676.9 (40%, $M+Na)^+$.

N^1,N^{10}-*bis*(Phthaloyl)-N^5-(4-benzyloxycarbonyl-oxyacetic acid)-1,5,10-triazadecane (144)

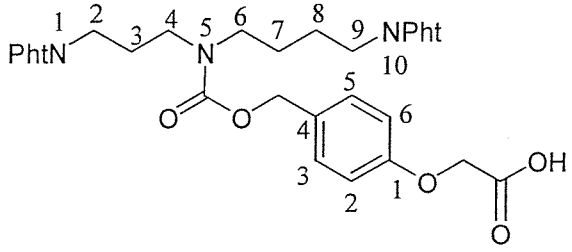

N^1,N^{10}-*bis*(Phthaloyl)-N^5-(4-benzyloxycarbonyl-oxyacetic acid allyl ester)-1,5,10-triazadecane (1.16 g, 1.4 mmol) was dissolved in dry dichloromethane (20 mL) and tetrahydrofuran (20 mL). The reaction mixture was stirred and degassed for 1 hour with a gentle flow of nitrogen. Thiosalicylic acid (0.96g, 6.2 mmol) and $Pd(PPh_3)_4$ (0.62g, 0.5 mmol) were added and the mixture stirred under nitrogen for 3 hours at room

temperature. The solution was concentrated under reduced pressure and the residue redissoved in dichloromethane (200 mL). The organic layer was washed with 2M $KHSO_4$ (2x50 mL) and saturated aqueous sodium chloride (50 mL), dried ($MgSO_4$) and the solvent evaporated *in vacuo* to give yellow liquid. Purification by flash chromatography (eluting with hexane: ethyl acetate; 1:1 ethyl acetate: methanol; 9: 1) provided the title compound as a yellow foam.

TLC: $R_f = 0.38$ (hexane / ethyl acetate (1:1)

Yield: 2.45 g (96 %).

IR (ν_{max}/ cm^{-1}) 1770 (C=O, urethane), 1709 (C=O).

δ_H (300MHz, $CDCl_3$): 1.63 (4H, m, $C^{7+8}H_2$), 1.91 (2H, m, C^3H_2), 3.32 (4H, m, $C^{4+6}H_2$), 3.70 (4H, m, $C^{2+9}H_2$), 4.63 (2H, s, $OC\underline{H}_2CO$), 5.06 (2H, s, $ArC\underline{H}_2O$), 6.83 (2H, m, Ar<u>H</u>), 7.24 (2H, m, Ar<u>H</u>), 7.70 (4H, m, Ar<u>H</u>), 7.82 (4H, m, Ar<u>H</u>).

δ_C (75MHz, $CDCl_3$) (rotameric forms observed): 25.5, 26.0, 27.4, 27.9, 35.8, 37.6, 44.9, 45.4, 46.5, 47.1, 65.0, 66.9, 114.8, 123.4, 129.9, 130.2, 132.2, 134.1, 156.4, 157.5, 168.5, 168.6, 172.4.

ES-MS (-ve): m/z = 726.9 (100%, M+TFA-H)$^-$

N^1,N^{10}-*bis*(Phthaloyl)-N^5-(4-benzyloxycarbonyl-oxyacetamidomethyl resin)-1,5,10-triazadecane (121)

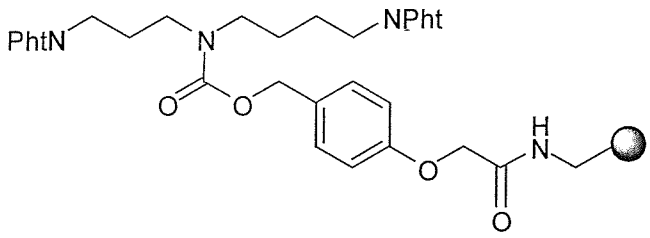

N^1,N^{10}-*bis*(Phthaloyl)-N^5-(4-benzyloxycarbonyl-oxyacetic acid)-1,5,10-triazadecane (0.84g, 1.4 mmol) was dissolved in dichloromethane (5 mL) at room temperature and HOBt (0.25g, 1.6 mmol) was added with DIC (0.25 mL, 1.6 mmol). After 10 min the solution was added to aminomethyl resin (pre-swollen in CH_2Cl_2 for 30 min. and filtered) (0.93g, 1.5 mmol, 1.6 $mmolg^{-1}$). The suspension was shaken at room temperature overnight. The resin was filtered and washed with CH_2Cl_2 (2x20 mL), DMF (2x20 mL), MeOH (2x20 mL), and Et_2O (2x20 mL). The resin was dried under vacuum and gave negative ninhydrin test.

N^5-(4-Benzyloxycarbonyl-oxyacetamidomethyl resin)-1,5,10-triazadecane (145)

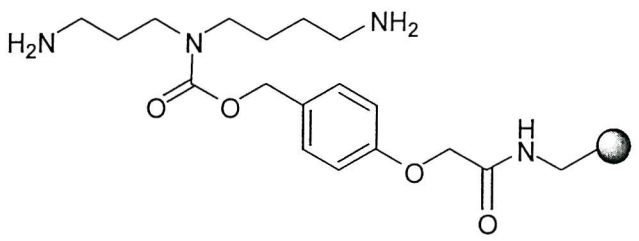

N^1,N^{10}-*bis*(Phthaloyl)-N^5-(4-benzyloxycarbonyl-oxyacetamidomethyl resin)-1,5,10-triazadecane (1.50 g) was added to absolute ethanol (50 mL) and hydrazine monohydrate (1 mL, 20.6 mmol). The solution was heated at 80 °C overnight. The resin was filtered and washed successively with hot water (2x20 mL), EtOH (2x20 mL), MeOH (2x20 mL), CH_2Cl_2 (2x20 v) and ether (2x20 mL). The resin was dried under vacuum. A quantitative ninhydrin test gave a loading of 0.9 $mmol.g^{-1}$ (1.31g).

General procedure for preparation of spermidine analogues

To a shaken suspension of N^5-(4-benzyloxycarbonyl-oxyacetamidomethyl resin)-1,5,10-triazadecane (**145**) (1 equiv. pre-swollen in CH_2Cl_2 and filtered) was added a solution of the carboxylic acid (4 equiv.) dissolved in CH_2Cl_2 (2-3 mL) and a few drops of DMF, HOBt (4 equiv.) and DIC (4 equiv.). The suspension was shaken at room temperature for 3-5 hours. The resin was filtered and washed with CH_2Cl_2 (2x10 mL), DMF (2x10 mL), MeOH (2x10 mL) and Et_2O (2x10 mL). The resin was dried under vacuum and gave a negative ninhydrin test. The resin was treated with a cleavage cocktail of TFA/water/CH_2Cl_2/thioanisole (16:1:1:2, 3 mL) and the suspension was shaken at room temperature for 2-3 hours. The resin was filtered and washed with CH_2Cl_2 (2 mL). The solution was concentrated under reduced pressure to a volume of approximate 1 mL. The product was precipitated by dropping into cold *tert*-butylmethylether 25 mL. The precipitate was collected by centrifugation and washed with hexane before re-dissolving into water with few drops of acetonitrile and freeze-dried.

N^1,N^{10}-*bis*(3,4-Dihydroxydihydrocinnamoyl)-1,5,10-triazadecane (148a)

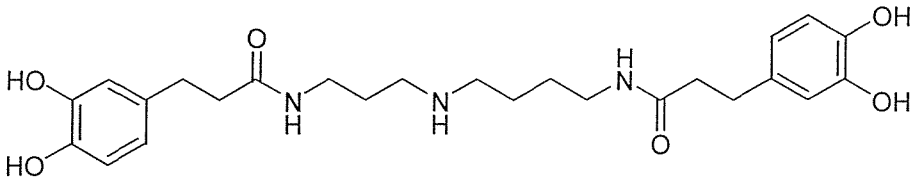

RP-HPLC: R_t = 8.4 min.

Yield: 78 mg (46%).

IR (ν_{max}/ cm^{-1}) 1676 (C=O).

δ_H (300MHz, CD_3OD): 0.76 (4H, m, $C^{7+8}H_2$), 1.06 (2H, m, C^3H_2), 1.72 (2H, t, *J* 7, $ArCH_2C\underline{H}_2$), 1.80 (2H, t, *J* 7, $ArCH_2C\underline{H}_2$), 1.94 (t, *J* 7, C^4H_2), 2.08 (6H, m, C^6H_2 and $ArC\underline{H}_2x2$), 2.48 (2H, t, *J* 7, C^9H_2), 2.55 (2H, t, *J* 7, C^2H_2), 5.85 (2H, m, $Ar\underline{H}$), 6.01 (4H, m, $Ar\underline{H}$).

δ_C (75MHz, CD_3OD): 24.4, 27.3, 27.4, 31.9, 32.4, 36.6, 38.5, 39.3, 39.4, 45.9, 48.6, 116.5, 116.8, 120.8, 120.9, 133.3, 133.7, 144.3, 144.5, 145.9, 146.0, 163.0, 163.4, 175.6, 176.5.

ES-MS (+ve): m/z = 474.3 (100%, $M+H)^+$.

HRMS (FTMS): $C_{25}H_{36}N_3O_6$ Calc. 474.2599, Found 474.2601.

N^1,N^{10}-*bis*(2,3-Dimethoxydihydrocinnamoyl)-1,5,10-triazadecane(148b)

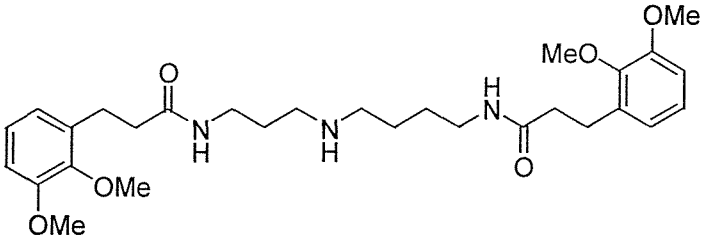

RP-HPLC: R_t = 11.5 min.

Yield 6 mg (21%).

δ_H (300MHz, CD_3OD): 0.93 (4H, m, $C^{7+8}H_2$), 1.12 (2H, m, C^3H_2), 1.81 (2H, t, *J* 7, $ArCH_2C\underline{H}_2$), 1.88 (2H, t, *J* 7, $ArCH_2C\underline{H}_2$), 2.11 (2H, t, *J* 7, C^4H_2), 2.26 (6H, m, $2xArC\underline{H}_2CH_2CO$ + C^6H_2), 2.54 (2H, t, *J* 7, C^9H_2), 2.59 (2H, t, *J* 7, C^2H_2), 3.15 (3H, s,

OCH_3), 3.16 (3H, s, OCH_3), 3.18 (6H, s, 2xOCH_3), 6.13 (2H, m, ArH), 6.21 (2H, m, ArH), 6.33 (2H, dd, *J* 8, 7, ArH).

ES-MS (+ve): m/z = 530.9 (100%, $M+H)^+$.

HRMS (FTMS): $C_{29}H_{44}N_3O_6$ Calc. 530.3225, Found 530.3226.

N^1,N^{10}-bis(4-Methoxycinnamoyl)-1,5,10-triazadecane(148d)

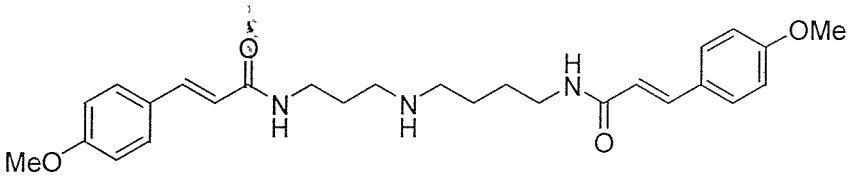

RP-HPLC: R_t = 11.1min.

Yield 42 mg (46%).

IR (ν_{max}/ cm^{-1}) 1677 (C=O).

Assignments based on H^1-H^1 and H^1-C^{13} correlations. δ_H (300MHz, CD_3OD): 1.69 (2H, m, C^8H_2), 1.79 (2H, m, C^7H_2) 1.55 (2H, m, C^3H_2), 3.07 (4H, m, $C^{4+6}H_2$), 3.38 (2H, t, *J* 7.4, C^9H_2), 3.04 (2H, t, *J* 7, C^2H_2), 3.78 (6H, s, OCH_3), 6.50 (2H, d *J* 16, ArCH=CH), 6.91 (4H, m, ArH), 7.52 (6H, m, ArCH=CH and ArH).

δ_C (75MHz, CD_3OD): 25.0, 28.0, 28.3, 37.4, 39.9, 46.7, 49.0, 56.2, 115.8, 118.9, 119.6, 128.3, 129.7, 130.2, 130.8, 130.9, 142.1, 142.7.

ES-MS (+ve): m/z = 466.4 (100%, $M+H)^+$.

HRMS (FTMS): $C_{27}H_{36}N_3O_4$ Calc. 466.2700, Found 466.2696.

N^1,N^{10}-bis(3-Methoxycinamoyl)-1,5,10-triazadecane(148e)

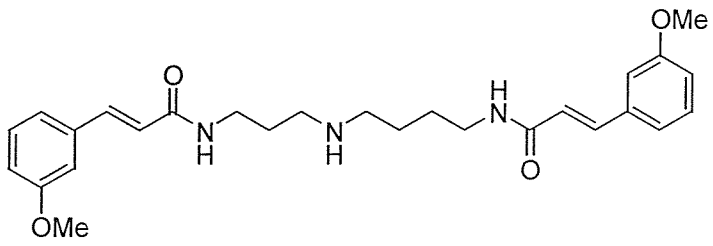

RP-HPLC: R_t = 11.1min.

Yield 12 mg (16%).

IR (ν_{max}/ cm^{-1}) 1677 (C=O).

δ_H (300MHz, CD_3OD): 0.91 (4H, m, $C^{7+8}H_2$), 1.10 (2H, m, C^3H_2), 2.03 (4H, m, $C^{4+6}H_2$), 2.65 (4H, m, $C^{2+9}H_2$), 3.10 (6H, s, 2xOCH_3), 5.83 and 5.85 (2H, 2xd, *J* 15, 15 ArCH=C<u>H</u>CO), 6.21 (2H, d, *J* 8, Ar<u>H</u>), 6.35 (2H, s, Ar<u>H</u>), 6.41 (2H, d, *J* 8, Ar<u>H</u>), 6.59 (2H, t, *J* 8, Ar<u>H</u>), 6.80 (2H, d, *J* 15 ArC<u>H</u>=CHCO).

ES-MS (+ve): m/z = 466.0 (100%, $M+H)^+$.

HRMS (FTMS): $C_{27}H_{36}N_3O_4$ Calc. 466.2700, Found 466.2698.

***N*^{1},*N*^{10}-*bis*(2,4-Dihydroxydihydrocinnamoyl)-1,5,10-triazadecane (148g)**

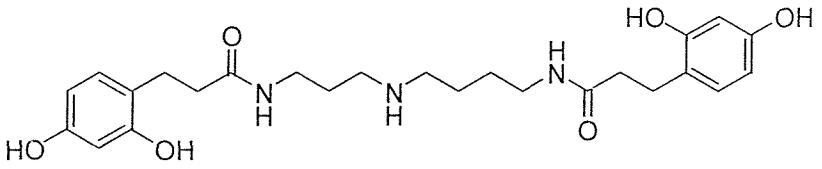

RP-HPLC: R_t = 11.5 min.

Yield 10 mg (36%).

IR (ν_{max}/ cm^{-1}) 1679 (C=O).

δ_H (300MHz, CD_3OD): 0.87 (4H, m, $C^{7+8}H_2$), 1.08 (2H, m, C^3H_2), 1.78 (2H, t, *J* 7, $ArCH_2C\underline{H}_2$), 1.85 (2H, t, *J* 7, $ArCH_2C\underline{H}_2$), 2.04 (2H, t, *J* 7, C^4H_2), 2.08-2.22 (6H, m, 2x$ArC\underline{H}_2CH_2CO$ + C^6H_2), 2.51 (2H, t, *J* 7, C^9H_2), 2.57 (2H, t, *J* 7, C^2H_2), 5.54 (2H, dt, *J* 10, 2 Ar<u>H</u>), 5.60 (2H, t, *J* 2, Ar<u>H</u>), 6.18 (2H, 2xd, *J* 2x8, Ar<u>H</u>).

ES-MS (+ve): m/z = 474.7 (100%, $M+H)^+$.

HRMS (FTMS): $C_{25}H_{36}N_3O_6$ Calc. 474.2599, Found 474.2604.

***N*^{1},*N*^{10}-*bis*(3,4-Methylenedioxycinnamoyl)-1,5,10-triazadecane (148h)**

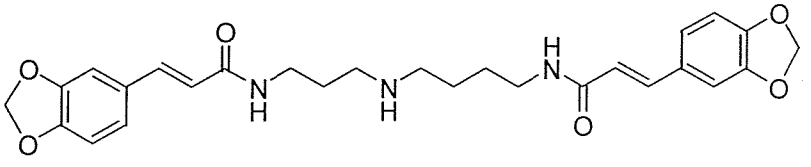

RP-HPLC: R_t = 12 min.

Yield 45 mg (48%).

IR (ν_{max}/ cm^{-1}) 1657 (C=O).

δ_H (300MHz, CD_3OD): 0.92-1.15 (4H, br m, $C^{7+8}H_2$), 1.25 (2H, m, C^3H_2), 2.33 (4H, m, $C^{4+6}H_2$), 2.67 (4H, m, $C^{2+9}H_2$), 5.29 (4H, s, 2xOCH_2O), 5.73 (2H, d, *J* 15, 2xArCH=C<u>H</u>), 6.10 (2H, dd, *J* 8, 2, Ar<u>H</u>), 6.28 (2H, m, Ar<u>H</u>), 6.37 (2H, dd, *J* 2, 2, Ar<u>H</u>), 6.75 (1H, d, *J* 15, ArC<u>H</u>=CHCO), 6.78 (1H, d, *J* 15, ArC<u>H</u>=CHCO).

δ_C (75MHz, CD_3OD): 24.5, 27.5, 27.7, 37.0, 39.5, 46.2, 48.5, 102.8, 107.2, 107.2, 109.4, 118.9, 119.5, 125.1, 125.2, 130.3, 130.4, 141.7, 142.4, 149.7, 150.6, 150.7, 169.1, 169.9.

ES-MS (+ve): m/z = 494.4 (100%, $M+H)^+$.

HRMS (FTMS): $C_{27}H_{32}N_3O_6$ Calc. 494.2286, Found 494.2291.

N^1,*N*^{10}-*bis*(2,5-Dihydroxyphenylacetyl)-1,5,10-triazadecane (148i)

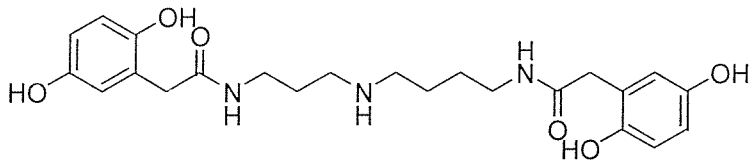

RP-HPLC: R_t = 7.8 min.

Yield 38 mg (59%).

IR (ν_{max}/ cm^{-1}) 1670 (C=O).

δ_H (300MHz, CD_3OD): 1.10 (4H, m, $C^{7+8}H_2$), 1.37 (2H, apparent quint, C^3H_2), 2.43 (4H, m, $C^{4+6}H_2$), 2.74 (2H, t, *J* 7, C^9H_2), 2.85 (2H, t, *J* 7,C^2H_2), 2.99 (2H, s, Ar$C\underline{H}_2$CO), 3.02 (2H, s, Ar$C\underline{H}_2$CO), 6.07-6.19 (6H, br m, Ar<u>H</u>).

δ_C (75MHz, CD_3OD): 24.1, 27.3, 27.6, 36.4, 39.0, 39.2, 45.6, 48.3, 115.7, 115.8, 116.8, 117.1, 118.4, 118.7, 124.0, 149.5, 151.3, 171.3.

ES-MS (+ve): m/z = 446.3 (100%, $M+H)^+$.

N^1,*N*^{10}-*bis*(3-Hydroxyphenylacetyl)-1,5,10-triazadecane (148j)

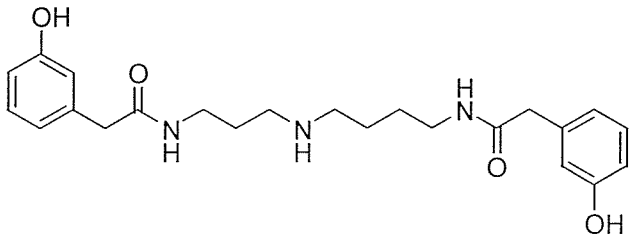

RP-HPLC: R_t = 9.9 min.

Yield 50 mg (76%).

IR (ν_{max}/ cm^{-1}) 1673 (C=O).

δ_H (300MHz, CD_3OD): 1.16 (4H, m, $C^{7+8}H_2$), 1.42 (2H, m, C^3H_2), 2.43 (4H, m, $C^{4+6}H_2$), 2.77 (2H, t, *J* 7, C^9H_2), 2.85 (2H, t, *J* 7, C^2H_2), 3.01 (2H, s, $ArC\underline{H}_2CO$), 3.02 (2H, s, $ArC\underline{H}_2CO$), 6.26 (2H, d, *J* 8, Ar<u>H</u>), 6.33 (4H, m, Ar<u>H</u>), 6.69 (2H, dt, *J* 8, 2, Ar<u>H</u>).

δ_C (75MHz, CD_3OD): 24.3, 27.2, 27.4, 36.8, 39.5, 43.7, 43.8, 46.0, 48.4, 114.8, 114.9, 116.9, 121.2, 130.5, 130.6, 138.2, 158.5, 162.8, 163.2 174.2, 175.2.

ES-MS (+ve): m/z = 414.3 (100%, $M+H)^+$.

HRMS (FTMS): $C_{23}H_{32}N_3O_4$ Calc. 414.2387, Found 414.2390.

N^1,N^{10}-bis(2-Quinoxaline carboxyl)-1,5,10-triazadecane (148k)

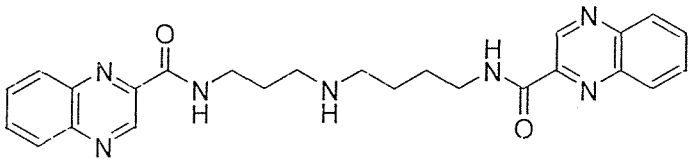

RP-HPLC: R_t = 10.7 min.

Yield 30 mg (39%).

IR (ν_{max}/ cm^{-1}) 1666 (C=O).

δ_H (300MHz, CD_3OD): 1.37 (4H, m, $C^{7+8}H_2$), 1.62 (2H, m, C^3H_2), 2.68 (4H, t, *J* 7, $C^{4+6}H_2$), 3.12 (2H, t, *J* 7, C^9H_2), 3.17 (2H, t, *J* 7, C^2H_2), 7.46 (4H, m Ar<u>H</u>), 7.69 (4H, m, Ar<u>H</u>), 9.01 (2H, s, Ar<u>H</u>).

δ_C (75MHz, CD_3OD): 24.5, 27.5, 27.7, 37.1, 39.5, 46.4, 48.5, 129.9, 130.8, 132.3, 133.1, 133.2, 141.7, 144.4, 144.5, 144.6, 145.0, 145.3, 165.6, 166.4.

ES-MS (+ve): m/z = 458.4 (100%, $M+H)^+$.

N^1,N^{10}-bis(3-Hydroxy-2-quinoxaline carboxyl)-1,5,10-triazadecane (148l)

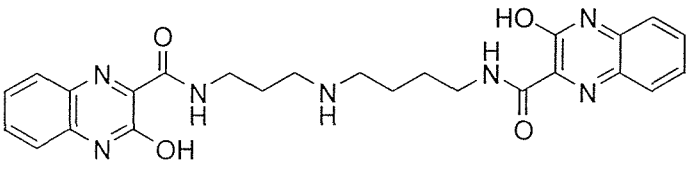

RP-HPLC: R_t = 8.6 min.

Yield 38 mg (38%).

IR (ν_{max}/ cm^{-1}) 1674 (C=O).

δ_H (300MHz, CD_3OD): 1.48 (4H, m, $C^{7+8}H_2$), 1.75 (2H, m, C^3H_2), 2.81 (4H, m, $C^{4+6}H_2$), 3.20 (2H, t, *J* 7, C^9H_2), 3.27 (2H, t, *J* 7, C^2H_2), 7.02 (2H, d, *J* 9, Ar<u>H</u>), 7.09 (2H, m, Ar<u>H</u>), 7.32 (2H, m, Ar<u>H</u>), 7.58 (2H, d, *J* 9, Ar<u>H</u>).

δ_C (75MHz, CD_3OD): 24.4, 27.1, 27.2, 37.7, 40.1, 46.3, 48.5, 117.0, 126.5, 131.2, 133.3, 133.6, 134.8, 134.9, 146.8, 147.0, 156.7, 164.6, 165.2.

N^1,N^{10}-*bis*(4-Hydroxy-7-trifluoromethyl-3-quinolinecarboxyl)-1,5,10-triazadecane (148m)

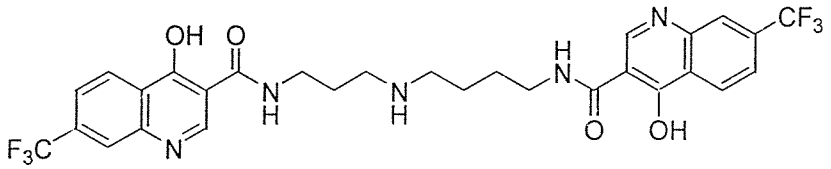

RP-HPLC: R_t = 12.7 min.

Yield: 56 mg (53%).

IR: (ν_{max}/ cm^{-1}) 1676 (C=O).

δ_H (300MHz, CD_3OD): 1.10 (4H, m, $C^{7+8}H_2$), 1.33 (2H, m, C^3H_2), 2.43 (4H, t, *J* 7, $C^{4+6}H_2$), 2.81 (2H, t, *J* 7, C^9H_2), 2.89 (2H, t, *J* 7, C^2H_2), 6.94 (2H, d, *J* 8, Ar<u>H</u>), 7.16 (2H, s, Ar<u>H</u>), 7.70 (1H, m, Ar<u>H</u>), 7.72 (1H, d, *J* 8, Ar<u>H</u>), 8.00 (2H, d, *J* 8, Ar<u>H</u>)

δ_C (75MHz, CD_3OD): 24.6, 27.4, 27.9, 36.5, 39.1, 46.2, 48.5, 112.6, 117.4, 122.0, 128.4, 129.6, 140.1, 145.8, 146.0, 167.0, 168.0.

ES-MS (+ve) m/z = 624.3 (100%, $M+H)^+$.

HRMS (FTMS): $C_{29}H_{28}N_5O_4F_6$ Calc. 624.2040, Found 624.2039.

N^1,N^{10}-*bis*(2-Hydroxyphenylacetyl)-1,5,10-triazadecane (148n)

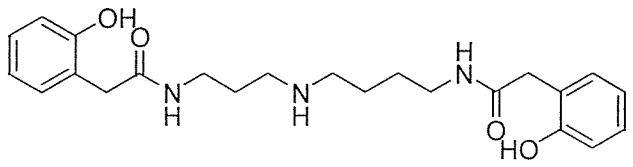

RP-HPLC: R_t = 9.8 min.

Yield: 31 mg (40%).

IR (ν_{max}/ cm^{-1}) 1678 (C=O).

δ_H (300MHz, CD_3OD): 0.87 (4H, m, $C^{7+8}H_2$), 1.13 (2H, m, C^3H_2), 2.18 (4H, m, $C^{4+6}H_2$), 2.46 (2H, m, C^9H_2), 2.60 (2H, m, C^2H_2), 2.82 (2H, $ArC\underline{H}_2$), 2.84 (2H, $ArC\underline{H}_2$), 6.10 (4H, m, Ar<u>H</u>), 6.40 (4H, m, Ar<u>H</u>).

δ_C (75MHz, CD_3OD): 24.2, 27.3, 27.5, 36.6, 39.0, 39.1, 39.3, 45.8, 48.4, 116.2, 116.4, 120.7, 123.1, 123.2, 129.4, 129.6, 132.0, 132.2, 156.7, 175.0, 176.1.

ES-MS (+ve): m/z = 414.4 (100%, $M+H)^+$.

HRMS (FTMS): $C_{23}H_{32}N_3O_4$ Calc. 414.2387, Found 414.2389.

***N*^{1},*N*^{10}-*bis*(Pyrrole-2-carboxyl)-1,5,10-triazadecane (148o)**

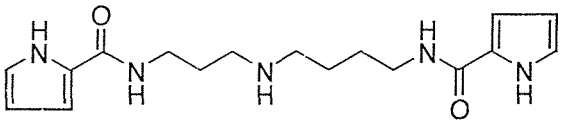

RP-HPLC: R_t = 9.1 min.

Yield 30 mg (51%).

IR (ν_{max}/ cm^{-1}) 1633 (C=O).

δ_H (300MHz, CD_3OD): 1.18 (4H, m, $C^{7+8}H_2$), 1.37 (2H, m, C^3H_2), 2.28 (4H, m, $C^{4+6}H_2$), 2.91 (4H, m, $C^{2+9}H_2$), 5.70 (2H, m, Ar<u>H</u>), 6.32 (2H, d, *J 4*, Ar<u>H</u>), 6.45 (2H, m, Ar<u>H</u>).

δ_C (75MHz, CD_3OD): 26.7, 28.2, 29.6, 37.4, 39.7, 47.3, 49.7, 110.07/110.14, 111.46/111.57, 111.6, 122.7, 122.9, 126.6, 164.1.

ES-MS (+ve): m/z = 332.3 (100%, $M+H)^+$.

***N*^{1},*N*^{10}-*bis*(2-Thiophenecarboxyl)-1,5,10-triazadecane (148p)**

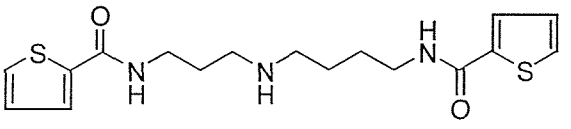

RP-HPLC: R_t = 9.6 min.

Yield 16 mg (42%).

IR (ν_{max}/ cm^{-1}) 1678 (C=O).

δ_H (300MHz, CD_3OD): 1.09 (4H, m, $C^{7+8}H_2$), 1.31 (2H, m, C^3H_2), 2.36 (4H, m, $C^{4+6}H_2$), 2.72 (4H, m, $C^{2+9}H_2$), 6.42 (2H, m, Ar<u>H</u>), 6.95 (4H, m, Ar<u>H</u>).

δ_C (75MHz, CD_3OD): 24.5, 27.6, 27.8 37.3, 39.7, 46.4, 128.9, 129.1, 129.6, 130.1, 131.7, 132.1.

ES-MS (+ve): m/z = 366.2 (100%, $M+H)^+$

HRMS (FTMS): $C_{17}H_{24}N_3O_2S_2$ Calc. 366.1304, Found 366.1310.

***N^1,N^{10}-bis*(2-Thiopheneacetyl)-1,5,10-triazadecane (148q)**

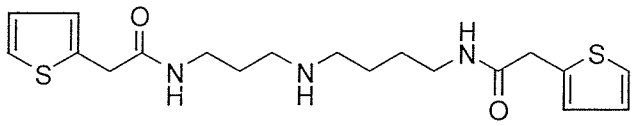

RP-HPLC: R_t = 10 min.

Yield 14 mg (42%).

IR (ν_{max}/ cm^{-1}) 1652 (C=O).

δ_H (300MHz, CD_3OD): 1.10 (4H, m, $C^{7+8}H_2$), 1.28 (2H, m, C^3H_2), 2.13 (4H, m, $C^{4+6}H_2$), 2.79 (4H, t, *J* 7, C^9H_2), 2.84 (2H, t, *J* 7, C^2H_2), 3.30 (4H, br s, 2xAr$C\underline{H}_2$), 6.53 (4H, m, Ar<u>H</u>), 6.85 (2H, m, Ar<u>H</u>).

δ_C (75MHz, CD_3OD): 27.4, 27.9, 29.9, 37.9, 38.1, 40.2, 47.4, 50.0, 125.67/125.72, 127.44/127.52, 127.8, 138.2, 172.7, 173.0.

ES-MS (+ve): m/z = 394.3 (100%, $M+H)^+$.

HRMS (FTMS): $C_{19}H_{28}N_3O_2S_2$ Calc. 394.1617, Found 394.1623.

***N^1,N^{10}-bis*(5-Bromofuroyl)-1,5,10-triazadecane (148r)**

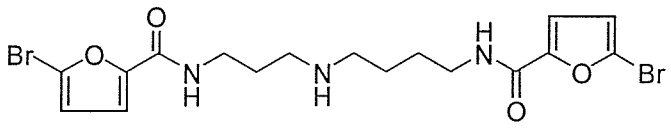

RP-HPLC: R_t = 10.5 min (91% purity).

Yield :15 mg (45%).

IR: (ν_{max}/ cm^{-1}) 1652 (C=O).

δ_H (300MHz, CD_3OD): 0.95 (4H, m, $C^{7+8}H_2$), 1.23 (2H, m, C^3H_2), 2.36 (4H, m, $C^{4+6}H_2$), 2.66 (2H, t, *J* 7, C^9H_2), 2.72 (2H, t, *J* 7, C^2H_2), 5.86 (2H, m, Ar<u>H</u>), 6.36 (2H, m, Ar<u>H</u>).

ES-MS (+ve): m/z = 490.0, 492.0, 493.9 (45%, 100%, 55%, $M+H)^+$.

HRMS (FTMS): $C_{17}H_{22}N_3O_4Br_2$ Calc. 489.9972, Found 489.9973.

***N*^{1},*N*^{10}-*bis*(4-Hydroxy-2-methoxy-phenylacetyl)-1,5,10-triazadecane (148s)**

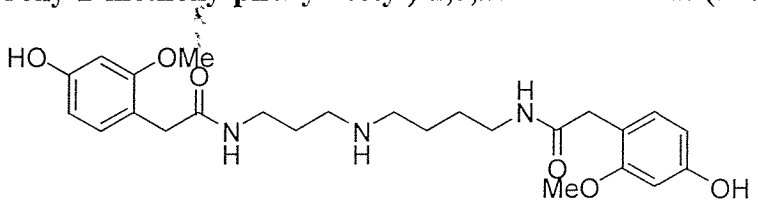

RP-HPLC: R_t = 10.5 min.

Yield :45 mg (56%).

IR: (ν_{max}/ cm^{-1}) 1652 (C=O).

δ_H (300MHz, CD_3OD): 1.15 (4H, m, $C^{7+8}H_2$), 1.39 (2H, m, C^3H_2), 2.41 (4H, m, $C^{4+6}H_2$), 2.76 (2H, t, *J* 7, C^9H_2), 2.85 (2H, t, *J* 7, C^2H_2), 2.98 (2H, s, $ArCH_2$), 3.00 (2H, s, $ArCH_2$), 3.41 (6H, s, 2xOMe), 6.30 (4H, m, Ar<u>H</u>), 6.46 (2H, br s, Ar<u>H</u>).

δ_C (75MHz, CD_3OD): 24.3, 27.3, 27.4, 36.8, 39.4, 43.3, 43.4, 45.9, 48.4, 56.3, 113.7, 116.2, 116.3, 122.6, 128.1, 128.2, 146.5, 146.6, 148.88/148.93, 174.7, 175.8.

ES-MS (+ve): m/z = 474.4 (100 %, $M+H)^+$.

***N*^{1},*N*^{10}-*bis*(3,4-Dihydroxyphenyl acetyl)-1,5,10-triazadecane (148t)**

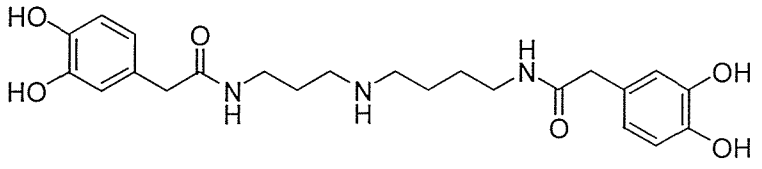

RP-HPLC: R_t = 11.0 min.

Yield 50 mg (42%).

IR (ν_{max}/ cm^{-1}) 1674 (C=O).

δ_H (300MHz, CD_3OD) : 1.07 (4H, m, $C^{7+8}H_2$), 1.32 (2H, m, C^3H_2), 2.30 (2H, t, *J* 7,C^4H_2), 2.36 (2H, t, *J* 7, C^6H_2), 2.71 (2H, t, *J* 7, C^9H_2), 2.80 (2H, t, *J* 7, C^2H_2), 2.86 (2H, s, $ArC\underline{H}_2$), 2.89 (2H, s, $ArC\underline{H}_2$), 6.13 (2H, m, Ar<u>H</u>), 6.24 (4H, m, Ar<u>H</u>).

δ_C (75MHz, CD_3OD): 24.2, 27.3, 27.5, 36.6, 39.3, 43.1, 43.3, 45.8, 48.3, 116.4, 117.1, 121.4, 128.1, 128.2, 145.3, 145.5, 146.3, 146.4, 174.9, 176.1.

N^1,N^{10}-bis(Phenylcarboxyl)-1,5,10-triazadecane (148u)

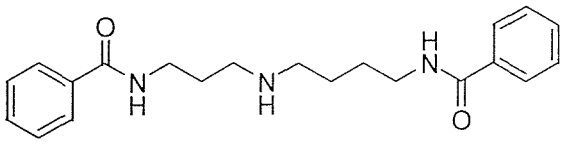

RP-HPLC: R_t = 10.1 min.

Yield 6 mg (13%).

IR: (ν_{max}/ cm^{-1}) 1677 (C=O).

δ_H (300MHz, CD_3OD): 1.22 (4H, m, $C^{7+8}H_2$), 1.50 (2H, m, C^3H_2), 2.50 (4H, m, $C^{4+6}H_2$), 2.90 (4H, m, $C^{2+9}H_2$), 6.85 (6H, m, ArH), 7.30 (4H, m, Ar<u>H</u>).

ES-MS (+ve): m/z = 354.2 (100%, $M+H)^+$.

HRMS (FTMS): $C_{21}H_{28}N_3O_2$ Calc. 354.2176, Found 354.2181.

N^1,N^{10}-bis(3,4-Methylenedioxyphenylcarboxyl)-1,5,10-triazadecane (148v)

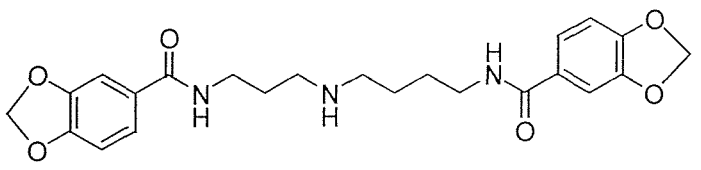

RP-HPLC: R_t = 10.4 min.

Yield: 29 mg (73%).

IR: (ν_{max}/ cm^{-1}) 1677 (C=O).

δ_H (300MHz, CD_3OD): 1.32 (4H, m, $C^{7+8}H_2$), 1.52 (2H, m, C^3H_2), 2.38 (4H, m, $C^{4+6}H_2$), 3.08 (2H, t, *J* 7, C^9H_2), 3.13 (2H, t, *J* 7, C^2H_2), 5.72 (4H, s, $2xOCH_2O$), 6.55 (2H, t, *J* 8, Ar<u>H</u>), 6.99 (1H, d, *J* 2, Ar<u>H</u>), 7.01 (1H, d, *J* 2, Ar<u>H</u>), 7.08 (2H, d, *J* 8, Ar<u>H</u>).

δ_C (75MHz, CD_3OD): 27.6, 28.1, 29.9, 38.7, 40.8, 47.8, 50.0, 103.0, 108.56/108.96 123.2, 129.5, 129.6, 149.5, 151.0, 169.5.

ES-MS (+ve): m/z = 442.2 (100%, $M+H)^+$.

N^1,N^{10}-*bis*(-4-Chlorobenzoyl)-1,5,10-triazadecane (148w)

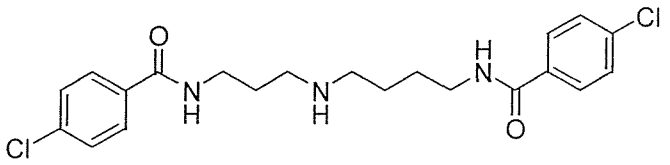

RP-HPLC: R_t = 11.0 min.

Yield: 7 mg (20 %).

IR: (ν_{max}/ cm^{-1}) 1668 (C=O).

δ_H (400MHz, CD_3OD): 1.75 (4H, m, $C^{7+8}H_2$), 1.99 (2H, m, C^3H_2), 3.10 (4H, m, $C^{4+6}H_2$), 3.46 (2H, t, *J* 7, C^9H_2), 3.52 (2H, t, *J* 7, C^2H_2), 7.44 (4H, d, *J* 8, Ar<u>H</u>), 7.81 (4H, d, *J* 8, Ar<u>H</u>).

δ_C (100MHz, CD_3OD): 25.0, 27.9, 28.1, 38.0, 40.5, 43.2, 46.9, 49.1, 130.2, 130.3, 130.4, 130.5, 133.8, 134.5, 139.3, 139.6, 169.6, 170.3.

ES-MS (+ve): m/z = 422.3, 424.1 (100%, 80% $M+H)^+$.

HRMS (FTMS): $C_{21}H_{26}N_3O_2Cl_2$ Calc. 422.1397, Found 422.1401.

N^1,N^{10}-*bis*(6-Chloronicotinyl)-1,5,10-triazadecane (148x)

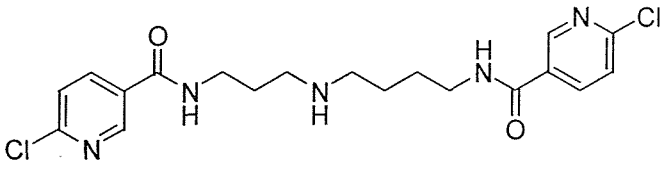

RP-HPLC: R_t = 10.5 min.

Yield: 12 mg (27%).

IR: (ν_{max}/ cm^{-1}) 1674 (C=O).

δ_H (300MHz, CD_3OD): 1.40 (4H, m, $C^{7+8}H_2$), 1.58 (2H, m, C^3H_2), 2.45 (4H, m, $C^{4+6}H_2$), 3.20 (4H, m, $C^{2+9}H_2$), 7.25 (2H, d, *J* 9, Ar<u>H</u>), 7.93 (2H, dd, *J* 9, 2, Ar<u>H</u>), 8.55 (2H, d, *J* 2, Ar<u>H</u>).

δ_C (75MHz, CD_3OD): 27.6, 28.0, 29.8, 38.9, 40.9, 47.8, 125.5, 130.6, 139.6, 149.8, 154.8, 171.4.

ES-MS (+ve): m/z = 424.2, 426.0 (100 %, 80%, $M+H)^+$.

HRMS (FTMS): $C_{19}H_{24}N_5O_2Cl_2$ Calc. 424.1302, Found 424.1300.

N^{1},*N*^{10}-*bis*(3-Indoleacetyl)-1,5,10-triazadecane (148y)

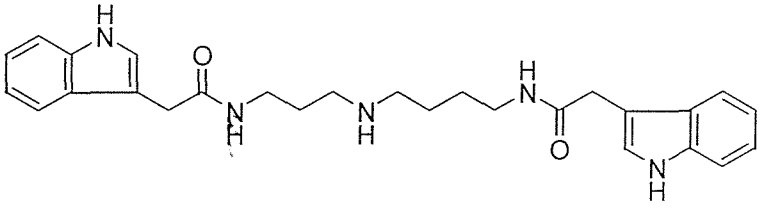

RP-HPLC: R_t = 10.7 min.

Yield: 23 mg (59%).

IR: (ν_{max}/ cm^{-1}) 1676 (C=O).

δ_H (300MHz, CD_3OD): 1.41 (4H, m, $C^{7+8}H_2$), 1.67 (2H, m, $C^{3}H_2$), 2.44 (4H, m $C^{4+6}H_2$), 3.22 (4H, t, *J* 7, $C^{9}H_2$), 3.28 (2H, t, *J* 7, $C^{2}H_2$), 3.73 (4H, s, Ar$C\underline{H}_2$), 7.10 (2H, m, Ar$\underline{H}$), 7.19 (1H, m, Ar$\underline{H}$), 7.26 (2H, m, Ar$\underline{H}$), 7.43 (1H, d, *J* 8, Ar$\underline{H}$), 7.45 (1H, d *J* 8, Ar$\underline{H}$), 7.63 (1H, dd, *J* 8, 2, Ar$\underline{H}$), 7.65 (1H, dd, *J* 8, 2, Ar$\underline{H}$).

δ_C (75MHz, CD_3OD): 27.2, 27.9, 29.7, 34.0, 38.0, 40.1, 47.2, 48.3, 109.3, 112.3, 119.3, 119.9, 119.9, 122.5, 125.0, 128.4, 138.1, 174.8, 175.1.

ES-MS (+ve): m/z = 460.3 (100%, $M+H)^+$.

HRMS (FTMS): $C_{27}H_{34}N_5O_2$ Calc 460.2707, Found 460.2706.

N^{1},*N*^{10}-*bis*(3,4-Dimethoxyphenylacetyl)-1,5,10-triazadecane (148z)

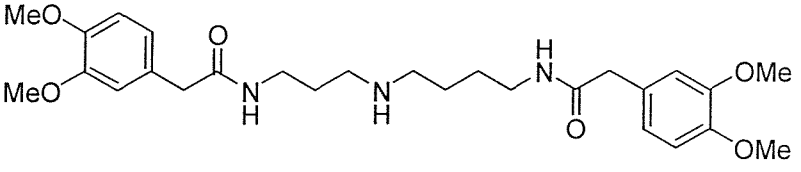

RP-HPLC: R_t = 11.0 min.

Yield: 75 mg (65%).

IR: (ν_{max}/ cm^{-1}) 1661(C=O).

δ_H (300MHz, CD_3OD): 0.86 (4H, m, $C^{7+8}H_2$), 1.12 (2H, m, C^3H_2), 2.16 (4H, m, $C^{4+6}H_2$), 2.48 (2H, t, *J* 7, C^9H_2), 2.57 (2H, t, *J* 7, C^2H_2), 2.72 (2H, s, $ArC\underline{H}_2$), 2.75 (2H, s, $ArC\underline{H}_2$), 3.07 (6H, s, 2xOMe), 3.10 (6H, s, 2xOMe), 6.22-6.10 (6H, m, Ar<u>H</u>).

δ_C(75MHz, CD_3OD): 24.3, 27.3, 27.4, 36.9, 39.5, 43.2, 43.4, 46.0, 48.1, 48.4, 56.4, 113.0, 114.0, 122.5, 129.5, 129.7, 149.4, 149.5, 150.3, 150.3, 174.4, 175.4.

ES-MS (+ve): m/z = 502.4 (100%, $M+H)^+$.

HRMS (FTMS): $C_{27}H_{40}N_3O_6$ Calc. 502.2912, Found 502.2913.

***N*^{1},*N*^{10}-*bis*(5-Hydroxy-3-indoleacetyl)-1,5,10-triazadecane (148I)**

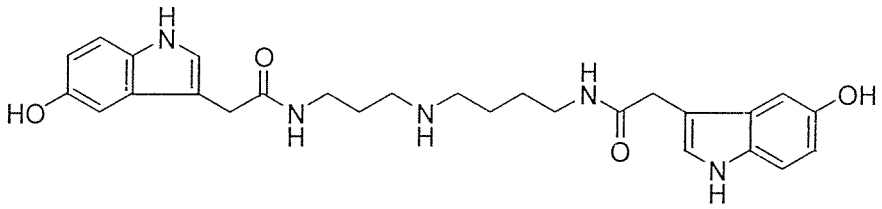

RP-HPLC: R_t = 11.0 min.

Yield: 30 mg (38%).

IR: (ν_{max}/ cm^{-1}) 1676 (C=O).

δ_H (300MHz, CD_3OD): 1.01 (4H, m, $C^{7+8}H_2$), 1.28 (2H, m, C^3H_2), 2.19 (4H, m, $C^{4+6}H_2$), 2.71 (2H, t, *J* 7, C^9H_2), 2.81 (2H, t, *J* 7, C^2H_2), 3.14 and 3.16 (4H, 2xs, $2xArC\underline{H}_2$), 6.25 (2H, d, *J* 9, Ar<u>H</u>), 6.48 (2H, s, Ar<u>H</u>), 6.68 (2H, s, Ar<u>H</u>), 6.75 (2H, d, *J* 9, Ar<u>H</u>).

δ_C(75MHz, CD_3OD): 24.2, 27.2, 27.4, 34.0, 36.5, 39.3, 45.7, 48.3, 103.47/103.52, 108.5, 112.6, 112.9, 113.0, 125.9, 129.0, 133.0, 151.3, 175.2, 176.3.

***N*^{1},*N*^{10}-*bis*(3-Indole propanoyl)-1,5,10-triazadecane (148II)**

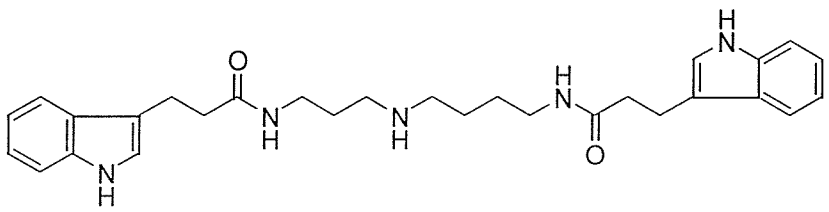

RP-HPLC: R_t = 12 min.

Yield: 35 mg (43%).

IR: (ν_{max}/ cm^{-1}) 1676 (C=O).

δ_H (300MHz, CD_3OD): 0.54 (4H, m, $C^{7+8}H_2$), 0.80 (2H, m, C^3H_2), 1.59 (4H, m, $ArC^{\alpha}H_2$), 2.71 (4H, m, $ArC^{\beta}H_2$), 2.21 (4H, m, $C^{4+6}H_2$), 2.26 (2H, t, *J* 7, C^9H_2), 2.34 (2H, t, *J* 7, C^2H_2), 6.20 (6H, m, ArH), 6.47 (2H, dd *J* 8, 8, ArH), 6.70 (1H, d, *J* 8, ArH).

δ_C(75MHz, CD_3OD): 22.2, 22.6, 24.3, 27.2, 36.3, 37.5, 38.2, 39.2, 45.5, 48.4, 112.2, 112.3, 114.7, 114.9, 119.3,119.4, 119.5, 119.7, 122.3, 122.4, 123.0, 123.1, 128.3, 128.6, 137.9, 138.0, 176.2, 177.9.

ES-MS (+ve): m/z = 488.6 (100%, $M+H)^+$.

HRMS (FTMS): $C_{29}H_{38}N_5O_2$ Calc. 488.3020, Found 488.3024.

***N*^{1},*N*^{10}-*bis*(2-Methyl-3-indoleacetyl)-1,5,10-triazadecane (148III)**

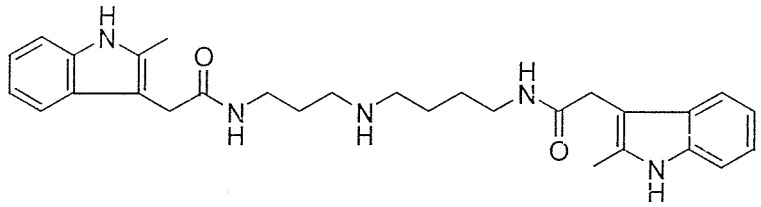

RP-HPLC: R_t = 11.6 min.

Yield: 45.4 mg (58 %).

IR: (ν_{max}/cm^{-1}) 1674 (C=O).

δ_H (300MHz, CD_3OD): 0.99 (4H, m, $C^{7+8}H_2$), 1.24 (2H, m, C^3H_2), 1.95 (6H, 2xs, $2xCH_3$), 2.09 (2H, t, *J* 7, C^4H_2), 2.11 (2H, t, *J* 7, C^6H_2), 2.66 (2H, t, *J* 7, C^2H_2), 2.76 (2H, t, *J* 7, C^9H_2), 3.15 (2H, s, $ArCH_2$), 3.16 (2H, s, $ArCH_2$), 6.49 2x (1H, m, ArH), 6.60 (1H, m, ArH), 6.61 (1H, m, ArH), 6.83 (H, dd, *J* 7, 3, ArH), 6.98 (2H, m, ArH).

δ_C (75MHz, CD_3OD): 11.4, 24.1, 27.3, 32.6, 32.7, 36.6, 39.4, 45.7, 48.1, 105.0, 111.5, 111.6, 118.4, 119.9, 121.7, 121.8, 129.5, 129.7, 134.7, 134.8, 137.0, 175.1, 176.1.

ES-MS (+ve): m/z = 488.6 (100%, $M+H)^+$.

***N*^{1},*N*^{10}-*bis*(5-Hydroxyindole-2-carboxyl)-1,5,10-triazadecane (148IV)**

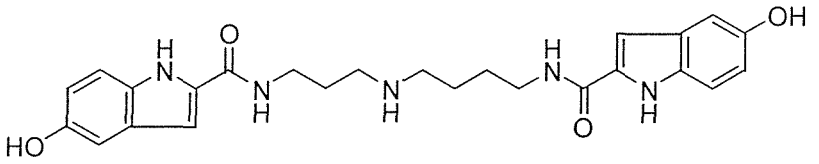

RP-HPLC: R_t = 9.4 min.

Yield: 40 mg (51 %).

IR: (ν_{max}/cm^{-1}) 1674 (C=O).

δ_H (300MHz, CD_3OD): 1.43 (4H, m, $C^{7+8}H_2$), 1.60 (2H, m, $C^{3}H_2$), 2.69 (4H, m, $C^{4+6}H_2$), 3.06 (2H, t, *J* 7, $C^{9}H_2$), 3.12 (2H, t, *J* 7, $C^{2}H_2$), 6.42 (2H, m, Ar<u>H</u>), 6.51 and 6.52 (2H, 2xs, 2xAr<u>H</u>), 6.55 (2H, dd, *J* 2, 2, Ar<u>H</u>), 6.88 (1H, d, *J* 8, Ar<u>H</u>).

δ_C (75MHz, CD_3OD): 24.6, 27.7, 27.9, 36.8, 39.4, 46.2, 48.5, 103.4, 103.8, 105.7, 113.6, 116.0, 116.2, 129.6, 130.2, 133.4, 152.3, 164.4, 165.1.

ES-MS (+ve): m/z = 464.1 (100%, $M+H)^+$.

***N*^{1},*N*^{10}-*bis*(*E*-3-Indoleacryl)-1,5,10-triazadecane (148V)**

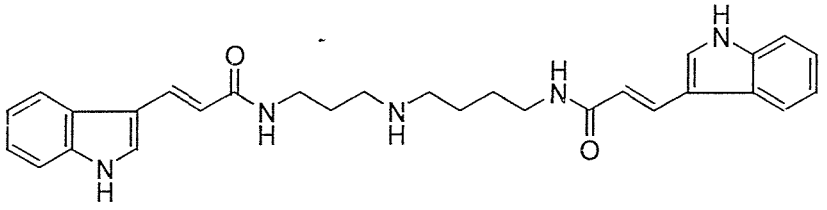

Yield: 10 mg (13%).

IR: (ν_{max}/ cm^{-1}) 1675 (C=O).

δ_H (300MHz, CD_3OD): 0.80 (4H, m, $C^{7+8}H_2$), 1.09 (2H, m, $C^{3}H_2$), 2.03 (4H, m, $C^{4+6}H_2$), 2.49 (2H, m, $C^{9}H_2$), 2.58 (2H, m, $C^{2}H_2$), 6.43-6.62 (8H, m, Ar<u>H</u>), 7.04 (2H, m, Ar<u>H</u>).

δ_C(75MHz, CD_3OD): 24.2, 27.3, 33.7, 36.7, 39.4, 45.8, 48.3, 109.3, 113.1, 114.1, 114.2, 122.0, 125.2, 125.3, 126.5, 126.6, 130.1, 130.2, 136.7, 140.0, 175.7, 174.7.

N^1,N^{10}-*bis*(5-Methoxyindole-3-acetyl)-1,5,10-triazadecane (148VI)

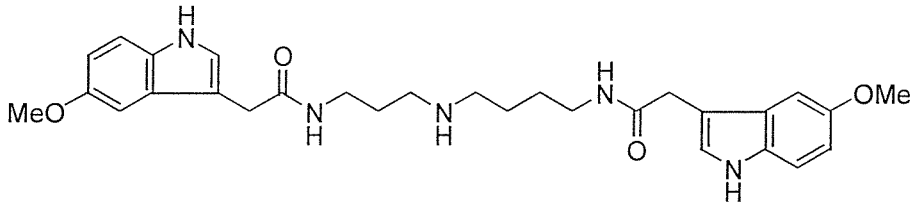

RP-HPLC: R_t = 8.9 min.

Yield 43.3 mg (49%).

IR (ν_{max}/cm^{-1}) 1676 (C=O)

δ_H (300MHz, CD_3OD): 0.75 (4H, m, $C^{7+8}H_2$), 1.03 (2H, m, C^3H_2), 1.92 (4H, m, $C^{4+6}H_2$), 2.45 (2H, m, C^9H_2), 2.56 (2H, t, *J* 7, C^2H_2), 2.93 and 2.95 (4H, 2xs, 2xArC$\underline{H}_2$), 3.19 (2H, s, ArC$\underline{H}_2$CO), 3.11 and 3.14 (6H, 2xs, 2xOMe) 6.09 (2H, m, Ar$\underline{H}$), 6.37 (2H, m, Ar$\underline{H}$), 6.47 (2H, s, Ar$\underline{H}$), 6.56 and 6.57 (2H, 2xd, *J* 9, 2xArH).

δ_C (75MHz, CD_3OD): 24.1, 27.3, 27.4, 33.9, 34.1, 36.6, 39.4, 45.7, 48.2, 101.4, 101.6, 109.2, 112.6, 112.7, 113.1, 113.2, 125.7, 125.8, 128.6, 128.8, 133.3, 155.1, 175.1, 176.2.

ES-MS (+ve): m/z = 520.6 (100%, $M+H)^+$.

HRMS (FTMS): $C_{29}H_{38}N_5O_4$ Calc 520.2918, Found 530.2921.

N^1,N^{10}-*bis*(Indole-2-carboxyl)-1,5,10-triazadecane (148VII)

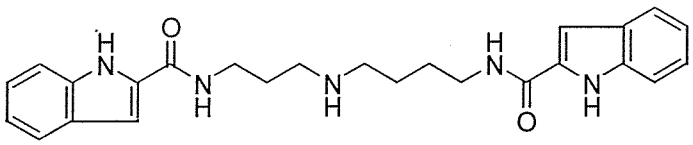

RP-HPLC: R_t = 12.3 min.

Yield: 23 mg (35%).

δ_H (300MHz, CD_3OD): 1.12 (4H, m, $C^{7+8}H_2$), 1.35 (2H, m, C^3H_2), 2.42 (4H, t, *J* 7, $C^{4+6}H_2$), 2.80 (2H, t, *J* 7, C^9H_2), 2.86 (2H, t, *J* 7, C^2H_2), 6.33-6.43 (4H, m, Ar$\underline{H}$), 6.48-6.56 (2H, m, Ar$\underline{H}$), 6.76 (2H, d, *J* 8, Ar$\underline{H}$), 6.91 and 6.92 (2H, 2xd, *J* 8, 2xAr$\underline{H}$).

δ_C (75MHz, CD_3OD): 24.5, 27.5, 27.8, 36.9, 39.4, 46.2, 48.6, 112.9, 121.1, 122.6, 125.1, 129.0, 138.0, 144.0, 160.2, 160.7.

N^1,N^{10}-*bis*(Tryptophanyl)-1,5,10-triazadecane (148VIII)

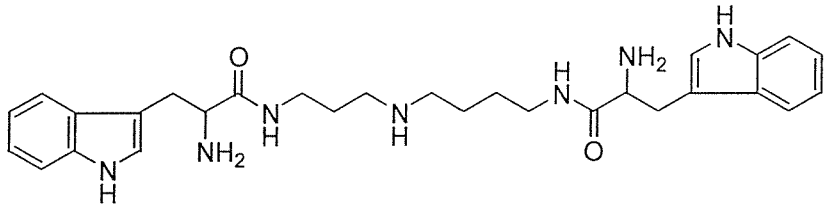

RP-HPLC: R_t = 8.8 min.

Yield: 35 mg (43%).

IR: (ν_{max}/ cm^{-1}) 1656 (C=O).

δ_H (300MHz, CD_3OD): 0.69 (2H, m, C^8H_2), 0.81 (2H, m, C^7H_2), 1.03 (2H, m, C^3H_2), 1.95 (2H, t, *J* 7, C^6H_2), 2.05 (2H, t, *J* 7, C^4H_2), 2.47 (2H, m, C^9H_2), 2.53 (2H, m, C^2H_2), 2.66 (4H, m, 2xAr$C^{\beta}\underline{H}_2$), 3.42 (2H, m, 2xAr$C^{\alpha}\underline{H}$), 6.33-6.49 (4H, m, Ar$\underline{H}$), 6.56 (2H, m, Ar$\underline{H}$), 6.71 (2H, d, *J* 7, Ar$\underline{H}$), 6.94 (2H, d, *J* 7, Ar$\underline{H}$).

δ_C(75MHz, CD_3OD): 24.3, 27.0, 28.8, 28.7, 37.2, 39.7, 46.0, 48.4, 55.3, 108.1, 112.6, 119.2, 120.1, 120.2, 122.8, 122.9, 125.5, 128.3, 138.1, 170.2, 170.8.

ES-MS (+ve): m/z = 518.5 (10%, $M+H)^+$.

N^1,N^{10}-*bis*(2-Methyl-5-methoxyindole-3-acetyl)-1,5,10-triazadecane (148IX)

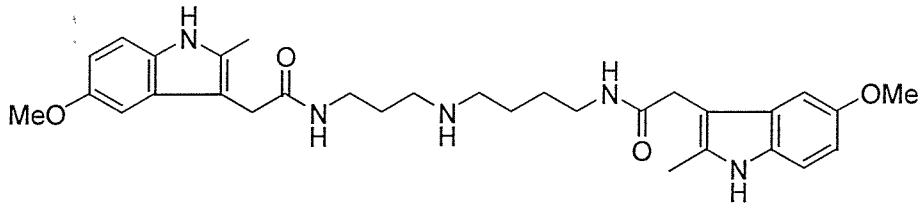

RP-HPLC: R_t = 11.5 min.

Yield: 7.9 mg

IR (ν_{max}/cm^{-1}) 1674 (C=O).

δ_H (300MHz, CD_3OD): 0.75 (4H, m, $C^{7+8}H_2$), 1.03 (2H, m, C^3H_2), 1.70 (6H, s, 2xCH_3), 1.95 (4H, m, $C^{4+6}H_2$), 2.43 (2H, m, C^9H_2), 2.53 (2H, t, *J* 7, C^2H_2), 2.87 and 2.88 (4H, 2xs, 2xAr$C\underline{H}_2$), 3.09 and 3.10 (6H, 2xs, 2xOMe), 6.00 (2H, m, Ar$\underline{H}$), 6.25 (2H, m, Ar$\underline{H}$), 6.44 (2H, m, Ar$\underline{H}$).

δ_C (75MHz, CD_3OD): 11.5, 24.2, 27.4, 32.7, 32.8, 36.6, 39.3, 45.7, 48.4, 56.4, 101.2, 104.9, 111.0, 111.2, 112.1, 130.0, 130.1, 132.2, 135.6, 155.1, 175.1, 175.3.

ES-MS (+ve): m/z = 548.6 (100%, $M+H)^+$.

***N*^{1},*N*^{10}-*bis*(Indole-3-carboxyl)-1,5,10-triazadecane (148X)**

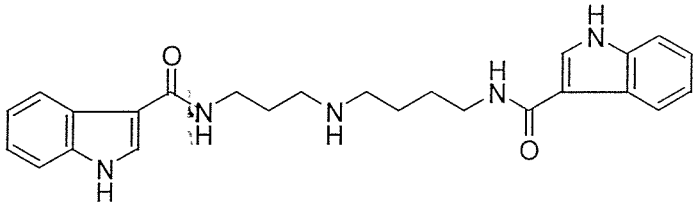

Yield: 21 mg

IR (ν_{max}/cm^{-1}) 1676 (C=O).

δ_H (300MHz, CD_3OD): 1.10 (4H, m, $C^{7+8}H_2$), 1.30 (2H, m, C^3H_2), 2.39 (4H, m, $C^{4+6}H_2$), 2.78 (2H, t, *J* 7, C^9H_2), 2.84 (2H, t, *J* 7, C^2H_2), 6.49 (4H, m, Ar<u>H</u>), 6.73 (2H, d, *J* 8, Ar<u>H</u>), 7.01 and 7.24 (2H, 2xs, 2xAr<u>H</u>), 7.41 (2H, d, *J* 8, Ar<u>H</u>).

δ_C (75MHz, CD_3OD): 24.7, 27.9, 28.1, 36.6, 39.2, 46.2, 48.6, 111.0, 111.6, 112.8, 121.6, 121.9, 122.1, 123.4, 123.5, 127.0, 128.9, 129.3, 138.0, 178.7, 169.5.

***N*^{1},*N*^{10}-*bis*(Indole-3-butanoyl)-1,5,10-triazadecane (148XI)**

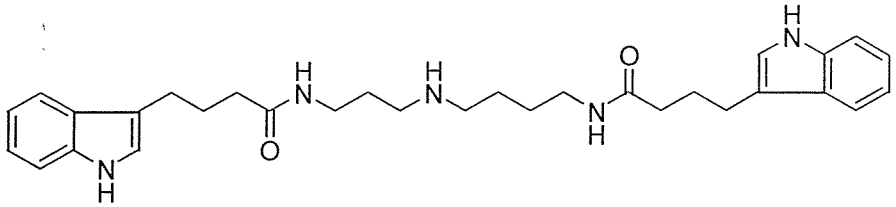

RP-HPLC: R_t = 10.2 min.

Yield: 15 mg

IR: (ν_{max}/ cm^{-1}) 1676 (C=O).

δ_H (300MHz, CD_3OD): 0.85 (4H, m, $C^{7+8}H_2$), 0.99 (2H, m, C^3H_2), 1.18 (4H, m, $ArC^{\beta}H_2$), 1.38 (4H, m, $ArC^{\alpha}H_2$), 2.10 (8H, m, $ArC^{\gamma}H_2$ and $C^{4+6}H_2$), 2.42 (4H, m, $C^{2+9}H_2$), 6.19 (2H, t, *J* 8, Ar<u>H</u>), 6.30 (2H, d, *J* 8, Ar<u>H</u>), 6.50 (2H, m, Ar<u>H</u>), 6.62 (2H, m, Ar<u>H</u>), 6.75 (2H, m, Ar<u>H</u>).

δ_C (75MHz, CD_3OD): 23.3, 23.5, 24.1, 27.2, 27.4, 28.6, 35.7, 35.9, 36.8, 37.0, 38.2, 38.9, 48.3, 112.4, 114.7, 114.9, 119.8, 120, 120.2, 120.3, 125.6, 125.8, 129.6, 138.2, 140.6, 176.2, 176.4, 177.4.

ES-MS (+ve): m/z =516.3 (30%, $M+H)^+$.

***N*^{1},*N*^{10}-*bis*(5-Bromoindole-3-acetyl)-1,5,10-triazadecane(148XII)**

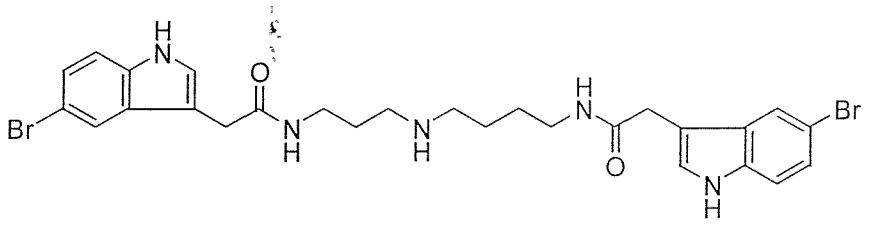

RP-HPLC: R_t = 12.6 min.

Yield 45 mg (45%).

IR (ν_{max}/cm^{-1}) 1673 (C=O).

δ_H (300MHz, CD_3OD): 0.80 (4H, m, $C^{7+8}H_2$), 1.07 (2H, m, C^3H_2), 2.01 (4H, m, $C^{4+6}H_2$), 2.48 (2H, t, *J* 7, C^9H_2), 2.57 (2H, t, *J* 7, C^2H_2), 2.92 and 2.94 (4H, 2xs, 2xArC$\underline{H}_2$), 6.48-6.55 (4H, m, Ar$\underline{H}$), 6.60 (2H, 2xs, 2xAr$\underline{H}$), 7.04 (2H, m, Ar$\underline{H}$).

δ_C (75MHz, CD_3OD): 24.3, 27.4, 27.5, 33.7, 33.8, 36.7, 39.4, 45.8, 48.4, 101.3, 109.3, 113.1, 114.1, 114.2, 122.1, 125.2, 125.3, 126.5, 130.2, 136.7, 174.7, 175.8.

ES-MS (+ve): m/z = 616.3, 618.2, 620.2 (48%, 100%, 52%, $M+H)^+$.

N^1,N^9-*bis*(Phthaloyl)-1,5,9-triazanonane (150)

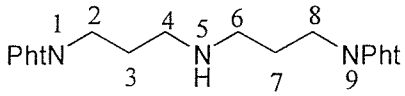

To a solution of norspermidine (9.38 g, 74.5 mmol) in $CHCl_3$ (100 mL) was added a solution of *N*-(ethoxycarbonyl)-phathalimide (34.5 g, 157.3 mmol) in $CHCl_3$ (50 mL) at room temperature over in 30 min. After stirring for 12 hours, the solvent was evaporated *in vacuo* and the residue was recrystallised in methanol. The solid was collected by filtralic and washed with diethyl ether (3x50 mL) and dried under vacuum to give N^1,N^9-*bis*(phthaloyl)-1,5,9-triazanonane as a colourless solid.

Yield: 17.55 g (62.7%)

m.p: 131-133°C.

IR (ν_{max}/cm^{-1}) 1705 (C=O).

δ_H (300MHz, $CDCl_3$): 1.81 (4H, m, $C^{3+7}H_2$), 2.60 (4H, t, *J* 7, $C^{4+6}H_2$), 3.72 (4H, t, *J* 7, $C^{2+8}H_2$), 7.67 (4H, m, ArH), 7.79 (4H, m, ArH).

δ_C (75MHz, $CDCl_3$): 29.0, 36.0, 47.0, 123.3, 132.2, 134.0, 168.6.

ES-MS (+ve): m/z 392.1 (100%, $M+H)^+$.

N^1,N^9-*bis*(Phthaloyl)-N^5-(4-benzyloxycarbonyl-oxyacetic acid allyl ester)-1,5,9-triaza decane (152)

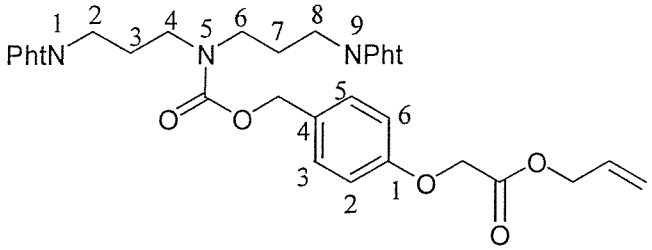

N^1,N^9-*bis*(Phthaloyl)-1,5,9-triazanonane (1.0 g, 2.6 mmol) was dissolved in DMF (30 mL) and Et3N (1.2 mL, 7.5 mmol). The solution was cooled in an ice bath to 0°C and a solution of [4-(4'-Nitro-phenoxycarbonyloxymethyl)-phenoxy]-acetic acid allyl ester (1.12 g, 3.1 mmol) in DMF (10 mL) was added dropwise over 10 min followed by the addition of DMAP (~50 mg). After 30 min at 0°C the mixture was allowed warm to

room temperature and was stirred overnight, before partitioning between 1M $KHSO_4$ (50 mL) and ethyl acetate (100 mL). The organic extract was washed with 10% sodium bicarbonate (2x50 mL) and saturated aqueous sodium chloride (2x50 mL), dried ($MgSO_4$) and the solvent was evaporated *in vacuo* to give a yellow liquid. Purification by flash chromatography on silica gel (eluting with hexane: ethyl acetate; 1:1) provided the title compound as a colourless liquid.

Yield: 1.45 g, 88 %

TLC: R_f = 0.4 hexane / ethyl acetate (1:1)

IR (ν_{max}/cm^{-1}) 1766 (C=O), 1704 (C=O).

δ_H (300MHz, $CDCl_3$): 1.90 (4H, m, $C^{3+7}H_2$), 3.33 (4H, m, $C^{4+6}H_2$), 3.65 (4H, m, $C^{2+8}H_2$), 4.60 (2H, s, $OC\underline{H}_2CO$), 4.68 (2H, d, *J* 6, $C\underline{H}_2CH{=}CH_2$), 4.99 (2H, s, $ArC\underline{H}_2O$), 5.25 (1H, d, *J* 10, $CH{=}C\underline{H}_{cis}$), 5.32 (1H, d, *J* 17, $CH{=}C\underline{H}_{trans}$), 5.90 (1H, m, $OCH_2C\underline{H}{=}CH_2$), 6.82 (2H, d, *J* 8, Ar$\underline{H}$), 7.21 (2H, d, *J* 8, Ar$\underline{H}$), 7.68 (4H, m, Ar$\underline{H}$), 7.76 (4H, m, Ar$\underline{H}$).

δ_C (75MHz, $CDCl_3$): 27.5, 28.0, 35.4, 45.0 45.5, 65.5 66.0, 66.8, 114.8, 119.3, 123.4, 129.7, 130.1, 131.6, 132.2, 134.1, 156.1, 157.6, 168.4, 168.7.

ES-MS (+ve): m/z 662.5 (100%, $M+Na)^+$.

N^1,*N*^{9}-*bis*(Phthaloyl)-*N*^{5}-(4-benzyloxycarbonyl-oxyacetic acid)-1,5,9-triaza decane (153)

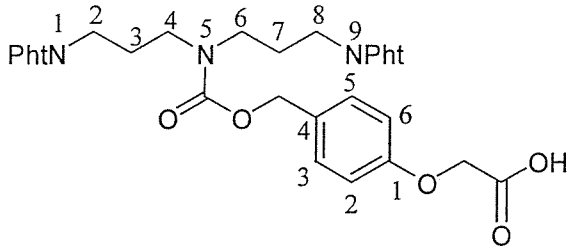

N^1,*N*^{9}-*bis*(Phthaloyl)-*N*^{5}-(4-benzyloxycarbonyl-oxyallyacetic acid allyl ester)-1,5,9-triazadecane (1.13 g, 1.7 mmol) in dry dichloromethane (20 mL) and tetrahydrofuran (20 mL). After the reaction mixture was stirred and degassed for 1 hour with a gentle flow of nitrogen though the solution. Thiosalicylic acid (0.4 g, 2.6 mmol) and $Pd(PPh_3)_4$ (0.26 g, 0.2 mmol) were added and the mixture stirred under nitrogen for 3 hours at room temperature. The solution was concentrated under reduced pressure and the residue redissoved in dichloromethane (200 mL). The organic layer was washed with 1M

$KHSO_4$ (2x50 mL) and brine (50 mL), dried (Na_2SO_4) and the solvent evaporated *in vacuo* to give yellow liquid. Purification by flash chromatography (eluting with hexane: ethyl acetate; 1:1 ethyl acetate: methanol; 9: 1) provided the title compound as a yellow foam.

TLC: R_f = 0.5 hexane / ethyl acetate (1:1)

Yield: 0.98 g, 96 %

IR (ν_{max}/cm^{-1}) 1707 (C=O).

δ_H (300MHz, $CDCl_3$): 1.88 (4H, m, $C^{3+7}H_2$), 3.32 (4H, m, $C^{4+6}H_2$), 3.65 (4H, m, $C^{2+8}H_2$), 4.58 (2H, s, $OC\underline{H}_2CO$), 4.96 (2H, s, $ArC\underline{H}_2O$), 6.80 (2H, d, *J* 8, Ar<u>H</u>), 7.17 (2H, d, *J* 8, Ar<u>H</u>), 7.40-7.88 (8H, m, Ar<u>H</u>).

δ_C (75MHz, $CDCl_3$): 31.3, 31.8, 39.7, 48.9, 49.4, 69.5, 71.0, 118.6, 127.3, 130.1, 136.1, 138.2, 144.3, 160.3, 161.7, 172.6.

N^1,N^9-*bis*(Phthaloyl)-N^5-(4-benzyloxycarbonyl-oxyacetamidomethyl resin)-1,5,9-triazadecane (149)

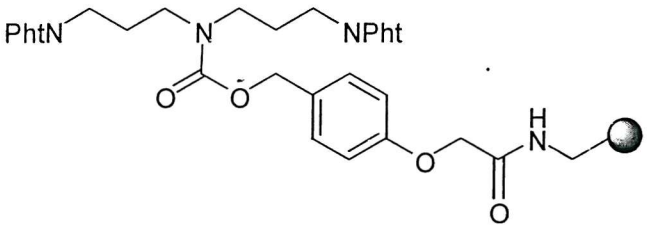

N^1,N^9-*bis*(Phthaloyl)-N^5-(4-benzyloxycarbonyl-oxyacetic acid allyl ester)-1,5,9-triaza decane (2.11 g, 3.5 mmol) was dissolved in dichloromethane (10 mL) at room temperature and HOBt (0.66 g, 4.2 mmol) was added with DIC (0.5 mL, 4.2 mmol). After 10 min the solution was added to amino resin (pre-swelled in CH_2Cl_2 for 30 mims and filtered) (2.35 g, 2.12 mmol, 0.9 $mmolg^{-1}$) and suspension was shaken at room temperature overnight. The resin was filtered and washed with CH_2Cl_2 (2x30 mL), DMF (2x30 mL), MeOH (2x30 mL), and Et_2O (2x30 mL). The resin was dried under vacuum and gave nagative nihydrin test.

N^5-(4-Benzyloxycarbonyl-oxyacetamidomethyl resin)-1,5,9-triazadecane (154)

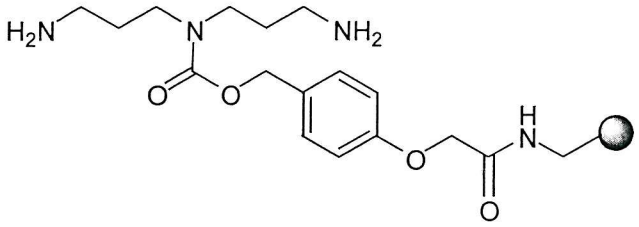

N^1,N^9-*bis*(Phthaloyl)-N^5-(4-benzyloxycarbonyl-oxyacetamidomethylresin)-1,5,9-triazadecane (4.0 g) was added to absolute ethanol (100 mL) and hydrazine monohydrate (2 mL, 40 mmol). The solution was heated under reflux at 80 °C overnight. The resin was filtered and washed successively with hot water (2x30 mL), EtOH (2x30 mL), MeOH (2x30 mL), CH_2Cl_2 (2x30 v) and ether (2x30 mL). The resin was dried under vacuum and the quantitative ninhydrin test gave a loading of 0.5 mmol.g^{-1}, 3.3 g.

N^1,N^9-*bis*(3,4-Dihydroxydihydrocinnamoyl)-1,5,9-triazanonane (156a)

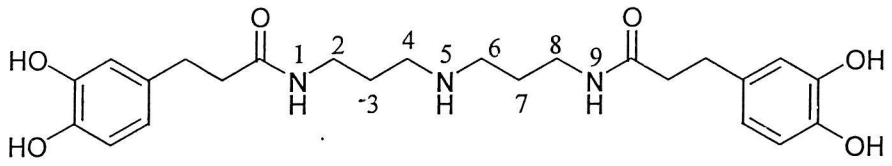

RP-HPLC: R_t = 7.5 min.

Yield 14 mg (48%).

IR (ν_{max}/ cm^{-1}) 1676 (C=O).

δ_H (400MHz, CD_3OD): 1.64 (4H, m, $C^{3+7}H_2$), 2.39 (4H, t, *J* 7, $ArCH_2C\underline{H}_2$), 2.51 (4H, t, *J* 7, $C^{4+6}H_2$), 2.69 (4H, t, *J* 7, $ArC\underline{H}_2CH_2$), 3.15 (4H, t, *J* 7, $C^{2+8}H_2$), 6.44 (2H, dd, *J* 8, 2, Ar<u>H</u>), 6.55 (2H, d, *J* 2, Ar<u>H</u>), 6.58 (2H, d, *J* 8, Ar<u>H</u>).

δ_C (100MHz, CD_3OD): 28.0, 32.4, 37.0, 39.0, 46.6, 48.7, 116.9, 117.2, 121.1, 133.8, 145.1, 146.6, 176.9.

ES-MS (+ve): m/z 460.3 (100%, $M+H)^+$.

N^1,N^9-*bis*(4-Hydroxy-7-trifluoromethyl-3-quinolinecarboxyl)-1,5,9-triazanonane (156m)

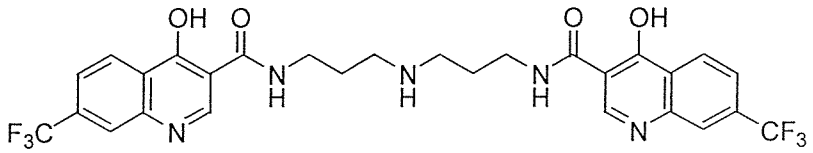

RP-HPLC: R_t = 11.4 min.

Yield 18.9 mg

IR (ν_{max}/cm^{-1}) 1676 (C=O).

δ_H (300MHz, CD_3OD): 1.40 (4H, m, $C^{3+7}H_2$), 2.48 (4H, m, $C^{4+6}H_2$), 2.95 (2H, m, $C^{2+8}H_2$), 6.94 (2H, d, *J* 8, ArH), 7.16 (2H, s, ArH), 7.69 (2H, d, *J* 8, ArH), 8.13 (2H, s, ArH).

δ_C (75MHz, CD_3OD): 27.9, 36.6, 46.4, 112.6, 117.6, 121.9, 128.4, 129.6, 140.4, 146.3, 167.9, 177.5.

ES-MS (+ve): m/z 610.4 (100%, $M+H)^+$.

N^1,N^9-*bis*(Indole-3-acetyl)-1,5,9-triazanonane (156y)

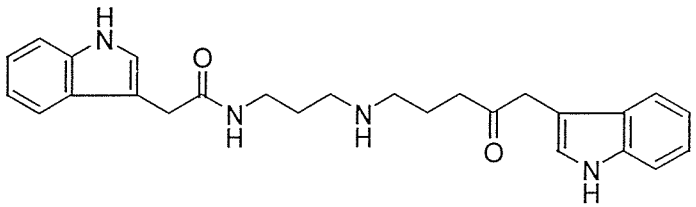

RP-HPLC: R_t = 10.9 min.

Yield 8.3 mg.

IR (ν_{max}/cm^{-1}) 1676 (C=O).

δ_H (300MHz, CD_3OD): 0.98 (4H, m, $C^{3+7}H_2$), 1.89 (2H, t, *J* 7, C^4H_2), 2.01 (2H, t, *J* 7, C^6H_2), 2.43 (2H, t, *J* 7, C^2H_2), 2.50 (2H, t, *J* 7, C^8H_2), 2.94 and 2.98 (4H, 2xs, 2xArCH_2), 6.33 (2H, m, ArH), 6.41 (2H, m, ArH), 6.46 and 6.50 (2H, 2xs, 2xArH), 6.67 (2H, t, *J* 8, ArH), 6.84 (2H, m, ArH).

δ_C (75MHz, CD_3OD): 26.6, 27.3, 29.5, 31.8, 33.9, 34.1, 46.0, 47.3, 109.0, 112.4, 119.2, 120.0, 122.6, 124.3, 125.2, 138.1, 176.0.

N^1,N^9-*bis*(5-Hydroxyindole-3-acetyl)-1,5,9-triazanonane (156I)

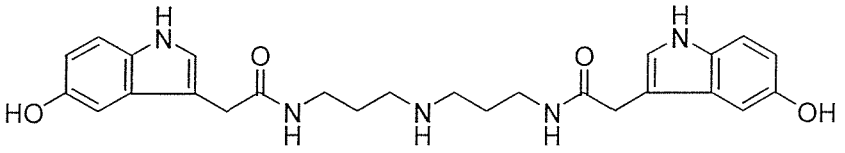

Yield 15 mg (37%).

IR (ν_{max}/ cm^{-1}) 1667 (C=O).

δ_H (300MHz, CD_3OD): 1.06 (4H, m, $C^{3+7}H_2$), 2.01 (4H, t, *J* 7, $C^{4+6}H_2$), 2.58 (4H, t, *J* 7, $C^{2+8}H_2$), 2.94 (4H, s, $ArCH_2$), 6.54 (4H, m, Ar<u>H</u>), 6.60 (2H, d, *J* 9, Ar<u>H</u>), 7.03 (2H, s, Ar<u>H</u>).

N^1,N^9-*bis*(Indole-3-propionyl)-1,5,9-triazanonane (156II)

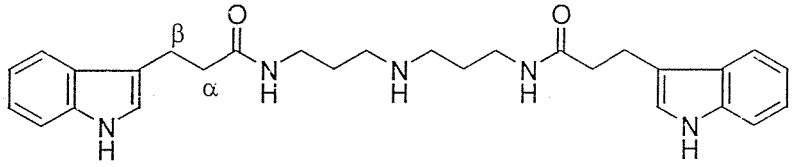

RP-HPLC: R_t = 11.7 min.

Yield 23 mg (61%).

IR (ν_{max}/ cm^{-1}) 1671 (C=O).

δ_H (300MHz, CD_3OD): 0.92 (4H, m, $C^{3+7}H_2$), 1.56 (4H, t, *J* 7, $ArC^{\alpha}H_2$), 1.95 (2H, t, *J* 7, $C^{4+6}H_2$), 2.40 (4H, t, *J* 7, $C^{2+8}H_2$), 2.50 (4H, t, *J* 7, $ArC^{\beta}H_2$), 6.37 (6H, m, Ar<u>H</u>), 6.64 (2H, d, *J* 8, Ar<u>H</u>), 6.86 (2H, d, *J* 8, Ar<u>H</u>).

δ_C (75MHz, CD_3OD): 22.3, 27.5, 36.4, 37.8, 45.6, 112.2, 114.7, 119.3, 119.6, 122.4, 123.1, 129.0, 138.0, 177.0.

ES-MS (+ve): m/z = 474.3 (100%, $M+H)^+$.

HRMS (EI): $C_{28}H_{36}N_5O_2$ Calc. 474.2864, Found 474.2869.

***N*^{1},*N*^{9}-*bis*(5-Methoxyindole-3-acetyl)-1,5,9-triazanonane (156VI)**

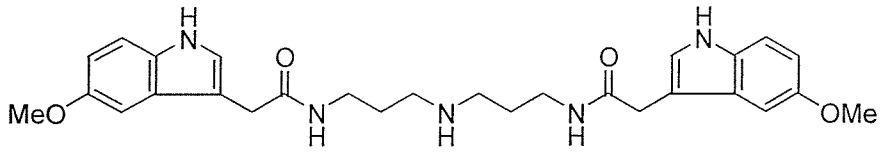

RP-HPLC: R_t = 10.8 min.

Yield 18 mg (64%).

IR (ν_{max}/ cm^{-1}) 1676 (C=O).

δ_H (300MHz, CD_3OD)**:** 1.14 (2H, m, C^3H_2), 1.28 (2H, m, C^7H_2), 2.18 (4H, m, $C^{4+6}H_2$), 2.30 (4H, t, *J* 7, $C^{2+8}H_2$), 2.65 (4H, s, $ArCH_2$), 3.14 (6H, s, 2xOMe), 6.12 (2H, dd, *J* 9, 2, ArH), 6.39 (2H, d, *J* 2, ArH), 6.50 (2H, s, ArH), 6.60 (2H, d, *J* 9, ArH).

δ_C (75MHz, CD_3OD): 25.3, 27.6, 33.9, 36.5, 37.6, 45.7, 56.4, 101.6, 109.0, 112.6, 125.8, 125.2, 138.1, 176.0.

***N*^{1},*N*^{9}-*bis*(Indole-3-buthyl)-1,5,9-triazanonane (156XI)**

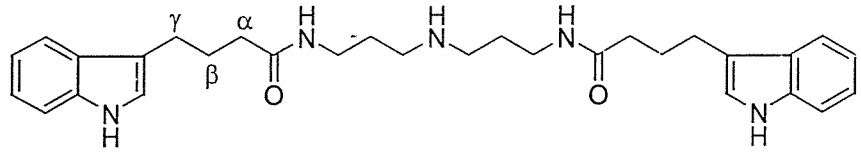

RP-HPLC: R_t = 9.8 min.

Yield: 18 mg.

IR (ν_{max}/ cm^{-1}) 1671 (C=O).

δ_H (300MHz, CD_3OD)**:** 1.00 (4H, m, $C^{3+7}H_2$), 1.22 (4H, m, $ArC^{\beta}H_2$); 1.36 (4H, m, $ArC^{\alpha}H_2$), 1.56 (4H, t, *J* 7, $ArC^{\gamma}H_2$), 1.72 (4H, m, $C^{4+6}H_2$), 2.21 (4H, m, $C^{2+8}H_2$), 6.38 (2H, t, *J* 7, ArH), 6.47 (2H, t, *J* 7, ArH), 6.66 (2H, m, ArH), 6.75 (2H, d, *J* 8, ArH), 6.91 (2H, d, *J* 8, ArH).

δ_C (75MHz, CD_3OD): 23.9, 24.5, 27.8, 28.5, 33.8, 36.1, 36.5, 46.1, 46.4, 112.3, 115.8, 119.8, 120.1, 123.5, 125.5, 130.2, 137.0, 177, 177.3.

ES-MS (+ve): m/z 502.3 (80%, $M+H)^+$.

N^{1},*N*^{9}-*bis*(5-Bromo-indole-3-acetyl)-1,5,9-triazanonane (156XII)

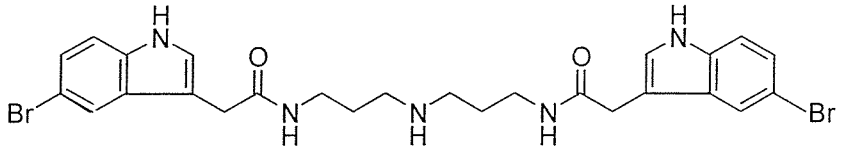

RP-HPLC: R_t = 10.8 min (93 % purity).

Yield 25 mg (61%).

IR (ν_{max}/ cm^{-1}) 1670 (C=O).

δ_H (300MHz, CD_3OD): 1.06 (4H, m, $C^{3+7}H_2$), 2.01 (4H, t, *J* 7, $C^{4+6}H_2$), 2.58 (4H, t, *J* 7, $C^{2+8}H_2$), 2.94 (4H, s, $ArC\underline{H}_2$), 6.54 (4H, m, Ar$\underline{H}$), 6.60 (2H, d, *J* 9, Ar$\underline{H}$), 7.03 (2H, s, Ar$\underline{H}$).

δ_C (75MHz, CD_3OD): 27.5, 33.7, 36.8, 46.1, 109.2, 113.1, 114.1, 122.0, 125.3, 126.6, 130.1, 136.7, 175.7.

ES-MS (+ve): m/z = 602.1, 604.0, 606.1 (48%, 100%, 46%, $M+H)^+$.

HRMS (EI): $C_{26}H_{30}N_5O_2Br_2$ Calc. 602.0761, Found 602.0763.

Results of inhibition studies

Compound 141a

[Substrate] (μM)	Initial Rate ($\Delta A\ sec^{-1}$; x 10^{-3} at specified inhibitor			
	0 μM	5 μM	10 μM	15 μM
10	0.65	0.41	0.47	0.36
20	1.22	0.69	0.71	0.47
40	2.11	0.78	0.96	0.85
80	2.78	1.64	2.32	1.23
160	3.08	2.11	3.02	1.43
200	3.15	2.25	3.65	1.73
V_{max}	4.8	3.7	3.2	2.5

Compound 141c

[Substrate] (μM)	Initial Rate ($\Delta A\ sec^{-1}$; x 10^{-3} at specified inhibitor			
	0 μM	10 μM	20 μM	30 μM
10	0.666	0.394	0.508	0.302
20	1.025	0.876	1.001	1.126
40	1.396	1.597	1.848	1.319
80	3.752	2.523	3.421	3.397
160	6.046	5.672	5.816	5.125
200	6.840	6.8570	6.8890	5.952
V_{max}	14.5	13.7	12.8	12.0

Compound 141m

[Substrate] (μM)	Initial Rate ($\Delta A\ sec^{-1}$; x 10^{-3} at specified inhibitor			
	0 μM	5 μM	10 μM	20 μM
7.5	2.65	1.97	0.94	0.46
15	3.09	3.96	1.87	0.92
45	5.83	5.19	3.86	1.33
90	8.56	7.84	5.16	2.39
120	8.51	8.99	6.50	3.13
180	9.00	9.73	8.88	5.60
V_{max}	4.8	3.7	3.2	2.5

Compound 148y

[Substrate] (μM)	Initial Rate ($\Delta A\ sec^{-1}$; x 10^{-3} at specified inhibitor			
	-0 μM	0.5 μM	1.0 μM	2.5 μM
10	0.80	0.61	0.20	0.20
25	1.15	1.38	0.52	0.51
50	1.94	1.76	0.80	0.87
75	2.16	2.28	0.94	1.06
125	2.43	2.82	1.27	1.35
200	2.80	3.27	1.47	1.72
V_{max}	4.0	3.1	2.5	1.9

Compound 141y

[Substrate] (μM)	Initial Rate ($\Delta A\ sec^{-1}$; x 10^{-4} at specified inhibitor			
	0 μM	1.0 μM	2.5 μM	5.0 μM
10	2.66	3.58	0.46	0.52
20	6.49	7.38	2.92	1.08
40	12.10	9.27	3.74	1.32
80	14.33	10.37	5.03	2.17
160	18.15	12.81	6.69	2.93
200	17.13	13.27	7.30	6.55
V_{max}	23.2	13.5	9.8	6.1

Compound 141II

[Substrate] (μM)	Initial Rate ($\Delta A\ sec^{-1}$; x 10^{-4} at specified inhibitor			
	0 μM	1.0 μM	2.5 μM	5.0 μM
10	2.66	1.47	0.80	1.22
20	6.49	4.02	2.36	1.28
40	12.10	5.63	5.32	2.06
80	14.33	5.96	4.80	2.86
160	18.15	10.43	6.81	4.15
200	17.13	16.46	7.25	4.41
V_{max}	24.8	14.2	10.0	6.2

Compound 141VI

[Substrate] (μM)	Initial Rate ($\Delta A\ sec^{-1}$; x 10^{-4} at specified inhibitor			
	0 μM	0.1 μM	0.25 μM	0.5 μM
10	0.27	0.18	0.15	0.81
20	0.49	0.38	0.24	0.12
40	1.04	0.63	0.39	0.21
80	1.74	0.91	0.46	0.26
120	2.15	1.27	0.77	0.42
V_{max}	4.7	2.3	1.5	0.7

Compound 141XI

[Substrate] (μM)	Initial Rate ($\Delta A\ sec^{-1}$; x 10^{-3} at specified inhibitor			
	0 μM	0.1 μM	0.5 μM	1.0 μM
10	0.65	0.58	0.43	0.29
20	0.75	0.70	0.56	0.43
40	1.15	1.22	1.27	0.60
80	1.91	1.78	1.44	0.80
120	2.45	2.32	1.88	1.32
V_{max}	4.2	3.5	3.0	2.3

Compound 141XII

[Substrate] (μM)	Initial Rate ($\Delta A\ sec^{-1}$; x 10^{-4} at specified inhibitor			
	0 μM	0.5 μM	1.0 μM	2.5 μM
20	5.47	1.33	0.58	0.43
40	9.60	2.04	1.20	0.58
80	14.60	2.78	1.23	0.87
160	18.22	4.77	1.92	1.15
200	15.70	4.72	1.72	1.37
V_{max}	29	11.4	9.9	6.4

5.4 Experimental for Chapter 3

5 -Formyl-2-hydroxybenzamidomethyl resin (200b) and 5-Formyl-2-hydroxy-benzamide-(5-carbamoylpentyl)-N^5-amidomethyl resin (200c).

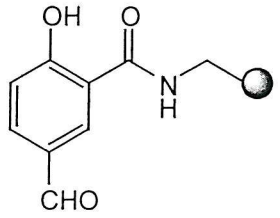

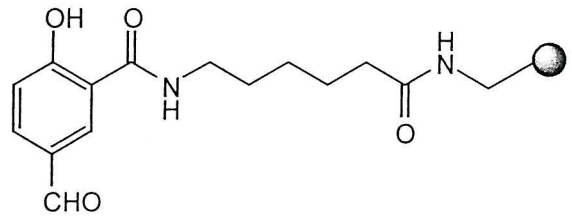

To a solution of 5-formyl salicylic acid (5 equiv.) in CH_2Cl_2 (10 mL) and HOBt (5 equiv.) in DMF (2 mL) was added with DIC (5 equiv.). After 10 min the solution was added to aminomethyl resin (or 1-amino-6-hexanamido methyl resin) (1 g, 1.1 mmol.g^{-1}) and the suspension was shaken overnight. The coupling process was repeated as above for 5 hours. The resin was filtered and washed with CH_2Cl_2 (2x30 mL), MeOH (2x30mL) and Et_2O (2x30 mL) and dried *in vacuo.*

IR (ν_{max}/ cm^{-1}) 1733, 1691, 1640, 1583.

2-Hydroxy-5-hydroxymethyl benzyl *N-(Boc)*-aminomethyl resin (201b).[136]

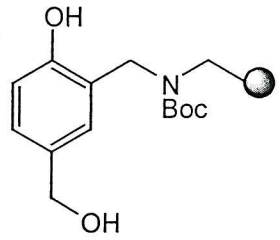

Resin (**200b**) (1g, 1 equiv.) was swollen in dry THF (10 mL) under nitrogen. Diborane (1M in THF, 10 mL) was added dropwise at room temperature and the suspension stirred gently at 55-65°C for 48 hours. Upon cooling the resin suspension was transferred to a polypropylene vessel. The resin was swollen in THF-AcOH-DIPEA (7:2:1) and iodine (2 equiv.) in THF (5 mL) was added and the reaction mixture was shaken for 1 hour. The resin was washed with THF, DMF/Et_3N (3:1), MeOH, CH_2Cl_2 and Et_2O and dried under vacuum. The resin was swollen in CH_2Cl_2 for 30 min. and a solution of Boc_2O (1 equiv.) was added. After 4 hours, the resin was filtered and washed with CH_2Cl_2 (2x20 mL), MeOH (2x20mL) and Et_2O (2x20 mL) and dried *in vacuo*.

General procedure for selective acetylation on the solid-phase[137]

Resin (**201**) was suspended in THF (3mL) and 1M NaOH (2 mL). A solution of the triazolide (2 equiv.) was added and the mixture was shaken overnight. The resin was filtrated and washed with H_2O, (2x10 mL), MeOH (2x10 mL) CH_2Cl_2 (2x10 mL), and Et_2O (2x10 mL) and dried under vacuum to give (**202**)

Preparation of active-carbonate safety-catch resin (209).

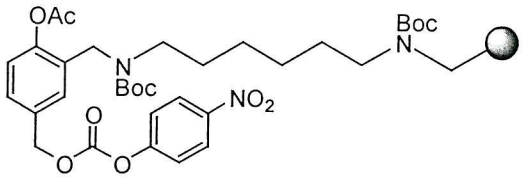

Resin (**202c**) was suspended in CH_2Cl_2 (10 mL), pyridine (0.5 mL) and *p*-nitrophenyl chloroformate (0.27 g, 1.32 mmol), dissolved in CH_2Cl_2 (3 mL), was slowly added at room temperature. The resin was shaken for 1 hour, then washed with dry CH_2Cl_2 (3x20 mL), MeOH (2x20 mL), Et_2O (2x20 mL) and dried *in vacuo*.

General procedure for loading the safety-catch linker with spermine (tetraazatetradecane) (210)

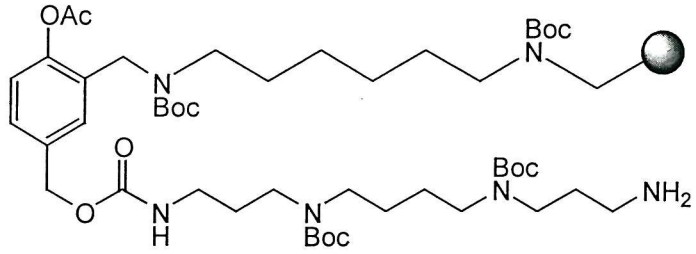

A ten-fold molar excess of N^5,N^{10}-*bis*(Boc)-tetraazatetradecane was dissolved in DMF (10 mL) and added to the active-carbonate safety-catch resin 1.0 g (0.3 mmol). The reaction mixture was shaken overnight at room temperature. The solution was filtered and the resin beads were washed with (3x20 mL) of DMF, H_2O, MeOH, CH_2Cl_2 and Et_2O and dried *in vacuo*.

General procedure for preparing squalamine derivatives

The carboxylic acid (4 equiv.) and DIC (4 equiv.) were dissolved in CH_2Cl_2 (3 ml) and a solution of HOBt (4 equiv.) in DMF was added. The mixtures were left at room

temperature for 10 min before adding to the resin pre-swollen in CH_2Cl_2 (5 ml) and the mixture was shaken at room temperature overnight. A quantitative ninhydrin test indicated that the reaction was complete. The resin was filtered and washed with (3x15 ml) DMF, CH_2Cl_2, MeOH, and Et_2O respectively. The resin was suspended in $CHCl_3$ (5 mL) and sulfur trioxide pyridine complex (5 equiv.) was added. The reaction was left overnight and the resin was filtered and washed with (3x15 ml) DMF, CH_2Cl_2, MeOH, and Et_2O respectively.

General procedure for resin cleavage

To the pre-swollen resin in CH_2Cl_2 was added a solution of CH_2Cl_2/TFA (1:1) and the resin was shaken for 1h. The resin was then washed with CH_2Cl_2, DMF, CH_2Cl_2, MeOH and water. A solution of sodium phosphate buffer (pH 8.0, 50 mM) was added (1 mL per 10 mg of resin). The resin was shaken at room temperature for 24 h, filtered and the supernatant was quenched with 0.1 % TFA before analysis by RP-HPLC.

N^1-(3β-Sulfoxy-23,24-bisnor-5-cholenyl-22-carbonyl)-1,5,10,14-tetraazatetradecane (213)

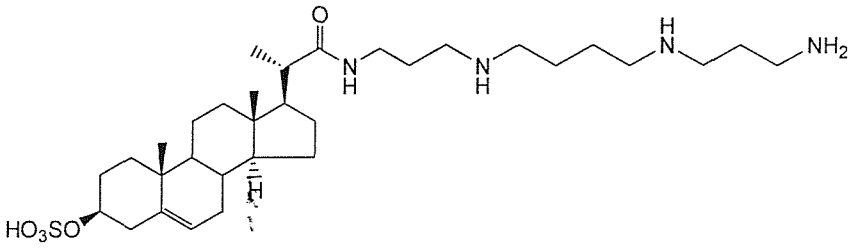

Yield 33 mg (60%).

Data in accordance with the literature.[138]

IR (ν_{max}/ cm^{-1}) 1667 (C=O).

δ_H (400 MHz, DMSO-d_6) 0.69 (3H, s, 18-CH_3), 0.81-2.81 (47H, series of multiplets, 1′β-CH, 2′β-CH, 8′β-CH, 11′α-CH, 11′β-CH, 12′α-CH, 14′α-CH, 15′α-CH, 16′β-CH, 17′α-CH, 19′-CH_3, 20′-CH, 21′-CH_3, 3-CH_2, 7-CH_2, 8-CH_2, 12-CH_2, 1′α-CH, 4′α-CH, 4′β-CH, 12′β-CH, 15′β-CH, 16′α-CH, 2′-$C^{\alpha}H$, 7′α-CH, 7′β-CH, 9′α-CH, 4-CH_2, 6-CH_2, 9-CH_2, 11-CH_2, 13-CH_2, 2-CH_2), 4.69 (1H, m, 3′-$C^{\alpha}H$), 5.35 (1H, br s, 6′-CH), 6.98 and 7.28 (7H, 2 x br m, NH_3^+ and NH_2^+) .

δ_C (100 MHz, $CDCl_3/CD_3OD$): 14.9, 21.8, 22.4, 24.4, 25.3, 27.6, 31.5, 32.9, 34.4, 35.3, 36.1, 36.2, 39.1, 39.8, 40.7, 44.1, 46.0, 50.0, 52.1, 54.5, 59.3, 60.2, 74.6, 124.7, 144.3, 178.0.

General procedure for preparing libraries

The carboxylic acid (4 equiv.) and DIC (4 equiv.) were dissolved in CH_2Cl_2 (3 ml) and a solution of HOBt (4 equiv.) in DMF was added. The mixtures were left for 10 min before adding to the resin, pre-swollen in CH_2Cl_2 (5 ml) and the mixture was shaken at room temperature overnight. A quantitative ninhydrin test indicated that the reaction was complete. The resin was filtered and washed with (3x15 ml) DMF, CH_2Cl_2, MeOH, and Et_2O respectively and dried *in vacuo*. All compounds were purified by semi-preparative RP HPLC.

5.5 Experimental for Chapter 4

N^1-(3β-Hydroxy-23,24-bisnor-5-cholenyl-22-carbonyl)-1,5,10,14-tetraazatetradecane (230a)

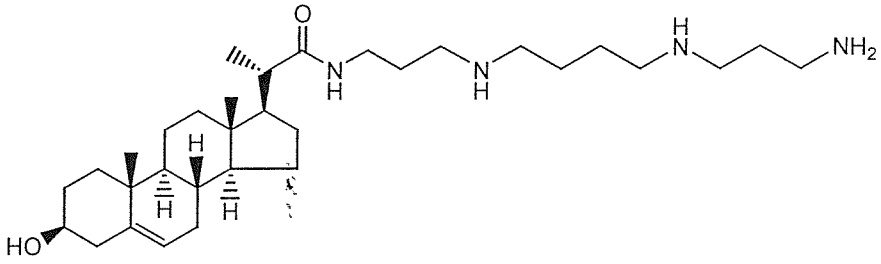

Yield 25 mg (78%)

IR (ν_{max}/ cm^{-1}) 1667 (C=O).

Data in accordance with the literature.[187]

δ_H (400 MHz, DMSO-d_6) 0.43 (3H, s, 18′-CH_3), 0.65-1.42 (31H, series of multiplets, 1′β-CH, 2′β-CH, 8′β-CH, 11′α-CH, 11′β-CH, 12′α-CH, 14′α-CH, 15′α-CH, 16′β-CH, 17′α-CH, 19′-CH_3, 20′-CH, 21′-CH_3, 3-CH_2, 7-CH_2, 8-CH_2, 12-CH_2, 1′α-CH, 4′α-CH, 4′β-CH, 12′β-CH, 15′β-CH, 16′α-CH), 1.49-2.20 (17H, series of multiplets, 2′-$C^{\alpha}H$, 3′-$C^{\alpha}H$, 7′α-CH, 7′β-CH, 9′α-CH, 4-CH_2, 6-CH_2, 9-CH_2, 11-CH_2, 13-CH_2, 2-CH_2), 5.11 (1H, br s, 6′-CH).

δ_C (100 MHz, DMSO-d_6): 11.9, 18.6, 19.4, 21.0, 22.6, 24.2, 28.1, 30.0, 31.6, 31.8, 35.6, 36.5, 36.9, 37.3, 39.7, 42.3, 50.0, 55.9, 56.6, 70.9, 121.0, 141.3, 159.8.

N^1-(3α-7α-Dihydroxy-5β-cholan-24-carbonyl)-1,5,10,14-tetraazatetradecane (230b)

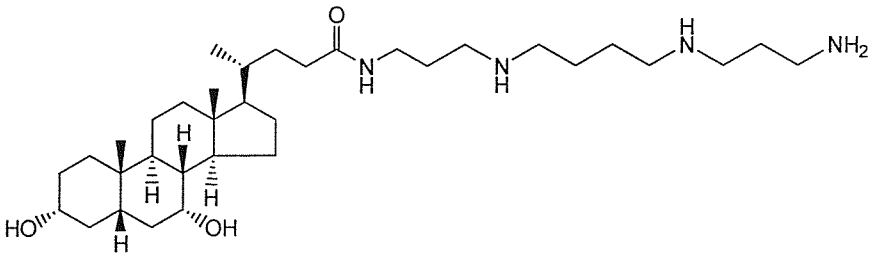

Spectroscopic data agreed with the literature.[187]

Yield 29 mg (72%).

IR (ν_{max}/ cm^{-1}) 1624 (C=O, amide).

Based on the literature assignment. [186] δ_H (400MHz, DMSO-d_6): 0.68 (3H, s, 18′-CH_3), 0.91 (3H, s, 19′-CH_3), 0.93-2.40 (37H, series of multiplets, 1′β-CH, 2′β-CH, 2′α-CH, 5′β-CH, 8′β-CH, 9′α-CH, 11′α-CH, 11′β-CH, 12′α-CH, 14′α-CH, 15′α-CH, 16′β-CH, 17′α-CH, 20′-CH, 21′-CH_3, 3-CH_2, 7-CH_2, 8-CH_2, 12-CH_2, 1′α-CH, 4′α-CH, 4′β-CH, 6′α-CH, 6′β-CH, 12′β-CH, 15′β-CH, 16′α-CH, 22′CH_2, 23′CH_2), 2.83, 2.93, 3.14 and 3.35-3.50 (13H, br multiplets, 4-CH_2, 6-CH_2, 9-CH_2, 11-CH_2, 13-CH_2, 2-CH_2, 3′β-CH), 3.89 (1H, m, 7′β-CH), 4.40 and 4.56 (2H, 2 x br s, 2 x OH), 8.08 and 8.27 (7H, 2 x br m, NH_3^+ and NH_2^+).

δ_C(100MHz, DMSO-d_6): 12.0, 18.6, 20.6, 22.9, 23.4, 25.6, 27.9, 28.3, 30.4, 30.6, 31.3, 31.6, 32,7, 34.1, 34.9, 35.2, 35.2, 35.4, 36.9, 39.2, 39.7, 39.9, 44.8, 47.7, 50.5, 55.8, 67.3, 71.3, 173.6.

N^1-(3α-Hydroxy-5β-cholan-24-carbonyl)-1,5,10,14-tetraazatetradecane (230c)

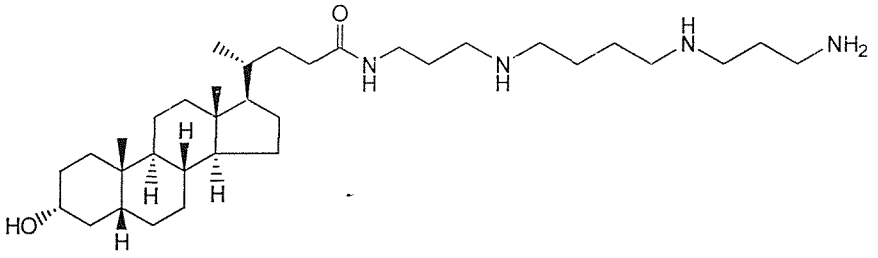

Data in accordance with the literature.[187]

RP-HPLC: R_t = 19.5 mins.

Yield 22 mg (67%).

IR (ν_{max}/ cm^{-1}) 1665 (C=O, amide)

Based on literature assignments.[186] δ_H (400MHz, DMSO-d_6): 0.68 (3H, s, 18′-CH_3), 0.94 and 0.97 (6H, 2 xs, 19′-CH_3 and 21′-CH_3), 1.00-2.40, (36H, series of multiplets, 1′β-CH, 15′α-CH, 2′β-CH, 2′β-CH, 5′β-CH, 8′β-CH, 9′α-CH, 7′CH_2, 11′α-CH, 11′β-CH, 12′α-CH, 14′α-CH, 16′β-CH, 17′α-CH, 20′-CH, 7-CH_2, 8-CH_2, 12-CH_2, 3-CH_2, 1′α-CH, 4′α-CH, 4′β-CH, 6′α-CH, 6′β-CH, 12′β-CH, 15′β-CH, 16′α-CH, 22′CH_2, 23′CH_2), 2.86, 2.96, 3.01 and 3.14-3.80 (13H series of multiplets, 4-CH_2, 6-CH_2, 9-CH_2, 11-CH_2, 13-CH_2, 2-CH_2, 3′β-CH), 4.60 (1H, br, s, 7'-OH), 8.26 and 8.46 (7H 2x br m, NH_3^+ and NH_2^+)

δ_C(100MHz, DMSO-d_6): 12.1, 18.6, 20.8, 23.4, 23.5, 24.2, 26.5, 28.2, 30.5, 31.6, 34.6 35.5, 35.5, 35.8, 36.4, 36.9, 42.0, 42.7, 47.8, 56.1, 56.5, 70.7, 173.3.

N^1-(3α-12α-Dihydroxy-5β-cholan-24-carbonyl)-1,5,10,14-tetraazatetradecane (230d)

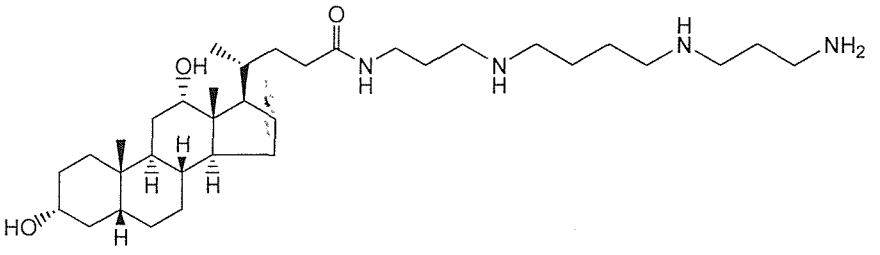

Yield 29 mg (70 %).

IR (ν_{max}/ cm^{-1}) 1666(C=O).

Data in accordance with the literature.[187]

δ_H (400MHz, $CDCl_3/CD_3OD$): 0.69 (3H, s, 18′-CH_3), 0.84 (3H, s, 19′-CH_3), 0.93 (3H, m, 21′-CH_3), 1.05-2.50 (34H series of multiplets, 1′β-CH, 15′α-CH, 2′β-CH, 2′α-CH, 5′β-CH, 8′β-CH, 9′α-CH, 11′α-CH, 11′β-CH, 14′α-CH, 16′β-CH, 17′α-CH, 20′-CH, 7-CH_2, 8-CH_2, 12-CH_2, 3-CH_2, 1′α-CH, 4′α-CH, 4′β-CH, 6′α-CH, 6′β-CH, 7′CH_2, 15′β-CH, 16′α-CH, 22′CH_2, 23′CH_2), 2.85, 2.94 and 3.13-3.85 (12H, series of multiplets, 4-CH_2, 6-CH_2, 9-CH_2, 11-CH_2, 13-CH_2, 2-CH_2), 3.50 (1H, m, 3′β-CH), 3.93 (1H, br s, 12′β-CH), 4.49 and 4.69 (2H, 2 x br, s, 2 x OH), 8.18 and 8.39 (7H, br m, NH_3^+ and NH_2^+).

δ_C(100MHz, $CDCl_3/CD_3OD$): 12.3, 12.7, 17.8, 21.2, 23.2, 23.3, 23.8, 25.5, 25.9, 26.3, 27.0, 27.7, 28.9, 30.3, 30.5, 31.6, 33.4, 34.3, 36.0, 41.8, 42.1, 45.1, 47.5, 47.9, 49.4, 70.8, 71.9, 173.0.

N^1-Eicosanoyl-1,5,10,14-tetraazatetradecane (230e)

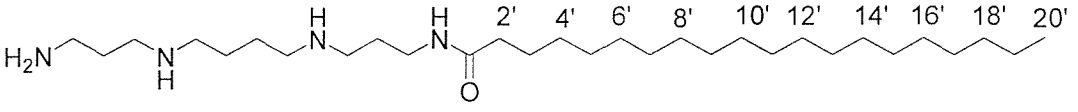

RP-HPLC (ELS): R_t = 17.4 mins.

Yield 35 mg (80%).

IR (ν_{max}/ cm^{-1}) 1666 (C=O).

δ_H (400MHz, DMSO-d_6)**:** 0.96 (3H, t, 20′-CH_3), 1.28-1.40 (33H, m, 4′ to 19′ CH_2), 1.60 (2H, m, 3′-CH_2), 1.78 (4H, m, 7-CH_2, 8-CH_2), 1.86 (2H, m, 12-CH_2), 2.65 (2H, m, 3-CH_2), 2.17 (2H, t, *J*=8, 2′-CH_2), 2.95-3.15 (m, 8H, 6-CH_2, 9-CH_2, 11-CH_2, 13-CH_2), 3.17 (2H, m, 4-CH_2) 3.23 (2H, m, 2-CH_2) 8.21, 8.95, 9.16 (3 x br s, NH_3^+, NH_2^+).

δ_C(100MHz, DMSO-d_6): 14.3, 22.6, 23.0, 23.1, 24.2, 24.9, 25.7, 26.5, 29.2, 29.3, 29.5, 31.8, 33.8, 34.2, 35.9, 36.7, 40.7, 44.4, 45.1, 46.6, 173.4.

ES-MS (+ve): m/z = 497.3 (40%, $M+H)^+$.

N^1-Docosanoyl-1,5,10,14-tetraazatetradecane (230f)

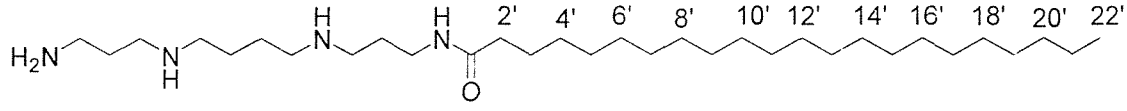

RP-HPLC (ELS): R_t = 19.0 mins.

Yield 38 mg (73%).

IR (ν_{max}/ cm^{-1}) 1685 (C=O).

δ_H (400MHz, DMSO-d_6)**:** 0.94 (3H, t, 22′-CH_3), 1.10-1.40, (36H, m, 4′ to 21′-CH_2), 1.60 (2H, m, 3′-CH_2), 1.68-1.90 (6H, m, 7-CH_2, 8-CH_2 12-CH_2), 2.06 (2H, t, *J* 8, 3-CH_2), 2.18 (2H, t, *J* 8, 2′-CH_2), 2.90-3.14 (10H, m, 4-CH_2, 6-CH_2, 9-CH_2, 11-CH_2, 13-CH_2), 3.24 (2H, t, *J* 6, 2-CH_2), 8.10, 8.80, 9.03 (3 x br s, NH_3^+, NH_2^+).

δ_C(100MHz, DMSO-d_6): 14.2, 22.5, 23.0, 23.1, 24.1, 24.9, 25.7, 26.5, 29.1, 29.2, 29.3, 31.8, 33.7, 35.8, 35.9, 36.2, 36.6, 44.4, 45.1, 46.7, 173.9.

ES-MS (+ve): m/z = 525.2 (20%, $M+H)^+$.

N^1-Tetracosanoyl-1,5,10,14-tetraazatetradecane (230g)

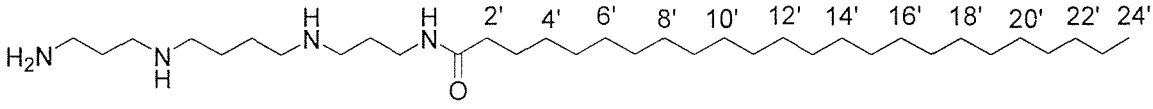

RP-HPLC (ELS): R_t = 20.9 mins.

Yield 35 mg (69%).

IR (ν_{max}/ cm^{-1}) 1689 (C=O).

δ_H (400MHz, DMSO-d_6): 0.94 (3H, m, 24′-CH_3), 1.10-1.50, (40H, m, 4′ to 23′-CH_2), 1.59 (2H, m, 3′-CH_2), 1.67-1.95 (6H, m, 7-CH_2, 8-CH_2, 12-CH_2), 2.04 (2H, m, 3-CH_2), 2.17 (2H, m, 2′-CH_2), 2.90-3.15 (10H, m, 4-CH_2, 6-CH_2, 9-CH_2, 11-CH_2, 13-CH_2), 3.23 (2H, m, 2-CH_2), 8.10, 8.80, 9.03 (3 x br s, NH_3^+, NH_2^+).

δ_C (100MHz, DMSO-d_6): 14.2, 22.5, 23.0, 23.1, 24.2, 24.8, 25.7, 26.5, 29.1, 29.2,29.3, 29.5, 31.7, 33.7, 35.8, 35.9, 36.1, 36.7, 44.4, 45.1, 46.7, 173.6.

ES-MS (+ve): m/z = 575.0 $(M+H)^+$.

N^1-Eicos-11-enoyl-1,5,10,14-tetraazatetradecane (230h)

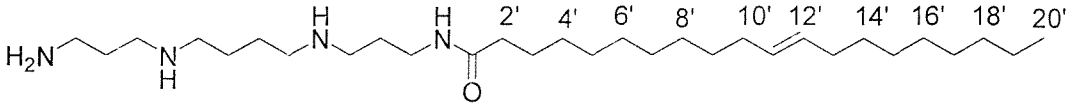

RP-HPLC: R_t = 16.2 mins.

Yield 35 mg (65%).

IR (ν_{max}/ cm^{-1}) 1679 (C=O).

δ_H (400MHz, DMSO-d_6): 0.96 (3H, m, 20′-CH_3), 1.10-1.28, (2H, m, 19′-CH_2), 1.30-1.45 (26H, m, 4′ to 10′-CH_2 and 13′ to 18′-CH_2), 1.59 (2H, m, 3′-CH_2), 1.76 (4H, m, 7-CH_2, 8-CH_2), 1.85 (2H, m, 12-CH_2), 2.07 (2H, m, 3-CH_2), 2.17 (2H, t, *J* 8, 2′-CH_2), 2.95-3.15 (10H, m, 4-CH_2, 6-CH_2, 9-CH_2, 11-CH_2, 13-CH_2), 3.23 (2H, m, 2-CH_2) 5.41 (2H, m, 11′-CH and 12′-CH), 8.08, 8.77, 8.97 (3 x br s, NH_3^+, NH_2^+).

δ_C(100MHz, DMSO-d_6): 14.3, 22.5, 23.0, 23.1, 24.2, 24.9, 25.7, 27.0, 29.0, 29.1, 29.2, 29.3, 29.4, 33.8, 35.8, 36.7, 44.4, 46.6, 129.4, 173.4.

ES-MS (+ve): m/z = 495.3 (20%, $M+H)^+$.

N^1-Docos-13-enoyl-1,5,10,14-tetraazatetradecane (230i)

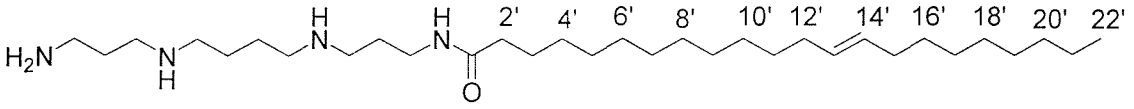

RP-HPLC: R_t = 17.6 mins.

Yield 30 mg (78%).

IR (ν_{max}/ cm^{-1}) 1689 (C=O).

δ_H (400MHz, DMSO-d_6): 0.95 (3H, m, 22′-CH_3), 1.30-1.43, (26H, m, 4′ to12′-CH_2 and 15′ to 21′CH_2), 1.60 (2H, m, 3′-CH_2), 1.77 (4H, m, 7-CH_2, 8-CH_2), 1.85 (2H, t, *J* 8, 12-CH_2), 2.07 (4H, m, 11′-CH, 14′-CH), 2.17 (2H, t, *J* 8, 2′-CH_2), 2.26 (2H, t, *J* 8, 2′-CH_2), 2.90-3.15 (10H, m, 4-CH_2, 6-CH_2, 9-CH_2, 11-CH_2, 13-CH_2), 3.23 (2H, m, 2-CH_2) 5.38 (2H, m, 13′-CH_2 and 14′-CH_2), 8.18, 8.90, 9.09 (3 x br s, NH_3^+, NH_2^+).

δ_C(100MHz, DMSO-d_6): 14.2, 22.5, 23.0, 23.1, 24.2, 24.9, 25.0, 26.5, 27.0, 29.1, 29.2, 29.3, 29.4 29.6, 31.8, 35.9, 36.0, 44.4, 45.1, 46.6, 51.3, 129.3, 173.4.

ES-MS (+ve): m/z = 523.0 (20%, $M+H)^+$.

5.5.2 Preparing stocks of (HB101) *E. coli.*

A single colony of HB101 *E. coli* was placed into LB (Luria-Bertani) broth (5mL, bactotryptone 10 gL^{-1}), yeast extract (5 gL^{-1}), NaCl (10 gL^{-1})) overnight. To 0.85 ml of bacterial culture, was added 0.15 ml of sterile glycerol (sterilised by autoclaving for 20 min). The culture was vortexed to ensure that the glycerol was evenly dispersed. The culture was frozen in liquid nitrogen and transferred to –70°C for long-term storage.

5.5.3 Transformation of plasmid DNA in Bacteria (*E. coli.*)

250 µl of transformation solution (sterile 50 mM of $CaCl_2$) was transferred using a sterile pipette into a sterile micro-centrifuge tube and the tube was placed on ice. A sterile loop was used to pick up one single colony of bacteria from a starter plate. The loop was immersed into the transformation solution at the bottom of tube. The sterile loop was immersed into the plasmid DNA stock tube and the loop was mixed into the cell suspension. The tube was incubated on ice for 10 min. The tube was transfered into the water bath set at 42 ^{0}C for exactly 50 seconds. The tube was placed back on ice and incubated for 2 min. 250 µl of LB broth was added to the tube and the tube incubated for 10 min at room temperature. 100µl of transformation mixture was spread onto the plate containing 100µg ml^{-1} ampicilin and left to grow overnight. A single colony from plate was grown overnight a 37°C in 5 ml of LB broth medium containing 100µg ml^{-1} ampicilin. 1 ml of this culture was used for preparing plasmid DNA.

5.5.4 Expression plasmids

Two types of plasmid DNA were used in this study: pGLO containing an arabinose (araC) promoter was obtained from Bio-Rad. This plasmid was carried a gene encoding for Green Fluorescent Protein (GFP). The second plasmid used was pEGFPLuc which encodes a fusion of enhanced green fluorescent protein and luciferase. Protein expression is under the control of the human cytomegatovirus (CMV) promoter. pEGFPLuc is a cotransfection marker that allows determination of transfection efficiencies in mammalian cells by fluorescence microscopy or a standard luciferase assay.

Plasmid DNA was isolated by the method of Laura Machesky.[7] Briefly, an overnight culture of bacteria (200 mL) was centrifuged and the pellet re-suspended in 50mM glucose, 50 mM, 25 mM Tris.HCl, pH 7.5, 10 mM, EDTA) (10 mL) and 1 mL of lysozyme solution (40 mg/mL) was added followed by incubating at room temperature for 10 min. To the solution was then added 20 mL of 0.2 M NaOH, 1% SDS. The solution was mixed by swirling and incubated for 5 min on ice. To the solution was added 5M potassium acetate (pH 4.8) (10 mL) The solution was mixed by swirling and incubated for 15 min on ice. The mixture was centrifuged at 8K rps for 10 min and the supernatant was poured through cheesecloth into a 50 mL tube. The plasmid DNA was precipitated using isopropanol (25 mL), mixed and centrifuged at 8K rps for 10 min. The pellet was washed with 70% ethanol (30 mL) and centrifuged at 8K rps for 10 min. The pellet was dried on the bench for 20-30 min before dissolving in TE (10 mM Tris-HCl, pH 8.0, 1 mM EDTA) (2 mL). The solution of DNA was added to a solution of diatomaceous earth (1g/10 mL of resin buffer) (10 mL). The DNA and resin were mixed by inverting. The resin-DNA slurry was poured into column and the column was fitted onto a vaccum line using a water pump. The resin-DNA was filtered and washed with 13 mL of column wash solution (50% ethanol, 100 mM NaCl, 10 mM Tris-HCl, pH 7.5, 5 mM EDTA). The column was washed with 5 mL of 80% ethanol, filtered and dried under vacuum for 10 min. The column was removed from the vacuum line and 1.5 mL of TE added. The column was preheated to 65-70°C for 1 min. The DNA was eluted by spinning at 1.3K for 5 min. The elute was collected in the tube and transferred to a 1.5 mL tube and stored at -20°C. The typical yield from this method was between 0.13-0.3 $\mu g/\mu L$ ($A_{260}/A_{280} > 1.8$).

5.5.5 Formulation of cationic liposomes

Liposomes were prepared by adding 2 mM of transfection agent to 2 mM of dioleolyl L-α-phosphatidylethanolamine (DOPE) (in $CHCl_3$). The solvent was removed under a stream of nitrogen gas and the resultant films were dried under vacuum for 2 h to remove traces of organic solvent. The lipid films were hydrated in 0.2 μm filtered water and vortexed 2-3 min at room temperature. Liposome preparations were stored at 4°C under nitrogen gas before use.

5.5.6 Transfection in bacteria

A single colony of HB101 *E. Coli* was placed into LB broth (5mL, bacto-tryptone $10gL^{-1}$), bacto-yeast extract ($5gL^{-1}$), NaCl ($10gL^{-1}$) overnight. 0.5 mL of this culture was transferred to an eppendorf centrifuge and the cells were harvested at 3000 rpm for 5 minutes at room temperature. The cells were washed with 1 mL of sterile water and re-harvested by centrifugation for 2 minutes at 3000 rpm. The cells were suspended in 0.5 mL of LB broth. For each transfection, the DNA and transfection solution were prepared in separated sterile tubes. 5 μg of plasmid DNA in 100 μL of LB broth was added to the first tube. 10-40 μL of transfection agents in 100 μL of LB broth was added to the second tube. After incubation at room temperature for 30 minutes, plasmid DNA/liposome complex mixtures (200μl) were added to each well. One hour after transfection, 1.0 mL LB broth was added to the transfected cells. The cells were returned to the incubator 1 hour at 37°C. 100μl of transformation mixture was pipetted on the plate containing $100\mu gml^{-1}$ ampicilin, 0.2 % (+)-arabinose and left to grow overnight. The transfection efficiency was analysed using a hand held UV lamp.

5.5.7 Cell counting

ND7 cell concentrations were calculated using a hemacytometer. Cells were mixed with 0.4 % trypan blue to determine the live/dead count (dead cells are blue). Both sides of the hemacytometer were loaded with the cell suspension covering both counting grids. The number of cells in 5 out of the 9 squares from each counting grid were counted (a total of 10 squares counted). The total number of cells counted from 10 squares were divided by 10 to get the average number of cells per square. The average count per square was multiplied by 10^4 then by the dilution facter to get the number of cells per mL of the original cell suspension.

5.5.8 Protein quantification by fluorescence

Generation of a GFP standard curve: A serial dilution of GFP was prepared in sonication buffer (50 mM NaH_2PO_4, 10 mM Tris-HCl, 200 mM NaCl, pH 8.0). Dilutions of GFP were assayed using a fluorometer and the relative fluorescence was plotted as a function of the concentration of each sample.

Preparation of cell lysates: Bacteria cell cultures were pelleted using micro-centrifugation and the supernatant was removed. The pellet was washed twice with 1 mL of PBS. The pellet was resuspended in 5 mL of sonication buffer. The cells were lysed by sonification (2x1min) with cooling on ice. The cell lysate was centrifuged at 12K rpm for 5 min at 4 ^{o}C. The supernatant was collected and the protein concentration determined using a standard Bradford assay. The results were compared with those of the standard curve to determine the amount of GFP protein expressed.

5.5.9 Cells culture and transfection

ND7 cells (Mouse neuroblastoma x rat neurone hybrid cell line) were maintained in DMEM + 2 mM Glutamine + 10% foetal bovine serum (FBS). Twenty-four hours before transfection, 500 µl of ND7 cells were seeded into 24-well culture plates at a concentration of 5x 10^4/mL. This dilution showed approximately 80% confluency after 24 hours.

5.5.10 Transfection by calcium phosphate

The cells were washed with medium and incubated with 200 µl of fresh growth media 3 h prior to transfection. To 1 µg of DNA in 26 µL water was added $CaCl_2$ (2 M, 3.7 µL) and mixed. 30 µL of 2XHBS solution (HEPES-buffered saline) was then added. Working in a tissue culture hood the tube was gently vortexed. Vortexing was continued while the prepared DNA solution was added dropwise. When the DNA addition was complete the solution appeared slightly opaque due to the formation of a fine calcium phosphate-DNA co-precipitate. The solution was incubated at room temperature for 30 mins. The transfection solution was vortexed again prior to the addition to the cells in the plates, which were then incubated at 37^{o}C.

5.5.11 Transfection using a liposome complex

The cells were washed with serum free medium just before transfection and incubated with 200 µl of serum free medium. Plasmid DNA/liposome complex mixtures (100µl)

were added to each well. Two hours after transfection the cells were gently over-layed with 0.8 mL of medium containing serum. The cells were returned to the incubator for 24-48 hours at 37°C. The transfection efficiency was assayed by microscopy and cytotoxicity assessed using the fluorescent exclusion dye propidium iodide (PI). PI (5μg/mL) was present in the medium throughout the experiment. PI is highly polar and is excluded from live cells but may enter damaged cells and becomes highly fluorescent upon binding to DNA. Fluorescence was exited at 450-490 nm or 515-560 nm using a standard Leica inverted microscope with either a FITC or a rhodamine filter block, respectively.

References

1. Cohen, S. S. *A Guide to Polyamines*; Oxford University Press: Oxford, 1998.

2. Matsuzaki, S.; Xiao, L. P.; Suzuki, M.; Hamana, K.; Niitsu, M.; Samejima, K. *Biochem. Int.* **1987**, *15*, 817-822.

3. Gale, E. F. *Biochem. J.* **1940** *34*, 392-413; Gale, E. F *Advances in Enzymology* **1946**, *6*, 1-32.

4. Djurhuus, R. *Anal. Biochem.* **1981**, *113*, 352-355; Heerze, L. D.; Kang, Y. J.; Palcic, M. M. *Anal. Biochem.* **1990**, *185*, 201-205.

5. Cantani, G. L. In *Biochemistry of S-adenosylmethionene and Related Compounds*; Uddin, E.; Borchardt, R. T.; Creveling, C. R. Eds.; Macmillin Press: London, 1982; pp 3-10.

6. Orr, G.; Danz, D.; Pontoni, G.; Prabhak, P.; Gould, S.; Coward, J. K. *J Am. Chem. Soc.* **1988**, *110*, 5791-5799.

7. Tabor, C. W.; Tabor, H. *Ann. Rev. Biochem.* **1976**, *45*, 285-306; Kahn, A. U.; Mei, Y. H.; Wilson, T. *Proc. Natl. Acad. Sci. USA.* **1992**, *89*, 11426-11427; Ha, H. C.; Yager, J.D.; Woster, P.A.; Casero jr, R. A. *Biochem. Biphy. Res. Commun.* **1998**, *244*, 298-303.

8. Tropp, J. S.; Redfield, A. G. *Nucleic Acid Res.* **1983**, *11*, 2121-2134.

9. Tabor, C. W.; Tabor, H. *Ann. Rev. Biochem.* **1984**, 53, 749-790; Frydman, B.; Westler, K.; Samejima, K. *J. Org. Chem.* **1996**, *61*, 2588-2589; Kusama-Eguchi, K, Watanabe, S.; Irisawa, M.; Waranabe, K.; Igarashi, K. *Biochem. Biphy. Res. Commun.* **1991**, *177*, 745-750.

10. Marton, L. J.; Pegg, A. E. *Ann. Rev. Phamacol. Toxicol.* **1995**, *35, 55-91*; Pegg, A. E. *Cancer Res.* **1988**, *48, 759-774.*

11. Kashiwagi, K.; Pahk, A. J.; Masulo, T.; Igarashi, K.; Williams, K. *Mol. Pharmacol* **1997**, *52*, 701-713; Bergeon, R. J.; Weimar, W. R.; Wu, Q.; Feng, Y.; McManis, J. S. *J. Med. Chem.* **1996**, *39, 5257-5266.*

12. Johnson, T. *Trends Pharmacol. Science* **1996**, *17*, 22-27; Williams, K. *Neuroscience. Lett.* **1995**, *184*, 181-184; Williams, K.; Romano, C.; Dichter, M. A.; Molinoff, P. B. *Life Sciences* **1991**, *48*, 469-498.

13. Overman, L.; Tomasi, A. L. *J. Am. Chem. Soc.* **1998**, *120*, 4039-4040.

14. Tsukamoto, S.; Kato, S.; Hirota, H.; Fusetani, N. *Tetrahedron Lett.* **1996**, *37*, 1439-1440; Ponasik, J. A.; Kassab, D. J.; Ganem, B. *Tetrahedron Lett.* **1996**, 37, 6041-6044.

15. Kurylo-Browska, Z.; Heaney-Kieras, J. *Methods Enzymol.* **1983**, *94,* 441-451.

16. Kurylo-Browska, Z. *Bull. Inst. Mar. Med.* **1959**, *10*, 151; Kurylo-Borowska, Z.; Heaney-Kieras, J. *Methods in Enzymology* **1983**, *94,* 441-451.

17. Moore, K. S.; Wehrli, H.; Roder, M.; Rogers, J.N.; Mccrimmon, D.; Zasloloff, M. *Proc. Natl. Acad. Sci. USA* **1993**, *90*, 1354-1358.

18. Clark, R. B.; Donaldson, P. K.; Gratin, K. A. F.; Lambert, J. J.; Piek, T.; Ramsay, R.; Spanjer, W.; Usherwood, P. N. R. *Brain Research* **1982**, *241*, 105-114; Huang, D.; Jiang, H.; Nakanishi, K.; Usherwood, P. N. R. *Tetrahedron* **1997**, *53*, 12391-12404.

19. Blagbrough, I. S.; Usherwood, P. N. R. *Proy. Soc. Edin.* **1992**, *99*, 67-81.

20. Blagbrough, I. S.; Moya, E. *Tetrahedron Lett.* **1994**, *35*, 2057-2060; Moya, E.; Blagbrough, I. S. *Tetrahedron Lett.* **1994**, *35*, 2061-2062.

21. Mc Manis, J. S.; Ganem, B. *J. Org. Chem.* **1980**, *45,* 2041-2042.

22. Werner, C.; Hu, W.; Lorenzi-Riatsch, A.; Hesse, M. *Phytochemistry* **1995**, *40,* 461-465.

23. Funayama, S.; Yoshida, K.; Konno, C.; Hikino, H. *Tetrahedron Lett.* **1980**, *21*, 1355-1356; Funayama, S.; Zhang, G. R.; Nozoe, S. *Phytochemmistry* **1995**, *38,* 1529-1531.

24. Ponasik, J. A.; Strickland C.; Faerman, C.; Savvides, S.; Karplus, P. A.; Garnam, B. *Biochem. J.* **1995**, *311*, 371-375.

25. Ina, H.; Ito, M; Kibayashi, C. *Chem. Commun.* **1995**, 1015-1016; Doll, M. K. H.; Guggisberg, A.; Hesse, M. *Helv. Chim. Acta* **1996**, *81*, 973-981.

26. Fairlamb, A. H.; Blackburn, P.; Ulrich, P.; Chait, B. T.; Cerami, A. *Science* **1985**, *227*, 1485-1487; Fairlamb, A. H. *Annu. Rev. Microbiol.* **1992**, *46*, 695-729.

27. Bergeron, R. J.; Hawthorne, T. R.; Vinson, J. R. T.; Beck, D. E.; Ingeno, M. J. *Cancer Res.* **1989**, *49*, 2959-2964.

28. Carrington, S.; Qarawi, M. A.; Blagbrough, I. S.; Moss, S. H.; Pouton, C. W. *Pharm. Sci.* **1996**, *2*, 25-27; Qarawi, M. A.; Carrington, S.; Blagbrough, I. S.; Moss, S. H.; Pouton, C. W. *Pharm. Sci* **1997**, *3*, 235-239.

29. Zhuo, J. C.; Cai, J.; Soloway, A. H.; Barth, R. F.; Adams, D. M.; Ji, W.; Tjarks, W. *J. Med. Chem.* **1999**, *42*, 1282-1292; Cai, J.; Soloway, A. H. *Tetrahedron Lett.* **1996**, *9283-9286.*

30. Lakanen, J. R.; Pegg, A. E.; Coward, J. K. *J. Med. Chem.* **1995**, *38*, 2714-2727.

31. Dessolin, J.; Galea, P.; Vlieghe, P; Chermann, J. C.; Kuras, J. C. *J. Med. Chem.* **1999**, *42*, 229-241.

32. Cooper, R. G.; Etheride, C. J.; Steward, L.; Marshall, J.; Rudgisky, S.; Cheng, S. H.; Milloe, A. D. *Chem. Eur. J.* **1998**, *4*, 137-151.

33. Geall, A. J.; Alhadithi, D; Blagbrough, I. S. *Chem. Commun.* **1998**, 2035-2036.

34. Geall, A. J.; Blagbrough, I. S. *Tetrahedron Lett.* **1998**, *39*, 443-446.

35. Gallop, M. A.; Barrett, R. W.; Dower, W. J.; Fodor, S. P. A.; Gordon, E. M. *J. Med. Chem.* **1994**, *37*, 1233-1254; Jung, G.; Becksichinger, A. G. *Angew. Chem., Int. Ed. Engl.* **1992**, *31*, 367-383.

36. Gersen, H. M.; Meloen, R. H.; Bartelling, S. J. *Proc. Natl. Acad. Sci. USA.* **1984**, *81*, 3998-4002.

37. Furka, A.; Sebestyen, F.; Asgedome, M.; Dico, G. *Int. J. Pep. Prot. Res.* **1991**, *37*, 487-493; Furka, A. *Drug. Dev. Res.* **1995**, *36*, 1-12.

38. Houghten, R. A.; Pinilla, C.; Blondelle, S. E.; Appel, J. R.; Dooley, C. T.; Cuerro, J. H. *Nature* **1991**, *354*, 84-86.

39. Dooley, C. T.; Houghten, R. A. *Life Sci.* **1993**, *52*, 1509-1517; Pinilla, C.; Appel, J. R.; Blondelle, S. E.; Dooley, C. T.; Eichler, J.; Ostresh, J. M.; Houghten, R. A. *Drug. Del. Res.* **1994**, *33*, 133-145.

40. Déprez, B.; Williard, X.; Bourel, L.; Coste, H.; Hyafil, F.; Tartar, A. *J. Am. Chem. Soc.* **1995**, *117*, 5405-5406.

41. Merrifield, R. B. *J. Am. Chem. Soc.* **1963**, *85*, 2149-2154.

42. Bayer, E. *Angew. Chem., Int. Ed. Engl.* **1991**, *30*, 113-129; Bayer, E.; Rapp, W. Dtsch. Offen. DE. Pat. 3,500,180, 1986.

43. Barany, G.; Albericcio, F; Biancalana, S.; Bontems, S. L.; Chang, J. L. Eritja, R.; Ferrer, M.; Fields, C. G.; Fields, G. B.; Lyttle, M. H.; Sole, N. A.; Tian, Z.; Van Abel, R. J.; Wright, P. B.; Zalipsky, S.; Hudson, D. In *Peptides;* Proc. 12th APS; Smith, J. A.; River, J. E. Eds.; ESCOM: Leiden, 1992, p. 603.

44. Adams, J. H.; Cook, R. M.; Hudson, D.; Jammalamadaka, V.; Lyttle, M. H.; Songster, M. F. *J. Org. Chem.* **1998**, *63*, 3706-3716.

45. Meldal, M. *Tetrahedron Lett.* **1992**, *33*, 3077-3080; Meldal, M.; Auzanneau, F. I.; Hindsgaul, O.; Palcic, M. M. *Chem. Commun.* **1994**, 1849-1850.

46. Kempe, M.; Barany, G. *J. Am. Chem. Soc.* **1996**, *118*, 7083-7093.

47. Phillips, G. B.; Wei, G. P. *Tetrahedron Lett.* **1996**, *37*, 4887-4891; Buckman, B. O.; Mohan, R. *Tetrahedron Lett.* **1996**, *37*, 4439-4443; Plunkett, M. J.; Ellman, J. A. *J. Org. Chem.* **1995**, *60*, 6006-6007.

48. Wang, S. S. *J Am.Chem.Soc.* **1973**, *95*, 1328-1333.

49. Mergler, M.; Tanner, R.; Gosteli, J.; Groee, P. *Tetrahedron Lett.* **1988**, *29*, 4005-4008.

50. Rink, H. *Tetrahedron Lett.* **1987**, *28*, 3787-3790.

51. Hone, N. D. *Tetrahedron Lett.* **1998**, *39*, 897-900.

52. Bycroft, B. W.; Chan, W. C.; Hone, N. D.; Milington, S.; Nash, I. A. *J Am. Chem. Soc.* **1994**, *116*, 7415-7416.

53. Nash, I. A.; Bycroft, B.W.; Chan, W. C. *Tetrahedron Lett.* **1996**, *37, 2625-2628.*

54. Feuchet, V.; Bourel, L.; Tartar, A.; Sergheraert, C. *Bioorg. Med. Chem. Lett.* **1994**, *4*, 2559-2562.

55. Byk, G.; Frederic, M.; Scherman, D. *Tetrahedron Lett.* **1997**, *38*, 17317-17334.

56. Byk, G.; Soto, J.; Mattler, C.; Frederic, M.; Scherman, D. *J. Comb. Chem.* **1998**, *2*, 81-87.

57. WHO data obtained from http://www.WHO.ch.

58. Brener, Z. *Annu. Rev. Microbiol.* **1973**, *27*, 347-382.

59. Moncayo, A.; *Eleventh Program Report of the UNPD/World Bank/WHO Special Program for Research And Training in Tropical Disease (TDR);* World Health Organisation: Geneva, 1991. pp 67-75.

60. Pepin, J.; Milord, F. *Advances in Parasitology* **1994**, *33*, 2-47.

61. Iten, M.; Matovu, R.; Brun, R.; Kaminsky, R. *Tropical Medicine and Parasitology* **1995**, *46*, 190-194.

62. Taelman, H; Clerinx, J.; Bogaerts, J.; Vervoort, T. *Transactions of the Royal Society of Tropical Medicine and Hygiene* **1996**, *90*, 572-573.

63. Brener, Z. *Pharmacol. Ther.* **1979**, *7*, 71-90; Schmunis, G. A.; Szarfman, A.; Coarasa, L.; Guilleron, C.; Peralta, G. M. *Am. J. Trop. Med. Hyg.* **1980**, *29*, 170-178.

64. Nussenzweig, V.; Sonntag, R.; Biancalana, A.; Pedreira de Fleitas, J. L.; Amatoneto, V.; Kleotzel, J. *Hospital* **1953**, 53, 731-744.

65. Docampo, R.; Moreno, S. N. J. *Rev. Biochem. Toxicol.* **1985**, *7*, 159-204.

66. Cohen, S. S. *Science* **1979**, *205*, 964-971; Wang, C. C. *J. Med. Chem.* **1984**, *27*, 1-9.

67. Nere, E.; Chance, M. L.; Hanboula, S. Y.; Monsigny, M.; Roche, A. C.; Mayer, R. M.; Hommel, M. *Antimicrobial Agents and Chemotherapy* **1992**, *36*, 2228-2232.

68. Hol, W. G. J. *Angew. Chem. Int. Ed. Engl.* **1986**, *25*, 767-778.

69. Goodford, P. J. *J. Med. Chem.* **1985**, *28*, 849-857.

70. Müller, J. G.; Bücheler, U. S.; Kayser, K.; Schirmer, R. H.; Werner, D.; Krauth-Siegel, R. L. *Cell. Mol. Biol.* **1993**, *39*, 389-396.

71. Schirmer, R. H.; Krauth-Siegel, R. L.; Schulz, G. E. In *Glutathione, Part A,* Dolphin, D.; Poulson, R.; Avramovic, O., Eds.; Wiely: New York, 1989; pp. 553-596; William, Jr. C. H. In *Chemistry and Biochemistry of Flavoenzymes, Vol.III;* Müller, F. Ed., CRC Press, Boca Raton, 1992, pp.121-211.

72. Fairlamb, A. H.; Cerami, A. *Ann. Rev. Microbiol.* **1992**, *46*, 695-729.

73. Schirmer, R. H.; Schoellhammer, T.; Eisenbrand, G.; Krauth-Siegel, R. L. *Free Radical Res. Commun.* **1997**, *3*, 3-12; Golenser, J.; Marva, E.; Chevion, A. *Parasitology Today* **1991**, *7*, 142-146.

74. Fairlamb, A. H.; Blackburn, P.; Ulrich, P.; Chait, B. T.; Cerami, A. *Science* **1985**, *227*, 1485-1487; Fairlamb, A. H.; Cerami, A. *Mol. Biochem. Parsitol.* **1995**, *14*, 187-198.

75. Krauth-Siegel, R. L.; Blatterspiel, R.; Saleh, M.; Schiltz, E; Schirmer, R. H.; Untucht-Grau, R. *Eur. J. Biochem.* **1982**, *121*, 259-267.

76. Karplus, P. A.; Schulz, G. E. *J. Mol. Biol.* **1987**, *195*, 701-729.

77. Karplus, P. A.; Schulz, G. E. *J. Mol. Biol.* **1989**, *210*, 163-180.

78. Karplus, P. A.; Krauth-Siegel, R. L.; Schirmer, R. H.; Schulz, G. E. *Eur. J. Biochem.* **1988**, *171*, 193-198; Bilzer, M.; Krauth-Siegel, R. L.; Schirmer, R. H.; Akerboom, T. P.; Schulz, G. E. *Eur. J. Biochem* **1984**, *138*, 373-378.

79. Pei, E. F.; Schulz, G. E. *J. Biol. Chem.* **1983**, *258,* 1752-1757.

80. Bücheler, U. S.; Werner, D.; Schirmer, R. H. *Nucleic Acids Res.* **1992**, *20,* 3127-3133; Leister, B.; Perham, R. N. *Biochem.* **1994**, *33*, 2773-2781.

81. Kuriyan, J.; Kong, X. P.; Krishna, T. S. R.; Sweet, R. M.; Murgolo, N. J.; Field, H.; Cerami, A.; Henderson, G. B. *Proc. Natl. Acad. Sci. USA* **1991**, *88*, 8764-8768; Hunter, W. N.; Bailey, S.; Habash, J.; Harrop, S.J.; Helliwell, J. R.; Aboarye-Kwarteng, T.; Smith, K.; Fairlamb, A. H. *J. Mol. Biol.* **1992**, *227*, 322-333; Bailey, S.; Smith, K.; Fairlamb, A.; H. Hunter, W. N. *Eur. J. Biochem.* **1993**, *213*, 67-75; Bailey, S.; Smith, K.; Fairlamb, A. H.; Hunter, W. N. *Acta Crystallogr. D* **1994**, *50,* 139-154.

82. Lantwin, C. B.; Schlichting, I.; Kabsch, W.; Pei, E. F.; Krauth-Siegel, R. L. *Prot. Struct. Funct. Genet.* **1994**, *18*, 161-173.

83. Benson, T. J.; Mc Kie, J. H., Garforth, J.; Borges, A.; Fairlamb, A. H.; Douglas, K. T. *Biochem. J.* **1992**, *286*, 2-11.

84. Krauth-Siegel, R. L.; Lohrer, H.; Bucheler, U. S.; Schirmer, R. H. In *Biochemical Protozoology*; Coombs, G. H.; North, M., Eds.; Taylor and Francis: London, 1991, pp. 493-505.

85. Williams, D. H.; Cox, J. P. L.; Doig, A. J.; Gardner, M.; Gerhard, U.; Kaye, P. T.; Lal, A. R.; Nicholls, I. A.; Salter, C. J.; Mitchell, R. C. *J. Am. Chem. Soc.* **1991**, *113*, 7020-7030; Williams, D. H. *Proc. Natl. Acad. Sci. USA* **1993**, *90*, 1172-1178.

86. Grafort, J.; Yin, H.; Mc Kie, J. H.; Douglas, K. T.; Fairlamb, A. H. *J. Enz. Inhib.* **1997**, *12*, 161-173.

87. Omar, M.; Khan, F.; Austin, S. E.; Chan, C.; Yin, H., Marks, D.; Vaghjiani, S. N.; Kendrick, H.; Yardley, V.; Croft, S. L.; Douglas, K. T. *J. Med. Chem.* **2000**, *43*, 3148-3156.

88. Garforth, J.; McKie, J. H.; Jaouhari, R.; Benson, T.J.; Fairlamb, A.H.; Douglas, K. T. *Amino Acids* **1994**, *6*, 295-299; McKie, J. H.; Garforth, J.; Jaouhari, R.; Chan, C.; Yin, H.; Besheya, T.; Fairlamb, A. H.; Douglas, K. T. *Amino Acids* **1994**, 20, 295-299.

89 Majumder, S.; Kierzenbaum F. *Antimicrobial Agents and Chemotherapy* **1993**, *37*, 2235-2238.

90. O'Sullivan, M. C.; Zhou, Q. *Bioorg. Med. Chem. Lett.* **1995**, *5*, 1957-1960.

91. Baillet, S.; Buisine, E.; Horvath, D.; Maes, L.; Bonnet, B.; Sergherert, C. *Bioorg. Med. Chem.* **1996**, *4*, 891-899.

92. Bonnet, B.; Sollez, D.; Davioud- Charvet, V; Landry , V.; Horvath, D.; Sergherert, C. *Bioorg. Med. Chem.* **1997**, *5*, 1249-1256.

93. Nefkins, G. H. L. *Nature* **1960**, *185*, 309; Sosnovsky, G.; Lukszo, J. *Z. Naturforsch.* **1986**, *41b*, 122-129.

94. Murahashi, S. I.; Naota, T.; Nakajima, N. *Chem. Lett.* **1987**, 879-882.

95. Itoh, M. *Bull. Chem. Soc. Jpn.* **1974**, *47*, 471-475; Adamczyk, M.; Fishpaugh, J. R.; Heuser, K. J. *Org. Prep. Proc. Int.* **1998**. *30*, 339-348.

96. Mitchinson, A.; Golding, B. T.; Griffin, R. J.; O'Sullivan, M. C. *Chem. Commun.* **1994**, 2613-2614; O'Sullivan, M. C., Dalrymple; D. M. *Tetrahedron Lett.* **1995**, *36*,

3451-3452; Xu, D.; Prasad, K.; Repic, O.; Blacklock, T. J. *Tetrahedron Lett.* **1995**, *36*, 7357-7360.

97. Zang, E.; Sadler, P. J. *Synth. Commun.* **1997**, *27*, 3145-3150.

98. Bycroft, B. W.; Chan, W. C.; Chabra, S. R.; Hone, N. D. *Chem. Commun.* **1993**, 778-779; Kellem, B.; Bycroft, B. W.; Chabra, S. R. *Tetrahedron Lett.* **1997**, *27*, 4849-4852.

99. Doll, M. K. H.; Guggisberg, A.; Hesse, M. *Helv. Chim. Acta* **1996**, *79*, 541-547.

100. Golding, B. T.; Mitchinson, W.; Clegg, W.; Elsegood, M. R. J. Griffin, R. J. *J. Chem. Soc. Perkin Trans. 1* **1999**, 349-356.

101. Marsh, I. R.; Bradley, M. *Chem. Commun.* **1996**, 941-942; Marsh, I. R.; Bradley, M. *Eur. J. Biochemistry.* **1997**, *243*, 690-694; Marsh, I. R.; Smith, H. K.; Leblanc, C. J.; Bradley, M. *Molecular Diversity* **1996,** *2*, 165-170.

102. Marsh, I. R.; Bradley, M. *Tetrahedron.* **1997**, *4*, 17317-17334; Smith, H. K; Bradley, M. *J. Comb. Chem.* **1999**, *1*, 326-332.

103. Jantagens, C.; Hoffmann, R; Guggisberg, A.; Bienz, S.; Hesse, M. *Helv. Chim. Acta* **1997**, *80*, 966-978.

104. Kunz, H.; Unverzagt, C. *Angew. Chem. Int. Ed. Engl.* **1984**, *23*, 436-437.

105. Guibe, F. *Tetrahedron* **1998**, 54, 2967-3042.

106. Mitchell, A. R.; Erickson, B. W.; Ryabtsev, M. N.; Hodges, R. S.; Merrifield, R. B. *J. Am. Chem. Soc.* **1976**, *98*, 7357-7362.

107. Sarin V. K.; Kent S. B. H.; Tam, J. P.; Merrifield, R. B. *Anal. Biochem* **1981**, *117*, 147-157; Kaiser, E; Colescott, R. L.; Bossingere, C. D.; Cook, R. I. *Anal. Biochem.* **1970**, *34*, 595-598.

108. Pearson, D. A. *Tetrahedron Lett.* **1989**, *30*, 2739-2743.

109. Nishino, N.; Mihara, H.; Izumi, Fujimoto, T. *Tetrahedron Lett.* **1993**, *34*, 1295-1298.

110. O'Sullivan, F. X.; Walsh, C. T. *Mol. Biochem. Parasitol.* **1991**, *44*, 145-148.

111. Sambrook, J.; Fritsch, E. F.; Maniatis, T. *Molecular Cloning: A Laboratory Manual*, 2nd ed.; Cold Spring Harbour Laboratory Press: New York, 1989.

112. Bradford, M. M. *Anal. Biochem.* **1976**, *72*, 248-254.

113 Eadie, G. S. *J. Biol. Chem.* **1942**, *146*, 85, 142b; Hofstee, B. H. J. *Nature* **1959**,*184*, 1296.

114 Gallop, M. A.; Barrett, R. W.; Dower, W. J.; Fodor, S. P. A.; Gordon, E. M. *J. Med. Chem.* **1994**, *37*, 1233-1251; Terrett, N. K.; Gardner, M.; Gordon, D. W.;

Kobylecki R. J.; Steele, J. *Tetrahedron* **1995**, *51*, 8135-8173; Rinnova, M.; Lebl, M. *Collect. Czech. Chem. Commun.* **1996**, *61*, 171-231.

115. Guillier, F.; Orain, D.; Bradley, M. *Chem. Rev.* **2000**, *100*, 2091-2157; James, I. W. *Tetrahedron* **1999**, *55*, 4855-4946.

116. Wang, S. S. *J. Am. Chem. Soc.* **1973**, *95*, 1328-1333; Rink, H. *Tetrahedron Lett.* **1987**, *28*, 3787-3790; Fyles, T. M.; Leznoff, C. C. *Can. J. Chem.* **1976**, *54*, 935-943, Fréchet, J. M.; Haque, K. E. *Tetrahedron Lett.* **1975**, *16*, 3055-3056; Fréchet, J. M.; Nuyens, L. J. *Can. J. Chem.* **1976**, *54*, 926-934.

117. Kenner, G. W.; McDermott, J. R.; Sheppard, R. C. *Chem. Commun.* **1971**, 636-637; Marshall, D. L. Liener, I. E. *J. Org. Chem.* **1970**, *35*, 867-868; Hoffmann, S.; Frank, R. *Tetrahedron Lett.* **1994**, *35*, 7763-7766.

118. Burbaum, J. J.; Ohlmeyer, M. H.; Reader, V; Henderson, I.; Dillard, L. W.; Li Troy, G.; Randle; T. L.; Sigal, N. H.; Chelsky D.; Baldwin, J. J. *Proc. Natl. Acad. Sci. USA* **1995**, *91*, 6027-6031; Baldwin, J. J.; Burbaum, J. J.; Henderson, I.; Ohlmeyer, M. H. *J. Am. Chem. Soc.* **1995**, *117*, 5588-5589; Holmes, C. P.; Jones, D. G. *J. Org. Chem.* **1995**, *60*, 2318-2319.

119. Sauerbrei, B.; Jungmann, V.; Waldmann, H. *Angew. Chem. Int. Ed. Engl.* **1998**, *37*, 1143-1346.

120. Pátek, M.; Lebl, M. *Biopoly.* **1998**, *47*, 353-363.

121. Kenner, G. W.; Dermott, G. R.; Sheppard, R. C. *Chem. Commun.* **1971**, *636-637.*

122. Backes, B. J.; Elmann, J. A. *J. Am. Chem. Soc.* **1994**, *116*, 11171-11172.

123. Backes, B. J.; Virgilio A. A.; Elmann, J. A. *J. Am. Chem. Soc.* **1996**, *118*, 3055-3056.

124. Marshall, D. L.; Leiner, I. E. *J. Org. Chem.* **1970**, *35*, 867-868; Flanigan, E., Marshall, G, R. *Tetrahedron Lett.* **1970**, 2403-2406.

125. Morphy, J. R.; Rankovic, Z.; Rees, D. C. *Tetrahedron Lett.* **1996**, *37*, 3209-3212; Brown, A. R.; Rees, D. C.; Rankovic, Z.; Morphy, J. R. *J. Am. Chem. Soc.* **1997**, *119*, 3288-3295.

126. Samanen, J. M.; Brandeis, E. *J. Org. Chem.* **1988**, *53*, 561-569.

127. Pátek, M.; Lebl, M. *Tetrahedron Lett.* **1991**, *32*, 3891-3894.

128. Hoffmann, S.; Frank, R. *Tetrahedron Lett.* **1994**, *35*, 7763-7766; Panke, G.; Frank, R. *Tetrahedron Lett.* **1998**, *39*, 17-18.

129. Alfred, J. C.; Aubagnac, J. L.; Calmes, M.; Daunis, J. *Tetrahedron* **1988**, *44*, 4407-4410.

130. Stowell, M. H.; Rock, R. S.; Rees, D. C.; Chan, S. I. *Tetrahedron Lett.* **1996**, *37*, 307-310; Rock, R. S.; Chan, S. I.. *J. Org. Chem.* **1996**, *61*, 1526-1529.

131. Routledge, A.; Abell, C.; Balasubramanian, S. *Tetrahedron Lett.* **1997**, *38*, 1227-1230.

132. Bray, A. M.; Maeji, N. J.; Valerio, R. M.; Campbell, R. A.; Geysen, H. M. *J. Org. Chem.* **1991**, *56*, 6659-6666.

133. Atrash, B.; Bradley, M. *Chem. Commun.* **1997**, 1397-1398.

134. Li, J.; Luo, X.; Wang, Q.; Zheng, L.; King, I.; Doyle, T. W.; Chen, S. H. *Bioorg. Med. Chem. Lett.* **1998**, *8*, 3159-3164.

135. Atrash, B. *Southampton University*, Personal Communication.

136. Hall, D. G.; Lapplante, C.; Manku, S.; Nagendran, J. *J. Org. Chem.* **1999**, *64*, 698-699.

137. Paradisi, M. P.; Zecchini, G. P.; Torrini, I. *Tetrahedron Lett.* **1998**, *39*, 439-442.

138. Khabnadideh; S.; Tan, C. H.; Croft, S. L.; Kendrick, H.; Yardley, V.; Gilbert, I. H. *Bioorg. Med. Chem. Lett.* **2000**, *10*, 1237-1239; Merritt, M.; Lanier, M.; Deng, G.; Regen, L. *J. Am. Chem. Soc.* **1998**, *120*, 8494-8501, Sadownik, A.; Deng, G.; Janout, V.; Regen, S.L.; Bernard, E.N.; Kikuchi, K.; Armstrong, D. *J. Am. Chem. Soc.* **1995**, *117*, 6138-6139.

139. Miller, A. D. *Angew. Chem. Intl. Ed. Engl.* **1998**, *37*, 1768-1885.

140. Crystal R. G.; McElvancy, N. G.; Rosenfeld, M. A.; Chu, C. S.; Mastrangeli A.; Hey, J. G.; Brody, S. L.; Jaffe, H. A.; Eissa, N. T.; Danel, C. *Nat. Genet.* **1994**, *8*, 42-51; Yang, Y.; Nunes, F. A.; Berencsi, K.; Gonczon, E.; Engelhardt, J. F.; Wilson, J. M. *Nat. Genet.* **1994**, *7*, 362-369.

141. Wong, T. K.; Neumann, E. *Biochem. Biophys. Res. Commun.* **1982**, 107, 584-588; Fraley R.; Subramani, S.; Berg, P.; Papahadjopoulos, D. *J. Biol. Chem.* **1980**, 255, 10431-10435.

142. Graham, F. L.; Van der Eb, A. J. *Virology* **1973**, *52*, 456-467.

143. MacCutchan, J. H.; Pagano, J. S. *J. Natl. Cancer Inst.* **1968**, *41*, 351-355.

144. Gluzman, Y. *Cell* **1981**, *23*, 175-182.

145. Kawai, S.; Nishizawa, M. *Mol. Cell. Biol.* **1984**, 4, 1172-1179.

146. Boussif, O.; Lezoualch, F.; Zanta, M. A.; Mergny, M. D.; Scherman, D.; Demenex, B.; Behr, J.–P. *Proc. Natl. Acad. Sci. USA* **1995**, *92*, 7297-7301.

147. Haensler, J.; Szoka, F. C. *Biocon. Chem* **1993**, *4*, 372-379; Kukowska-Latallo, J. F.; Bielinska, A. U.; Johnson. J.; Spinder, R.; Tomalia, D. A.; Baker, R. J. *Proc. Natl. Acad. Sci. USA* **1996**, *93*, 4897-4902.

148. Cappechi, M. R. *Cell* **1980**, *22*, 479-488.

149. Shigekawa, K.; Dower, W. J. *Biotechnique* **1988**, *6*, 742-751.

150. Ye, G. N.; Danielle, H.; Sanford, J. C. *Plant. Molec. Bol.* **1990**, *15*, 809-819.

151. Klein, T. M.; Wolf E. D.; Wu R.; Sanford J. C. *Nature* **1987**, *327*, 70-73.

152. Flegner P. L.; Gadek. T R; Home, M.; Roman, R.; Chan, H. W.; Wenz, J. P.; Nothrop, J. P.; Ringold, R. M.; Danielsen, M. *Proc. Natl. Acad. Sci. USA* **1987**, *84*, 7413-7417.

153. Behr, J. P.;Demeniex, B.; Loeffeler, J. P.; Perez-Mutul, J. *Proc. Natl. Acad. Sci. USA.* **1989**, *86*, 6982-6986.

154. Walker, S.; Sofia, M. J.; Kakarla, R.; Kogan, N. A.; Wierichs, L.; Longley, C. B.; Bruker, K.; Axelrod, H. R.; Midha, S.; Babu, S. *Proc. Natl. Acad. Sci. USA* **1996**, *93*, 1585-1590.

155. Gao, X.; Huang, L.; *Biochem. Biophys. Res. Commun.* **1991**, *179*, 280-285.

156. Guy-Caffey, J. K.; Bodepudi, V.; Bishop, J. S.; Jayaraman, K.; Chaudhary, N. *J. Biol. Chem.* **1995**, *270*, 31391-31396.

157. Moradpour, D.; Schauer, J. I.; Zurawski, V. R., Jr.; Wands, J. R.; Boutin, R. H. *Biochem. Biophys. Res. Commun.* **1996**, *221*, 82-88.

158. Vigneron, J. P.; Oudrhiri, N.; Fauquet, M.; Vergely, L.; Bradley, J. C.; Basseville, M.; Lehn, P.; Lehn, J.-M. *Proc. Natl. Acad. Sci. U.S.A* **1996**, *93*, 9682-9686.

159. Felgner, J. H.; Kumar, R.; Sridhar, C. N.; Wheeler, C. J.; Tsai, Y. J.; Border, R.; Ramsey, P.; Martiun, M.; Felger, P. L. *J. Biol. Chem.* **1994**, *269, 2550*-2561; Balasubramaniam, R. P.; Bennett, M. J.; Alberle, A. M.; Malone, J. G.; Nantz, M. H.; Malone, H. W. *Gene Therapy* **1996**, *3*, 163-172; Wheeler, C. J.; Felger, P. L.; Tsai, Y. J.; Marshall, J.; Sukhu, L.; Doh, S. G.; Hartikka, J.; Nietupski, J.; Manthorpe, M.; Nichols, M.; Plewe, M.; Liang, X.; Norman, J.; Smith, A.; Cheng, S. H. *Proc. Natl. Acad. USA* **1996**, *93*, 11454-11459.

160. Farhood, H.; Bottega, R.; Epand, R. M.; Huang, L. *Biochem. Biophys. Acta* **1992**, *111*, 239-246.

161. Felger, P. L.; Ringold, G. M. *Nature* **1989**, *337*, 387-388.

162. Gershon, H., Ghirlando, R.; Guttman, S. B. Minsky, A. *Biochemistry* **1993**, *32*, 7143-7151.

163. Smith, J. G.; Walzem, R. L.; German, J. B. *Biochem. Biophys. Acta* **1993**, *1154*, 327-340.

164 Leventis, R.; Silvius, J. R. *Biochem. Biophys. Acta* **1990**, *1023*, 124-132.

165. Farhood, H.; Serbina, N.; Huang, L. *Biochem. Biophys. Acta* **1995**, *1235*, 289-295; Zelphati, O.; Szoka Jr., F. C. *Pharm, Res.* **1996**, *13*, 1367-1372; Friend, D. S.; Papahadjopoulos, D.; Debs, R. J. *Biochem. Biophys. Acta* **1996**, *1278*, 41-50.

166. Mislick, K. A.; Baldeschwieler, J. D. *Proc. Nat, Acad. USA* **1996**, *93, 12349-*12354; Labet-Moleur, F.; Steffan, A. M.; Brission, C.; Perron, H.; Feugeas, O.; Furstenberger, P.; Oberling, F; Brambilla, E.; Behr, J.-P. *Gene Therapy* **1996**, *3,* 1010-1017.

167. Behr, J. P.; Demeneix, B.; Loeffler, J. P.; Multul J. P. *Proc. Nat. Acad. USA* **1989**, *86,* 6982-6986; Behr, J.-P. *Acc. Chem. Res.* **1993,** *26,* 274-278.

168. Zabner, J.; Fasbender, A. J.; Morninger, T.; Poelinger, K. A.; Welsh, M.J. *J. Biol. Chem.* **1995**, *270*, 18997-19007.

169. Xu, Y.; Szoka, F. C. *Biochem.* **1996**, *35*, 5616-5623.

170. Lewis, J. C.; Feltus, A.; Ensor, C. M.; Daunert, S. *Anal. Chem.* **1998**, 579A-585A.

171. Alam, J.; Cook, J. L. *Anal. Biochem.* **1990**, *188*, 245-254.

172. Rosenthal, N. *Meth. Enzymol.* **1987**, *152, 704.*

173. Haugland, R. P. *Handbook of Fluorescent Probes and Research Chemicals*, 6th ed.; Molecular Probes: Eugene, 1996; Chapter 10.

174. Naleway, J. J. *GUS Protocols: Using the GUS Gene as a Reporter of Gene Expression*; Academic Press: San Diego, 1992.

175. Campbell, K. *Chemiluminescence*; Ellis Horwood: Chichester, 1988.

176. Bronstein, I.; Fortin, J.; Stanley, P. E.; Stewart, G. S.; Kricka, L. J. *Anal. Biochem.* **1994**, *219*, 169-181.

177. Chalfie, M. Y.; Tu, G.; Euskirchen, G.; Ward, W. W.; Prasher, D. C. *Science* **1994**, *263*, 802-804; Tsien, R.Y. *Ann. Rev. Biochem.* **1988**, *67*, 509-544.

178. Prasher, D. C.; Eckenrode, V. K.; Ward, W. W.; Prendergast, F. G.; Cormier, M. J. *Gene* **1992**, *111*, 229-33.

179. Gerdes, H. H.; Kaether, C. *FEBS Lett.* **1996**, *389*, 44-47.

180. Reid, B. G.; Flynn, G. C. *Biochemistry* **1997**, *36*, 6786-6791.

181. Ormo, M.; Cubitt, A. B.; Kallio, K.; Gross, L. A.; Tsien, R. Y.; Remington, S. J. *Science* **1996**, *273*, 1392-1395.

182. *Liposomes*: *A Practical Approach*; New, R. R. C. Ed.; IRL: Oxford, 1990.

183. Machesky, L. In *Basic RNA and DNA protocols;* Harwood, A. Ed.; Humana Press Inc: Totowa; 1996; Vol. 58, pp 269-271.

184. Carter, M. J.; Milton, I. D. *Nucleic Acids Res.* **1993**, *21*, 1044.

185. Atherton, E.; Sheppard, R.C. *Solod Phase Peptide Synthesis: A Practical Approach*; IRL Oxford Univ. Press: Oxford, **1989**.

186. Page, P.; Burrage, S.; Baldock, L.; Bradley, M. *Bioorg. & Med. Chem. Lett.* **1998**, *8*, 1751-1756.

187. Blagbrough, I. S.; Al-Hadithi, D.; Geall, A. J., *Tetrahedron* **2000**, *56*, 3439-3447.